4

Modelling of Total Suspended Particulates in Malaysian Coastal Waters Using Remote Sensing Techniques

ANISAH LEE ABDULLAH

submitted in partial fulfillment of the requirement of
Middlesex University for the degree of Doctor of Philosophy

April 2004

TABLE OF CONTENTS

LIST OF FIGURES

CHAPTER 4

CHAPTER 5

CHAPTER 6

CHAPTER 7

LIST OF TABLES

LIST OF APPENDICES

ABSTRACT

This study focused on environmental remote sensing with the objective of constructing a remote sensing algorithm to determine Total Suspended Particulate (TSP) concentrations in Malaysian coastal surface waters. Other objectives included coral reef mapping and production of quantitative map of [TSP] using the remote sensing algorithm at the study area which was Tanjung Rhu, located northeast of Pulau Langkawi, Peninsular Malaysia. Measured [TSP] varied from 93.92 ± 50.10 mg/L to 148.65 ± 45.39 mg/L. The biogeographic distribution of the reef in Tanjung Rhu was mapped and the hermatypic coral species was identified taxonomically. Results were compared to a control site, Teluk Datai, located northwest of Pulau Langkawi. There were 37 coral species in Tanjung Rhu and 76 species in Teluk Datai. The Jaccard's score was 27% indicating that the two reefs were quite diverse in their coral compositions. The development of a remote sensing algorithm is deemed necessary to provide a synoptic view of the potential problem within the coastal waters due to the early coastal development in Tanjung Rhu. Sedimentation studies showed sediment fractions were mainly biogenic materials and lithified sediments. Sediment fallout rates in Tanjung Rhu were 1,403.48 ± 125.60 g/m^2/day (dry season) and 6,550.77 ± 641.43 g/m^2/day (wet season). In Teluk Datai the sediment fallout rates were 1,532.99 ± 201.81 g/m^2/day (dry season) and 12,446.45 ± 237.81 g/m^2/day (wet season). The remote sensing algorithm, *Suspended Particulate Algorithm for Coastal Remote Sensing* (SPACoRS) developed from a modified Simple Radiative Transfer Model is defined as [TSP] (mg/L) = $0.6668e^{4.3892x}$, where x represents ($R_{rs\text{-}toaTM3}/R_{rs\text{-}toaTM2}$) ratio. SPACoRS is designed to determine [TSP] of 30 – 275 mg/L with primary material of TSP having high backscattering and low absorbance values. Sensitivity of SPACoRS to produce higher accuracies was limited to TSP ≤ 150mg/L. SPACoRS's accuracy using Landsat Thematic Mapper data was 66%.

ACKNOWLEDGEMENT

I am very grateful to a great number of people and institutions for without their enormous help and involvement this thesis would not have been completed.

Firstly, I wish to thank Prof. Brian R. Shutes (Middlesex University), Dr. Mark Fitzsimons (University of Plymouth), and Assoc. Prof. Dr. Wan Ruslan Ismail (Universiti Sains Malaysia) for being my supervisors, for their advices, guidance, support and patience given to me throughout my study.

I am forever indebted to my husband, Assoc. Prof. Dr. Zulfigar Yasin, for his supervision in all aspects of my thesis, his time, invaluable advices, utmost patience, and everything anyone could ask for especially when I almost given up. Most importantly I am grateful for him being whom he is and for being with me through thick and thin.

I am also very grateful to Dr. Roland Doerffer and Dr. Hansjörg Krasemann (GFE, GKSS, Germany) for their enormous help in my remote sensing work and to Carl-Duisberg Gesellschaft e.V. for giving me the opportunity to work with them; all members of Reef Research Group Universiti Sains Malaysia for their never-ending assistance; to Universiti Sains Malaysia for the provision of short-term research grant to carry out my field study; to Dr. Khiruddin Abdullah for his valuable advice and help; to the technical staffs of USM (particularly Mukahead Marine Research Station and School of Biological Sciences) and MACRES for their kind assistance; and to my circle of supportive friends from near and far.

I owe this especially to my family whom are always there for me; for their generous support, continuous encouragement, patience, understandings and love they've always given me.

Above all I am most grateful to *Allah S.W.T.* for *He* has forgotten me not and had always generously showered me with *rezeki.....Syukur Alhamdulillah.....*

Anisah Lee Abdullah

Chapter 1

INTRODUCTION

1.1 A GENERAL OVERVIEW

Until two decades ago, coral reefs were utilized on a small-scale for harvesting food and craft materials; and although these activities had a severe impact on the coral environments, the effects were localized. Through time the deleterious effects of human activities intensified, broadened in scale, and changed in nature. Excessive harvesting using unselective methods, widespread pollution of many different types, and the massive spread of tourism have resulted in the deterioration of many reefs and the destruction of some. According to Buddemeier (1999), "it is logical to conclude that coral reefs are doomed -- probably within the next few decades". Stoddart (1981) implied that reef scientists must determine their research priorities in the light of the rapidly expanding impact of man on coral reefs.

The accelerating degradation of the reef environment, which takes a variety of forms (Stoddart, 1968) results from the direct activities of man, in the collection of shells and corals, in fishing, and in the modification of reef topography. It results too from pollution of the seas on a variety of scales. At the local scale, there is abundant evidence of the effects of sewage from densely populated areas and hotels on adjacent coral reefs, of dumping wastes in coastal waters, and of thermal pollution near power stations are also apparent. At the regional scale, there are effects in increased sedimentation resulting from commercial development in the tourism trade, and deforestation along the coastlines. Even the most remote reefs are no longer immune from pollution. There is a need to raise awareness of the fragility of reef ecosystems, and the possible irreversibility of these changes, at least on a timescale measured in decades, in spite of the fact that reefs are adapted to cope with a variety of natural disturbances (Pearson, 1981). We cannot escape the conclusion that many of the environmental disruptions triggered by man involve elements of carelessness, lack of foresight, and ignorance, as well as simple economic pressures.

The management strategies adopted for reefs have been diverse but the two main strategies have been controls over areas and controls over species. There is a need to develop an explicit recognition of the diversity of the management requirement and the multiplicity of the possible response. Strategies need to operate at different levels where some sites are protected with great vigour, but others utilised both to control and to generate income from tourists and other modes of exploitation.

There should not be pessimism because the ocean is wide, the reefs are vast; many are still untouched. But it *is* a shrinking world, shrinking very much more rapidly than any of us would have anticipated or thought possible only some two decades ago. It would be inappropriate to concentrate our energies exclusively on the disasters of the past but rather try to anticipate what will happen on the unspoiled reefs in the future. It was with this strategy that this study was carried out.

In Southeast Asia, people have coexisted with the coral reef ecosystems for thousand of years. With more than 350 million people living within 50 km of the coast, coral reefs are important not only in local communities' cultures, but are also critical to the economic health of these nations (WRI, 2000). Coral reef fisheries, in particular, are a vital source of food and employment. The large yields obtained from marine fisheries supported by the reef system is not limited to the fishes and crustaceans harvested from within the reef system, but also include a larger variety and quantity of organisms caught elsewhere but whose existence is dependent upon the reef. In addition to fisheries, coral reefs provide many other exceptionally valuable services. Their beauty draws millions of tourists from around the world each year. Corals posses a yet untold value as biochemical materials for pharmaceuticals and other products. Reefs also facilitate the growth of mangroves and seagrasses, provide sheltering habitat essential to a variety of marine species, and help prevent shoreline erosion. The coral reefs in the Malacca Straits alone which, also encompassed the study area of this research, have a total assessed economic value of US$563 million for tourism, shoreline protection, fishery resources, and their research potential (IMO, 1999).

For colour, sheer beauty of form and design, and tremendous variety of life, perhaps no natural area in the world can equal coral reefs. Their beauty has fascinated generations of people, both scientific and lay, down through the years. By the same token, few areas of the marine environment have less initial aesthetic appeal than the dark, mud-wreathed areas known as mangrove forests, where passage is barred by a maze of tangled roots standing above soft mud surface. Yet these two very different associations are characteristic of vast tropical regions of the world, are unique, and must be considered if one is to understand the functioning of shallow water areas in the tropics.

1.2 THREATS TO THE MALAYSIAN REEFS

One of the major sources of coral reef degradation which is now a growing concern, is associated with mismanagement of upland areas particularly coastal development resulting in high rates of sedimentation which effectively suffocate the corals (DuBois and Towle, 1984; Kinsey, 1988; Birkeland, 1997). Although highly diverse and extraordinarily valuable, the

World Resources Institute, (WRI) (2002) reported that coral reefs of Southeast Asia are also severely threatened. The Malaysian reefs are no exception. The heavy reliance on marine resources across the region has resulted in the overexploitation and degradation of many coral reefs, particularly those near major population centers.

According to WRI report (2002) coastal development and land-use changes put significant pressure on coral reefs in this region, affecting 25% and 21% of reefs, respectively. The combined sedimentation and pollution from these two activities place 37% of the region's reefs at risk. From the major categories of threats evaluated, marine-based pollution is the least pervasive threat, affecting only 7% of reefs (Figure 1.1). When all of these threats are aggregated, human activities threaten the vast majority of coral reefs in the region by 88%. Nearly 50% of those threatened coral reefs are under high or very high threat.

Figure 1.1: Threat estimates in percentage for Southeast Asia coral reefs by type of threat.
(Source: WRI Report, 2002)

WRI made a study by assessing the reefs at risk within the Asian region in year 2000 and summarised the threat index in the various countries as shown in Table 1.1. The Southeast Asian countries have the highest percentage of threat index. Malaysia and Indonesia each have over 85% of their coral reefs threatened.

Malaysia encompasses 11 states and 2 federal territories on the Malay Peninsula and 2 states on the island of Borneo. The wide geographic range that Malaysia covers means that diverse coral reefs can be found in varied condition across the country. Little reef development occurs along the west coast of Peninsular (or West) Malaysia, but the east coast of West Malaysia has some

fringing reefs along the coast and many reefs around the offshore islands. Overall, more than 350 coral species are found in Malaysia (Jameson and Smith, 1997).

Table 1.1: A Summary of Reefs at Risk Threat Index by Country (or area). (Source: WRI Report, 2000)

Threats facing Malaysian reefs differ according to location. Peninsular Malaysia reefs are most affected by development. High-traffic shipping lanes run along the western coast of Peninsular Malaysia through the Straits of Malacca. Reefs in this area are subjected to oil spills and anchor damage. Agriculture and development on the peninsula have caused increased sediment and nutrient runoff. Some west coast reefs are now damaged by seasonal macroalgae blooms (Jameson *et al.*, 1995). Information about coral cover in Peninsular Malaysia is limited. Surveys of coral reefs along the east coast of Peninsular Malaysia suggest relatively high coral cover, 55 -70% on most fringing reefs. On the west coast of the peninsula, the estimated percentage of live coral cover is generally lower, from 25 - 45% (UNEP/IUCN, 1988).

According to studies conducted by the WRI on Reefs at Risk (2000), it was found that over 85 % of Malaysian reefs are threatened by human activities (Figure 1.2). Destructive fishing and overfishing was the primary threats, impacting 68% and 56% of the reefs, respectively. Coastal development and sedimentation from upland sources each affect approximately 23% of coral reefs in Malaysia. Impacts of these two primary threats causing sedimentation and suspended particulate problems in coastal waters are discussed in the following sections.

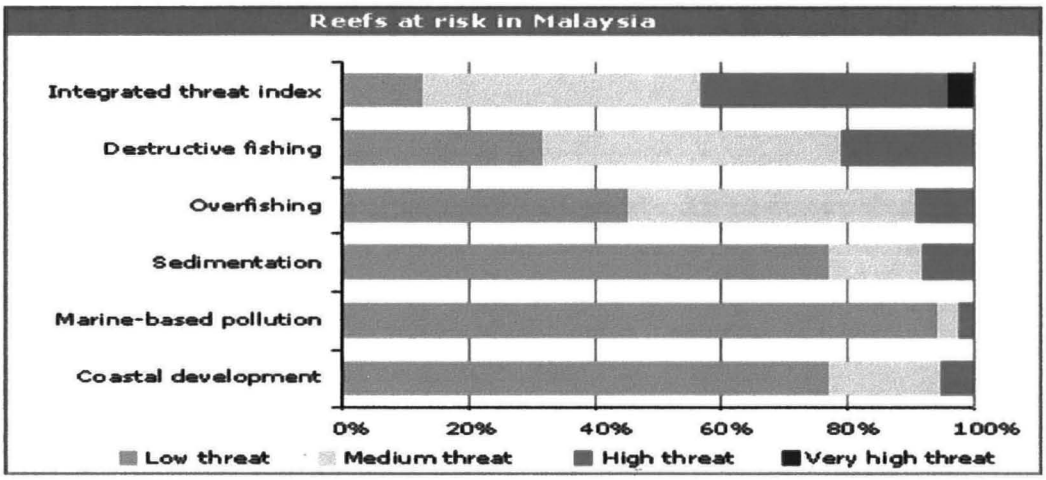

Figure 1.2: Threat estimates in percentage for Malaysian reefs by type of threat. (Source: WRI Report, 2002)

1.3 IMPACT OF SEDIMENTATION ON THE CORAL REEF ECOSYSTEM

Sediments affect reefs through a number of ways both directly and indirectly. Such effects may be subtle if sediment concentrations are low and manifest itself as physiological stress. If the sediment loads are high, acute effects and even colony die-offs may be observed. Sediments may be objectionable in water for several reasons. It is aesthetically displeasing and provides adsorption sites for chemical and biological agents. The damaging effects of sediments on coral reefs are numerous and will be summarized in the following subsections.

1.3.1 Sediment Attenuation of the Light Spectrum

Sediment in water, particularly suspended particulates, attenuates light which is important for coral photosynthesis. Light limits the growth of coral to about 5% of surface illumination (Jerlov, 1976). Corals in deeper waters are affected as the amount of light reaching the bottom is reduced. Optimal light intensities allow the maximum species diversity to develop round about 20m depth. At greater depths, the attenuation of light causes species diversity to decline (Sheppard, 1980).

In the west coast of Peninsular Malaysia the average maximum depth of fringing reefs are between 2.5 - 3.5m (Pulau Langkawi and Pulau Songsong) to 8m (Pulau Payar). Hence the waters are turbid. On the east coast of Peninsular Malaysia where the waters are clearer the reefs extended to greater depths (Yasin, *pers. comm.*).

Selective wavelength attenuation of light is dependent on sediment and its origin. Resuspended sediments tended to act as neutral density filter reducing light over the whole of the visible spectrum.

1.3.2 Sediment Smothers Corals Causing Suffocation

Heavy sediment falling on the reef will smother the coral and suffocate it if the rate of sedimentation is higher than the rate at which the corals are able to shed them. Mechanisms of sediment rejection in corals are discussed in the following subsections.

1.3.2.1 Energy and Material Expended To Remove Sediment on Corals

Energy is expended by corals to remove sediment falling onto the colonies. Increased sedimentation meant that higher proportion of the energy of the corals be spent removing the sediment and lower proportion of the energy expended for feeding, growth and reproduction.

Dodge and Vaisnys (1977) and Bak (1978) discovered that a much larger mucus production is produced by corals in response to sedimentation. The mucus is used to trap sediments and sediment saturated mucus is easier to remove than sediment alone. This method of sediment removal can only be sustained over a short period of time after which deleterious effects begin to show on the corals (Antonius, 1981). There are five methods of sediment rejection by corals. These are:

1. removal by ciliary action;
2. distension of the body causing accumulated sediment to be shed off;
3. production of mucus where sediments are in turn collected;
4. removal of sediment by coral tentacles, and
5. morphological adaptation of the coral colony.

Different species may use different methods of sediment rejection or a use of combination of the above methods. There are also variations within the same species found in different environment. The same species of corals may develop different colony shapes, ecomorphs,

depending whether they are found in clear or turbid waters. However, given the strategies above the ability of corals to withstand sedimentation is not limitless.

1.3.2.2 Reproduction and Dispersal Of Corals

Since corals are sedentary animals, its mode of dispersal for the purpose of reproduction is through tiny planktonic larvae called planulae. To compensate for the hazards of passive transportation in water currents, these planulae are produced in large numbers. Only when the aquatic environment is favourable do these planulae settle on suitable substrate to form corals. Coral larvae require a hard and stable substratum to settle. Sediment rain changes the bottom type and may render it unsuitable for coral planulae settlement. This might also cause higher mortality rates of coral planulae before settlement. After larval settlement mortality rates are normally lower but in such situation the rate may still be quite high until colonies have increased in size, thereby gaining some immunity and tolerances to risk of mechanical damage due to unfavourable environmental condition (Barnes, 1973).

Total fecundity is determined by the number of polyps and will continue to increase with colonial growth. Sedimentation on top of the coral heads will cause a decrease of polyp cover due to suffocation and eventually death of polyps on coral heads. This will in turn result in the reduction of total fecundity. Since coral growth is an extremely slow process, a reduction in total fecundity will also affect coral spreading or its extension in the shallow water region.

1.3.2.3 Inherent Toxic Properties of Sediment

Sediment from terrigenous inputs may have toxic properties. These may be in the form of metal ions such as iron which are toxic to marine invertebrates. The toxicity may also be imparted as nutrients contained in the sediments. Increased nutrient in a naturally nutrient-poor environment such as a coral reef can result in algal blooms.

1.3.2.4 Particle Size and Its Effect

The size of particles in sediments affects both its horizontal and vertical distribution as this factor influence sediment transport. The size of sediments also determines the success of sediment rejection in corals. In determining the effect of sediments on corals, it is necessary to study the spatial distribution and concentrations of sediments in the water.

1.3.2.5 Horizontal Variation

The horizontal distribution of sediments in the sea is caused by sediment transport by waves and prevailing currents as well as the size and shape of the particles concerned. Larger heavier particles are retained near the point source but light silt size particles can be carried over great distances. At Pulau Songsong (Malaysia), located further south of Pulau Langkawi where the proposed research area is located, the turbid waters were caused by silt particles transported from the Muda estuary on the mainland at a distance of more than 6 km away (Yasin, 1993).

Oceanographic features may modify the distribution of sediments. Eddies may cause the deposition of sediments during transportation. Where sediment deposition and resuspension is high, coral diversity and coral cover is low.

1.3.2.6 Variation with Depth

Stoke's Law stated that fall velocity of a sphere is proportional to the sphere diameter. Stoke's Law correspond to silt-size and finer particles with the density of quartz. For larger grain size particles fluid inertial forces causes a drag behind the particle therefore retarding its fall. Fall of particles is again slowed down in the presence of other grain. In standing water then there is a distribution of particles; the heavier particles lying near the bottom whilst the lighter particles are located in the upper layers or are continuously in suspension.

The gradation is further modified in the presence of a prevailing boundary current that induces resuspension of the settled sediment. This is important on the reef as even though the injection of fresh sediments into the system may have stopped, the effects of sedimentation may still be felt as resuspension of settled sediments occur.

1.3.2.7 Temporal Variation

The natural rate of sedimentation on reefs is subject to temporal variations. This is more pronounced on shallow reefs as it is subject to both wave actions and near shore current. In the shallow reefs of Pulau Songsong (Malaysia) where sedimentation rates are high, water turbidity is increased by an average of 112% during spring tides (Yasin, 1993). The local current velocity on the reef during spring tide is 3.5 times that of the neaps. Both the current and wave act on the settled sediment to bring it into resuspension.

Sediment concentration and water turbidity also increase during the peak of wet seasons on reefs of Peninsular Malaysia. This period is characterized by strong currents and high wave climate. In

addition, the fringing reefs that lie in close proximity to a river will receive a higher load of sediment from the riverine inputs.

1.3.2.8 Sediment Tolerant and Sediment Sensitive Species

It is a common misconception that turbid waters do not have corals. Even in the chronically turbid waters such as Pulau Kendi, Malaysia, where sedimentation can exceed 180 mg/cm^2/day a number of coral genera thrives (Thevathasapillai, 1990). However, coral communities found in turbid or sedimented waters are composed of different reef species. In the turbid waters the few coral genera that usually predominate are *Favites, Porites*, and *Favia*. As the sedimentation rate increases, scleractinians (the reef-building corals) begin to disappear and there is a predominance of the non-scleractinian corals and the soft corals. Jones and Endean (1981) discovered that reefs in turbid waters differ from clear water reefs in having lesser coral cover, lower diversity and growth rates, and has different species composition.

1.3.2.9 Degree Of Sedimentation And Its Effect On Reefs

Pastorok and Bilyard (1985) estimated the degree of impact of various sedimentation rates on coral communities (Table 1.2). No breakdown of particle sizes for the sediments is given but it is clear that the adverse effects of increased sedimentation on species diversity and coral cover are logarithmic. Their findings were based on Atlantic corals.

Table 1.2. Estimated degree of impact of various sedimentation rates on coral communities (Source: Pastorok and Bilyard, 1985).

Sedimentation Rate (mg/cm^2/day)		Degree of Impact
1 - 10	Slight To Moderate	▪ Decrease in abundance ▪ Altered growth forms ▪ Decreased growth rates ▪ Possible reductions in recruitment ▪ Possible reductions in numbers of species
10 - 50	Moderate To Severe:	▪ Greatly decreased abundance ▪ Greatly decreased growth rates ▪ Predominance of altered growth forms ▪ Reduced recruitment ▪ Decreased numbers of species ▪ Possible invasion of opportunistic species
>50	Severe To Catastrophic	▪ Severely decreased in abundance ▪ Severe degradation of communities of many species ▪ Many colonies die ▪ Recruitment severely reduced ▪ Regeneration slowed or stopped ▪ Invasion of opportunistic species

Following reef degradation there are other important effects that should be considered. These are:

1. The effect of reef degradation on the systems productivity and its consequent effect on higher trophic levels.
2. The effect of this degradation on other reef functions such as the provision of habitat for reefal organisms.
3. The maintenance of reef structure and integrity as reef sometimes function as breakwaters in coastal areas.
4. The effect of reef degradation on human uses.

Sedimentation lowers the value of reefs both biologically, aesthetically and economically.

1.3.2.10 Other Effects of Sedimentation on Coral Reefs

Sediment may affect fish or shellfish either by damaging the organisms physically or biologically or by damaging the habitat in which the organisms live.

Jones and Endean (1981) found that fish could tolerate turbidities up to 100,000 parts per million (ppm) for a week or longer, but the same fish died in turbidities above 175,000 ppm. Ellis (1937), studying fish and freshwater mollusks in turbid waters, observed the same phenomenon. In both cases, sediment-clogged gills ceased to function as oxygen exchange sites; with decreased aeration of the blood, the fish died from a combination of anoxemia and carbon dioxide retention.

Sediment and/or turbidity can damage aquatic ecosystems especially in coral reefs in a number of ways:

(1) Reduction of light penetration by sediment is marked (Ellis, 1936). This light reduction can inhibit photosynthesis (Corfitzen, 1939; Tarzwell and Gaufin, 1953), leading to a decline in food in the aquatic ecosystem and thereby limiting its capacity.

(2) A reduction of oxygen in water directly due to turbidity has not been exhibited experimentally or with field data (Cordone and Kelley, 1961), but decomposition of organic matter frequently deposited with sediment uses dissolved oxygen (Phelps, 1944), thereby effectively reducing the oxygen content in water.

(3) Mansueti (1961) estimated that sedimentation had destroyed system. Oysters, hard clams, and blue crabs need to attach to firm bottoms, free from heavy mud (Maurer and

Price, 1969; Maurer *et al.*, 1971). Sediment concentration is also related to the reduction of insect fauna (Cordone and Kelly, 1961; Chapman, 1962) and of bottom-growing plants (Langlois, 1941) as well as fish population reductions.

(4) Turbidity reduces the ability of fish to find food (Jones, 1964), but it may also allow young fish to escape predators.

Under most conditions the ecological effect of sediment on aquatic ecosystems especially the coral reefs is probably greater than the physiological effect of sediment on fish. But the combination of ecological and physiological effects creates an additional stress on fish populations which tends to change these populations either in number or in dominant fish species, thereby altering original coral reef ecosystems (Leletkin, 1981).

1.3.3 Protection And Conservation Of Coral Reefs

As in any other ecosystem, biodiversity is a fundamental property. The natural histories of organisms relate directly to ecosystem structure, and constraints imposed at higher scales of interaction determine both species occurrence and abundance, and community composition. If those constraints are altered either by natural phenomena or by human intervention, biodiversity will be altered as well. Therefore, understanding the distribution of biota among different systems and assessing their functional roles are keys both to understanding how ecosystems function and their conservation (Ray and Grassle, 1991).

Coastal and marine systems are extraordinarily diverse in all aspects, from genetic to taxonomic to ecological. As diversity is becoming widely recognized, the scientific literature and the public press are reporting that many marine systems, particularly coastal ones, are severely depleted, drastically altered, overfished, and polluted. The United Nations Environment Programme (UNEP, 1990) has documented pathogens, toxic substances, eutrophication, and disruption of ecological habitats in the coastal and marine environment. UNEP has also reported that biological diversity has been decreased.

It is necessary to consider coral reef as one of the important ecosystems since it is part of the coastal and marine systems which together with the terrestrial ecosystems and the atmosphere enveloping it forms the whole earth system that sustains life within it. This can also be considered in smaller scale such as in this study. The interrelationships and the connections are very complex and yet crucial for the need of protection and conservation. In tropical waters such as in Malaysia, the degree of sediment and suspended sediment impact varies depending on factors involving changes of wet and dry seasons of the year, the degree of anthropogenic

influences, the country's development phases and the level of care given in making marked changes to the natural environment.

How rainfall erosion within a forested area could have its effect on the existing connected ecosystem is summarized in Appendix 1. This summary only shows the natural occurrences. These impacts can be long-term or short-term, but the ecosystem will always have its ways of balancing these disturbances. It is when there are human interventions to such phenomena that normally cause longer term or perhaps even irreversible impacts. Typical examples of the degree of impacts humans have on the Malaysian coastal environment when deforestation occurs for the sake of coastal development is given in Appendix 2.

1.4 IMPACT OF TOTAL SUSPENDED PARTICULATES ON THE CORAL REEF ECOSYSTEM

The total suspended particulates (TSP) affect the reefs in various ways and the degree of impact varies depending on the extent of exposure and concentrations of these particulates. Some of the known major impacts associated with Malaysian coral reefs are:

(1) the reduction of coral growth rate
(2) the deterioration of coral health
(3) the reduction in gross productivity
(4) the decrease in fishery resources
(5) the decrease in reef aesthetic values
(6) the lowering of income generation for tourism-based industry (local and regional)

If concentrations of TSP in water increase, the much-needed light for photosynthesis by the symbiotic zooxanthellae in reef building corals will be reduced. These zooxanthellae are super-sensitive to light (Hoegh-Guldberg, 2000). The growth rates of corals will be significantly reduced if the exposure to high concentrations of TSP is prolonged. However, different species of coral show different tolerance levels to light intensity and TSP concentrations in water. Corals are known to require an extensive length of time to recover (White and Cruz-Trinidad, 1998), therefore high concentrations of TSP over long exposure period may naturally degrade a vast extent of healthy reef. The reef may be subjected to long term impact or short-term impact depending on several factors such as monitoring and management strategies and its effectiveness.

The presence of high concentrations of TSP will cause existing live and healthy corals to experience stress. Although it has not been scientifically proven, it is believed that when TSP concentration is high, it tends to absorb and retain heat resulting in increased water temperature (Buchheim, 2002). Coral bleaching, an important sign of disease in corals, may occur resulting in the expulsion of coral's symbiotic algae, zooxanthellae, after which the corals appear white or

"bleach'. Bleached corals can survive for sometime, but if conditions do not return to normal they die. Once dead, coral skeletons are covered by bacteria and fast-growing algae, and the reef ecosystem may go through a relatively rapid succession of opportunistic organisms. Algae and fast-growing invertebrates can potentially prevent re-establishment of the original coral community. Unless there is significant recovery of reef-building corals, physical break-down of reef structure may occur.

These impacts contribute greatly to general coral reef degradation and so related to potential economic loss. These impacts may be long-term or short-term ones depending on the extent of exposure and concentrations of the suspended particulates within the water column.

1.5 THE STUDY AREA

The chosen area for this study is Tanjung Rhu (*Tanjung* = Cape, *Rhu* = Casuarina), located at the northeast of Pulau Langkawi (*Pulau* = Island) in Peninsular Malaysia. Pulau Langkawi is located between the latitudes of 6° 10' N - 6° 30'N and 99° 35'E - 100° 00'E which is on the northwestern coast of Peninsular Malaysia. The size of the study area is approximately 63 km^2. Details of the study area are described in Chapter 2.

1.6 THE CONTROL SITE

A control site, Teluk Datai, was chosen for the purpose of this study and it is located at the northwest of Pulau Langkawi. Teluk Datai is the preferred control site for this study because it has similar existing major natural habitats as found in Tanjung Rhu. The differences lie in the riverine-estuarine network which, do not exist in Teluk Datai and the state of development of Teluk Datai that has stopped since 1994. The existing natural environment of Teluk Datai is well maintained and is considered pristine. The existing environment of Teluk Datai is also described in Chapter 2.

Comparisons of results in this study will be made particularly to the biogeographic distribution of the coral reef features and sedimentation between the study area (Tanjung Rhu) and the control site (Teluk Datai).

1.7 THE STUDY RATIONALE

Pulau Langkawi was declared a Free Port on January 1987. Since then the development on the island has rapidly progressed. This coincided with the increase in the development of infrastructure especially related to the tourism industry.

Initially the focus of the development was in Kuah, the largest town in Pulau Langkawi located in the southeast of the island. Later development spread to the beaches of Pantai Chenang on the west. This latter development is to support the tourism industry basically relying on the natural beauty of the coastline within the island.

Beachfront properties at Pantai Chenang were soon taken up and development proceeded to other areas such as the northwest coast of Pulau Langkawi (Lee, 1994). At present one of the new sites for development was on the northeast coast of Langkawi - the area which was studied by the author.

Tanjung Rhu is relatively undisturbed although there are some small scale developments occurring within this region. Its relatively pristine condition renders it a suitable area for this study. There are a number of existing natural habitats within this relatively small study area and these are coral reefs, mangrove forest, mudflats, sandflats and an estuarine-riverine system. These habitats, particularly the coral reefs, are complex ecosystems with high biological diversity that occur in shallow waters throughout the tropics. Their proximity to the coast exposes coral reefs not only to subsistence pressures but also to other human induced (anthropogenic) stresses such as pollution (industrial, chemical and sewage) and sedimentation (land clearing, reclamation, mining).

Given the potential economic impact of continued degradation of the coral reefs, suitable monitoring programs are required to detect any degradation and to facilitate the development of effective management plans to ensure the future viability of these resources. In order to determine the importance of natural reef ecosystems and to detect changes that occur through perturbations (man-made and natural), the distribution of the existing coral reefs should be mapped. Natural variability of the extent of the reefs could then be determined through monitoring.

Despite the complexity and high biological diversity of these ecosystems they are not stable, indeed they are sensitive to disturbance and are highly variable. Long-term quantitative studies of these complex ecosystems are necessary in order to decouple the effect of human impacts from natural variability in community structure.

1.8 THE STUDY OBJECTIVES

This study proposes a combination of techniques; synoptic satellite data, aerial photography, on-site sampling, and development of a suspended particulate algorithm to assist in the determination or estimation of suspended particulates in the surface coastal waters of Malaysia particularly at the coral reef regions of Pulau Langkawi.

The objectives of this study are:

(1) to ascertain the water quality profile of the study area,

(2) mapping of the coral reefs of the study area,

(3) to measure sediment fallout rates of the study area,

(4) construction of a satellite-based methodology, a theoretical algorithm, for the determination of suspended particulates concentrations on the surface coastal waters, and

(5) the production of quantitative maps of suspended particulates concentrations using the developed algorithm.

It is of importance to state here that this research study aims to construct a satellite-based algorithm that could be applied to the surface waters of the study area and not developing a programme that is used to construct the algorithm in mind.

1.9 APPROACH TO THE STUDY

This study applies Environmental Remote Sensing to the coastal waters of Peninsular Malaysia. There are four major components involved in this research study and these are water quality, remote sensing, GIS and impact studies. This research study is basically divided into five phases and these are given in a flow chart in Figure 1.3.

The methodology adopted in this study utilizes both conventional and advancing remote sensing technology to assess the existing coastal environment. The use of a remote sensing technique will provide a broad synoptic view of the distribution and concentration of suspended particulates.

TSP is the main target material in this study because it is one of the parameters that changes the optical characteristics of surface waters. It is also readily observed in the coastal zone and inland waters using optical spectral range instruments from aircraft and satellite platforms (Ritchie *et al.*, 1987). The objective of estimating concentrations of this material in water surface layer from reflectance or radiance measurements above the sea has so far been based mainly on statistical analysis of remotely-sensed and field data, leading to algorithms, with limited applicability and accuracy (Ritchie and Cooper, 1988).

Suspended particulates in surface waters can be a visible indicator of erosion and soil loss. Remote sensing can provide the synoptic view of the landscape and the ocean necessary to locate and monitor areas with significant suspended particulate/sediment problems.

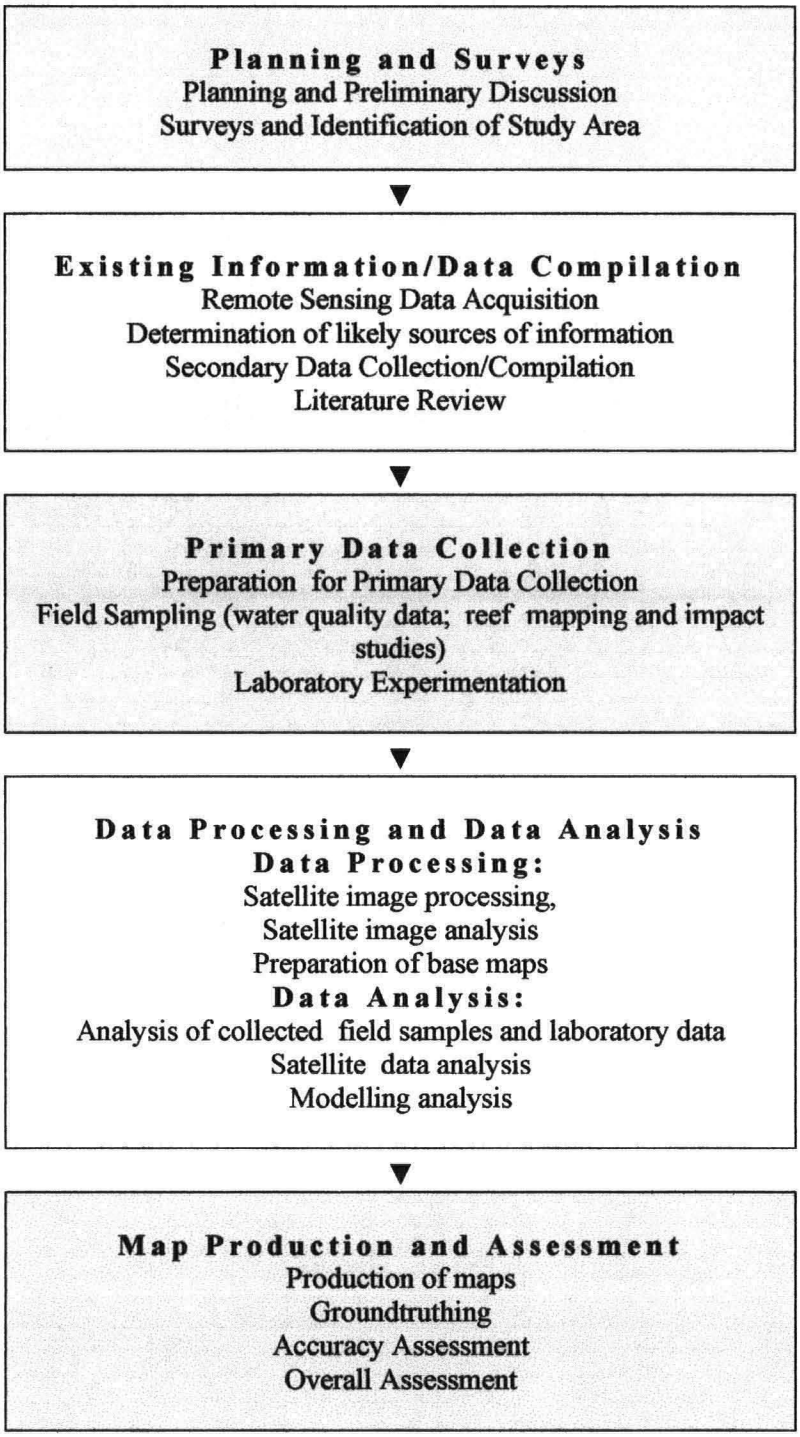

Figure 1.3. The Research Study Phases.

In the past, studies were based on statistical data analysis (Ritchie and Schiebe, 1986; Ritchie *et. al*, 1987; Curran and Novo, 1988; Ritchie and Cooper, 1988) until a radiative transfer model for temperate waters was developed by Doerffer *et al.* (1989). However, most Asian countries facing suspended particulates as the main polluter of coastal waters have not been using this remote sensing technique. Since there has been advancement in this technology, the radiative transfer

model is thought to be an appropriate method to be applied in this study. A modified version will be required since the original programme was designed specifically for temperate waters and not for the highly dynamic coastal tropical waters. Modifications will be made in this radiative transfer model to further transform the applicability of this method to the tropical coastal waters of Peninsular Malaysia. The modifications made in the radiative transfer model (the original programme) in this research study were done by Doerffer (the programmer) after having work with and getting inputs from the author.

Within a coastal ecosystem, sedimentation forms one of the primary environmental problems which affect the health of the coral ecosystem. Studies of the suspended particulates of surface waters, considered to be one of the main visible pollution indicators of the aquatic system, would provide invaluable information for impact studies and the monitoring of these complex ecosystems.

Satellite remote sensing provides an alternative means for obtaining relatively low-cost, simultaneous information on surface water conditions within a large geographic area. Previous experiments conducted by researchers (e.g. Morel, 1980; Ritchie and Schiebe, 1986; Ritchie *et. al*, 1987; Curran and Novo, 1988) have indicated that certain biological and water quality parameters have distinctive spectral characteristics. Even these limited demonstration experiments make it clear that remote sensing measurements provide critical complementary information to conventional oceanographic measurements for regional and global studies.

With the availability of remote sensing data, models or theoretical algorithms can be developed to enable the determination of water quality data over a vast area of study and predictions of suspended particulate plumes in surface waters. Development of such a model will not only provide relatively low-cost and simultaneous data but will also be very useful and applicable within the tropical waters. The use of satellite imagery to map vast areas of coastline is considered to be a valuable management tool, which will also form the basic path for future improvement of planning and management strategies.

1.10 SUMMARY

On the basis of the information collected, the world's coral in general show rapid decline as a result of environmental change. For Malaysia 87% of the reefs remain under medium and high threat. The ethical and practical dilemma we are facing now is similar to human medicine: when to discontinue heroic life-support measures for a terminally ill patient. With limited funds available for all conservation and research, the answer must be: sooner rather than later. It is time for comprehensive, objective assessment of the prospects for the coral reef ecosystem, and of the feasibility of effective human intervention.

To have assessment, monitoring, and/or restoration as objectives implies that we aim to manage coral-reef resources as we do wildlife, lacustrine fisheries, forests, or wetlands. But the complex relationships of biological environment with the physical environment make this kind of control of resource replenishment overly ambitious. Furthermore, the characteristics and the attributes of the ecosystem processes of coral reefs makes it unrealistic to expect reef systems to provide material resources for the expanding economies and human populations in the tropics. Basic biological and ecological principles make it rational to take the more successful approach in managing humans rather than reef resources. This is still not an easy task because some present economic principles such as depreciation are incompatible with sustainability, but it is feasible.

Coral reef habitats are important both biologically and economically. Our understanding of reef dynamics is based on our ability to detect biological differences, or effects, in time and space. Reefs are under increasing pressure from pollution and human-induced disturbance. There is an urgent need to locate, delineate, and determine the condition of corals at a scale that is efficient and cost effective. Due to the remote oceanic nature, large spatial extent, and relatively shallow depth of coral reefs, optical remote sensing techniques may provide valuable data on coral reef ecosystems.

With the background information collected, this study proposes to ascertain the physical water quality environment of the study area, to map the existing coral reef region within it and to measure sediment fallout rates as the primary data collection phase. Data collected particularly the TSP will be used to formulate the remote sensing algorithm. It is hoped that the combination of techniques used in this study would generate a reliable robust algorithm applicable especially to the coastal waters of Malaysia; which perhaps will be applicable too to other coastal waters within the Southeast Asia region.

Chapter 2

THE EXISTING ENVIRONMENT: THE NATURAL ECOSYSTEMS

2.1 GEOGRAPHICAL LOCATION OF THE STUDY AREA

The study site, Tanjung Rhu, is located in Pulau Langkawi ("pulau" = island), the largest island (32, 180 ha.) within Kepulauan Langkawi located at northwest Peninsular Malaysia ("kepulauan" = archipelago). This group of 44 islands is surrounded by the Straits of Melaka (Figure 2.1).

Figure 2.1: Location of the study area and control site in Pulau Langkawi, Malaysia

Kepulauan Langkawi is approximately 30 km from Kuala Perlis and 51.5 km from Kuala Kedah, the nearest mainland ports. These ports also form the main entry points to the islands.

The size of Tanjung Rhu study area was approximately 6,300ha (Figure 2.2). Tanjung Rhu, situated at northeast of Pulau Langkawi, is located within the Latitude/Longitude of N06°25.24' - N06°30.11' and E099°47.78' – E099°51.41' (UTM: E202000-209000m and N711000-720000m) (Figure 2.3).

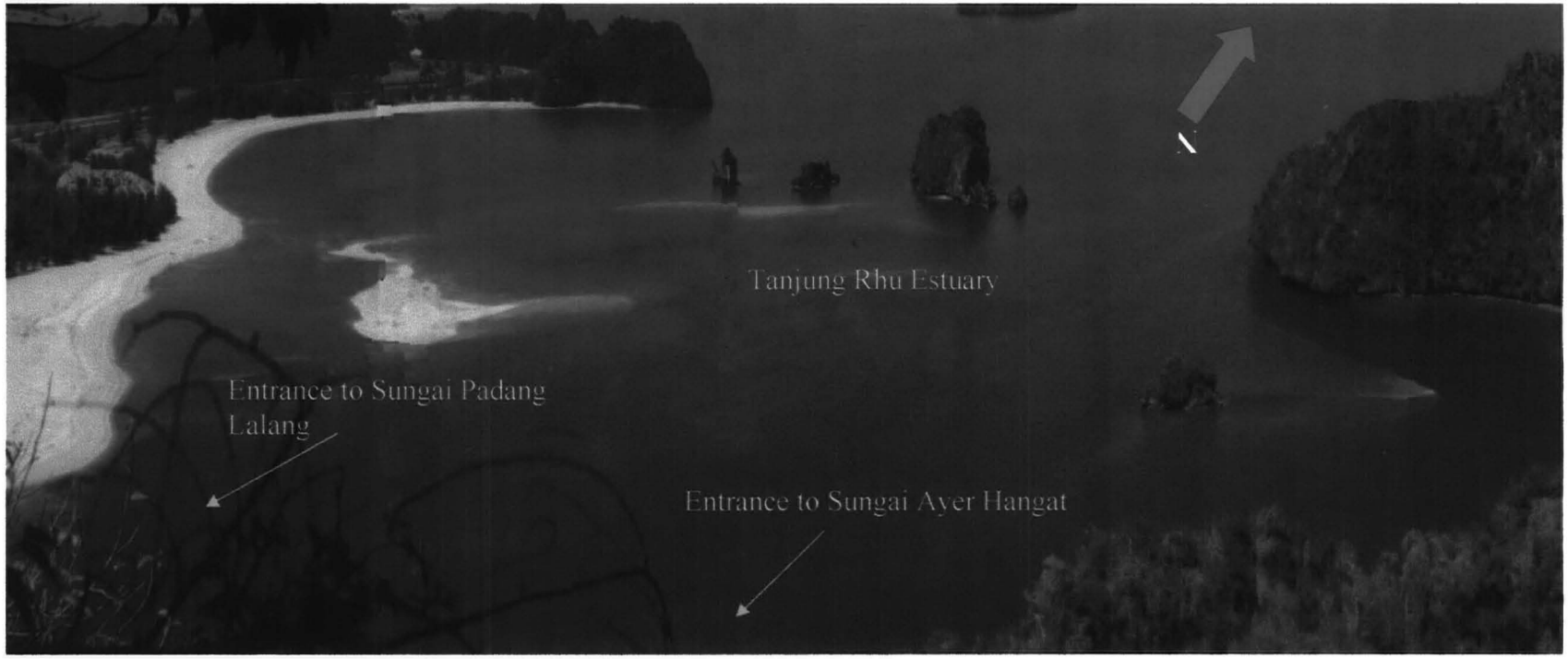

Figure 2.2: An aerial view of the study area, Tanjung Rhu, Pulau Langkawi, Malaysia.

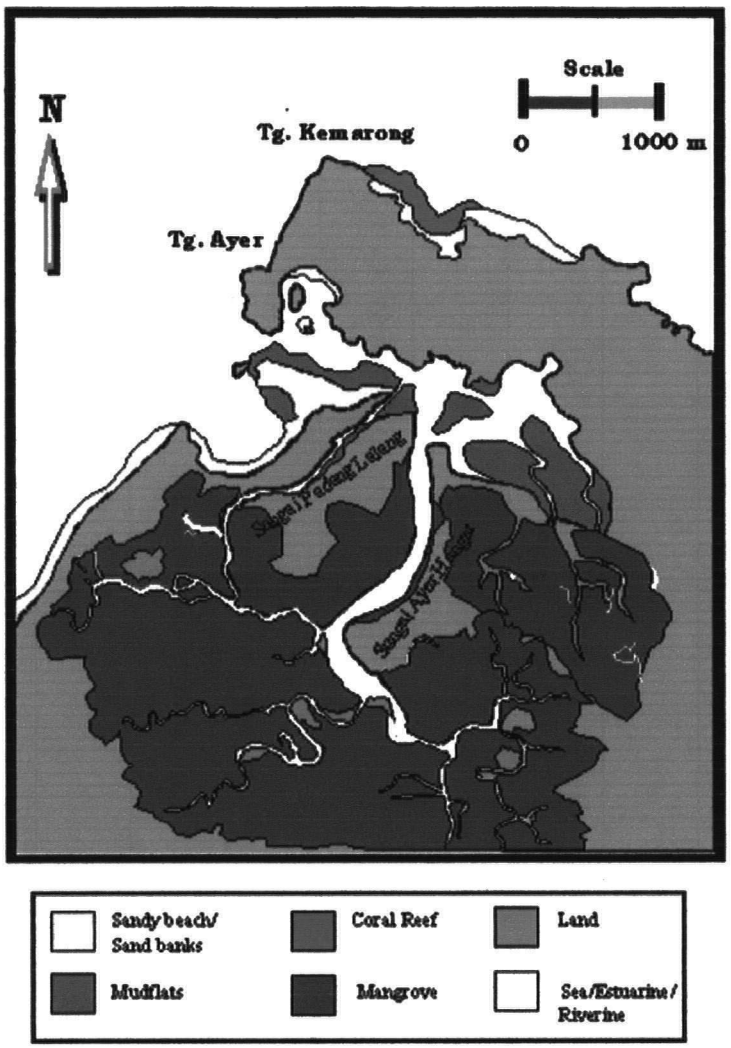

Figure 2.3: The Study Area, Tanjung Rhu, with its existing natural ecosystems.

2.2 EXISTING NATURAL ENVIRONMENT: THE PHYSICAL SYSTEM

2.2.1 Topography

The topography of Tanjung Rhu is mostly less than soft. The low area, at the central section of the study area is covered with mangrove, while the low area at the coast is dominated by casuarina and coconuts. Highland areas, consisting of mainly limestone outcrops, are found in Kuala Ayer Hangat Forest reserve (up to 250'), Tanjung Batu Kulat and south of this tanjung (up to 100').

2.2.2 Landuse

A major part of Langkawi is still in its natural state with about 57 % of the whole area being covered with forest reserves. Agriculture is the second important landuse in Langkawi accounting for 16.2%; scrubland/secondary forest with 12.8%; villages 7.1%, and swamps 2.4%. The rest are made up of other land uses such as industry, hotel/chalet, government institutions, commercial and housing. The

landuse types of Tanjung Rhu are simple. Three landuse predominates, i.e. mangrove forest, scrubland and tourism.

2.2.3 Hydrography

The shorelines of Tanjung Rhu consists of a continuous sandy beach extending from the river mouths of Sungai Padang Lalang and Sungai Ayer Hangat at the eastern part towards Tanjung Batu Kulat at the west end. The western part of the study site has a crest-shape coastline with a prominent feature in the form of a rocky headland. Towards the east there exist a massive sandspit, locally known as Tanjung Rhu sandspit, forms on the northern side of the rivers, and this remains a prominent feature of the area. This sandspit has an almost straight coastline and is generally aligned in an N 60° E direction. For most of the study area, the topography is low and flat with continuous and cyclic built-up and removal of sandy beaches and underwater sandspits on the northeastern part of the Tanjung Rhu sandspit. The river, Sungai Padang Lalang, has a moderately wide flood plain and the upper reaches are covered by mangrove forest. Sungai Ayer Hangat has a comparatively wide floodplain which is covered with lush swamp vegetations. The Tanjung Rhu sandspit, which has withstood the attack of waves so far, is covered by grass and casuarina trees.

The existing beaches have a distinctly different profile. However, both the foreshore (subject to normal tidal actions) and the backshore (reached by storm waves only) have about the same slope. The slope of the foreshore areas is considered steep at 1:10. The flood plains of Sungai Padang Lalang and Sungai Ayer Hangat lie slightly below the mean sea level (MSL) and are inundated at most parts during high tide.

2.2.4 Geology

Other than the sandspit and the mangrove areas, the remaining zone of tanjung Rhu is covered with almost vertical limestone escarpments which confer scenic beauty to the area.

The main geological formation of Tanjung Rhu is categorized by the raised sand beach, alluvial silts and clays and limestone hills. The raised sand beach is located in the spit facing the ocean and extends inland towards the northeastern part of the island. The alluvium silts and clays cover the mangrove area in the low-lying zone in the south of Tanjung Rhu and beneath the raised sands on the spit and island. Limestone hills containing near vertical cliffs can be found in the rest of the area, the largest of which is located in the southeast quadrant of Tanjung Rhu. The limestone is derived from the Setul Formation which is known to be strong rock. The rock has light to dark grey colour and is easily distinguished by its irregular rockhead with opened joints and cavities within the rock mass.

2.2.5 Coastal Environment

Tanjung Rhu is generally made up of beaches, limestone hills, intertidal flats, rivers, coastal flats, limestone islands, a sandspit, coral reefs and mangrove swamps. There beaches within Tanjung Rhu are quite stable generally except for one located immediately at the front of the narrow headland at the end of the Sungai Padang Lalang rivermouth.

Immediately offshore of Tanjung Rhu are three limestone islands which provide protection from strong waves to the beach especially towards the end of the spit. These islands are also giving protection to sediment deposited behind them and making the waters between them and the spit very shallow.

The eastern border of Tanjung Rhu is bordered by Sungai Ayer Hangat and in the middle lies the Sungai Padang Lalang which debouches at the mouth of Sungai Ayer Hangat. Sungai Padang Lalang also acts as a distributary of the main river at the southern part of the project area. Sungai Padang Lalang which runs behind the sandspit is very shallow river with mudflats and mangrove swamps along its length. The rest of the area is either made up of limestone outcrops or coastal lowland with signs of beach ridges at the back of the present beaches.

2.2.6 Water Resources and Hydrology

The tributary of Sungai Ayer Hangat joins the upstream of Sungai Padang Lalang at about 2.5 km away from its rivermouth. Studies carried out by Universiti Kebangsaan Malaysia (1995) showed that the sea water can only reach about 1 km upstream of Sungai Padang Lalang during lowest tide. Sungai Ayer Hangat is quite deep and does not dry up even during low tide. The depth of the river's cross-section near the first tributary junction was measured to be 5.2m during lowest tide.

The well-formed limestone escarpments that surround Tanjung Rhu have a big opening facing the sea in the north frontier. The boundary at the northern border is dynamically interacting with sea water. The exposed land that contracts and expands as the tide level changes may cover an area of up to 40 ha. These changes of land size markedly alter the appearance of the area.

The river water within and adjacent to Tanjung Rhu appears to be entirely influenced by tidal without runoff of freshwater during dry season. Sungai Padang Lalang is a fairly shallow river that flows between the sand spit and the limestone hill island. The widths of the river vary between 30 m and 180 m during low and high water respectively; the depth varies between 0.5m to 3 m respectively during low and high water. Sungai Ayer Hangat is moderately deep and drains most of the watershed area of Tanjung Rhu. The bay near the sand spit is generally shallow and is protected against sea

breeze. Towards the eastern part of the bay is an area of fairly deep water with shifted sand that extends to the Sungai Ayer Hangat river mouth.

2.3 EXISTING NATURAL ENVIRONMENT: THE BIOLOGICAL SYSTEM

2.3.1 Flora and Fauna

There are 4 main vegetation types in Tanjung Rhu and these are:

(i) Strand vegetation

This develops on and just behind marine beaches. The most characteristic species are the *Casuarina equisetifolia* (Rhu) and *Terminalia cattapa* (Ketapang) which occur naturally or are introduced into the area for protection from beach erosion and also as wind breakers.

(ii) Lowland Scrub vegetation

The lowland vegetation comprises one of the least important vegetation types notably *Axonopus compressus, Melastoma malabathricum, Ficus* sp. and *Chyropogon aciculatus.* Ecologically the sandy lowland is a harsh environment and probably contains poor faunistic and floristic elements compared to other habitats within Tanjung Rhu.

(iii) Lowland Swamp Forest (Mangrove Forest)

The mangrove forests are essentially similar to mangrove areas found throughout Malaysia and occur on tidal flats along the protected bays and on the banks of the two rivers. Further details of this forest are described in subsection 2.3.2.2 of this chapter.

(iv) Limestone Hill Forest

The vegetation of the limestone forest of Tanjung Rhu is still in its primary state. The vegetation is often stunted and reduced due to the prolonged dry season, the proximity to the sea and the poor water holding capacity of the limestones. Only in the area sheltered from the wind is the vegetation more luxuriant with a denser growth of larger trees. Many of the species found in the Langkawi limestones are not found on limestone further south of the mainland and some are endemic to the project area which include *Cycas siamensis, Euphorbia antiquorum, Grewia viminea, Hopea ferrea, Pentacme siamensis,* and *Diospyros ferrea.*

2.3.2 Coastal Habitat

There are several coastal habitats existing in Tanjung Rhu natural ecosystems (Figure 2.4). These habitats are:

1. River-Estuary
2. Mangrove

3. Coral reefs
4. Other intertidal habitats

2.3.2.1 River-Estuary

River

Rivers and streams can be simply defined as bodies of water flowing in an open channel (Summerfield, 1998). They have three important roles in landscape creation: they erode the channels in which they flow, they transport sediments and solutes provided by weathering and slope processes as well as by the other denudational agents, and they produce a wide range of erosional and depositional landforms. River systems are the primary agents of erosion, transportation and deposition in most landscapes, including many where surface water is not present for most of the time.

Fluvial systems can for convenience be regarded as consisting of three main elements: a zone of sediment production, a zone of sediment transfer and a zone of sediment deposition. This categorization is, of course, over-simplified because some erosion, transport and deposition occur in all three zones. Nevertheless, within each zone one of these three processes is usually dominant.

Estuary

Depending on the immediate point of view, an estuary can be defined in various ways. For most oceanographers, natural scientists and engineers, estuaries are defined as 'areas of interaction between fresh and salt water' (Dyer, 1973). The definition most commonly adopted is that of Cameron and Pritchard (1963) who state that '*An estuary is a semi-enclosed coastal body of water which has a free connection with the open sea and within which sea water is measurably diluted with fresh water derived from land drainage*'. Pritchard (1952b) included the terms positive estuaries and negative estuaries. Pritchard (1952b) defined a positive estuary as an estuary where fresh water inflow derived from river discharge and precipitation exceeds the outflow caused by evaporation, and therefore surface salinities are consequently lower within the estuary than in the open sea. Negative estuaries are those where evaporation exceeds river flow plus precipitation and hypersaline conditions exist.

Another commonly used definition for an estuary is given by Thurman & Trujillo (1999) stating that '*An estuary is a partially enclosed body of water where incoming seawater is mixed with freshwater coming from the land*'. Estuaries are very fragile because of the delicate combination of fresh and salt water. A small disturbance in the habitat can have serious repercussions. Because of the difference in density between fresh and salt water, salt water will move into the estuary along

the bottom, while freshwater will flow downstream to the ocean along the surface. This caused a layered condition.

The interaction of fresh and salt water provides a circulation of water and mixing processes that are driven by the density differences between the two waters. The density of seawater depends on both the salinity and temperature, but in estuaries the salinity range is large and the temperature range is generally small. Consequently temperature has a relatively small influence on the density and there is little information published on temperature fluctuations in estuaries. Many tropical estuaries have little river flow entering them during the hot season. Surface heating could then provide sufficient density difference between the estuary and the sea to maintain a gravitational circulation. Because of the diurnal variation of temperature, however, these effects would be transitory.

Estuaries are formed in the narrow boundary zone between the sea and the land and their life is generally short. Their forms and extent are being constantly altered by erosion and deposition of sediment and drastic effects are caused by a small raising or lowering of sea level. Estuaries have probably been extremely important in the world's development though they are a particularly ephemeral feature of the earth's surface. They have generally high inflows of nutrients from the land, but, because of their range of conditions, tend to have a lesser diversity of life than other aquatic environments. As freshwater meets the ocean, both land and ocean contribute to a beautiful and fragile ecosystem of specialized plants and animals. Individual species are numerous, but are specialised and often tolerant to large extremes of temperature and salinity.

An estuary provides:

1. *A place to live*: estuaries contain lots of potential food sources for animals or organisms that live in them full time
2. *A nursery ground for marine organisms*: many marine organisms depend on estuaries at some point during their development. Some fish only use estuaries at certain times of the year, while others use the natural protection for laying of eggs. Most commercially valuable fish and shellfish spawn, nurse, or feed in estuaries.
3. *A water filtration system*: rivers often contain lots of sediment, nutrients and pollutants. Estuaries remove sediments and nutrients before they reach the ocean. Otherwise, valuable topsoil and nutrients will be flushed into the open seas where they could not be used again. Salt marshes and the grass blades found in many estuaries filter out much of the sediment and nutrients. Estuaries, in fact, filter the water and create cleaner water. Water draining off the uplands carries a load of sediments and nutrients. As the water flows through salt marsh, peat

and the dense mesh of marsh grass blades, much of the sediment and nutrient load is filtered out. This filtration process creates cleaner and clearer water.

4. *A flood and storm control*: Salt marsh dominated estuaries act as natural buffers between the land and the ocean. Porous, resilient salt marsh soils and grasses absorb flood waters and dissipate storm surges. Like barrier islands, they protect the mainland and people from the brunt of heavy storms. So estuaries help protect human lives, upland animals, and billion of dollars of real estates.
5. *Food source*: a pristine estuary can produce 4 to 10 times the weight of food for aquatic animals than can be produced by a corn field of the same size.

Because of their fertile waters, sheltered anchorages and the navigational access they provide to a broad hinterland, estuaries have been the main centre of man's development. Deforestation of the land leads to increased run-off from the land, increased aperiodic discharge and increased sediment load in the rivers. Building and paving of large areas also produce a quick response of run-off to rainfall. Maintenance of river flow at a set level to control such effects (e.g. building of dams) will decrease the natural tendency for rivers to flush sediments out of their estuaries and consequently may aggravate shoaling problems. Deepening of the estuary by dredging will increase the estuary volume and reclamation of intertidal areas will decrease the tidal flow, alter the mixing process and circulation patterns and perhaps decreases the flushing time of the estuary.

2.3.2.2 Mangrove

Mangroves occupy the tropical and subtropical habitat equivalents of the saltmarshes of more temperate regions. Mangrove stands are dominated by woody species which, under optimal conditions, may form tall closed forest with the canopy trees more than 30m tall. Other mangrove stands are low shrub thickets, differing little in structure from communities dominated by the taller shrubby saltmarsh vegetation.

The mangrove flora consists of two phytogeographically distinct groups. One is restricted to the Indian Ocean and West Pacific, while the other and much smaller group of species, occurs in the Atlantic and on the west coast of South America (Chapman, 1962).

Taxonomically, the mangrove flora is diverse, with representatives from a number of different families (some 70 species in 20 families). The latitudinal limits of mangroves are generally regarded as being determined by the intolerance of most species to frost. Mangroves are best developed where the average temperature of the coldest month is above 20°C and the seasonal temperature range is 5°C or less. Although mangroves can withstand frequent tidal flooding and

tolerate soil salinities as high as that of seawater, in general they do not seem to tolerate hypersaline conditions. Except in the upper estuary or in sites influenced by percolating groundwater, soil salinities towards the landward edge of mangroves may reach high values. The success of mangroves within the tropics and the taxonomic diversity of the mangrove flora indicates that a range of families posses the ability to evolve tolerance of these conditions. The essential features of the mangrove habitat are generally high but variable (e.g. soil salinity and a poorly drained and frequently anaerobic substrate).

2.3.2.3 Coral Reefs

In the tropics, the shallow inshore waters are dominated by the formation of coral reefs and they are often used to define the limits of the tropical marine environment. Coral reefs are unique among marine associations or communities in that they are built up entirely by biological activity.

Hermatypic corals, such as those found in Tanjung Rhu study area, grow actively on the reef crest and face where the reef is growing seaward and upward or toward the sea surface. Though not responsible for the formation of reefs, the non-hermatypic corals may still be valuable as substrate and may provide the basis for diverse and productive communities. These species are found both inshore and in deeper waters and often are valuable in the formation of sediment substrates, including beaches and shoals.

Coral reefs are recognized as occurring in a number of major morphological, or structural, types. Fringing or shore reefs are the most common and widespread of the reef structural types. Such is the type of reef found at the study area of Tanjung Rhu where there is extensive exposure of the intertidal reef flat. They occur in the nearshore environment and are best developed along rocky coasts of uplifted continental coastlines and islands as well as along shores of exposed limestone islands where there is a firm substrate. Their inshore distribution renders them susceptible to coastal activities, more so than other reef structural types. Fringing reefs are nearly always found below the low-tide level, but extensive intertidal exposure forming broad tidal flats is known to occur in areas where there are moderate to large tides.

2.3.2.4 Other Intertidal Habitats

Mudflats, sandy beaches and rock shores are the remaining existing habitats found in Tanjung Rhu natural ecosystems.

The quite extensive mudflats within Tanjung Rhu study area are found along the Sungai Padang Lalang ("sungai" = river) river mouth and the Tanjung Rhu estuary. At some locations these

mudflats are fully exposed during low water at spring tide. Exposure of these mudflats could occur for up to 2 hours depending on the tidal range. Various organisms are normally found to be very active during the exposure especially of mudcrabs and the fiddler crabs. One of the common shells found in abundance here belonging to the Cerithideidae family is *Cerithidea cingulata*. A common name for it is 'girled horn shells'. The species of this genus usually live on the soft bottom mudflats of mangrove areas called the infralittoral zone.

Sandy beaches are found along most of the coastlines within the Tanjung Rhu study area. The exceptional areas are the small sporadic rocky shores and the entrance to the estuary. A small patch of mudflat is found at the extensive sandbanks found at Pantai Tanjung Rhu ("pantai" = beach). Here mussel beds are found on the mudflat patch. These can only be seen during low waters of spring tides. Stretches of sandy beaches are found along Teluk Dedap and Pasir Panjang which are located on the western side of the study area. Narrower and shorter sandy beaches are found here compared to the beaches of Pantai Tanjung Rhu.

On the rocky shoreline areas of Tanjung Rhu, huge boulders are common sights among steep cliffs. Layers of rock formation during different geological periods are also seen from this rocky area. The lower rocky coast which is the rocky intertidal zone generally exhibit distinct zones of high-tide area, barnacle or mussel zone and algae or seaweed areas (low-tide area). These zones are differentiated by the clear markings on the rock.

2.4 THE CONTROL SITE: TELUK DATAI

The control site for this study is Teluk Datai which is located at the northwest of Pulau Langkawi (Figure 2.4). Teluk Datai was seen as an appropriate control site for this study mainly because it has similar existing natural ecosystems as those found within the study area of Tanjung Rhu. The differences lie within the absence of riverine-estuarine system and the mangroves. However, Teluk Datai is surrounded by a forest reserve, the Machinchang Forest. The condition of the surrounding habitats of Teluk Datai is well maintained and is still pristine.

The major difference between the control site and the study area is that in Teluk Datai, coastal development has completely stopped since 1995. Part of this area had undergone heavy tourism-related infrastructure development between 1989 until 1992. Prior to that this segment underwent land clearings and leveling which alters the natural landscape. However, these activities no longer posed an environmental problem since there has been vegetation re-plantation and turfing.

Figure 2.4: The control site, Teluk Datai, Pulau Langkawi. View taken during low water spring tide exposing the coral boulders at the reef flat zone.

2.5 SUMMARY

Tanjung Rhu (the study area) and Teluk Datai (the control site) are considered the most spectacular sites on Pulau Langkawi in terms of coastal scenery, terrain, flora and forestry. These sites feature a spectacular combination of widespread beaches, outlying islands, mountain facade and ocean islets. These sites have varied natural topographical features comprising of sensitive habitats such as coral reefs, mangrove swamps, large natural vegetation, limestone outcrops on steep slopes, and a network of riverine-estuarine system. Since these areas are primarily considered to be still in their pristine condition, the State Government has assigned the task of overseeing the preservation of the natural environment during development to Langkawi stressing on the preservation of the natural environment and landscape, keeping in line with the Langkawi Declaration on Environment to transform the island into a "nature paradise". Known to be blessed with an unspoiled beautiful environment and an outstanding natural landscape, Langkawi is the most likely to become the regional hub for development between the Indonesia Malaysia, and Thailand Growth Triangle (IMT-GT). It would therefore be of crucial importance to ascertain the status of the environment on a continuous basis incorporating monitoring and environmental assessment programs in order to preserve its existing sensitive ecosystems.

Chapter 3

THE RIVERINE-ESTUARINE WATER QUALITY OF TANJUNG RHU

3.1 LITERATURE REVIEW

3.1.1 Introduction

Pollutants are basically of two types i.e. *primary pollutants* and *secondary pollutants*. Primary pollutants exert harmful effects in the form in which they enter the environment. Secondary pollutants which are synthesized as a result of chemical processes, often from less harmful precursors, in the environment. Although highly toxic substances are responsible for many cases of environmental pollution, under some circumstances materials which are normally considered harmless may cause pollution if they are present in excessive quantities or in the wrong place at the wrong time.

In all cases of pollution there is (1) a source of pollutants, (2) the pollutants themselves, (3) the transport medium (air, water or direct dumping onto land), and (4) the target (or receptor) which includes ecosystems, individual organisms (e.g. humans) and structures. These are shown in Figure 3.1. Pollution can be classified in several ways according to (1) the source (e.g. industrial pollution or agricultural pollution), (2) the media affected (e.g. air pollution or water pollution) or (3) by the nature of the pollutant (e.g. chemical pollution).

Figure 3.1: A simplified model of environmental pollution (from Holdgate, 1979)

Sources of pollutants can either be discrete point sources or diffuse sources (non-point sources). Pollutants have certain intrinsic properties that determine the likely effect that they will have after emission or discharge into the environment. Holdgate (1979) divided these into two types: effect generating properties, such as toxicity in living organisms or corrosion of metals, and pathway determining properties which determine the distance and the rate of dispersion of the pollutant in the environment.

3.1.2 Water Quality Parameters

This chapter focuses only on the physical water quality parameters, particularly Total Suspended Particulates (TSP) and turbidity. This is because, prior to this research, a short study was conducted and published by the author and the Reef Research Group from Universiti Sains Malaysia to ascertain the water quality problem of the study area, Tanjung Rhu. Three groups of water quality parameters (Table 3.1) were studied based on the requirements of the Department of Environment (DOE) Malaysia, namely physical, chemical and biological parameters. Studies were carried out on a monthly basis for a 12-month period commencing in January 1997 until December 1997. Results from the study showed that all water quality parameters measured did not exceed the permissible limit set by the DOE Malaysia except TSP. Turbidity is discussed here because, like TSP, it can alter light paths when present in the water column.

3.1.2.1 Total Suspended Particulates

Total Suspended Particulates (TSP) are comprised of settleable, floating, and non-soluble (colloidal suspension) components. TSP generally contains an inorganic fraction (silts, clays, etc.) and an organic fraction (algae, zooplankton, bacteria, and detritus) that are carried along by water as it runs off the land. The inorganic portion is usually considerably higher than the organic. Both contribute to turbidity, or cloudiness of the water. Waters with high sediment loads are very obvious because of their "muddy" appearance. This is especially evident in rivers, where the force of moving water keeps the sediment particles suspended. When these suspended particles settle to the bottom of a water body, they become sediments. TSP can be extremely variable, ranging from less than 5 mg/L to extremes of 30,000 mg/L in some rivers. TSP is not only an important measure of erosion in river basins; it is also closely linked to the transport of nutrients (especially phosphorus), metals, and a wide range of industrial and agricultural chemicals (Gower, 1980).

In most rivers, TSP is primarily composed of small mineral particles. TSP is often referred to as 'turbidity' and is frequently poorly measured. TSP-levels and fluctuations influence aquatic life, from phytoplankton to fish. TSP, especially when the individual particles are small (< 63μm), carry many substances that are harmful or toxic. As a result, suspended particles are often the primary carrier of these pollutants to estuaries and to coastal zones of oceans where they settle.

Table 3.1: Malaysian Department of Environment Standards/Permissible Levels for Water Quality Parameters (Source: Malaysian Department of Environment, 1990)

	Standard/Permissible Level
Physical Parameters:	
Dissolved Oxygen	NA
Temperature	40°C
Salinity	NA
Turbidity	50 FTU
pH	6.0 - 9.0
Total Suspended Particulates	50 mg/L
Chemical Parameters:	
Biological Oxygen Demand	20 mg/L
Chemical Oxygen Demand	50 mg/L
Ammoniacal Nitrogen	NA
Nitrate	10 mg/L
Phosphate	0/6 mg/L (Class IIA/IIB)
Copper	0.20 ppm
Lead	0.10 ppm
Zinc	1.0 ppm
Iron	1.0 ppm
Mercury	0.005 ppm
Chromium	0.20 ppm
Cadmium	0.01 ppm
Oil and Grease	0 ppm
Biological Parameter:	
Faecal Coliform	0 CFU/100ml

NA : *Not Available*
Class IIA : *Direct Contact Recreational Waters*
Class IIB : *Non-recreational Waters*

Environmental Impact: TSP can clog fish gills, either killing them or reducing their growth rate. They also reduce light penetration, reducing the ability of algae and other photosynthetic organisms to produce food and oxygen. When the water slows down, the suspended sediment settles out and drops

to the bottom, a process called siltation. This causes the water to clear, but as the silt or sediment settles it may change the bottom. The silt may smother bottom-dwelling organisms, cover breeding areas, and smother eggs.

Indirectly, the suspended solids affect other parameters such as temperature and dissolved oxygen. Because of the greater heat absorbency of the particulate matter, the surface water becomes warmer and this tends to stabilize the stratification (layering) in stream pools, embayments, and reservoirs. This, in turn, interferes with mixing, decreasing the dispersion of oxygen and nutrients to deeper layers.

3.1.2.2 Turbidity

Turbidity is a unit of measurement quantifying the degree to which light travelling through a water column is scattered by the suspended solids. Light scattering increases with increasing suspended load. Turbidity is often largely due to suspended sediment in the water column, particularly originating from anthropogenic activities. Turbidity is commonly measured in Nephelometric Turbidity Units (NTU), but may also be measured in Jackson Turbidity Units (JTU).

The velocity of the water resource largely determines the composition of the suspended load. Suspended loads are carried in both the gentle currents of lentic waters and the fast currents of lotic waters. Even in flowing waters, the suspended load usually consists of grains less than 0.5 mm in diameter (Table 3.2). Suspended loads in lentic waters usually consist of the smallest sediment fractions, such as silt and clay (Dunne and Leopold, 1978).

Table 3.2: Size Classification of sediments (Adapted from Friedman *et al.*, 1992)

Sediment class	Size (mm)
Sand	
Very Coarse	1.5
Medium	0.375
Very Fine	0.094
Silt	
Very Coarse	0.047
Medium	0.0117 (no longer visible to the human eye)
Very Fine	0.0049
Clay	< 0.00195

Environmental Effects: The series of turbidity-induced changes that can occur in a water body may change the composition of an aquatic community (Wilber, 1983). First, turbidity due to a large volume of suspended sediment will reduce light penetration, thereby suppressing photosynthetic activity of phytoplankton, algae, and macrophytes, especially those farther from the surface. If turbidity is largely due to algae, light will not penetrate very far into the water, and primary production will be limited to the uppermost layers of water. Cyanobacteria (blue-green algae) are favoured in this situation because they possess flotation mechanisms (McCabe and Sandretto, 1985). Overall, excess turbidity leads to fewer photosynthetic organisms available to serve as food sources for invertebrates. As a result, overall invertebrate numbers may also decline, which may adversely affect fish populations.

3.2 DESCRIPTION OF TIDAL FLOW OF TANJUNG RHU

3.2.1 Tidal condition

Tanjung Rhu is fronted by the Straits of Malacca and the Andaman Sea. The tides are semi-diurnal. Table 3.3 summarizes the various tidal elevations for the area.

Table 3.3: Summary of Tidal Elevations of Tanjung Rhu. (Source: Tide Prediction Tables of 1997, Department of Hydrography, The Royal Malaysian Navy).

Tide	Level (m) ACD
Highest Astronomical Tide (HAT)	3.8
Mean High High Water (MHHW)	3.1
Mean Low High Water (MLHW)	2.2
Mean Sea Level (MSL)	1.9
Mean High Low Water (MHLW)	1.5
Mean Low Low Water (MLLW)	0.6
Lowest Astronomical Tide (LAT)	0.0

From Table 3.3, it may be inferred that the study area has a significant spring tide range of 2.45 m. However, it must be emphasized that the tide levels above are only predicted results and in reality these may differ by a certain percentage primarily due to astronomical tides which can be observed only through actual site measurements. However, to a certain degree, the fluctuations are also the outcome of tidal impact resulting from the interaction between waves and river flows, and the effect of the landlocked nature of the water in the area. In addition, water level fluctuations near the site may also be affected by meteorological phenomenon such as storm surges and wave set-up/down. Nonetheless, in this area, these two events are not too significant since the storms are generally weak (*i.e.* the site is a

sheltered area) and the waves have moderate energy. Studies by UKM (1995) estimated wave set-up/down to be at about 0.04 m while storm surges along the west coast of Peninsular Malaysia were estimated to be relatively low.

3.2.2 Currents

There are four types of currents generated in the Straits of Malacca. These are:

(i) longshore currents

(ii) tidal currents which are generated solely by tides

(iii) surface currents, and

(iv) currents generated by discharges from rivers.

Ocean currents in the Straits of Malacca flow northerly from Singapore to the Andaman Sea and along Sumatera throughout the year. However, during the northeast monsoon season, ocean currents off the Perlis coast change direction, and southerly currents appear seasonally along the coast of the Peninsular.

Localised current characteristics along the northern coastlines and bays of Pulau Langkawi are complex due to the geography, bathymetry and seasonal ocean current variations. A review of the limited information available on ocean currents in the bay of Tanjung Rhu has revealed that the currents are predominantly tide generated and are reversing in direction with the flood and ebb tides. These characteristics are further complicated by the presence of river discharges from Sungai Ayer Hangat and Sungai Padang Lalang.

Previous studies (UKM, 1995) have indicated that littoral drift is usually responsible for moving suspended particles in constricted bays – this is a similar situation for Tanjung Rhu. Littoral drift is the wave breaking at an angle to shore and subsequently moving along the shore carrying beach material. Incoming waves are responsible for generating longshore transport and suspension of sediments within the limit of the surf zone. Once the suspended particles are transported beyond the surf zone, the tidal current is then responsible for moving the particles/sediments further offshore; thus, causing coastal erosion. This effect is more pronounced during ebb tide when the water retreats offshore. At the river mouth, the current generation process is further complicated by the presence of river discharges, and is further affected by the offshore and/or nearshore bathymetry and coastal configuration. The surface currents generated by winds are not significant in Tanjung Rhu. This is because the area is a narrow strip and has a relatively shallow depth of water.

The current patterns within the Tanjung Rhu, obtained from previous investigations by UKM (1995) are discussed in the succeeding paragraphs.

(i) River mouth current pattern

The flow pattern in the river mouth is cyclic or reversal corresponding to the tide cycles. During the ebb, the water movement is towards the bay (northwest direction), occurring 40% of the time of the tide cycle. During flood tides, the movement is towards the estuary and occurs almost 45% of the tide cycle. Studies by UKM (1995) have revealed that maximum current speed of Tanjung Rhu is 0.8 m/s, with a mean of approximately 0.45.

(ii) Current pattern within the bay

The current patterns within the enclosed bay of Tanjung Rhu are shown in Figures 3.2 and 3.3. These correspond with the conditions during the ebb and flood tides respectively. The directions of flow shown in both figures are the generalised ebb and flood tide circulation patterns.

Existing records by UKM (1995) reported that the circulation of currents within Tanjung Rhu is affected by tidal fluctuations. In the vicinity of the estuary, the current pattern during each tidal cycle is significantly influenced by the large amount of inflow and outflow of the river discharge. During ebb tide, the discharge of water flowing out through the river mouth generates strong undercurrents and these affect the flow patterns in the entire bay area.

During low tides, the main course of the river flow is through the deep channel extending seaward from the river mouth of Sungai Ayer Hangat (Figure 3.4). However, overflowing from the river across the riverbank or sandspit also occur. This is due to the inability of the river mouth (because of the configuration and bathymetry) to contain the entire retreating flow from the estuary, and the rivers of Sungai Padang Lalang and Sungai Ayer Hangat. Consequently a large portion of the flow moves seaward across the relatively shallow part of the bay.

The synoptic flow pattern within Tanjung Rhu during flood tide is almost identical to the generated ebb circulation – in the sense that it is strongly influenced by river discharges. In the western half of the bay, the offshore currents are reversing its flow direction with the flood current approaching from the southwest and northwest directions during flood tide. The seabed and topographical features within the bay contributed towards the formation of flow patterns. During the early stages of the flood tide, the sandbars are exposed and act as barriers to the flow. Most of the flow movement during this time is towards the river mouth via northern deep channel. As a result, the bay area, located east of the offshore island, has a strong inflow of water. The flow within the west-end crescent bay is therefore

relatively weak. During the last stages of the flood tidal cycle, the seabed features offer little resistance and the flow intruding from the west of the bay towards the river mouth attains the same speed as that in the northern deep channel.

Figure 3.3: Generalized Flood Tide Circulation Pattern. (Source: UKM, 1995)

Figure 3.4: The Flow Regime at the Rivermouth-Estuarine of Tanjung Rhu. (Source: UKM, 1995)

It should also be borne in mind that since 1982, several major changes have taken place in the proximity of Tanjung Rhu. These changes have had a direct influence on the river discharges and wave patterns. Similarly, during the same period, the Tanjung Rhu sandspit and the nearby sandbars have changed their shape and location, and these too have had an effect on the current patterns.

Overall, the current patterns in Tanjung Rhu may be simplified as follows: the flow during flood tide enters the inlet of Tanjung Rhu just north of the spit. Behind this inlet there is a lagoon which stores water during this period. The water from the flood tide is also sorted in the rivers and mangrove swamps, of which the swamps can store a significant amount of water. During ebb tide, the stored water is released. Since the amount of water is larger and the opening at the northern end of the

Tanjung Rhu sandspit is constricted, the water rushes seaward through this small opening. As a result, strong currents with high speeds of around 1 m/s are generated. The cross-sectional profile of the opening or inlet at the northern end of the sandspit is in a state of equilibrium. This is due to the combined effect of littoral drift (which builds the sandspit) and strong currents (which erode the sandspit).

3.3 SAMPLING METHODOLOGY

This section discusses the sampling methodologies used for water quality measurements on a monthly basis.

Results of monthly water quality monitoring data collected and published by the author and Reef Research Group (Universiti Sains Malaysia) were used in this study. A copy of the published work (Abdullah and Yasin, 2000) is attached in Appendix 3. The following subsections 3.3.1 and 3.3.2 were written based on the author's published work. In this study only measurements of the physical parameters were referred to *i.e.* TSP, dissolved oxygen (DO), salinity, pH and turbidity.

Water quality data collections (measurements and analysis) during all samplings were conducted by the author. Assistance from members of the Reef Research Group (Universiti Sains Malaysia) was also sought during these times.

The water quality of the control site, Teluk Datai, was not measured during this study. This was because the water quality condition in the area was assumed not to have significantly changed. This was based on previous water quality data collected in 1985, 1989 and 1994 (Lee, 1994) during which time the control site was experiencing heavy coastal developmental pressure between 1989 and 1992. Coastal development had since stopped in 1995. Measured levels of the water quality parameters showed values that were well below the DOE permissible limit. A summary of the marine water quality of Teluk Datai is given in Appendix 4.

3.3.1 Water Quality Field Sampling Methodology

There were 10 sampling points selected for water quality sampling for the riverine-estuarine of Tanjung Rhu (Figure 3.5). In general, the sampling methodology adopted which includes sampling techniques, containers and preservation methods were based on those recommended by APHA (1985) or UNESCO (1985). The following approaches were adopted during sampling:

1. water samples, wherever possible, were taken close to or at the middle of the river;

2. water samples were collected approximately 0.5m below the water surface except for shallow waters;
3. all sample bottles were rinsed thoroughly with river water or sea water (depending on sampling location) before water samples were collected.

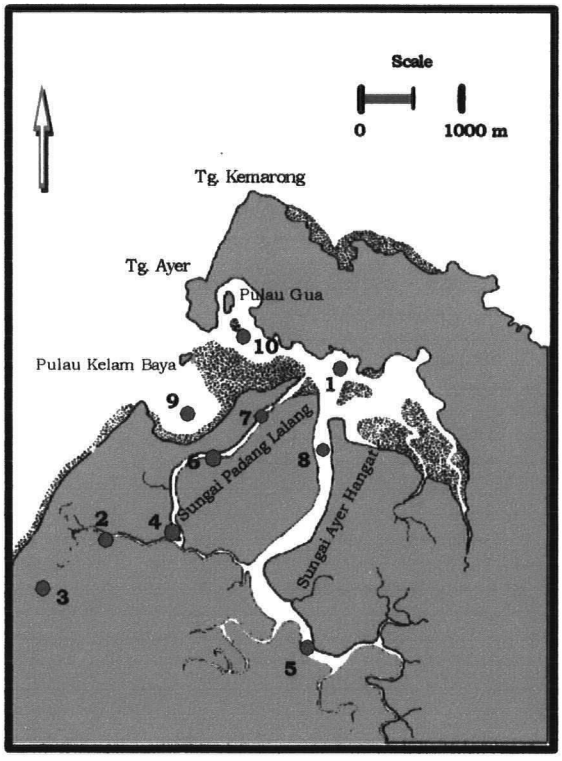

Station	Description	Position
1	Inner Main Estuary (Teluk Udang)	N 06° 27' 38.5" E 99° 49' 42.2"
2	Proposed Equestrian centre outlet	N 06° 26' 40.6" E 99° 48' 38.3"
3	Proposed Culvert near staff quarters	N 06° 26' 28.3" E 99° 48' 58.3"
4	Upstream Sungai Padang Lalang	N 06° 26' 38.3" E 99° 49' 09.1"
5	Upstream Sungai Air Hangat	N 06° 26' 13.0" E 99° 49' 37.8"
6	Downstream Sungai Padang Lalang	N 06° 27' 00.8" E 99° 49' 15.0"
7	Hotel Discharge Drain	N 06° 27' 16.6" E 99° 49' 36.6"
8	Downstream Sungai Air Hangat (estuary)	N 06° 27' 13.3" E 99° 49' 37.5"
9	Hotel Front	N 06° 27' 25.0" E 99° 49' 23.3"
10	Main estuary	N 06° 27' 42.2" E 99° 49' 29.7"

Figure 3.5: Location of monthly water quality sampling stations for Tanjung Rhu riverine-estuarine.

3.3.2 Monthly water quality sampling methodology

The water quality monitoring was carried out on a monthly basis from January 1997 until December 1997. A summary of the sampling dates with their corresponding tidal conditions were shown in Table 3.4. Predicted tides were relied on in this study because Tanjung Rhu is located at a distance of approximately 4 km from Teluk Ewa which is one of the standard tidal stations for tidal elevation measurements of the Department of Hydrography in the Royal Malaysian Navy.

Laboratory Analysis

Total Suspended Particulates (TSP)

Samples collected for TSP analyses were kept in an ice box immediately after sampling in polypropylene or polyethylene bottles and transported to the laboratory where filtrations and analyses

were carried out immediately. The APHA Method 2540D is employed for the determination of TSP level in the water samples. A volume of 500ml of water sample is filtered through a 0.45 μm pore size WHATMAN white plain cellulose nitrate membrane filter and dried at 105°C until a constant weight is achieved. The amount of TSP is then calculated in milligrams per litre unit. The mean amount of TSP and standard variations were calculated based on 3 replicates for each sampling point.

Table 3.4: Summary of Tanjung Rhu Monthly Water Quality Sampling Conditions for 1997.

Sampling Date	Tidal Condition	Tidal Height (m)	Tidal Flow During Sampling
28 January 1997	Spring	0.5 - 2.7	Flooding
28 February 1997	Spring	0.6 - 2.7	Flooding
31 March 1997	Mid-tide	1.3 - 2.3	Flooding
16 April 1997	Spring	2.0 - 1.7	Flooding
18 May 1997	Spring	1.2 - 2.9	Ebbing
20 June 1997	Spring	0.7 - 3.3	Ebbing
22 July 1997	Spring	0.6 -3.4	Flooding
23 August 1997	Spring	0.7 - 2.9	Flooding
24 September 1997	Neap	1.5 - 2.0	Flooding
26 October 1997	Mid-Tide	1.3 - 2.4	Ebbing
27 November 1997	Spring	1.0 - 2.7	Ebbing
21 December 1997	Mid-Tide	1.1 - 2.3	Flooding

Note: *Sampling hour falls between 0900hr to 1600hr*

In-Situ Measurements

For the following measurements, three replicates of readings were taken for each sample collected or at each sampling location. The means and standard deviations were then calculated.

Dissolved Oxygen

Dissolved oxygen (DO) content of the river water is measured using a YSI Salinity compensated DO meter with a 0.05mg/L precision. The probe is lowered into the river or seawater at 0.5m depth and readings were taken after steady values were obtained. The DO meter has been pre-calibrated against ambient saturated air as recommended by the instrument manual in the laboratory and re-checked in the field prior to each measurement.

Salinity

The salinity of the river and the sea were measured using an ATAGO hand-held refractometer with a ± 0.5‰ precision that has been calibrated using distilled water. A few drops of river water or seawater were placed on the glass plate and the reading is taken directly from the view finder facing against sunlight. The glass plate is rinsed with distilled water after each use.

pH

Water samples for pH measurements were carried out using glass-calomel electrode which has been pre-calibrated using buffer standards of pH 6.98 and 9.89 at ambient temperature. The electrode is cleaned with distilled water followed by rinsing with the river water prior to actual measurements. An ORION portable pH meter with a ± 0.01 pH unit precision is used.

Turbidity

The turbidity of water samples were measured using DREL 2000 HACH kit. Water samples were read against filtered distilled water as blank through a spectrophotometer at 750nm wavelength. Levels of turbidity were read as Formadazin Turbidity Unit and this is the equivalent to the Nephelometric Turbidity Unit.

3.4 ANNUAL FLUCTUATIONS OF THE TANJUNG RHU WATER QUALITY

This section summarises the monthly riverine-estuarine water quality results measured from over a 12-month period from January 1997 to December 1997 within the study area, Tanjung Rhu.

3.4.1 RESULTS: The Physical Environment

Dissolved oxygen

Surface water dissolved oxygen (DO) levels do indicate a fluctuation pattern but this pattern is clearly observed for most sampling stations except Station 3. The monthly surface water DO for each sampling station is shown in Figure 3.6(a). Lowest DO level (1.39 mg/L) is detected in February 1997 at Station 3 while highest DO (6.88 mg/L) is detected in December 1997 at Station 10. Results showed that ambient DO levels peaked generally in February-April 1997, June 1997 and December 1997. Lower DO levels were observed during the period of May 1997 and September-November 1997. Mean surface water DO levels were also calculated and these were shown in Figure 3.6(b). Statistical

analysis showed that the mean DO levels ranged between 3.91 ± 1.15 mg/L at Station 3 to 5.72 ± 0.72 mg/L at Station 9.

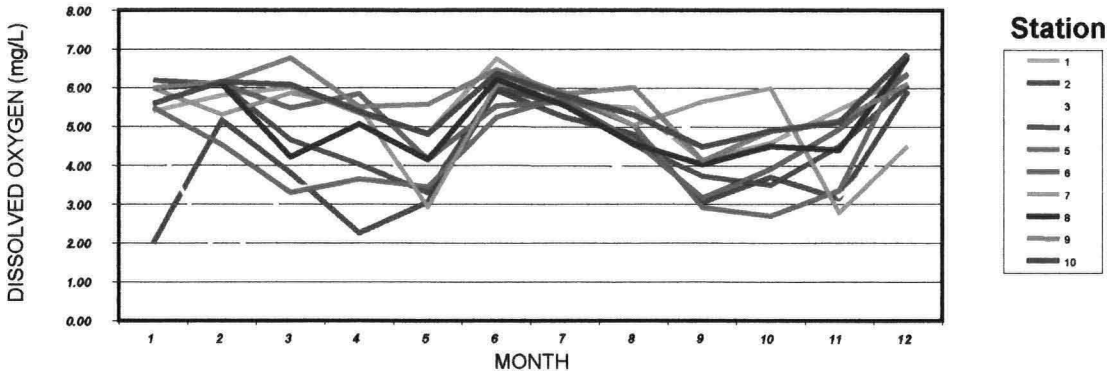

Figure 3.6(a): Monthly surface water dissolved oxygen at study sites in Tanjung Rhu, Pulau Langkawi for 1997. (Source: Abdullah and Yasin, 2000)

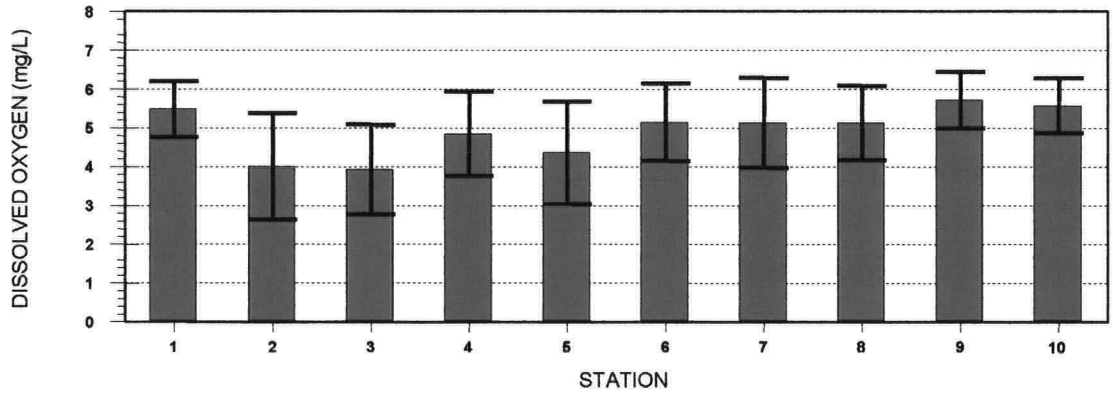

Figure 3.6(b): Mean annual surface water dissolved oxygen at study sites in Tanjung Rhu, Pulau Langkawi for 1997. (Source: Abdullah and Yasin, 2000)

Temperature

Collected data of surface water temperatures in degree Centigrade (°C) for each sampling station were shown in Figure 3.7(a). Like levels of TSP, there is a distinct pattern of temperature fluctuations observed in the 12-month data. Generally lower ambient temperature levels were observed during January, August and December 1997. Warmer surface water was detected between the months of March to May 1997 and September to November 1997. Most ambient temperature levels fell between 26 °C to 34 °C. However there were exceptions to collected data for Station 3 during March-April 1997 and Station 7 during September-October 1997. Very high ambient surface water temperatures were detected here. This phenomenon was probably due to the shallowness of these two sampling points. Mean ambient temperatures for each sampling station were given in Figure 3.7(b). Low

fluctuations were observed based on the standard deviations from the statistical analysis of this parameter except for Stations 3 and 7 where the standard deviation values were greater than 2.0 °C. Overall mean values were found to be between 29.1 ± 1.3 °C to 31.9 ± 2.5 °C.

Figure 3.7(a): Monthly surface temperature at study sites in Tanjung Rhu, Pulau Langkawi for 1997. (Source: Abdullah and Yasin, 2000)

Figure 3.7(b): Mean annual surface water temperature at study sites in Tanjung Rhu, Pulau Langkawi for 1997. (Source: Abdullah and Yasin, 2000)

Salinity

Levels of surface water salinity expressed in the unit of parts-per-thousand (ppt) sampled throughout the 12-month period for each sampling station were shown in Figure 3.8(a). Most sampling stations recorded ambient salinity levels ranging between the higher brackish water condition of 20 ppt to the typical coastal water salinity condition of 34 ppt. Salinity levels at Station 2 fluctuated at a greater range of 10 ppt to 33 ppt. Greatest salinity fluctuations were observed at Stations 3 and 7 where the measured levels ranged from 0 ppt which was purely freshwater condition to a typical coastal water salinity condition of 31 ppt. Mean salinity levels calculated were shown in Figure 3.8(b). Low salinity fluctuations within a sampling station were observed at Stations 1, 9 and 10. These were detected

based on the low standard deviations calculated. In contrast, very high salinity fluctuations were seen at Stations 3 and 7 where calculated standard deviations were nearly as high or slightly higher than the mean results.

Figure 3.8(a): Monthly surface water salinity at study sites in Tanjung Rhu, Pulau Langkawi for 1997. (Source: Abdullah and Yasin, 2000)

Figure 3.8(b). Mean annual surface water salinity level at study sites in Tanjung Rhu, Pulau Langkawi for 1997. (Source: Abdullah and Yasin, 2000)

Turbidity

Turbidity levels of the surface waters for each sampling station were given in Figure 3.9(a). This parameter was measured in Formadazin Turbidity Unit (FTU). Fluctuation pattern in the ambient turbidity levels were also detected in the collected data. Very high turbidity (150 FTU) was measured at Station 3 during August 1997. Another peak was also observed for Station 3 during April 1997 but the measured level was 59 FTU. Two equal consecutive peaks (65 FTU) were seen at Station 7 during September and October 1997. The general range of turbidity levels measured for the remaining 8 sampling stations generally fell between 0- 34 FTU. Mean surface water turbidities calculated were

shown in Figure 3.9(b). The overall range of calculated mean values were 5.75 ± 6.57 FTU to 36.35 ± 39.23 FTU. Statistical analysis showed that the standard deviations were higher than the mean values. This indicated the measured turbidity levels fluctuated greatly within each sampling station itself throughout the sampling period.

Figure 3.9(a): Monthly surface turbidity at study sites in Tanjung Rhu, Pulau Langkawi for 199 (Source: Abdullah and Yasin, 2000)

Figure 3.9(b). Mean annual surface water turbidity level at study sites in Tanjung Rhu, Pulau Langkawi for 1997. (Source: Abdullah and Yasin, 2000)

pH

Relatively large fluctuations were observed in the measured pH levels during the first 5 months of 1997 (Figure 3.10(a)). Large increase in pH levels were observed for most sampling stations from January to February 1997 ranging between 7.50 to 8.90. Waters at Station 3 were found to be exceptionally different because levels of pH here fluctuated the most throughout the 12-month period. Station 3 generally showed the lowest pH levels measured among all stations. Fluctuation patterns for Stations 1, 8, 9 and 10 were similar throughout the study period and this could be attributed to their locations within relative close proximity to each other. A sudden drop of pH levels were measured in

November which increased to the normal range measured in December. Mean annual surface water pH levels calculated for each station were shown in Figure 3.10(b). These means were found to range between 8.10 to 8.60. Lower pH mean was calculated for Station 3 (pH: 7.50) with higher standard deviations due to the greater fluctuations observed throughout the study period.

Figure 3.10(a): Monthly surface water pH at study sites in Tanjung Rhu, Pulau Langkawi for 1997. (Source: Abdullah and Yasin, 2000)

Figure 3.10(b): Mean annual surface water pH at study sites in Tanjung Rhu, Pulau Langkawi for 1997. (Source: Abdullah and Yasin, 2000)

Total Suspended Particulates (TSP)

Results of the monthly surface water TSP concentrations according to sampling stations for January 1997 to December 1997 were given in Figure 3.11(a). The results of TSP concentrations were expressed in the S.I. unit, which were milligrams per-litre (mg/L). There was a distinct pattern of fluctuation observed in all the collected data obtained during the 12-month period. Similar fluctuation patterns were observed for most sampling stations except two, Stations 3 and 7. High levels of TSP were found during the second and third quarter of the year, which was from April -August 1997. A

slightly lower TSP peak was seen in February 1997. Highest concentration of TSP recorded during the 12-month sampling period was at Station 7 during April 1997 (243.00 mg/L) while the lowest was recorded at Station 3 during February 1997 with a level of 27.00 mg/L. The mean surface water TSP for each sampling station in 1997 was calculated and charted in Figure 3.11(b). There was an undulating pattern observed in these mean values. Calculated mean values were high ranging from 93.92 ± 50.10 mg/L to 148.65 ± 45.39 mg/L.

Figure 3.11(a): Monthly surface TSP at study sites in Tanjung Rhu, Pulau Langkawi for 1997 (Source: Abdullah and Yasin, 2000)

Figure 3.11(b): Mean annual surface water TSP at study sites in Tanjung Rhu, Pulau Langkawi for 1997. (Source: Abdullah and Yasin, 2000)

3.4.2 DISCUSSION: The Physical Environment

The whole study area of Tanjung Rhu is under the influence of the semi-diurnal pattern of tidal condition. Based on the measured water conditions particularly of salinity levels, the water of Tanjung Rhu constantly appear to be of coastal or seawater range, much less of brackish condition. Freshwater

condition is rarely found except at certain sampling stations located at a distance from the tidal influence. Therefore, discussion on the water quality parameters of Tanjung Rhu is mainly attributed to its seawater and brackish water characteristics more than the freshwater.

Discussions on the measured parameters will also be referred to the Standards/Permissible Levels outlined by the Department of Environment (DOE), Malaysia shown in Table 3.1.

The fluctuations of DO concentrations measured during the 12-month study were found to coincide with the tidal range during sampling periods. Higher DO levels were observed during spring tidal conditions where ranges of tidal waters of the days were large. These were obvious during the months of January to March, June to August, and November to December. Lower magnitudes of DO concentrations were observed during lower tidal range. However, the tidal flow direction is also important because generally flooding tides from the sea especially of spring tidal condition tend to transport in bodies of well-aerated waters and fresh batches of nutrients due largely to the higher mixing activities. Ebbing tides tend to transport out 'used' water bodies depending on the physical environment of an area. In this case, the inner tributaries of Tanjung Rhu riverine system would flush out less oxygenated water bodies during ebbing tides as physical water activities would be more sluggish as compared to those occurring within the estuarine and the open sea.

The overall levels of DO concentrations measured for all representative sampling stations at Tanjung Rhu were indicatives of healthy and well-aerated aquatic environment. The high levels recorded during sampling period is the result of high mixing activity occurring at the time of sampling as the tide floods into the Tanjung Rhu aquatic system. Exceptionally lowered DO level measured at Stations 2 and 3 during the months of January to April were of no particular concern because these stations were located within the inner tributaries of Tanjung Rhu riverine system. Low DO concentrations would be expected to occur naturally as these locations were further away from the tidal influence and hence the flushing exchange of water bodies would be less frequent. Other physical factors also have its impact on these values such as the river depth which would influence the heat budget of the water column that will in turn influence the level of DO measured. There was no standard given by the DOE on the concentrations of DO as this particular parameter is highly subjective to its environmental condition *i.e.* the physical, chemical and biological environments.

Water temperature is a prime regulator of natural processes within the aquatic environment. It governs physiological functions in organisms and, acting directly or indirectly in combination with other water quality constituents, affects aquatic life with each change. The temperature level also controls the solubility of gases particularly the oxygen level. The amount of DO decreases as the temperature

increases over a specific function. This phenomenon can be observed from the two sets of measurements (surface water temperature and DO) obtained from all sampling sites at Tanjung Rhu. Measurements of these two parameters obtained from Station 3 with its distinctive peaks at the extreme ends would best describe this phenomenon.

Two peaks were obviously seen from the plotted levels of temperature measured for Stations 3 and 7 during March and September-October respectively. These extremes recorded temperatures as high as 37 °C which is not normal but acceptable. This is because both sampling sites fell onto the shallow water category of which the depth range varied between 0.5 m to 1.2 m depending on the tidal condition. When the water column is small (*i.e.* shallow), the amount of atmospheric heat received would be distributed within this small column hence the increased water temperature compared to another sampling site that was broader and deeper (> 5.0 m) receiving the same amount of atmospheric heat. The resulting heat budget distributed within a small water column would be higher than that of a larger one.

Generally the temperatures measured observed natural levels that normally occur within a natural ecosystem and the values obtained for Tanjung Rhu fluctuates between 26 °C to 33 °C. Cooler temperatures measured were normally due to the influence of ambient atmospheric temperature which were low during the earlier hours of sampling and partly also due to the in-flux of fresh seawater from the sea into the estuarine-riverine region.

Another important variable in coastal and estuarine waters is the salinity. It is of particular concern that changes in salinity can cause changes in the aquatic ecosystem relative to the types and relative abundance of organisms. Variations in salinity throughout the aquatic system depend almost entirely on the balance between evaporation and precipitation and the extent of mixing between surface and deeper waters. Salinity of an estuarine water ranges from 0.5 to 35.0 ppt. Salinity levels encountered at Tanjung Rhu is within the sea water range of 33 ppt with an exception at two sampling sites i.e. Station 3 (the innermost sampling station) and Station 7 where the hotel discharge outlet was located. Wastewater discharges have greater influence in lowering the salinity level hence the freshwater or lower brackish water conditions measured. However, such low salinities were not observed throughout the 12-month sampling period. These levels were detected during low water springs and coincidences of wastewater discharge times.

Influences of the tide can be observed from the measured salinities obtained throughout 1997. As an example, Station 2 which is the second innermost sampling site within the Tanjung Rhu riverine area, showed brackish water condition during the months of May and August to November 1997. These

sampling months coincided with spring, neap and mid-tidal conditions. This has shown that the in-flux of fresh seawater bodies during flooding tides had not fully influenced the water bodies here. Mixing had occurred only to a certain degree where it is possible to have measured freshwater (0 ppt) during ebbing neap tides at this particular station. Characteristics of this area would then be fully of freshwater and not brackish water. However, the type of water characteristics around this sampling area changes from freshwater to seawater and is subjective to the magnitude of tidal volume which brings in seawater from the sea region. Based on the measured salinities itself, the extent of tidal influence on Tanjung Rhu riverine-estuarine region can be determined from the tidal volume and also the physical characteristics of the area.

In rivers under flood conditions, turbidity will be primarily comprised of relatively coarse dispersions. Turbidity is of concern in surface water courses due to aesthetic considerations, filterability, and disinfection. Turbidity in water may result from naturally occurring materials, or from man-related activities such as construction projects and waste discharges. Most turbid water occurs at salinities from 1 ppt to 5 ppt known as "turbidity maxima" as a result of several physical and chemical changes which occur as the river and sea water mix. Exhibition of strong turbidity maxima is closely related to mixing zones where these locations are strongly affected by freshwater run-offs.

Water samples collected at Station 3 exhibited turbidity maxima during the 1997 water quality monitoring at Tanjung Rhu study area. Such were proven from the high turbidities and low salinities observed particularly during the months of April to June, August and November. Highest turbidity (149.7 FTU) peaked during August 1997 where salinity level at this point was about 2.0 ppt. Another possible explanation to the high turbidity and low salinity level may be the occurrence of trapped freshwater pockets or uneven mixing of sea water and freshwater even though high water has intruded the sampling location at the time of sampling. Turbidity maxima may have occurred at Station 7 where the hotel discharge outlet was located during September and October 1997 judging from the two subsequent peaks (>60 FTU) measured. However, the low salinities and high turbidities here may more so be attributed to the volume and the collective flocculation of materials or colloids observed from the wastewater discharge. The overall turbidity levels measured during the 12-month study period exhibited acceptable conditions as these values measured were far below the 50.0 FTU given by the DOE.

In estuaries, the change of pH as freshwater encounters the sea causes intense flocculation of clay and other particles, with increased adsorption of metals and other materials on the flocculation. Flocculation is generally defined as a process of contact and adhesion whereby the particles of dispersion form larger-size clusters or woolly cloudlike aggregations. Such occurrences (flocculation)

would contribute to the turbidity level. However, there was no indicative of pH change impacts from the measured pH levels during the study period. Therefore the contribution effect of pH change does not occur at Tanjung Rhu study area. This is because changes of pH measured during the 12-month period did not differ greatly as the buffering system of Tanjung Rhu was able to accommodate the changes occurring within it. Although there seem to be quite large fluctuations from the measured pHs between stations and over time, there was no particular concern at this point over pollution problem because these levels were of natural conditions and were also within the DOE pH standards of 6.0 - 9.0.

Although the study area of Tanjung Rhu is known to still lies within its natural condition, generally high levels of total suspended particulates (TSP) were observed in the study region throughout the 12-month study period. These values were observed have exceeded the DOE TSP standard of 50.00 mg/L. Based on the measured levels, TSP were observed to stay constantly high during the months of April to August. This period coincided with the usual peak rainfall season. A few factors may have great influences on the measured TSP. The first factor would probably be the whole study area which is highly subjected to high water movement and re-suspension of bottom sediments by tidal waters. While sedimentation takes place in all but the swiftest rivers, estuaries are subject to particularly heavy sedimentation, leading to extensive formation of mud-flats containing much of the organic material, metals and so on from the water column. Furthermore, Tanjung Rhu consists largely of mangrove ecosystems which, in nature act as sediment traps.

Lowered water clarity (high turbidity levels) was more so seen around Tanjung Rhu because mangroves, being the major forest type surrounding the study region, are known to be naturally highly sedimented area. Churning up of the settled bottom materials particularly during flooding spring tide had released the trapped and settled substances within the upper bottom layer of the rivers and streams. The high physical energies occurring at that time, serves both to replenish the oxygen to the underlying coarse sediments and to wash out finer materials which for several reasons, consume oxygen rapidly. This has resulted in the high turbidity level and the lowered DO observed. In areas of the estuaries underlain with fine sediments, a reduced zone is widespread; thus lowered DO is measured. This phenomenon is observed particularly in August where TSP reaches one of its peaks. The reverse is seen during neap tides.

Station 1, located at Teluk Udang which is within the inner main estuary of Tanjung Rhu study area falls within an area that is highly subjected to physical environmental changes or activities. Water quality profiles at this station is under the influences of the tidal waters occurring daily as this location forms part of the entrance border to the Tanjung Rhu estuarine-riverine network. This is also an area

generally known to have turbid waters and highly reducing and very fine sediments. The depth here was measured between 4 - 7 m during sampling times. High turbulence has churned up bottom sediments and materials resulting in considerable increase in the TSP level measured.

3.5 SUMMARY

Based on the monthly water quality monitoring data in 1997 carried out by the author (Abdullah and Yasin, 2000), the overall results obtained had indicated that most of Tanjung Rhu study area still is a relatively clean environment with regards to its water quality. Its physical environment showed no pollution although high TSP and frequent occurrence of high turbidities were measured. This is largely due to the natural existing environment, which consists of mangrove forest type that naturally acts as sediment traps. These high values should not be regarded as pollution since the nature of mangrove and estuarine ecosystems are subjective to high sedimentation. Turbid waters with high TSP are therefore expected from such environment. However, high TSP will be considered a problem if the tide flushes out high concentrations of TSP into the nearby highly sensitive natural habitats such as the coral reef within the study area.

The sampling area of Tanjung Rhu is under the influences of the tides. The tidal influence reached the uppermost stations (Stations 2, 3 and 5 of monthly water quality monitoring stations) located within the inner tributaries. This affected the levels of the measured parameters in two ways:

1. There is a general flushing of the system twice a day as the tide rises and falls. The rising tide has resulted in the high salinity readings in all the stations sampled rendering the Tanjung Rhu riverine area to be of saline and brackish water conditions most of the time.

2. This flushing also resulted in the movement of pollutants to both the upstream and downstream areas. This facilitates dilution and dispersion of potential periodical pollutants lessening its deleterious effects over time.

The tide therefore not only flushes pollutants away from high concentration areas it also transports the pollutants from the source to other areas following tidal movement. Most contaminants were found to originate from areas concentrated with human activities mainly at the downstream locations and at some areas at the upper streams.

Spatial and temporal distribution of the investigated parameters along with water circulation pattern if available will no doubt provide valuable baseline information for the planning and implementation of management strategies for potential pollution problems in similar aquatic ecosystems.

Chapter 4

THE BIOGEOGRAPHIC DISTRIBUTION OF TANJUNG RHU CORAL REEFS

4.1 WHAT ARE CORAL REEFS?

Over a vast region (millions of square miles) of the tropics, the shallow inshore waters are dominated by the formation of coral reefs and indeed, they are often used to define the limits of the tropical marine environment.

Coral reefs are one of the most productive ecosystems in the world in terms of support and maintenance of a large animal biomass (quantity of living matter). Although the gross primary productivity of the reef producers is equivalent to that for most productive plants, the reef system is also adapted to utilize a variety of organic and inorganic materials brought to the reef by water currents and by the diurnal migration of reef and nonreef species. Although the coral reef appears to be a discrete and self-contained ecological system, its productivity is wholly maintained by the characteristics of the surrounding environment. In this regard, the basis for the high productivity of the coral reef ecosystem is a result of the production of the reef itself, together with its surrounding and supporting environment (Odum, 1955). It is this level of productivity which is the basis for sustaining the reef's characteristically high diversity and abundance of fish biomass (estimates between 490 and 1450 kilograms/hectare) (Philippines Ministry of Natural Resources, 1979).

The coral reef ecosystem has a variety of useful roles, all of which have a relevant and positive influence on associated coastal habitats. The most prominent role is the provision of a diverse habitat for a large number of sessile and mobile organisms. In this regard, one notable feature is the large proportion of species that live within the reef system but forage and feed in contiguous areas on a diurnal cycle. Conversely, many nonreef species visit coral reefs at periodic intervals for the purpose of foraging and preying upon coral reef inhabitants. The coral reef ecosystem is thus both a habitat and source of nourishment for many species typically found in the coastal areas dominated by reefs.

Although the coral reef ecosystem depends on pristine seawater, the reef itself plays a role in maintaining the quality of local waters. Water currents that circulate over and within a coral reef are "filtered" as the reef system takes up and utilizes a variety of inorganic minerals, oxygen, organic detritus, and plankton. The outflowing water carries small concentrations of metabolic wastes away from the reef as well as planktonic larvae that are dispersed into other areas (Odum, 1955).

In general, coral reef development is greater in areas that are subject to strong wave action. Coral colonies with their dense, massive skeletons of calcium carbonate are very resistant to damage by wave action. Coral reefs tend to be positioned perpendicularly to the mean direction of wind-generated swell currents flowing over the reef. Depending on the reef's proximity to adjacent coastal areas, these characteristics can serve to weaken incoming waves, thus minimizing erosion and coastal hazards behind the reef. This creates a lagoon and a protected coastal environment. At the same time, the wave action provides a constant source of fresh, oxygenated sea water and prevents sediment from settling on the colony. Wave action is also responsible for renewing the plankton, which serves as food for the coral colony. Dead coral reefs will not be able to retain this ability to protect the coastal area from erosion and other natural coastal hazards, but increases such hazards instead.

Although the corals are the major organisms on coral reefs in that they form the basic reef structure, there is a bewildering array of other organisms associated with reefs such that these areas are perhaps the most diverse and species-rich areas that exist in the marine environment today. Coral reefs are large and complex associations of organisms that have a number of different habitat types all present in the same system. Thus, for example, there are areas of hard substrate upon which many sessile organisms attach and which are analogous to rocky shores; at the same time, there are areas of sand, which require a different set of adaptations, much as we saw for soft bottoms. Similarly, there are areas of heavy wave action and strong currents and areas of virtual calm where water movement is minimal. Still other areas may have a lush growth of calcareous green algae (*Halimeda* sp.) mimicking sea grass beds. All of these habitat types are found in a relatively small area. Therefore one of the reasons for the great diversity of life in coral reefs is the great diversity of habitats. As might be expected, these different habitat types, as well as others, vary in their extent or presence on reefs in different geographic areas (Nybakken, 1982).

4.2 METHODOLOGY

4.2.1 Mapping Methodology

4.2.1.1 Required Resources

(1) Ground Mapping

Ground mapping or *in situ* mapping of the fringing reefs of Tanjung Rhu (Teluk Dedap reef) is an on-site mapping which uses 50 m transect lines that has been tagged at every meter mark. Slates, data sheets and a base map of the working area are needed to assist recording of intercept data. Thick boots to walk on exposed reefs are also required for ground mapping. Snorkeling and SCUBA equipment are occasionally needed during sampling when the tide is high. Camera and photographic films are also used in ground mapping.

(2) Basic airphoto interpretation equipment

Photo interpretation equipment generally serves one of three fundamental purposes: viewing photographs, making measurements on photographs, and transferring interpreted information to base maps or digital data bases. The airphoto (or aerial photograph) process typically involves the utilization of stereoscopic viewing to provide a three-dimensional view of the study area. This effect is due to our binocular vision. A stereoscope facilitates the stereoviewing process. Aerial photos or stereograms taken at an altitude are required for such viewing. These stereograms need to be taken in pairs with 60 percent endlap.

Stereograms were used in this study for reef mapping of the control area which is Teluk Datai located at the western corner of north Pulau Langkawi. This study uses two dates of stereograms (1989 and 1994) from the archives of the Reef Research Group of Universiti Sains Malaysia. The first set of stereograms were taken at an altitude of 660m (2,200ft) in 1989 having the calculated scale of 1:3,260. The other set was taken in 1994 at an altitude of 600m (2,000ft) and the calculated scale was 1:3,000.

4.2.1.2 Preliminary Mapping (aerial photographs)

Eight types of reef features were identified from the aerial photographs and these are:

1. sandy beach
2. sand/pebble/rock
3. rocks
4. mud flat
5. coral debris
6. coral (≥50% live coverage)
7. coral (≤50% live coverage)
8. mangrove

A systematic study of aerial photographs usually involves several basic characteristics of features shown on a photograph. The exact characteristics useful for any specific task, and the manner in which they are considered, depend on the field of application. However, most applications consider the following basic characteristics or variations of them: shape, size, pattern, tone (or hue), texture, shadows, site, and association (Lillesand and Kiefer, 1987).

i. *Shape* refers to the general form, configuration, or outline of individual objects.

ii. *Size* of objects on photographs must be considered in the context of the photo scale. Relative sizes among objects on photographs of the same scale must also be considered.

iii. *Pattern* relates to the spatial arrangement of objects. The repetition of certain general forms or relationships is characteristic of many objects, both natural and constructed, and gives objects a pattern that aids the photo interpreter in recognizing them.

iv. *Tone* (or *hue*) refers to the relative brightness or colour of objects on photographs. Tonal patterns vary according to for example, the drainage conditions of soil where the lighter-toned areas are topographically higher and drier while the darker-toned areas are lower and wetter. Without tonal differences, the shapes, patterns, and textures of objects could not be discerned.

v. *Texture* is the frequency of tonal change on the photographic image. Texture is produced by an aggregation of unit features that may be too small to be discerned individually on the photograph. It is a product of their individual shape, size, pattern, shadow, and tone. It determines the overall visual "smoothness" or "coarseness" of image features.

vi. *Shadows* are important in two opposing respects: (1) the shape or outline of a shadow affords an impression of the profile view of objects which aids interpretation, and (2) objects within shadows reflect little light and are difficult to discern on photographs which hinders interpretation.

vii. *Site* refers to topographic or geographic location, and is a particularly important aid in the identification of vegetation types.

viii. *Association* refers to the occurrence of certain features in relation to others.

In this study, results of the reef features and their distribution at the control site (Teluk Datai) were based on Abdullah *et al.* (2002), a copy of which can be found in Appendix 5. The reef features and their distribution interpreted from the aerial photographs were used to detect changes occurring in the control site from 1989 to 1994. The area of coverage was estimated for the year 1989 and 1994.

4.2.1.3 Field Sampling/Preliminary Mapping

Line Transect Intercept (LIT) survey method (Loya, 1978; Marsh *et al.*, 1984) was used for field data collection *i.e.* the assessment of sessile benthic communities of coral reefs. Surveys were carried out by the author and members of the Reef Research Group of Universiti Sains Malaysia during low water spring tides between January to May 1999 for Teluk Dedap reef. Surveys were conducted during low water spring tides because during these times the reefs are exposed allowing easy access to mapping. Direct ground mapping would require a relatively longer time as sampling frequency needs to be increased. This is basically due to the short time span of reef exposure during low water spring tide which is about 6 hours and the fortnightly occurrence of spring tides. There were 150 transects being surveyed on Teluk Dedap reef and each transect were laid at 4m

apart (Figure 4.1).This would allow greatest coverage possible with the given time and space. On such surveys, the observer is normally required to walk on the reefs along transect lines. SCUBA diving and snorkeling techniques are involved only during higher seawater level. The benthic community is characterised using lifeform categories which provide a morphological description of the reef community. The LIT is used to estimate the cover of an object or group of objects within a specified area (Gates, 1979) by calculating the fraction of the length of the line that is intercepted by the object. A schematic representation of the percent cover used for the estimation of live and dead coral, sand/rubble is given in Figure 4.2. This measure of cover, usually expressed as a percentage, is considered to be an unbiased estimate of the proportion of the total area covered by that object with the assumptions that the size of the object (corals) is small relative to the length of the line, and that the length of the line is small relative to the area of interest (Lucas and Seber, 1977; Mundy, 1991).

The LIT has been used for objectives ranging from large-scale spatial problems (Benayahu and Loya, 1977: 1981) to morphological comparisons of coral communities (Bradbury *et al,*, 1986; Reichelt *et al.*, 1986), and studies assessing the impact of natural and anthropogenic disturbances (Mapstone *et al,*, 1989; Lee, 1994). These categories are recorded on data sheets by divers swimming along lines of plastic fibre tape which are placed roughly parallel to the reef crest at varying depths of 3m to 10m at each site. Transect lengths vary depending on location of the reef edge.

4.2.1.4 Cross-sectional Reef Profiles

Reef profiles of the study area (Teluk Dedap Reef) and the control site (Teluk Datai Reef) were also drawn (by the author) from reef surveys during low water spring tides. The purpose of this was to provide a cross-sectional view of the existing reefs. Locations of these reef profile transects are given in Figure 4.3 for Teluk Dedap reef and Figure 4.4 for Teluk Datai reef.

4.2.1.5 Ground Truthing/Accuracy Assessment

Basically, the general LIT survey method was also employed in the ground truthing process with one exception - points were selected at random. Ground truthing which is carried out after map production mainly means verifying information extracted from remote sensing data (stereograms, and photographs). From ground truths, accuracy assessments for reef maps were also calculated. This assessment was based on a set of reference points selected randomly on the study area as it is not practical to ground truth or test every unit area of the study region. A classification accuracy table is also generated from the ground truth results and two kinds of reports were derived, the error

matrix and the accuracy report. The accuracy report refers to the calculated statistics i.e. the percentages of accuracy based upon the results of the error matrix.

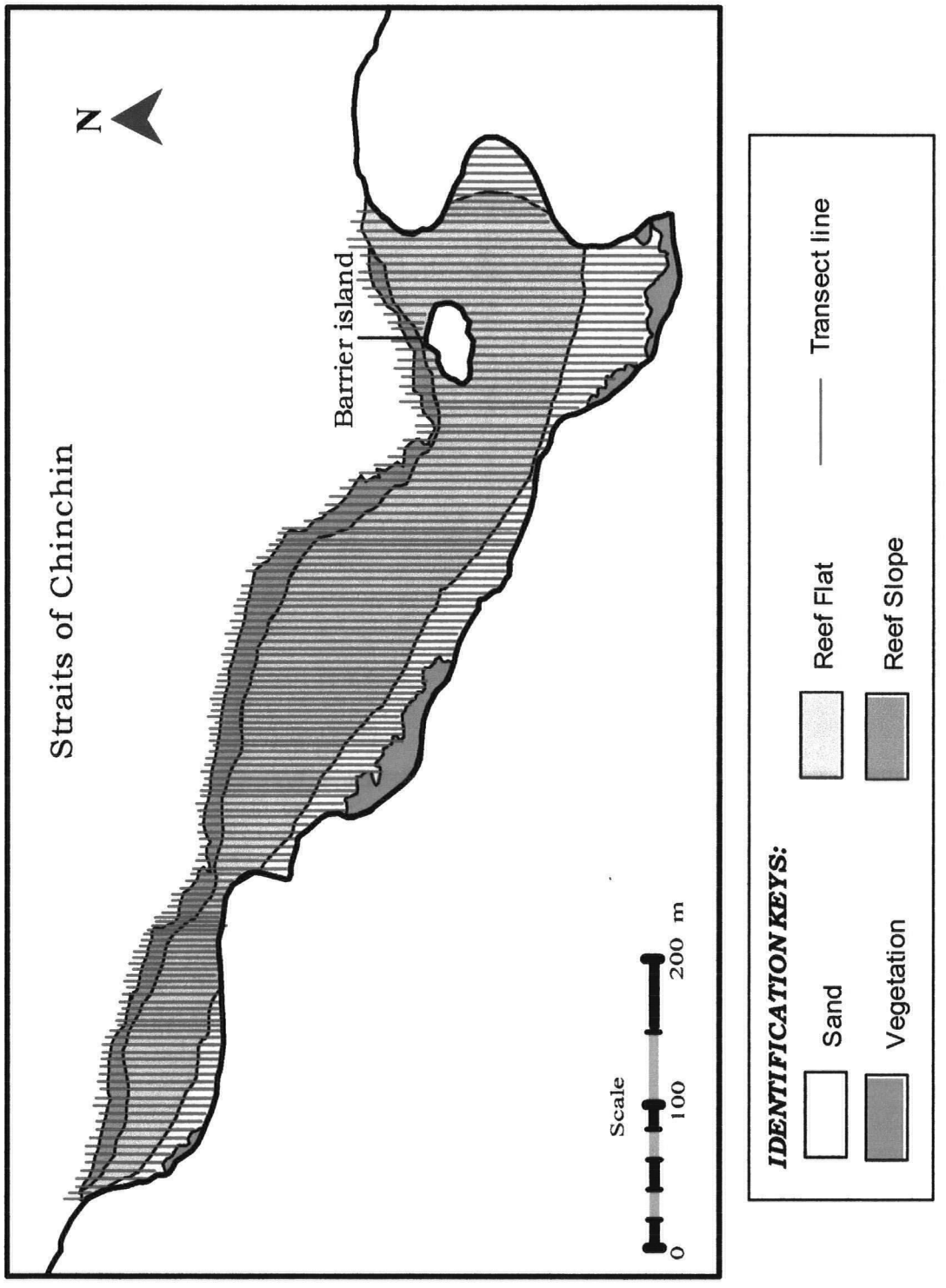

Figure 4.1. Location of Transect lines for coral reefmapping in Teluk Dedap, Tanjung Rhu.

Figure 4.2. Schematic representations of percent cover used for the estimation of live and dead coral, soft coral and sand/rubble (Source: English & Wilkinson, 1994)

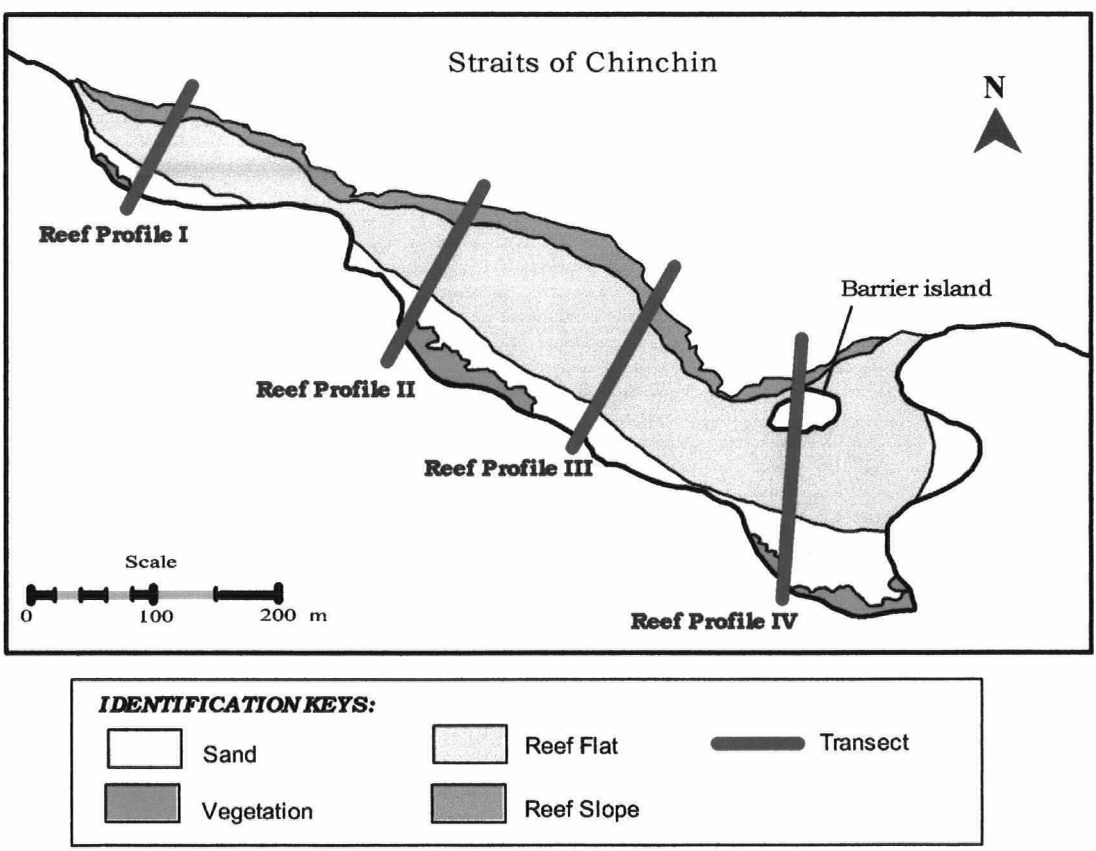

Figure 4.3: Location of transects surveyed for cross-sectional reef profiles (I - IV) of Teluk Dedap reef, Tanjung Rhu.

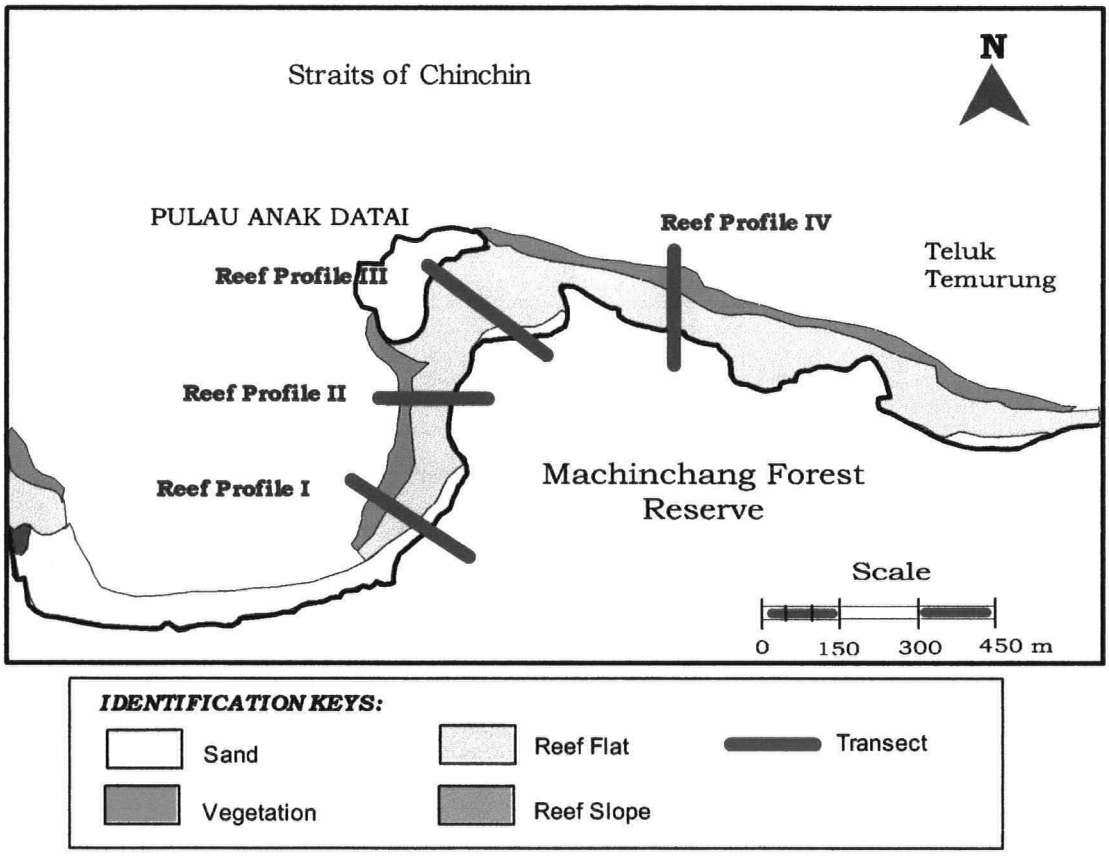

Figure4.4: Location of transects surveyed for cross-sectional reef profiles (I - IV) of Teluk Datai reef.

The error matrix is the most common way to represent classification accuracy of remotely sensed data as in this study. An error matrix is a square array of numbers that expresses the number of points assigned to a particular category relative to the actual category as verified on the ground. The columns usually represent reference data or the observed data while the rows indicate the classified data generated from the remotely sensed data. An error matrix is a very effective way to represent accuracy because the accuracies of each category are plainly described along with both the error of inclusion (commission errors) and errors of exclusion (omission errors) present in the classification or mapping.

The error matrix can be used as a starting point for a series of descriptive and analytical statistical measurements. The simplest descriptive statistic is overall accuracy, computed by dividing the total correct points or correct occurrences (*i.e.* the sum of major diagonal) by the total number of points or occurrences in the error matrix.

The total number of correct points in a category divided by the total number of points of that category as derived from the reference data (the column total) indicates the probability of a reference point being correctly classified and is really a measure of omission error. It is also known as "producer's accuracy" because it indicates how well a certain area can be classified. On the other hand, if the total number of correct points in a category is divided by the total number of points that were classified in that category, the result is a measure of commission error or the "user's accuracy". This is also a measure of reliability indicating the probability that a point classified on the map or image actually representing that category on the ground. A summary of the error matrix computation is as follows:

		Columns (Reference data)			
Rows (Classification data)		1	2	k	Row total
	1	n_{11}	n_{12}	n_{1k}	n_{1+}
	2	n_{21}	n_{22}	n_{2k}	n_{2+}
	k	n_{k1}	n_{k2}	n_{kk}	n_{k+}
	Column total	n_{+1}	n_{+2}	n_{+k}	n

$$\text{Overall Accuracy (\%)} = \frac{\text{Sum of correct occurrences } (n_{11} + n_{22} + \ldots n_{kk})}{\text{Sum of occurrences (n)}} \times 100$$

Producer's accuracy for class 1 (%) = $(n_{11} / n_{+1}) * 100$

User's accuracy for class 1 (%) = $(n_{11} / n_{1+}) * 100$

The ground truthing and generation of error matrices for this study were carried out by the author.

4.2.1.6 Map Production

Final maps were produced by the author after verification or ground truthing with satisfactory results has been conducted. In the process of map production, the scaled drawn maps were scanned and legends were assigned to each identified features allowing easy recognition of the various reef features.

4.2.2 Coral Taxonomy

Corals collected during field surveys were brought back to the laboratory for the cleaning process prior to identification or its taxonomic study. The corals were bleached and dried to rid the living organisms thus exposing only the skeletons that were made of calcareous materials. This needs great care in order to minimize damage to the skeletal structures which forms the principal classification features in coral taxonomy studies.

Useful equipment needed for this study include plastic rulers marked in centimeters and millimeters, magnifying glass and/or a stereomicroscope, and taxonomic keys to hard coral identification (Wood, 1984). The taxonomic keys used here are based on the concept of dichotomous key, a type of key used widely in the identification of plants and animals. Single or multiple characters are given in contrasting pairs (occasionally in groups) and a choice must be made between the alternatives thus eliminating each genus in turn. Some of the features used in coral identification include morphology of the corallum, corallites, septal arrangement, appearance of the columella, arrangement of the costae, etc. These features were used together with *in situ* identification of corals wherever possible as field observations and detail skeletal features form the basis of coral identification.

With the limited time available during low water spring tides and taking into consideration the size of the reefs, the author also sought the help from members of the Reef Research Group of Universiti Sains Malaysia to collect coral samples from the study area. Collected coral samples were then identified by the author and further verifications of the identified coral samples were obtained from Yasin (*pers. comm.).*

4.2.3 Computation of Species Diversity

In biogeography, Jaccard's Index (Jaccard's coefficient) is one of the simplest numerical methods used for comparing the species diversity between two different samples or communities. Jaccard's Index will be used to calculate the faunal similarity or diversity between the two coral communities found at Teluk Datai and Teluk Dedap.

The formula for Jaccard's Index used in this study is as follows:

$$\text{Jaccard's Index} = \frac{C}{(N_1 + N_2 - C)} \times 100$$

where, C = number of species shared between a pair of regions
N_1, N_2 = number of species in each of the two regions.

4.3 TANJUNG RHU CORAL REEFS

4.3.1 Condition of the reefs

The reef of Tanjung Rhu study area is located mainly at Teluk Dedap. Details of the reef drawn from the 150 line transects using Line Intercept Transect method is shown in Figure 4.5.

The breadth of the reef was measured to extend from 0 m to 120 m from shoreline. The area of each reef feature was estimated from the scaled map with the aid from data collected from the LIT method during survey, Malaysian Topology Map (series L7030 Sheet 3069, 1985) and Admiralty Chart (series N7030 Sheet 3069, 1989). Estimated area coverage of the mapped reef features at Teluk Dedap is shown in Table 4.1.

Live coral zone was observed to be at the lower reef flat and the reef edge. It is considered to be the richest zone in terms of live coral growth and scleractinian species diversity. Live corals covered an estimated area of 7,700 m^2 (12.2%) of 63,000 m^2 total reef at Teluk Dedap. Of this live coral cover, 7.9% (5,000 m^2) are dominated by $\leq$50% live corals and the remaining 4.28% (2,700 m^2) by $\geq$50% live corals. Comparatively, coral debris was quite extensive and the area of coverage was 18,000 m^2 (28.5%). The coral debris zone is sometimes termed "coral rubble zone" because as the name implies, broken corals normally cover this zone. However, this does not necessarily imply that the zone is a dead one. The two main features seen from the reef are the long sand strips along the beaches and the mudflats of Teluk Dedap. These alone constituted 35,550 m^2 (56.5%) of the estimated total reef area. Mudflats are easily considered the "dead" zone of the reef and appear to be gradually expanding itself onto the reef claiming the coral rubble zone. The only typical reef feature not found within Teluk Dedap fringing reef in Tanjung Rhu is the mangroves.

From Figure 4.5 the three main reef features of Teluk Dedap are very clearly signified by the landward corridors formed by each feature along the length of the reef. The sandy beach formed the shoreline followed by mudflats and irregular strips of coral debris preceded live coral coverage at the lower reef flats and the reef slopes. Typical reef profile of Teluk Dedap offering cross-sectional views were also drawn during surveys. Four reef profiles were able to be distinguished and the reef morphologies are shown in Figures 4.6(a)–(d). Basically the reef of Teluk Dedap is flat, narrow and shallow. These were based on the profiles drawn and the depth of which the reef is exposed during low water springs. The entire reef was observed to be exposed at water levels below 0.4m and fully submerged at water levels above 1.7m. Depths of the reef were found to be

approximately 0.6 m - 1.7 m at reef flats and 1.6m - 2.8m at the slopes during spring tides. The reef slope in this area is very narrow and the live corals are mainly massive or submassive boulders distributed quite sporadically.

Figure 4.5: Distribution of reef features of Teluk Dedap, Taniung Rhu (1999).

Table 4.1: Area coverage of the reef features of Teluk Dedap in Tanjung Rhu, Pulau Langkawi (1999)

Reef Feature	Area (m^2)
Sand	18,800
Sand/Pebble/Rock	1,000
Rock	750
Live Coral (≤50%)	5,000
Live Coral (≥50%)	2,700
Coral Debris	18,000
Mud	16,750
Mangrove	-
TOTAL	63,000

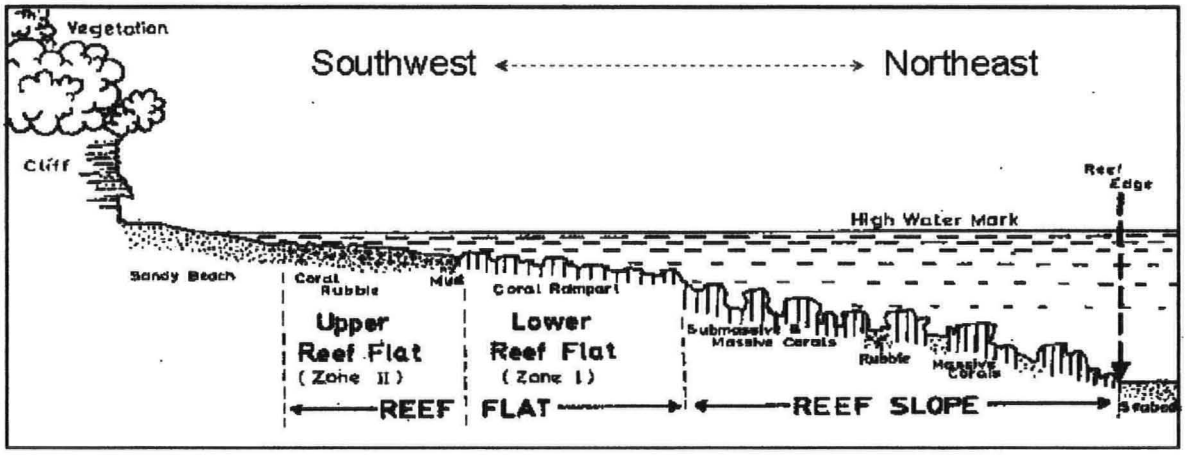

Figure 4.6 (a): Cross-sectional area of Reef Profile I, showing reef morphology of Teluk Dedap. (Drawn by the author)

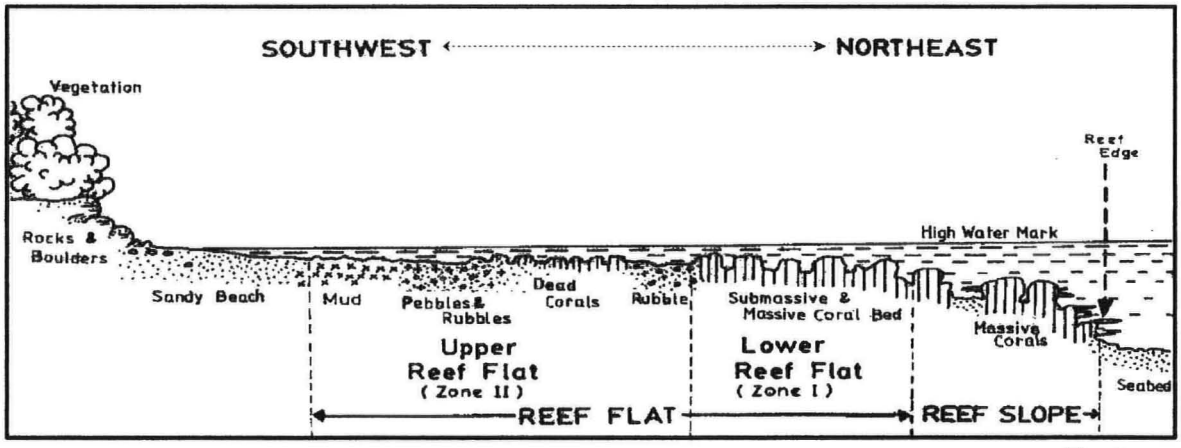

Figure 4.6 (b): Cross-sectional area of Reef Profile II, showing reef morphology of Teluk Dedap. (Drawn by the author)

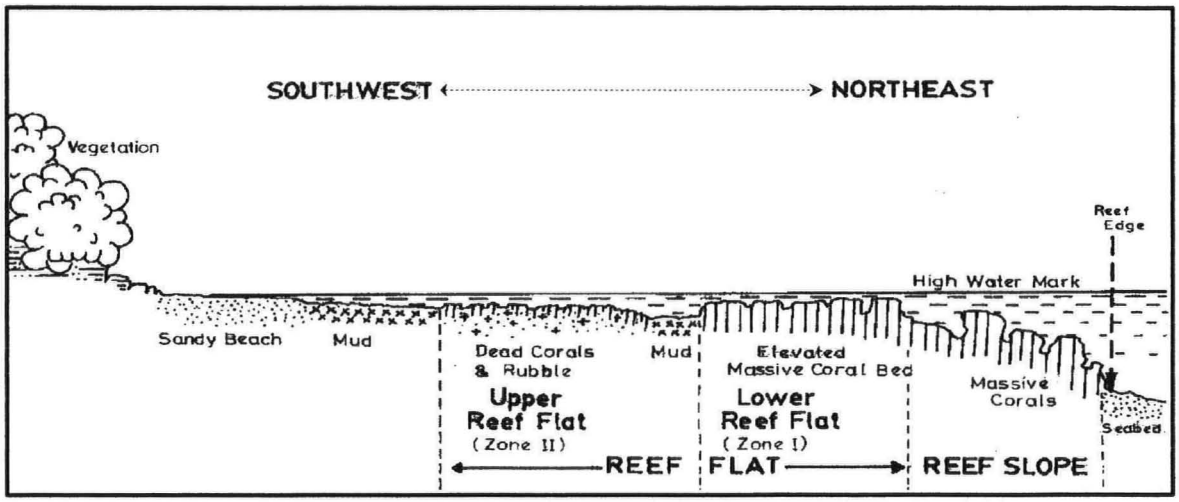

Figure 4.6 (c): Cross-sectional area of Reef Profile III, showing reef morphology of Teluk Dedap. (Drawn by the author)

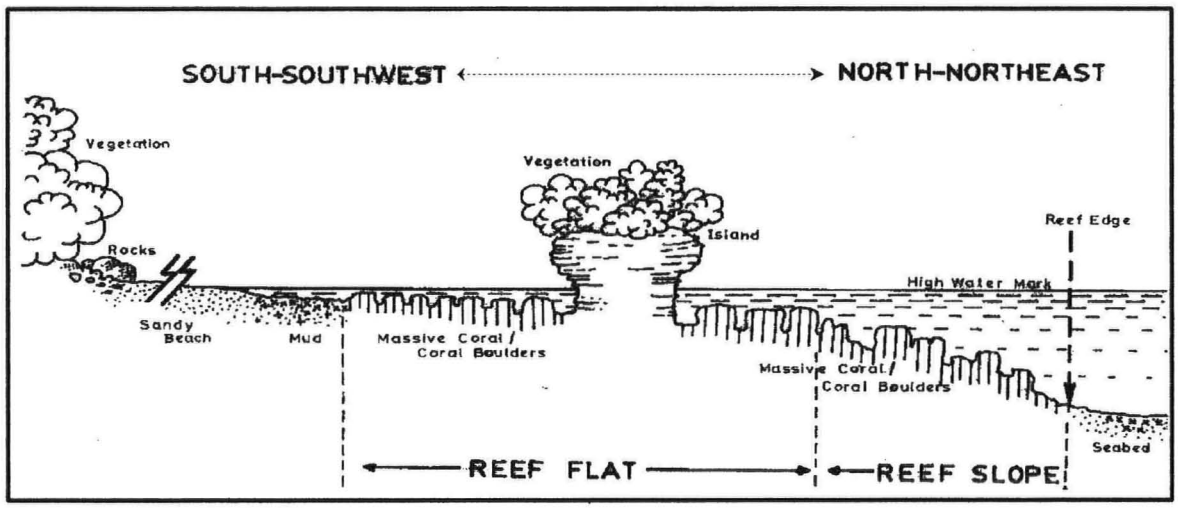

Figure 4.6 (d): Cross-sectional area of Reef Profile IV, showing reef morphology of Teluk Dedap. (Drawn by the author)

4.3.2 Accuracy Assessment

Accuracy assessment similar to that computed in remote sensing methods is employed in this section of reef mapping although reef features were identified through field surveys and not through aerial photographs. This is assumed to be possible because surveys carried out using LIT method is an estimation method which could not cover the entire reef in every unit area in detail. Errors are bound to occur and would therefore be logical to employ the error matrix in the accuracy assessment.

Table 4.2(a) showed the error matrix computed for Teluk Dedap reef surveyed in 1999. Overall accuracy computed was found to be good *i.e.* 90.3% and this was attributed by the survey method employed which is LIT. Inaccuracies were low because the method employs on the ground mapping instead of relying on aerial photographs. Producer's and user's accuracies (Table 4.2(b)) were also computed. Producer's accuracy ranged between 84.1% to 97.8% and the range for user's accuracy was slightly lower *i.e.* 82.0% to 96.0%. These good accuracies were expected due to the survey method used. If ground truthing was carried out much later *e.g.* a year later, the accuracies (overall, producer's and user's) are expected to be lower because of environmental changes over time.

Table 4.2(a). Error matrix of reef features showing classified and observed data with overall accuracy for year 1999 at Teluk Dedap, Tanjung Rhu, Pulau Langkawi.

		REFERENCE DATA (OBSERVED DATA)								
CLASSIFIED DATA	Reef Feature	SA	PE	RK	MD	MG	CD	CH	CS	Total
	SA	38	2	-	-	-	-	-	-	40
	PE	-	35	5	-	-	-	-	-	40
	RK	-	2	37	1	-	-	-	-	40
	MD	3	1	-	46	-	-	-	-	50
	MG	-	-	-	-	-	-	-	-	-
	CD	-	1	1	-	-	48	-	-	50
	CH	-	-	1	-	-	1	41	7	50
	CS	-	-	-	-	-	1	5	44	50
Total		41	41	44	47	-	50	46	51	320

Abbreviations to Reef Features:
SA - Sand
PE - Sand/Pebble/Rock
RK - Rock
MD - Mud
MG - Mangrove
CD - Coral Debris
CH - Live coral ≥ 50%
CS - Live coral ≤50%

Sum of major diagonal = 289
Overall Accuracy = (289/320) = **90.3 %**

Table 4.2(b). Computation of producer's and user's accuracy results (1999) for Teluk Dedap reef, Tanjung Rhu, Pulau Langkawi.

Producer's Accuracy			User's Accuracy		
SA	= 38/41	= 92.7%	SA	= 38/40	= 95.0%
PE	= 35/41	= 85.3%	PE	= 35/40	= 87.5%
RK	= 37/44	= 84.1%	RK	= 37/40	= 92.5%
MD	= 46/47	= 97.8%	MD	= 46/50	= 92.0%
MG	= -	= -	MG	= -	= -
CD	= 48/50	= 96.0%	CD	= 48/50	= 96.0%
CH	= 41/46	= 89.1%	CH	= 41/50	= 82.0%
CS	= 44/51	= 86.3%	CS	= 44/50	= 88.0%

4.4 TELUK DATAI CORAL REEFS

4.4.1 Condition of the reefs

Most reefs observed in the control area are located at Teluk Datai, Teluk Temurung and Teluk Nyiur. Details of the reefs drawn from the aerial photographs of 1989 are shown in Figure 4.7. Details of the reefs in 1994 are shown in Figure 4.8.

The breadth of the reef was estimated to extend from 50 m to 300 m from shoreline. The area of each reef feature was determined from the aerial photographs. These statistics of the area are given in Table 4.3. The corals dominated approximately 461,250 m^2 of the reef in 1989. About 326,250 m^2 of this particular area was covered by ≥50% live corals, while the remaining 135,000 m^2 was covered by ≤50% live corals. These coral areas were found distributed in patches. In 1994 the total area dominated by these corals was approximately 409,500 m^2. About 247,500 m^2 was covered by ≥50% live corals, while the remaining 162,000 m^2 was covered by ≤50% live corals. There is a decrease of 78,750 m^2 of ≥50% live coral coverage and an increase of 27,000 m^2 ≤50% live coral coverage. These changes indicated that the coral reef condition is deteriorating in terms of live coral coverage.

The sandy beach covered the second largest area *i.e.* about 236,250 m^2 in 1989. This sandy beach stretches mainly along Teluk Datai. In 1994, the sandy beach area was estimated as 210,000 m^2. There is a decrease of 36,250 m^2 of sandy beach within 5 years. This change could be due to beach erosion. The quality of the aerial photographs could also affect the area estimation of the sandy beach. The accuracy of reef feature boundary delineation may be reduced if the quality is not satisfactory.

Sand, pebbles, and rocks covered an area of approximately 180,000 m^2 in 1989 while in 1994, the area is approximately 181,250 m^2. The difference of 1,250 m^2 may be disregarded because errors that might occur during the reef feature boundary delineation.

The rocky shores covered 123,750 m^2 of the area in 1989. An increase was observed in 1994 where the rocky shores covered an area of about 135,500 m^2. The increase is probably due to the increase in dead coral coverage mentioned earlier.

Figure 4.7: Reef Characteristics of Teluk Datai Coastal Zone in 1989 (Source: Lee, 1994)

Figure 4.8: Reef Characteristics of Teluk Datai Coastal Zone in 1994 (Source: Lee, 1994)

Dead corals *i.e.* the coral debris covered an area of 56,250 m^2 in 1989 and this was found between Teluk Nyior and Teluk Temurung. Coral debris coverage increased two-fold by 1994, *i.e.* 108,000 m^2.

Table 4.3: Area coverage of the reef features on the reef flats of the sandy area in 1989 and 1994. (Source: Abdullah et. al, 2002)

Reef Feature	Area (m^2)	
	1989	1994
Sand	236,250	210,000
Sand/Pebble/Rock	180,000	181,250
Rock	123,750	135,500
Live Coral (≤50%)	135,000	162,000
Live Coral (≥50%)	326,250	247,500
Coral Debris	56,250	108,000
Mud	22,500	26,250
Mangrove	7,500	6,750
TOTAL	1,087,500	1,077,250

A patch of mud flat was detected near Teluk Nyior covering an area of approximately 22,500 m^2 in 1989. An area of 26,250 m^2 of mud flat was observed in 1994. This increase of 3,750 m^2 was probably the result of increasing sedimentation rate around Teluk Nyior.

A small mangrove area was also found at Teluk Datai and it covered about 7,500 m^2 in 1989. In 1994, the area was estimated as 6,750 m^2. Again this change may be disregarded because of errors that might have occurred during the reef feature boundary delineation.

Typical reef profile of Teluk Datai offering cross-sectional views were also drawn during ground truth surveys. Reef profiles of Teluk Datai drawn by the author with its reef morphology are given in Figures 4.9(a)-(d).

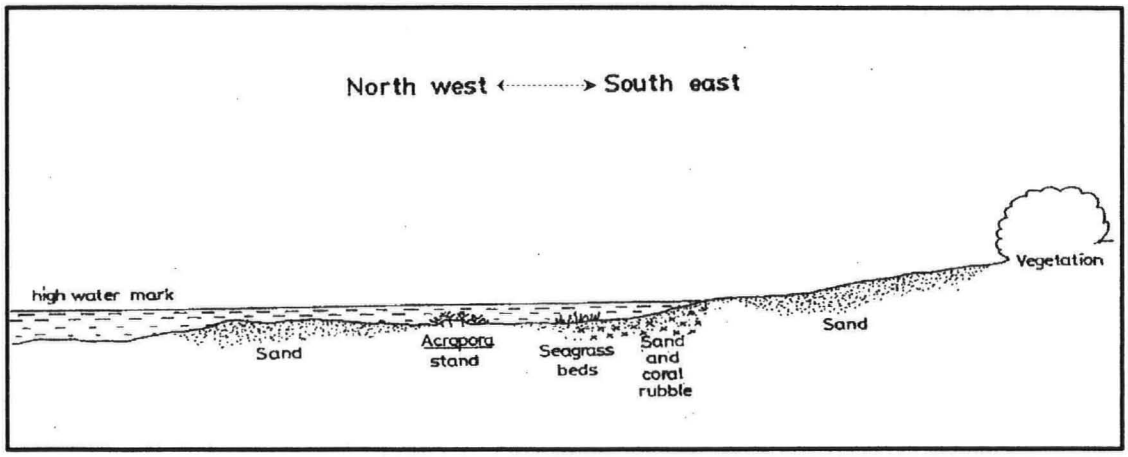

Figure 4.9 (a): Cross-sectional area of Reef Profile I, showing reef morphology of Teluk Datai (Drawn by the author)

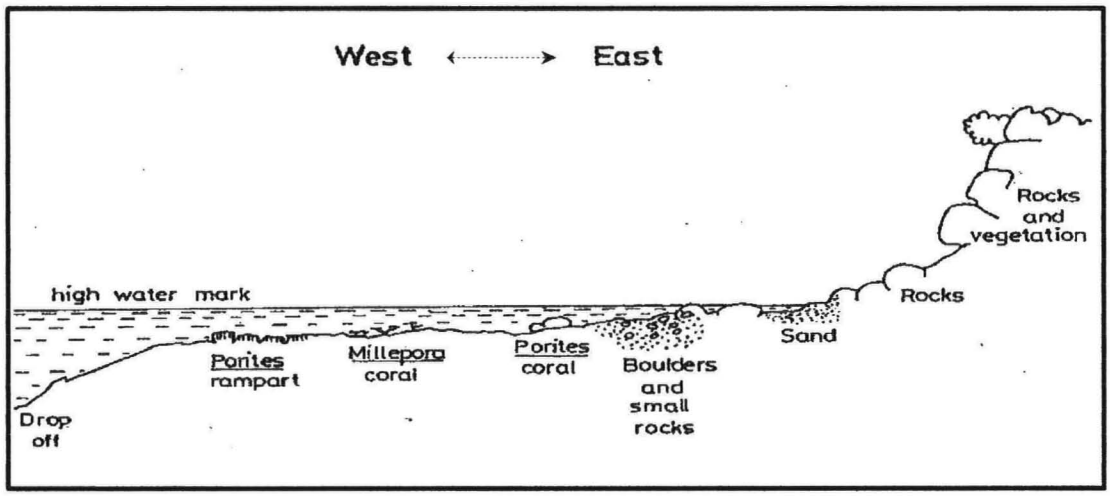

Figure 4.9 (b): Cross-sectional area of Reef Profile II, showing reef morphology of Teluk Datai (Drawn by the author)

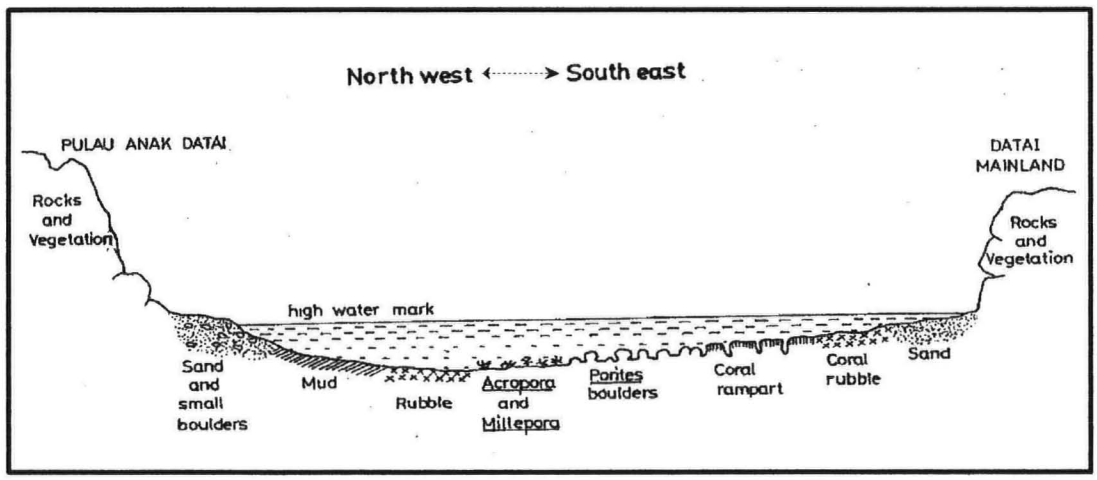

Figure 4.9 (c): Cross-sectional area of Reef Profile III, showing reef morphology of Teluk Datai (Drawn by the author)

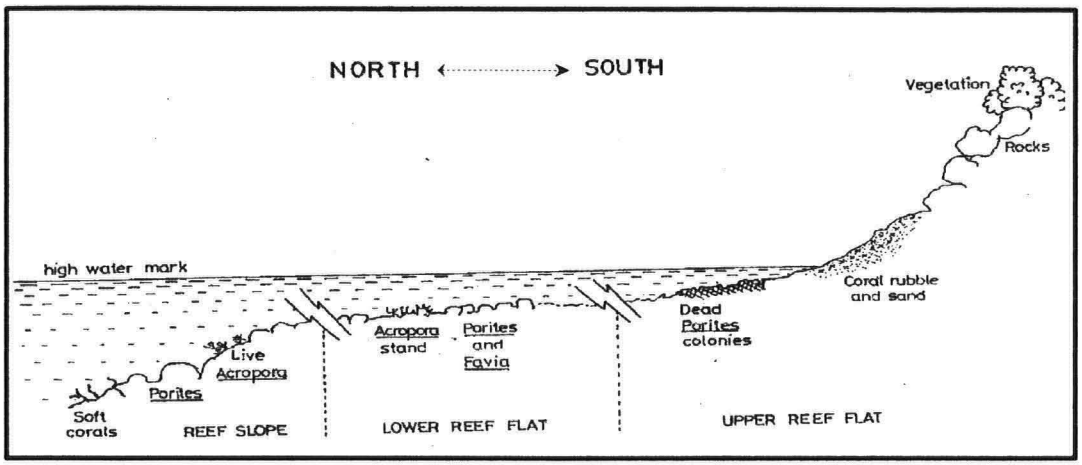

Figure 4.9 (d): Cross-sectional area of Reef Profile IV, showing reef morphology of Teluk Datai (Drawn by the author)

4.4.2 Accuracy Assessment

Results of accuracy assessment are given in the published work of the author, Abdullah *et al* (2002) in Appendix 5 (pages 6 – 8).

Overall accuracy computed for the reef features of 1989 map is 74.9% while the overall accuracy for 1994 map is 84.3%. The results of overall accuracy obtained were as expected *i.e.* higher in 1994 and much lower for 1989 map. This is because ground truthing was carried out in 1997. A large area had undergone changes since 1989, the pre-development period, and therefore overall accuracy should be much lower as the reference or observed data were based on the ground truthing date. If ground truthing was carried out the same year or time during data acquisition, accuracy would be expected to increase to possibly 90% or more depending on the quality of the remotely sensed data (aerial photographs) as well as the knowledge of the analyst on the study area.

Similarly, producer's and user's accuracy are expected to be higher for 1994 map compared to the 1989 map. Good accuracy results were obtained in this study because the percentage range obtained was high, 62.5% to 100% for producer's accuracy; and 64.8% to 100% for user's accuracy. This is also an indicative of good quality aerial photographs obtained where various reef features were clearly shown in different tones, texture and pattern.

4.4.3 A comparison of species diversity between Teluk Dedap and Teluk Datai

The list of hard coral species and commonly shared coral species of the study area, Teluk Dedap reef, and the control site, Teluk Datai reef are given in Appendix 6.

(1) Species Richness of Teluk Dedap Fringing Reefs

There are a total of 37 hard coral species within the study area. These species comprised of 4 sub-orders, 10 families, and 22 genera. The dominant family in this reef is the Faviidae, with the most number of species and live coral cover. Dominant species appeared to be *Goniastrea, Favia, Favites* and *Platygyra*. The next dominant family is Poritidae with its dominant species being the *Porites* that firmed the structural basis for the entire reef.

Other species appear to be randomly distributed throughout the reef. *Fungia* were normally found living in congregation in tidal pools during low water. Other genera seemed to occur in patches on the reef mainly the *Acropora, Montipora, Goniastrea* and *Galaxea* colonies. *Galaxea fascicularis* is dominant on the reef edge, forming large submassive colonies.

Various other organisms were found on Teluk Dedap reef and these include anthozoans, sponges, alcyonaceans, molluscs, and echinoderms. Most sponges found were the encrusting type with vivid hues of purples and reds. The common echinoderms found were mainly holothurians and echinoids. Submarine vegetation were also found here which include turf algaes and most common of all is the *Sargassum* sp.

(2) Species Richness of Teluk Datai Fringing Reefs

Both hard and soft corals were found in the coral reefs of the control site, Teluk Datai. The reef edge and slope are the most developed with higher species diversity compared to the reef flat which has fewer coral species. Diversity increases as one approaches the reef rim and slope. Most of the corals found here were the hard coral types while the soft corals were found mainly on the sea bed.

There are 76 species of corals found in Teluk Datai fringing reefs comprising of 35 genera. There are a total of 14 hard coral families within this fringing reef belonging to 4 sub-orders. Majority of the corals belong to Acroporidae, Faviidae and Poritidae families. These groups of corals are known to be tolerant to intermediate sediment load in the water column (Yasin, *pers. comm.*).

Submassive and branching corals were commonly found at the reef flats and these were dominated by the *Porites*, and *Acropora* species. Massive boulders of *Porites, Favia, Favites* and *Platygyra* species were found towards the reef edge where diversity is commonly higher. Encrusting and foliose corals were also found around these solid massive corals. Free-living corals of *Fungia* however, formed the solitary ones that were normally scattered throughout the reef. Few tabulated forms of *Acropora* corals were found mainly along the reef slope.

As in the case of a typical tropical fringing reef, other types of reef organisms were also found at Teluk Datai. These include the vivid coloured sponges, ascidians, molluscs, submarine vegetation (*Sargassum* sp.) and echinoderms (holothurians and echinoids).

Using the Jaccard's Index, faunal diversity or resemblance was calculated as follows:

If :

$C = 24$ (number of shared species)

$N_1 = 76$ (number of species in Teluk Datai)

$N_2 = 37$ (number of species in Teluk Dedap)

Jaccard's Index $= [24/(76 + 37 - 24)] * 100$

$= \mathbf{27\ \%}$

Result of the Jaccard's Index showed that there were only 27 % of coral similarity between the fringing reefs of Teluk Datai and Teluk Dedap. This would also mean that corals found (*i.e.* coral samples collected in the same year for both sampling locations) within these two regions are quite diverse. Studies by Abdullah and Yasin (2001; 2003) showed that Teluk Datai fringing reef was 17 times larger than the Teluk Dedap reef. The larger reef area would provide larger space for coral larval settlement.

4.5 NORTH LANGKAWI FRINGING REEF ASSESSMENT

Generally, the reef topography can be divided into three categories *i.e.* the reef flat, reef rim/slope, and sea bed. Coral diversity is relatively low on west coast reefs of Peninsular Malaysia because of the turbid water conditions and muddy substrate (Chua and Charles, 1980). Inflow of large rivers resulted in turbid water conditions along the Straits of Malacca region and restricted the ability of coral growth (Wood, 1984).

Comparing the two fringing reefs of north Pulau Langkawi, Teluk Datai reefs are found to be more extensive and diverse than the one found in Teluk Dedap. The reef features are more continuous in Teluk Datai resulting in large patches of live coral growths. In Teluk Dedap, live coral growths are also patchy but small and appeared to be more sporadic like.

The reefs in Teluk Datai covered an area of 1,077,250 m^2 (1994) and this is very extensive compared to the reef found in Teluk Dedap, Tanjung Rhu which is 63,000 m^2. Table 4.4 shows the percentage of each reef feature in relation to its total size for both Teluk Datai and Teluk Dedap fringing reefs. Dominant reef features at Teluk Dedap fringing reefs in descending order are sandy beach, coral debris and mudflats. In Teluk Datai the dominant reef features in the same order manner are ≥50% live corals, sandy beach, and combination of sand/pebble/rock area. Live coral coverage in Teluk Dedap in Tanjung Rhu study area is very small compared to the ones found in Teluk Datai. Total live coral area in Teluk Dedap reef is just about 12% while in Teluk Datai live corals covered approximately 38% of its reef. 'Dead' reef areas which is normally mudflats covered a large space in Teluk Dedap (26.59%) compared to only 2.43% in Teluk Datai. The reef in Teluk Datai is also rockier than that found in Teluk Dedap. However, no mangrove stands were found in Teluk Dedap mainly because there wasn't any existing river within the small study area.

Table 4.5 compares the hard coral species richness found in both Teluk Datai and Teluk Dedap fringing reefs of north Pulau Langkawi. Dominant hard coral families in Teluk Dedap reef belong to Faviidae and Poritidae. In Teluk Datai dominant hard coral families belong to Acroporidae, Faviidae and Poritidae. As mentioned earlier these groups of hard corals, Faviidae and Poriitidae, are the hardier ones that seemed to be able to tolerate intermediate sediment load hence more turbid waters (Yasin, *pers.comm.*). These groups of corals tend to form distinguishable submassive and massive coral boulders towards the reef edge.

Figure 4.10 compares the hermatypic coral species found in both Teluk Datai and Teluk Dedap fringing reefs of north Pulau Langkawi. This was based on the number species found in each family.

Table 4.4. Comparison of reef features in percentage area coverage for Teluk Datai and Teluk Dedap, Pulau Langkawi.

Reef feature	**Teluk Dedap (1999)**	**Teluk Datai (1994)** (Source: Abdullah *et. al*, 2002)
Sand	29.84	19.49
Sand/Pebble/Rock	1.59	16.83
Rock	1.19	12.58
Live coral (≤50%)	7.94	15.04
Live coral (≥ 50%)	4.28	22.98
Coral Debris	28.57	10.03
Mud	26.59	2.43
Mangrove	-	0.62

Table 4.5. Comparison of species richness of hard corals of Teluk Datai and Teluk Dedap, Pulau Langkawi.

	Teluk Dedap	Teluk Datai
Class	1	2
Order	1	2
Sub-order	4	4
Family	10	14
Genus	22	36
Species	37	76

Corals of the Hydrozoan class were found in Teluk Datai reef but absent in Teluk Dedap. However, only 2 species of this group were found in Teluk Datai. The number of coral species in Teluk Datai is twice of that found in Teluk Dedap. It is not valid to state that species richness is related to the extent of a reef because it is known that coral reefs are not uniform in their composition. In some areas they built from several hundred species such as that found in the Great Barrier Reef, and in others from 40 (Hawaii) or less (eastern Pacific) (Wood, 1984).

Studies by Wood (1984) stated that the richness of different reef areas, the position of faunal centers, the distribution of coral genera and species and the similarities between different reef areas are not attributable to any single factor. Instead, they result from the combination of past and present geological and environmental events.

Distribution of corals is governed by a multitude of factors and is not a predictable subject. Larval settlement involves a certain amount of choice of substrate and location. Environmental factors such as water depth, type of substrate and forces of swell and current also play important part both in successful establishment and subsequent growth. The final pattern of distribution of coral colonies and the way in which they and the reef grow produce a variety of habitats and microhabitats. These habitats each encourage growth of certain species or forms of coral and a particular type of associated or visiting fauna. The zone generally subjected to the most variable conditions is the reef crest or reef flat. Corals may be exposed to air and direct sunlight during low tides, to changes in salinity and to strong wave action. Species diversity is often limited because of these environmental constraints. Much the same applies to the back reef zone, which lies to the leeward and usually landward side of the reef crest. Here, corals have to withstand exposure to sun and air. In addition, there is relatively little water movement and sediments tend to accumulate. This is clearly seen from the mudflats fringing the sandy beach at the back reef zone of Teluk Dedap. The fore reef lies to the seaward side of the reef crest, and the shallower regions are typically the most actively growing and diverse within the reef habitat as a whole. This in itself explains the distribution of live corals on the lower reef flats of the study area.

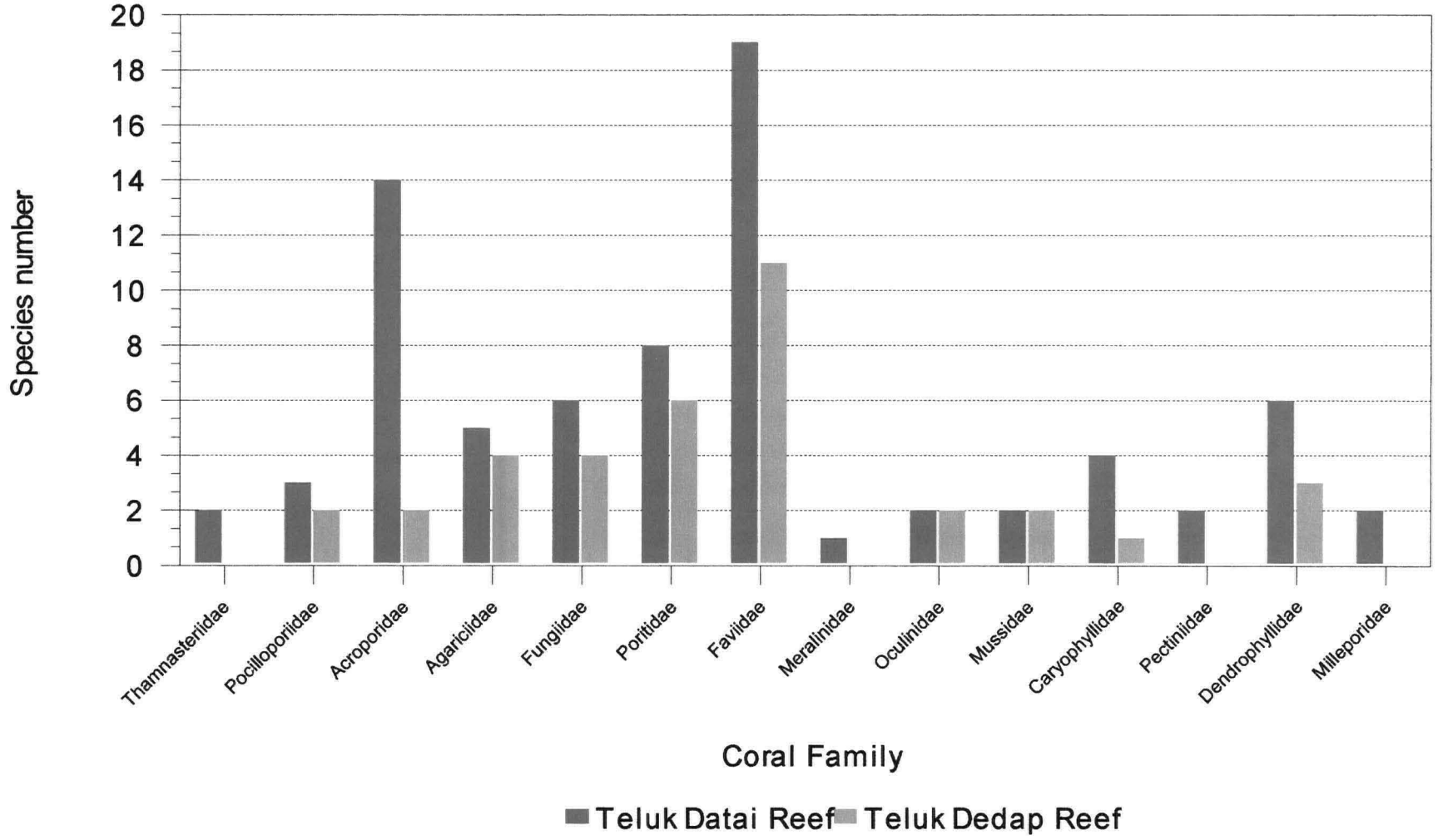

Figure 4.10. Hermatypic coral species compositions of Teluk Datai and Teluk Dedap fringing reefs.

4.6 SUMMARY

Based on the list of coral species found and surveyed at both Teluk Dedap and Teluk Datai reefs, it would be logical to say that Teluk Datai (the control area) is richer in terms of diversity. However, if the aspect of reef area coverage were to be considered in relation to species richness, it would be valid to state that Teluk Dedap (the study area) is richer in diversity as compared to the control site. This is because the size of estimated reef area in Teluk Datai is about 17 times larger than that found in Teluk Dedap but the difference is only two-fold in terms of species diversity at generic and species level. The Jaccard's Index calculated for the two fringing reefs showed a value of 27 % of which it can be concluded that the two fringing reefs set at opposite ends of north Langkawi are quite diverse in its hermatypic coral compositions.

The reef condition in Teluk Datai however, appeared to be healthier than that found in Teluk Dedap mainly because:

i. percentage of total live coral coverage is larger in Teluk Datai,
ii. percentage of $\geq$ 50% live coral coverage is much larger in Teluk Datai,
iii. coral debris (coral rubble zone) is larger in Teluk Dedap indicating possible increasing coral deaths and destruction,
iv. mudflats or the dead zone is larger in Teluk Dedap,
v. Teluk Datai reef is more extensive, an indication of larger space provision for coral larval settlement for reef building process.

The distribution of coral reefs does not necessarily reflect the limits of distribution of corals themselves. Hermatypic corals often grow successfully without actually forming reefs. Neither are coral reefs uniform in their composition. This is clearly seen from the two reefs mapped in the north of Pulau Langkawi itself, the Teluk Datai and Teluk Dedap fringing reefs. Therefore it is not crucial to look at the extent of a reef but rather its richness.

Chapter 5

SEDIMENT FALLOUT IN TANJUNG RHU CORAL REEFS

5.1 LITERATURE REVIEW

Erosion on upland soils is a major global problem around the world (Brown, 1984; Brown and Wolf, 1984; Pimentel *et al.*, 1987). About 50% of this detached soil reaches a waterway where it impacts water quality (Robinson, 1971), aquatic productivity (Cooper, 1986), wildlife habitats (Ritchie, 1972) and other components of aquatic ecosystem structure and function. Sedimentation is an explanation for the absence or paucity of coral reefs, especially in South and East Asia, Indonesia and Melanesia, where rivers deliver 70% of the global sediment transported to the oceans (e.g. Ganges-Brahmaputra: 1670 million tonnes/year; Yangtze/Chan Jiang:480 million tonnes/year; Irrawaddy:265 million tonnes/year; Mekong:160 million tonnes/year; Taiwan rivers:185 million tonnes/year; Purari and Fly in Papua New Guinea:110 million tonnes/year) (Milliman and Meade, 1983). Settled particles may be re-suspended several times before final burial in bottom sediments.

Sediment is defined as particulate organic or inorganic matter which accumulates in a loose, unconsolidated form. It may be chemically precipitated from solution, secreted by organisms, or transported from land by air, ice, wind, or water and deposited (Gross, 1972).

Classification of sediments

Sediment particles are classified in two different ways - by source and by size. The size of particles determines how far they can be transported by moving water or air. Small grains like clays can reach the middle of the ocean in very slow currents, while pebbles can be moved only by fast moving rivers or waves on beaches. In general larger particles are deposited close to land while the smallest particles dominate sediments in the open ocean.

By source, sediment particles are divided into the following groups:

- *lithogenous or terrigenous particles*

  These originated from land and are the products of erosion and weathering of rocks in the continents by wind and rain, glaciers and chemical reactions.

- *biogenous particles*

  These particles are produced by living creatures (plants and animals) in the ocean and consist of microscopic remains of predominantly planktonic (drifting) marine organisms

that secrete skeletons of calcium carbonate ($CaCO_3$) - mainly foraminifera and coccolithophores - or silica (SiO_2) - mainly radiolaria and diatoms.

- *hydrogenous particles*

  Also called authigenic sediments, these particles are deposited directly from seawater through chemical reactions. Examples are metalliferous sediments that precipitate from hydrothermal vents (black smokers) and manganese nodules in low sedimentation rate regions.

- *volcanic particles*

  These sediments come from ash ejected during eruptions, carried by winds and rivers.

- *cosmogenous particles*

  These are tiny fragments of meteorites and comets from space.

By size, sediment particles are classified into 7 categories (See Table 5.1). These size fractions are based on the Wentworth Scale. Particle size is an important property of sediments because it determines the mode of transport and also determines how far particles travel before settling to the bottom. How well sorted the sediments are in the environment depends greatly on the wave and current actions. A well-sorted sediment is one in which a limited size range of particles occurs, the other-sized particles have been removed usually by mechanical means such as that of the waves and currents. Beach sand is a typical well-sorted sediment, in which particles have been segregated by size. A poorly-sorted sediment contains particles of many sizes, usually indicating that little mechanical energy has been exerted to sort the different particle sizes.

Sand usually occurs along coastlines where waves and currents have removed the finer particles, depositing them in deeper water.

Sources of Sediments on Reefs

Sediments are usually defined as solid particles that fall under gravity to the bottom. It also includes the finer particles that remain in suspension in the water column which are normally termed Suspended Particulates or Suspended Solids.

Natural sedimentation does occur. The major contributor to this is re-suspension which on reefs is caused by the wave and current forcing on the sediment particles lifting them off the bottom. Such natural sedimentation is tolerated by the reef corals. Basically the sediment fallout on a coral reef can arise naturally from the resuspension of the bioeroded skeletal remains of reef organisms,

which are then transported by water movement to living corals elsewhere on the reef. The sediment naturally produced in the reef system consists predominantly of organic carbonates and are known as bioclastics (Randall and Birkeland, 1978). As these sediments are continuously produced, the organisms associated with reefs are generally adapted to such continuous long term patterns of production and distribution.

Table 5.1. Classification of sediment particles by size (Wentworth Scale). (Source: Briggs (1977))

Size Fraction	Particle Diameter (millimeters)
Boulders	>256
Cobbles	64 - 256
Pebbles	4 - 64
Granules	2 - 4
Sand	0.062 - 2 (62 - 2000 μm)
Silt	0.004 - 0.062 (4 - 62 μm)
Clay	< 0.004 (< 4 μm)

In addition to the natural sedimentation are the allochtonous inputs of materials onto reefs especially from terrigenous processes, such as the physical and chemical breakdown of soils, soil erosion, etc. These sediments consist largely of non-calcareous clay, silt and organic detritus. The sediment derived from terrestrial sources is not uniform in quality, quantity and time. Generally, the sediment is concentrated around river mouths, and is transported in the form of pulses associated with periods of heavy rainfall. The distance transported depends on the strength and continuity of local ocean currents. Fine particles, particularly clay, tend to stay in suspension longest and are transported furthest due to their low settling velocity. The degree of mixing of the river water in the sea will affect the concentration of suspended sediments, which is dependent on sea conditions and therefore weather. This suspended sediment gradually falling out of suspension may be considered true 'sedimentation' as opposed to 'sediment fallout', which includes re-suspended bioclastics. The suspended fine terrestrial sediments cause the water to be turbid, reducing visibility and light penetration.

Anthropogenic activities can lead to significant sedimentation which can be harmful to reefs. An example is the sediment arising as a result of coastal development from land reclamation,

(a) Sediment fraction > 1000 μm, Trap 1(reef flat), Teluk Dedap (Dry season, 2-19 February 1999)

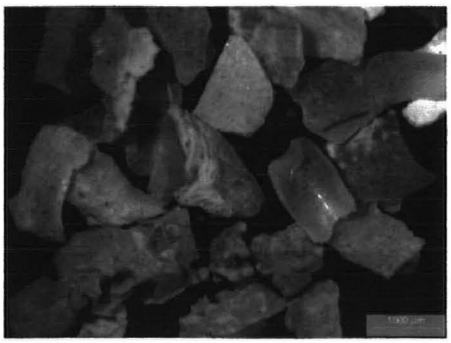

(b) Sediment fraction 710μm - 1000 μm, Trap 1 (reef flat), Teluk Dedap (Dry season, 2-19 February 1999)

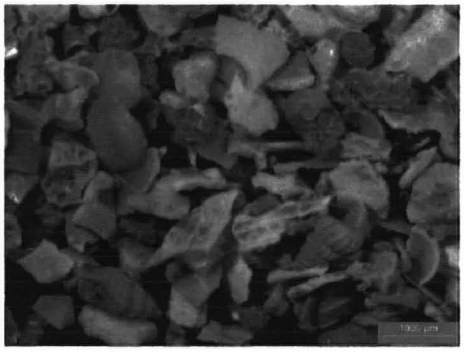

(c) Sediment fraction 500 μm - 710 μm, Trap 1 (reef flat), Teluk Dedap (Dry season, 2-19 February 1999)

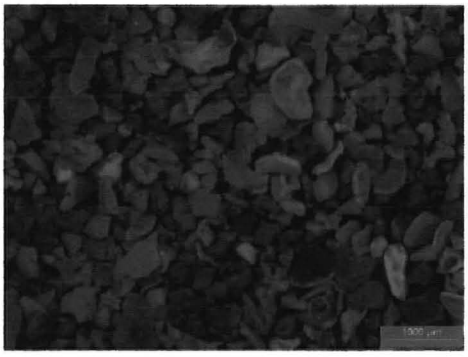

(d) Sediment fraction 250 μm - 500 μm, Trap 1 (reef flat), Teluk Dedap (Dry season, 2-19 February 1999)

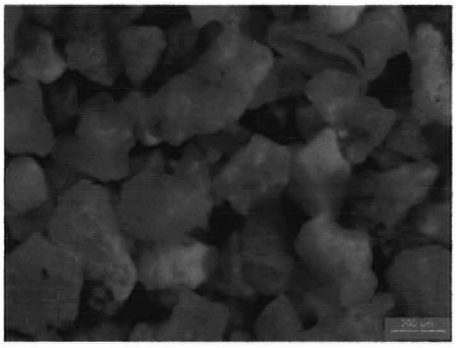

(e) Sediment fraction 212 μm - 250 μm, Trap 1 (reef flat), Teluk Dedap (Dry season, 2-19 February 1999)

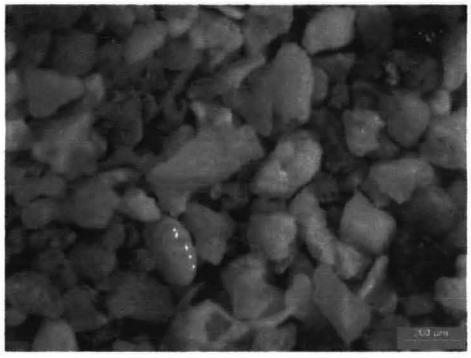

(f) Sediment fraction 125 μm - 212 μm, Trap 1 (reef flat), Teluk Dedap (Dry season, 2-19 February 1999)

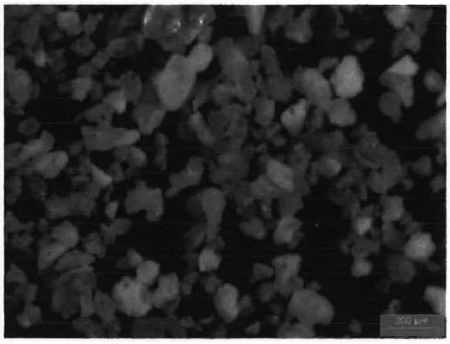

(g) Sediment fraction 63 μm – 125 μm, Trap 1 (reef flat), Teluk Dedap (Dry season, 2-19 February 1999)

Figure 5.14. Sediment particles observed under microscope for sediment fractions collected from Teluk Dedap (1999).

(a) Sediment fraction > 1000 μm, Trap 1 (reef flat), Teluk Datai (Dry season, 2-19 February 1999)

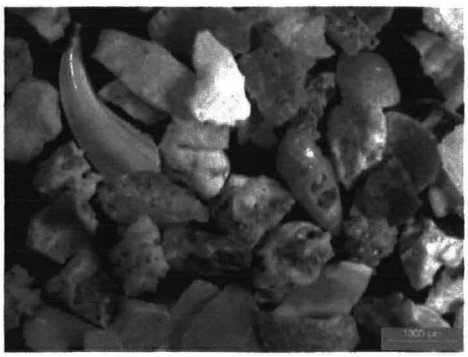

(b) Sediment fraction 710μm - 1000 μm, Trap 1 (reef flat), Teluk Datai (Dry season, 2-19 February 1999)

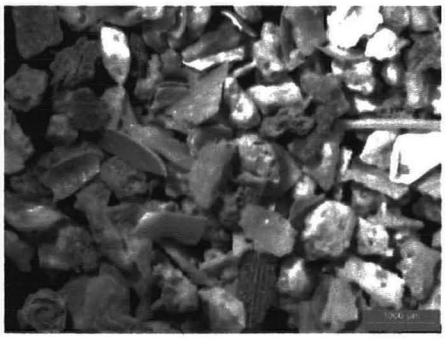

(c) Sediment fraction 500 μm - 710 μm, Trap 1 (reef flat), Teluk Datai (Dry season, 2-19 February 1999)

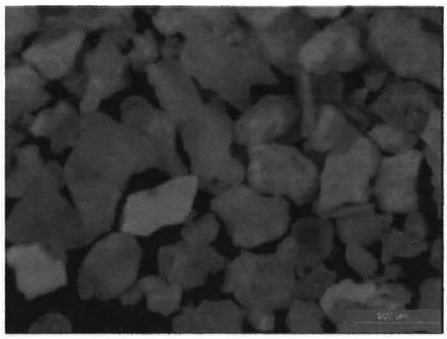

(d) Sediment fraction 250 μm - 500 μm, Trap 41 (reef slope), Teluk Datai (Dry season, 2-19 February 1999)

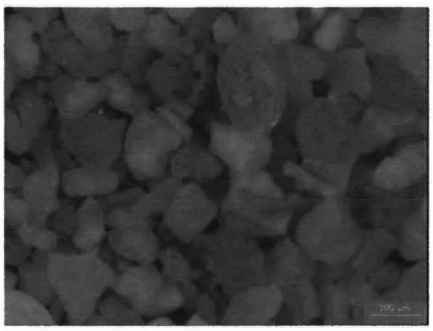

(e) Sediment fraction 212 μm - 250 μm, Trap 41 (reef slope), Teluk Datai (Dry season, 2-19 February 1999)

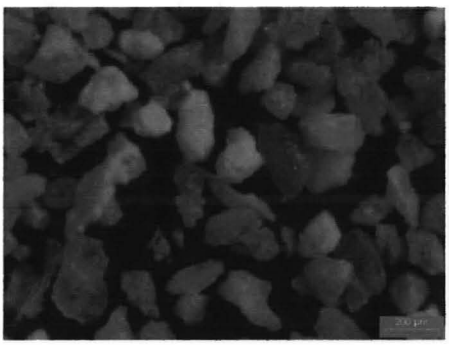

(f) Sediment fraction 125 μm - 212 μm, Trap 4 (reef slope), Teluk Datai (Dry season, 2-19 February 1999)

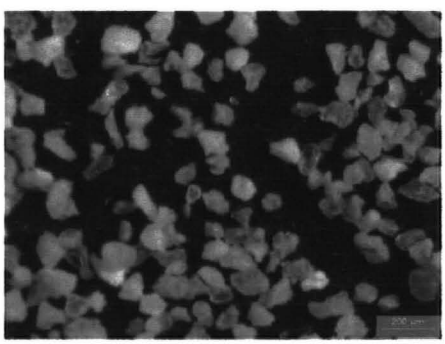

(g) Sediment fraction 63 μm – 125 μm, Trap 4 (reef slope), Teluk Datai (Dry season, 2-19 February 1999)

Figure 5.15 Sediments particles observed under microscope for sediment fractions collected from Teluk Datai (1999).

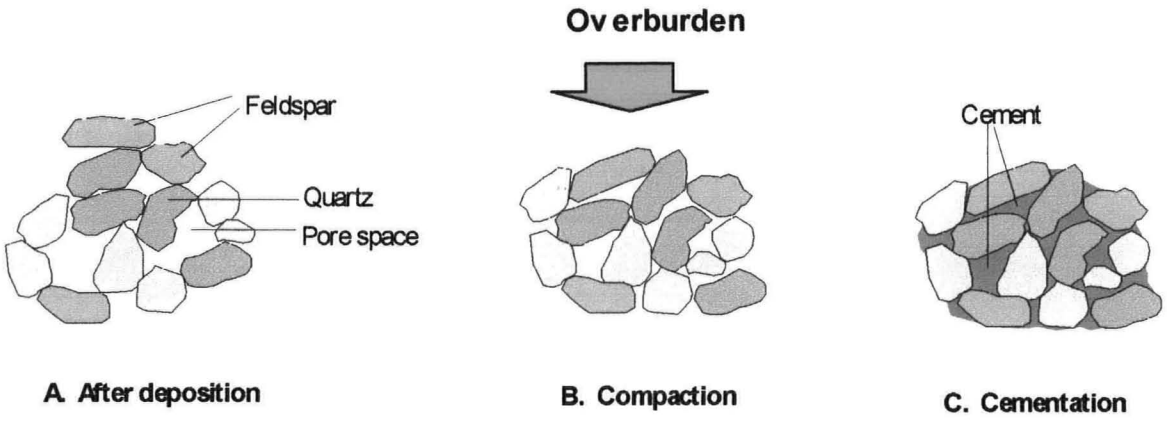

Figure 5.16: A schematic diagram on lithification of reef sediments: (a) deposition of loose grains, (b) weight of overburden compacts sediment particles into tighter arrangement, reducing pore space, (c) precipitation of cement in the pores to bind structure to form clastic texture. (Adapted from: Plummer *et al.*, 2003)

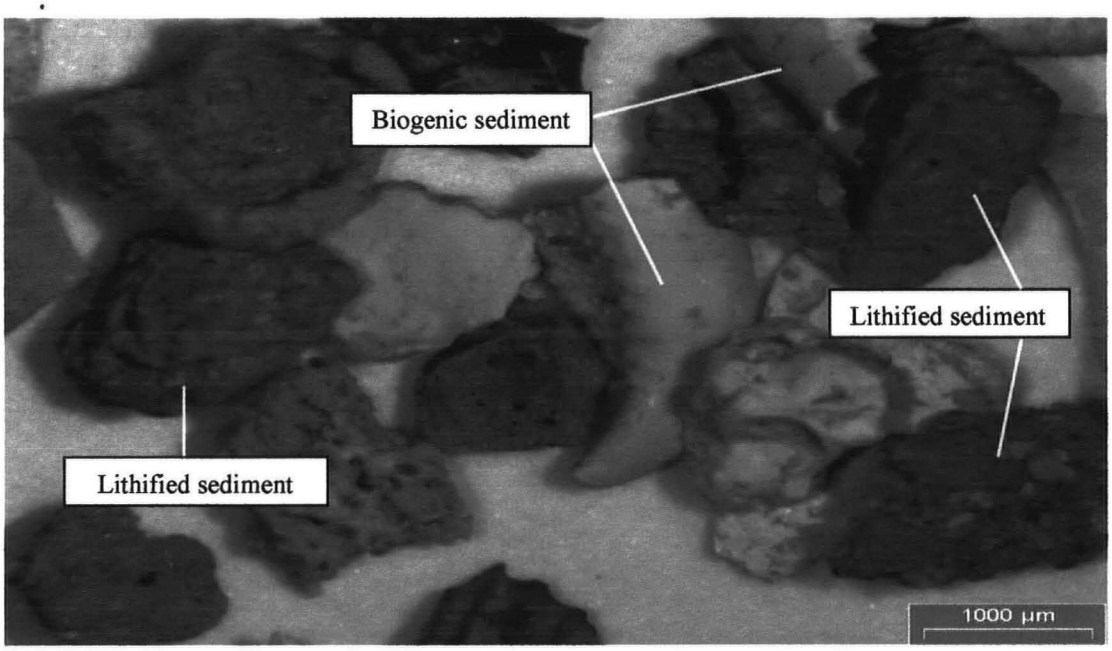

Figure 5.17: Lithified and biogenic sediments observed using microscope from sediment fraction size > 1000µm in Teluk Dedap during dry season (2-19 February 1999).

marina construction, golf course development, shrimp farm development, airport construction, tourist resort construction, coastal road construction, etc (Yasin, 1993).

The objective in this section of research study is to measure and compare the sediment fallout rates of Teluk Dedap in Tanjung Rhu with its control site in Teluk Datai during the wet and dry seasons. It was thought that this would provide an insight to the sedimentation problem which is also related to the suspended particulates present in the water column of Tanjung Rhu.

As mentioned in the previous chapter, Teluk Datai was chosen as the control site because it has an ecosystem similar to the impacted Teluk Dedap and both were located on the north of Pulau Langkawi.

5.2 SAMPLING METHODOLOGY

5.2.1 Sediment Trap Design

A survey of the literature revealed that there is no standard method of collecting sedimenting particles in a coral reef environment (Gardner, 1977, Newman, 1984). Methods to date have generally shown a high loss of samples (Randall and Birkeland, 1978) and a very high variability between traps within a group (Liew and Hoare, 1979).

Laboratory experiments carried out by Gardner (1977) and Lorenzen *et al.*, (1981) on the design of sediment traps revealed that the basic design used should incorporate a minimum aperture to a length ratio of 1:3 to prevent resuspension and eventual loss of material from the trap.

The rate of sediment fallout was proportional to the area of the base of the trap so a trap should be cylindrical in design although the absolute size was flexible. A trap too large would be unmanageable and hard to place, while one too narrow may present serious fouling problems. The narrow tubes used by Randall and Birkeland (1978) were often inhabited by fish which kept all the tubes clean. This can be overcome by using a grill or wire mesh.

Two other factors need crucial consideration in the designing of the trap for this study. First, it has to be heavy to provide stability and not affected, moved or swept away by the strong currents within the coastal region of Tanjung Rhu. Since the reef area of Tanjung Rhu and its control site, Teluk Datai, are highly subjected to the open ocean currents, heavy sediment trap base is preferable. The second important factor is the sediment fallout sample collection container. It needs to be secured to the heavy base of the trap so that the swift strong currents will not wash it ashore

or into the ocean. At the same time the container should be easily removed from the trap during the course of sampling period.

Based on previous experiments (e.g. Randall and Birkeland (1978), Lorenzen *et al.* (1981)), and the requirements in relation to the study area, a final design was chosen which incorporated the various possibility for a good and reliable sediment trap. The sediment trap designed by the author and constructed with the help from members of the Reef Research Group (Universiti Sains Malaysia) is shown in Figure 5.1. The trap consisted of a concrete base made from a cement and sand mixture to contain 4 collection bottles. Each collection bottle was made of glass and had an internal diameter of 7.2 cm and surface area of 41.87cm^2. The length or height of the bottle is 20.0 cm. The inner circle of the bottle plastic cap was cut out and a 1 cm size wire mesh was fitted to it. The mesh was to prevent large molluscs and fish from entering the collection bottles. Unused inner tyre tubes were cut into strips to be wrapped around each collection bottle and secured with copper wire. This was to ensure the collection bottles stayed intact and in place within the sediment trap.

The total height of the sediment trap (concrete base plus collection bottles) was approximately 30 cm. This allowed the traps to be placed amongst the coral heads or on the seabed with the top no higher than the upper edge of the coral heads. This was considered to provide satisfactory results in terms of collecting sediments that had been resuspended and sediment fallout.

5.2.2 Design of Sediment Sampling Program

Based on the topography of the reefs of Tanjung Rhu (Teluk Dedap) and its control site in Teluk Datai as described in the reef profiles in Chapter 4, two zones were selected for the sediment trap placement: reef flat and reef slope. Ideally there should be three zones i.e. reef flat, upper reef slope and lower reef slope which will allow a more comprehensive comparison. However, since the reef slopes within the study area (Teluk Dedap) were not steep but rather shallow and gradual, only two zones are considered. Although the reef slopes at the control site (Teluk Datai) were a little steeper, only two zones were selected to provide uniformity for data comparison at the later stage.

The locations of the sediment traps in Teluk Dedap and Teluk Datai are shown in Figures 5.2 and 5.3 respectively.

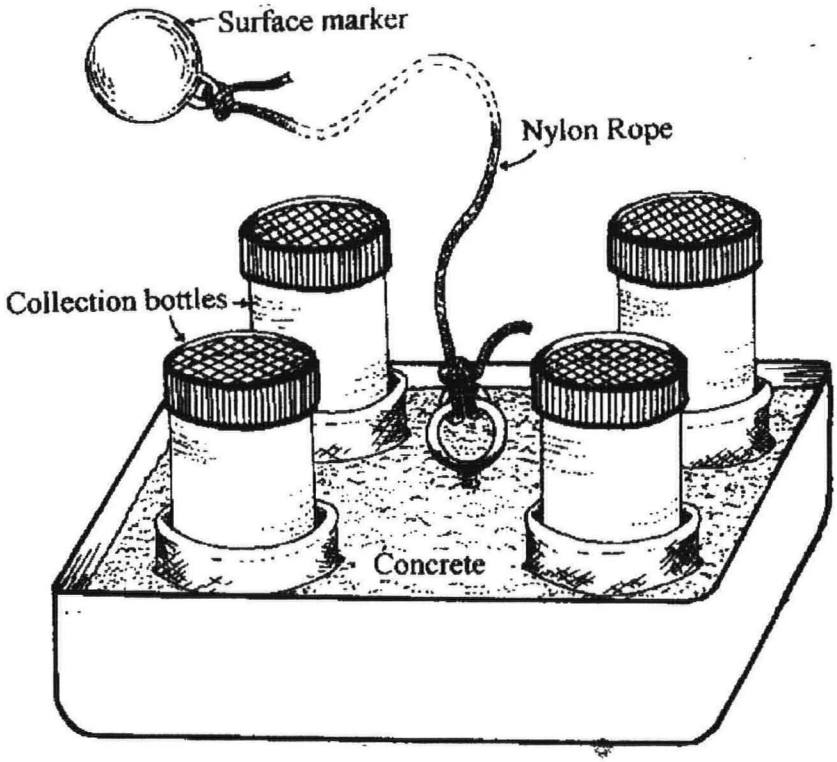

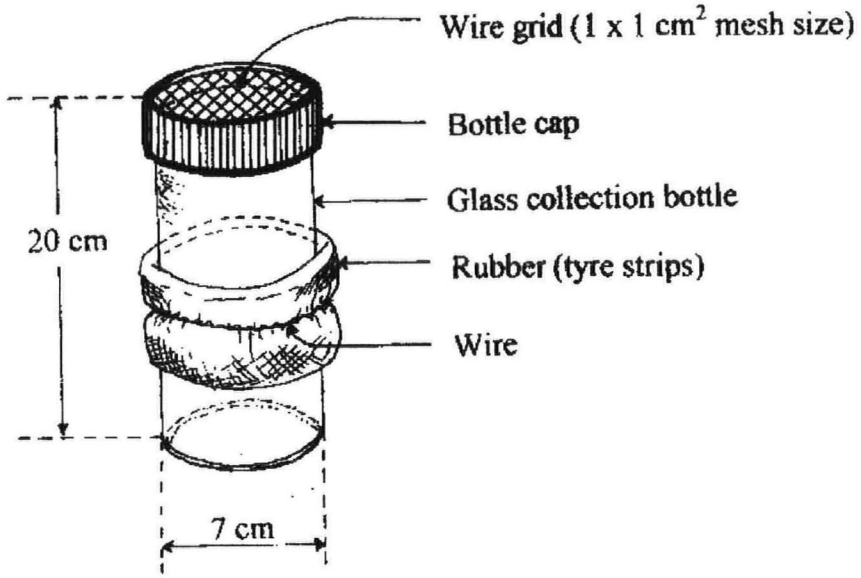

Figure 5.1 Sediment Trap (designed by the author)

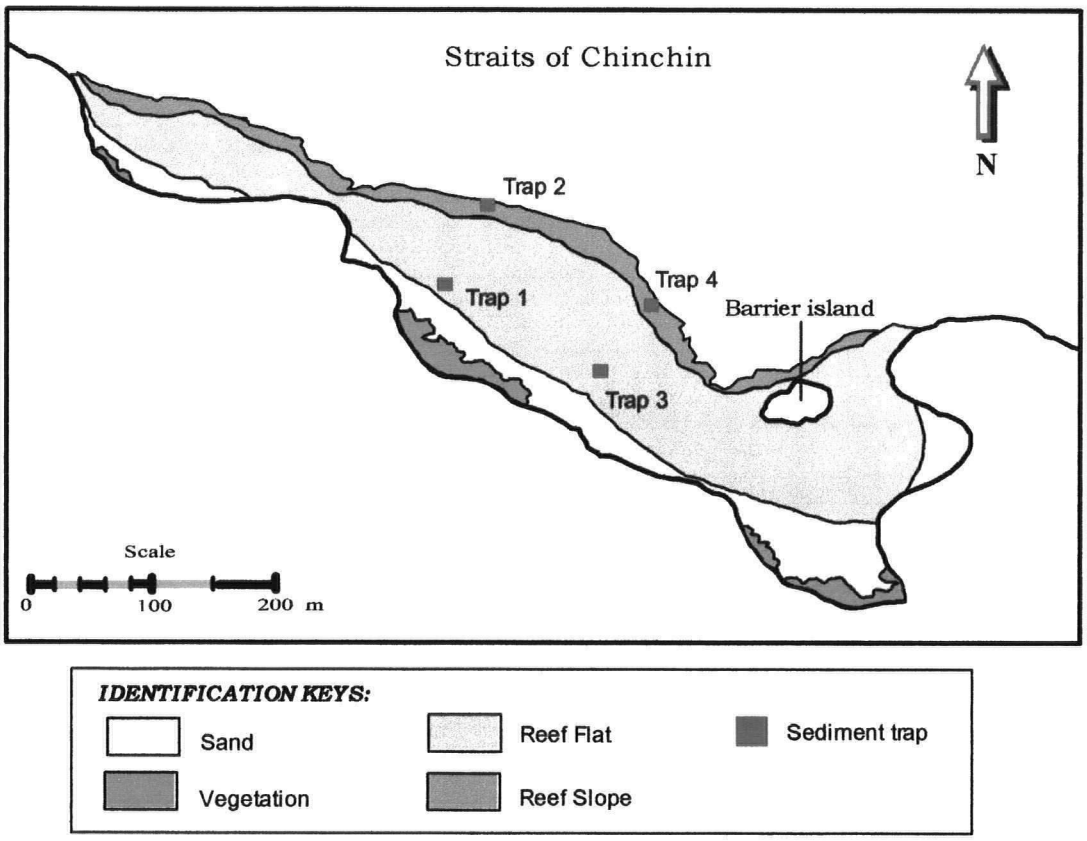

Figure 5.2: Location of sediment traps in Teluk Dedap, Tanjung Rhu.

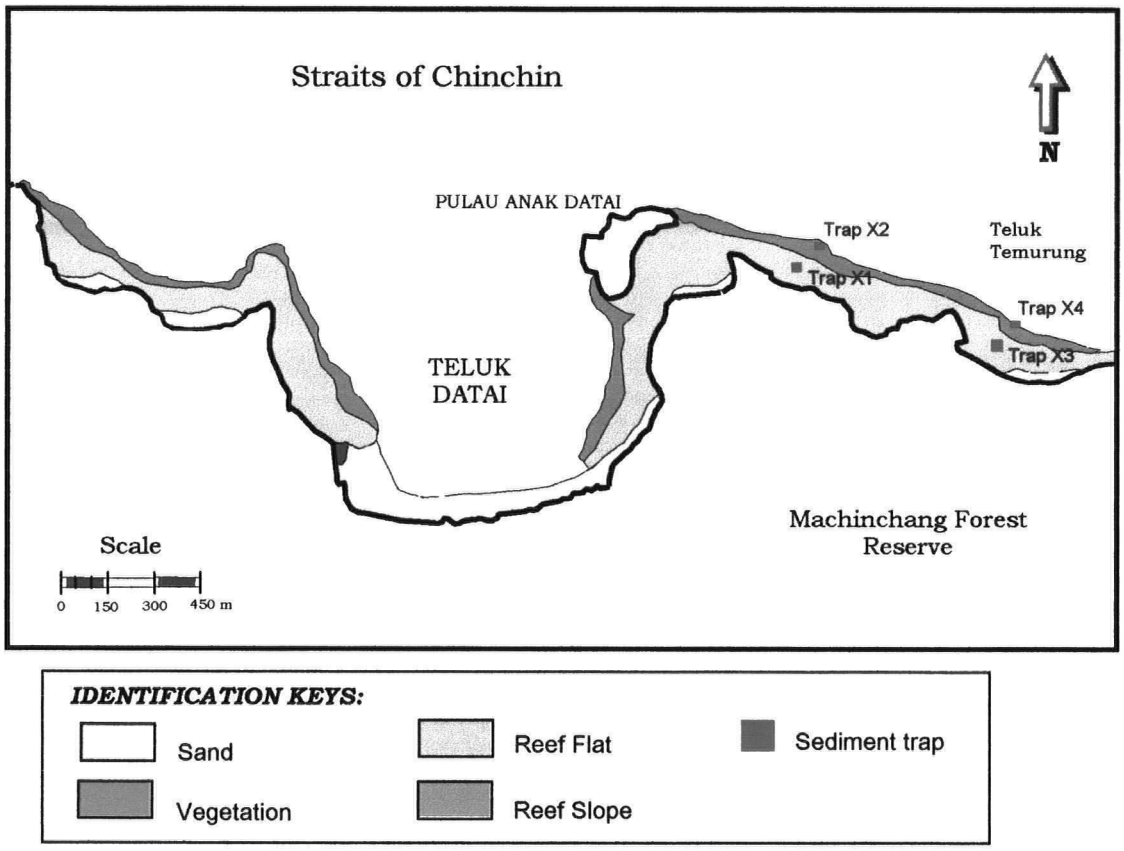

Figure 5.3: Location of sediment traps in Teluk Datai.

The sediment traps were placed on their respective locations during low water spring tides and collections were made in the following low water spring tides. Two replicates of the tidal cycles were carried out for the dry and wet seasons at both sampling sites of Teluk Dedap and Teluk Datai. The rationale behind the low water spring tidal condition chosen for this sampling was that highest sediment fallout was expected to occur during these times as compared to the neap tidal conditions. Lesser sediment fallout is expected during neap tides and therefore may not portray any greater sediment fallout scenario experienced by the reefs.

The tidal ranges during the two sampling periods of the dry and wet seasons are given in Figure 5.4 and Figure 5.5 respectively. The dry season sampling was carried out on 2 – 19 February 1999 for Teluk Dedap (17 days) and 3 – 19 February 1999 for Teluk Datai (16 days); while the wet season sampling was carried out on 10 – 24 July 1999 for Teluk Dedap (14 days) and 11 – 25 July 1999 for Teluk Datai (14 days). The tidal range was 2.9 m during the wet season and 3.1 m for the dry season.

5.2.3 Sediment Analysis

5.2.3.1 Particle Size Analysis (Wet Sieving Method)

The sediments collected were returned to the laboratory and emptied into glass beakers. The beakers were then filled with fresh water and fine material decanted off into a second beaker and allowed to settle. The clear water was siphoned off and replaced with fresh water in both beakers. This process was carried out a minimum of three times to remove salts and until most of the fine material was separated.

The fine material was then wet-sieved through a 63 μm sieve to separate the silt/clay particles. The washings were retained, allowed to settle and the clear water siphoned off. The coarser sediment remaining in the sieve was added to the beaker of coarse sediment and both beakers were placed in the oven at 105°C until they reached a constant weight. It was necessary to remove the fine material before oven drying as otherwise, due to the high proportion of clay, the sediment formed concretions when dried and could not be sieved for particle size and further analysis.

After oven drying the coarse sediment was sieved into the following size series:

- > 1000 μm
- 710 – 1000 μm
- 500 – 710 μm
- 250 – 500 μm
- 212 – 250 μm
- 125 – 212 μm

- 63 – 125 μm
- < 63 μm

The weight of each particle size fraction was recorded. From the total sediment data, a rate of sediment fallout in $g/m^2/day$ was calculated as follows.

To calculate mean weight of dry sediment fractions collected:

$$¼ (W_1 + W_2 + W_3 + W_4) = \mathbf{W} (g)$$

To calculate sediment fallout rate:

Sediment fallout rate = $\mathbf{W} / (\mathbf{A} * \mathbf{T})$ $(g/m^2/day)$

where W = mean weight of dry sediment fractions (g)

A = surface area of sediment trap bottle (41.87×10^{-4} m^2)

T = number of days during collection period

The particle size distribution is given as the percent contribution of each particle size for each sample.

Figure 5.4. Tidal range of dry season sediment sampling at Teluk Dedap, Tanjung Rhu (2 – 19 February 1999) and Teluk Datai (3 – 19 February 1999).
(Source: Tide Tables Malaysia 1999)

Figure 5.5. Tidal range of wet season sediment sampling at Teluk Dedap, Tanjung Rhu (10 – 24 July 1999) and at Teluk Datai (11 – 25 July 1999).
(Source: Tide Tables Malaysia 1999)

5.2.3.2 Microscopic Examination

Representative samples of each sediment sample collected from each zone for the collection periods were examined under the microscope. The purpose of this was to obtain a clearer view of the sediment types.

5.3 SEDIMENT FALLOUT DURING THE DRY SEASON (2 – 19 FEBRUARY 1999)

A comparison analysis of particle size for sediment collected in traps located at the reef flats of Teluk Dedap (Traps 1 and 3) and in Teluk Datai (Traps X1 and X3) showed that Teluk Datai experiences larger variations in its percentage range for different sediment fractions. This is particularly true for particles ranging up to 0.2mm in size. These variations are shown in Figure 5.6. Based on the summation curves shown in Figure 5.6, the composition of sediment collected within the western section of the reef flats of Teluk Dedap and Teluk Datai (Traps 1 and X1) tend to have lesser amount of finer sediment particles of < 0.2mm than in the eastern section of the reef flats (Traps 3 and X3). However, it is observed that larger amounts of finer sediment particles (<0.2mm) were collected within the reef flats of Teluk Dedap and Teluk Datai compared to the larger particles. The percentage for sediment particles of < 0.2mm size ranged approximately 15% to 80%, while for the larger particles of > 0.2mm size the amount collected approximated as 65% to 100%. The similarity of sediment trap placements between the two reefs (Teluk Dedap and Teluk Datai) coupled with the possibility of similar water circulation within these reefs may have

resulted in the similar characteristic of the general composition of larger and finer sediment particles collected during the dry season.

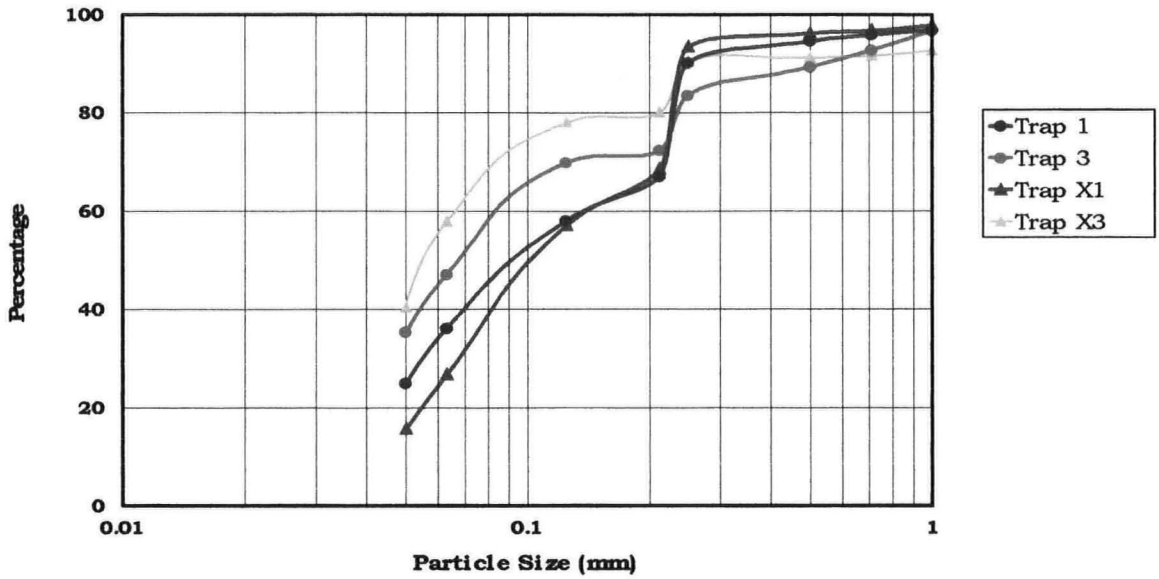

Figure 5.6 : Summation Curves Of Sediment Particle Size Analysis For Sediment Traps At Reef Flats Of Teluk Dedap (Traps 1 and 3) And Teluk Datai (Traps X1 and X3), Pulau Langkawi During The Dry Season (2 - 19 February 1999)

The summation curves in Figure 5.7 showed a different characteristic in the general composition of sediment collected in both reef slopes of Teluk Dedap and Teluk Datai during the dry season. The differences in the amount of different fractions of sediment particles analysed are large ranging from near 0% to 100% compared to the reef flats where the range is 15% to 100%. Within the reef slope regions of Teluk Dedap and Teluk Datai, larger amount of sediment were collected from Trap 2 (Teluk Dedap) and Trap X4 (Teluk Datai). There is no distinction between the east and west as seen in the sediment fractions collected for the reef flats. This shows that the sediment particles would be subjected to a more complex physical movement or activity within the water column at the reef slopes before finally settling to the bottom. The range of finer sediment particles collected is also broad. Trap 4 (Teluk Dedap) and Trap X2 (Teluk Datai) collected lower percentage of sediment particles of < 0.2mm size and this ranged between near 0% to a maximum of 35%. The reverse is observed for Trap 2 (Teluk Dedap) and Trap X4 (Teluk Datai).

Based on the two summation curves (Figures 5.6 and 5.7), it is apparent that most finer sediment particles ($0.06 < x < 0.2$ mm) settled rather quickly within the reef flats of Teluk Dedap and Teluk Datai. The shallowness of the reef flats and their full exposure to air during low water springs probably provide the explanations to the larger portion of finer materials settled within the reef flats here. Furthermore, the small depth and greater intensity of wave actions and erosion occurring

along the reef flats may have trapped the finer particles and resulted in more of such materials being settled here. It is also observed here that the following assumptions (i) finer particles are able to be carried a far greater distance to settle further out into the sea, and (ii) that larger particles will be carried only a shorter distance and settle faster due to their weight, do not apply for the reef flats of Teluk Dedap and Teluk Datai. These however are probably applicable in conditions where the fringing reef areas are relatively deeper and perhaps larger as well. The other aspect that explains the lesser amount of finer sediment particles collected within the reef slope region would be the higher physical wave activity, constant movement of finer materials and the subtidal condition during low water springs would have made lighter, finer materials more difficult to settle.

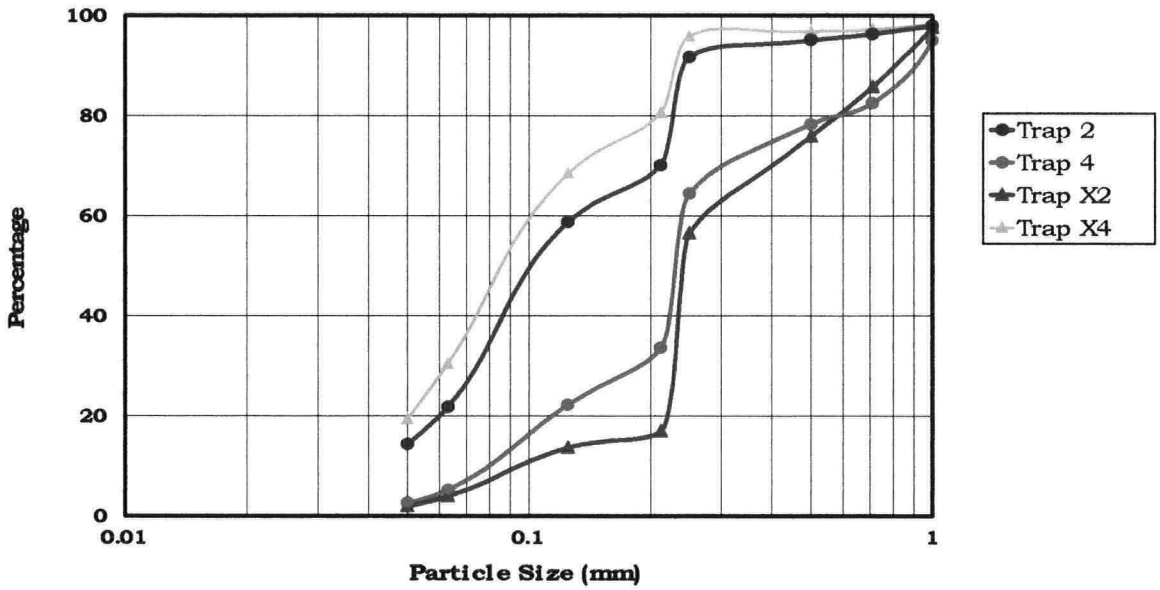

Figure 5.7 : Summation Curves Of Sediment Particle Size Analysis For Sediment Traps At Reef Slopes Of Teluk Dedap (Traps 2 and 4) And Teluk Datai (Traps X2 and X4), Pulau Langkawi During The Dry Season (2 - 19 February 1999)

Figure 5.8 shows a breakdown of the sediment fractions analysed during the dry season for both Teluk Dedap and Teluk Datai. In Teluk Dedap, sediment fraction of >1000 μm were collected mostly in Traps 3 and 4 which were located on the eastern reef flat and reef slope respectively.

Generally, the sediments collected from Teluk Dedap showed higher composition of sediment fractions having > 1000 μm size. At least 60% of the sediment fractions collected for Teluk Dedap fell within the ≤ 212 μm range with the exception for Trap 4. By comparing the sediment fractions collected for traps in Teluk Dedap alone, it was expected that Trap 2 which was directly located at a sudden slope would naturally have a larger portion of finer materials of < 0.06 mm. This was because particularly during low water spring, most fine materials would have been swept directly down from the reef flat onto the slope. Trap 4 on the other hand was placed on a more

gradual slope and lesser finer materials would have been trapped here. Trap 4 also contained the largest portion of sediment fraction size > 1000μm. For Teluk Datai, sediment fractions collected showed greater variations in its composition. Similar to Teluk Dedap, larger amount of sediment fractions were also from the ≤ 212 μm range.

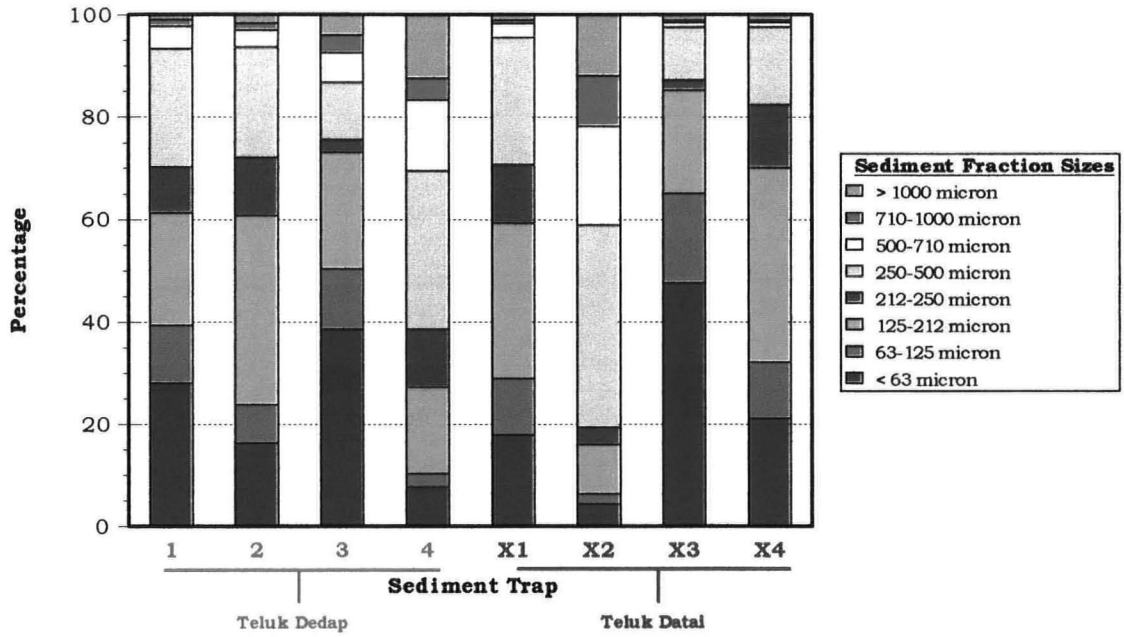

Figure 5.8 : Distribution Of Particle Size Fractions At Teluk Dedap (2-19 February 1999) And Teluk Datai (3 – 19 February 1999), Pulau Langkawi During Dry Season.

A summary of the mean total sediment measured in grams collected during the dry season for Teluk Dedap and Teluk Datai is given in Table 5.2. Almost similar mean total sediment and standard deviation values were measured for the reef flats of the study area of Teluk Dedap (112.5 ± 28.84 g – 119.2 ± 27.08 g). Higher variation is observed for sediment traps located on the reef slope of Teluk Dedap (99.9 ± 8.94 g – 338.4 ± 38.30 g). The same cannot be said for the control site (Teluk Datai) because the measured mean total sediments varied considerably 102.7 ± 13.52 g – 680.8 ± 26.64 g). Mean total sediment appears to be comparatively lower for sediment traps placed on the western region of Teluk Dedap reef (i.e. Traps 1 and 2) as compared to Teluk Datai (Traps X1 and X2). The reverse is observed for sediment traps placed on the eastern region of both reefs.

Table 5.2: Summary of mean total sediment collected during the dry season in Teluk Dedap and Teluk Datai (2 – 19 February 1999).

☐ Reef Flat

Teluk Dedap		Teluk Datai	
Trap	**Mean ± S.D. (g)**	**Trap**	**Mean ± S.D. (g)**
1	112.50 ± 29.84	X1	268.20 ± 64.68
2	99.90 ± 8.94	X2	680.80 ± 26.64
3	119.20 ± 27.08	X3	102.70 ± 13.52
4	338.40 ± 38.30	X4	135.20 ± 17.05

5.4 SEDIMENT FALLOUT DURING THE WET SEASON (10 - 25 JULY 1999)

The profile of summation curves for sediment collected at the reef flats of Teluk Dedap and Teluk Datai is shown in Figure 5.9. A larger percentage of sediment particles of ≤ 0.2mm was collected in sediment Traps 1 and 3 of Teluk Dedap while smaller percentage was collected for sediment Traps X1 and X3 at Teluk Datai. Sediment fractions ≥ 0.25mm were almost equally collected in Traps 3, X1 and X3 with the exception for Trap 1. Again it is observed here that the reef flats tended to trap more of the finer sediment fractions even during the wet season. The percentage of these fractions however is smaller than that measured during the dry season. This may be possible because during the wet season, the physical water activity is of greater magnitude where vertical and horizontal mixing may have occurred more frequently compared to the dry season. Therefore, coarser sediment particles would be able to settle in comparatively greater proportion within the reef flat during this time.

Figure 5.10 shows the summation curves of sediment fractions collected for the reef slopes in Teluk Dedap and Teluk Datai during the wet season. Larger amounts of coarser sediment fractions were collected in Traps 2 and 4 in Teluk Dedap and Trap X2 in Teluk Datai. The percentage of sediment fractions of ≥ 0.25mm size collected in these traps was also similar. There is an exception in Trap X4 (Teluk Datai) where larger proportions were from finer sediment particles having the size of ≤ 0.2mm.

The comparison of summation curves for reef slopes during the dry (Figure 5.7) and wet season (Figure 5.10) showed that during the wet season, the variation is much smaller due to the higher physical activity occurring within the coastal and shallow marine system of both Teluk Dedap and Teluk Datai. The constant high physical activity such as wave actions and turbulence may have resulted in a more even distribution of sediment fractions compared to the dry season. However,

the physical condition of the reef, such as its structures and degree of slopes may have contributed to the varying degree of variations in the sediment fractions analysed.

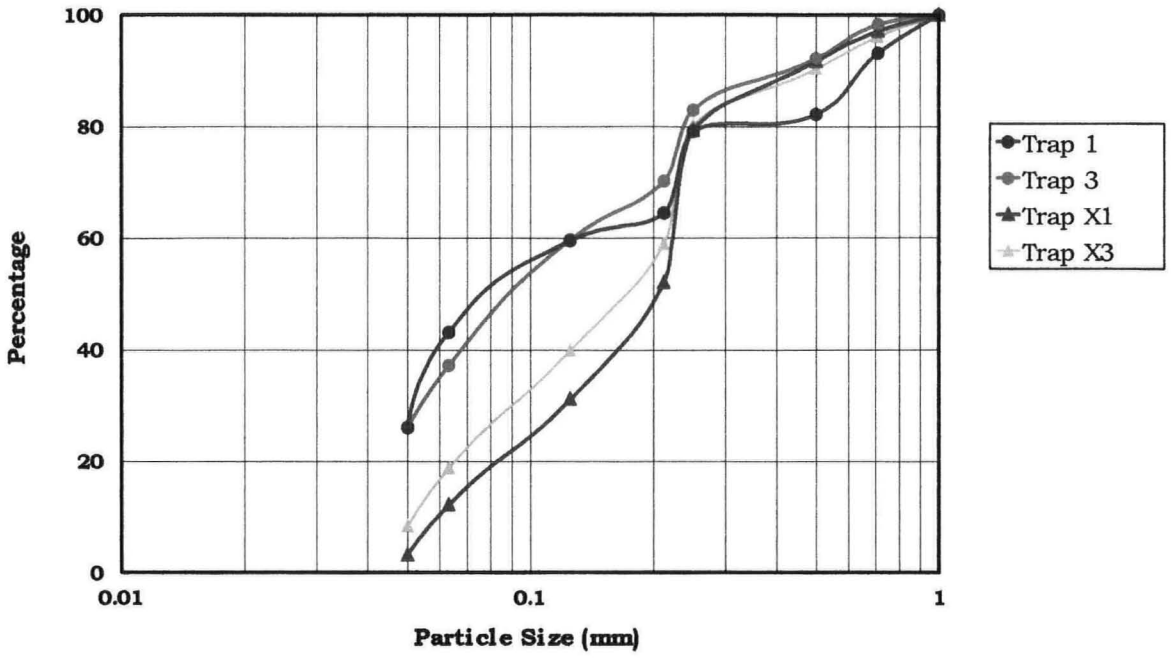

Figure 5.9: Summation Curves Of Particle Size Analysis For Sediment Traps At Reef Flats Of Teluk Dedap (Traps 1 and 3) And Teluk Datai (Traps X1 and X3), Pulau Langkawi During The Wet Season (10 – 25 July 1999).

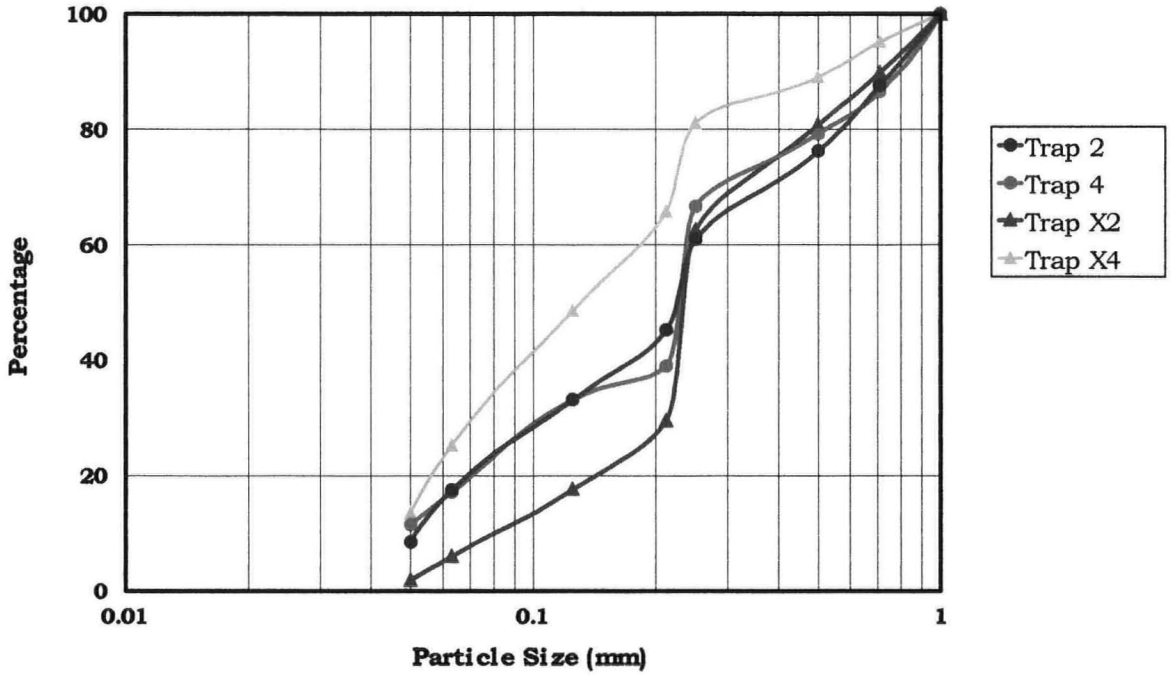

Figure 5.10: Summation Curves Of Particle Size Analysis For Sediment Traps At Reef Slopes Of Teluk Dedap (Traps 2 and 4) And Teluk Datai (Traps X2 and X4), Pulau Langkawi During The Wet Season (10 – 25 July 1999).

Figure 5.11 shows the different fractions of sediment collected from all the sediment traps in Teluk Dedap and Teluk Datai. The amount of fine sediment fraction (< 63 μm) was relatively much lower than that measured during the dry season. These fine particles may have more difficulty settling but would probably stay suspended within the water column during this period, hence the lesser amount trapped in the sediment traps. Sediment fractions ranging from 500 μm - > 1000 μm were measured in greater proportions during the wet season. This is probably because most reefal materials will either be eroded or broken of more during the higher and longer physical wave actions during the wet season.

A summary of mean total sediment collected and standard deviations calculated for Teluk Dedap and Teluk Datai during the wet season is given in Table 5.3. Almost similar mean total sediments were collected in the sediment traps on the reef flats of Teluk Dedap (160.5 ± 4.45 g - 165.9 ± 2.12 g) and also Teluk Datai (302.2 ± 12.58 g - 350.6 ± 12.41 g) was observed. This shows lesser variations in the sediment fallout within the reef flats during the wet season. The means calculated for sediment traps placed within the reef slopes showed considerable variation. The comparative difference in means for Teluk Dedap reef slope sediments was two-fold (182.5 ± 10.36 g - 384.0 ± 37.6 g) while for Teluk Datai was more than almost three-fold (207.3 ± 13.44 g - 729.6 ± 13.94g).

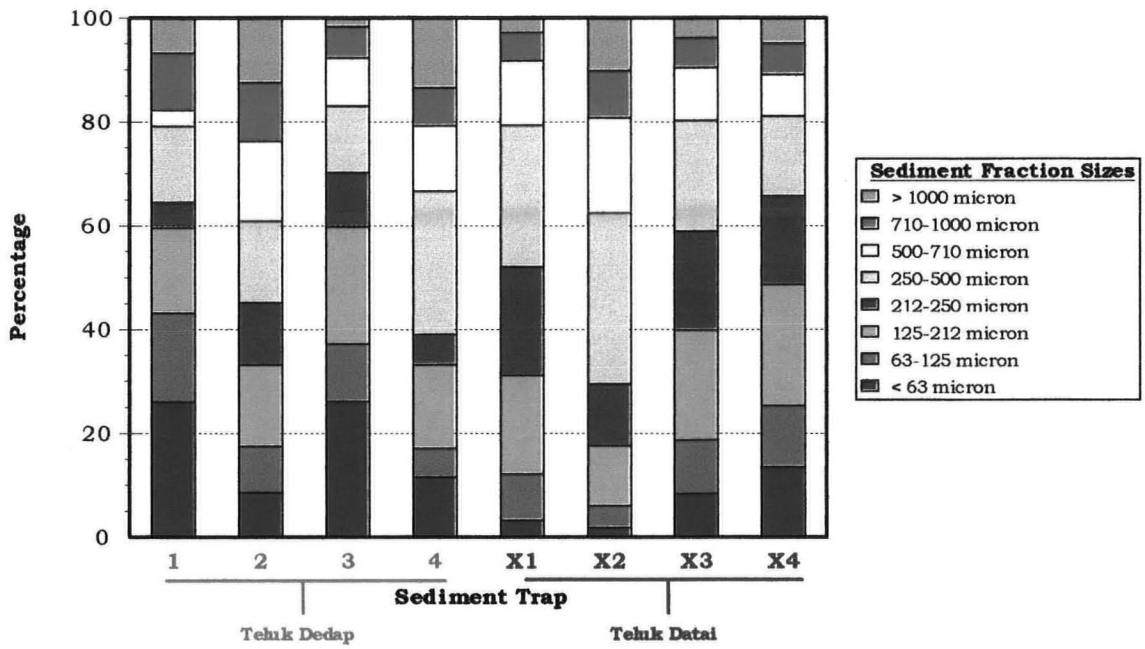

Figure 5.11: Distribution Of Particle Size Fractions At Teluk Dedap And Teluk Datai, Pulau Langkawi During Wet Dry Season (10 – 25 July 1999).

Table 5.3: Summary of mean total sediment collected during the wet season in Teluk Dedap and Teluk Datai (10 – 25 July 1999).

☐ Reef Flat

Teluk Dedap		Teluk Datai	
Trap	**Mean ± S.D. (g)**	**Trap**	**Mean ± S.D. (g)**
1	160.50 ± 4.45	X1	350.60 ± 12.41
2	182.50 ± 10.36	X2	729.60 ± 13.94
3	165.90 ± 2.12	X3	302.20 ± 12.58
4	384.00 ± 37.6	X4	207.30 ± 13.44

5.5 A COMPARISON OF SEDIMENT FALLOUT BETWEEN THE DRY AND WET SEASONS

5.5.1 Teluk Dedap

Sediment fractions fallout of Teluk Dedap is compared for the dry and wet seasons as shown in Figure 5.12. It is clearly seen that during the dry season, finer sediment particles mainly < 212 μm was the main composition in all sediment traps collected except for Trap 4 which was placed in the east of the reef slope in Teluk Dedap. In some traps these finer sediment fractions also dominate the total collection during the wet season. However, the compositions are relatively lower during the wet season than in the dry season, with the exception of Trap 4. On the reef flats of Teluk Dedap where Traps 1 and 3 were placed, the sediment fractions showed that at least 60% of the compositions are made up of sediment particles of ≤ 212 μm. In the reef slope, the main composition consists of sediment fractions ≥ 250 μm. However, there is an exception for Trap 2 during the dry season. More quantities of sediment fraction with > 1000 μm size is measured during the wet season, particularly Traps 1, 2, and 4.

5.5.2 Teluk Datai

From Figure 5.13, it is observed that the main composition of sediment collected during the dry season (Traps Dry X1 – Dry X4) is the finer sediment fractions of ≤ 212 μm. These fractions were less abundant during the wet season in all sediment traps placed in both the reef flat and the reef slope. It is also observed that larger quantities of finer sediment fractions ≤ 212 μm were collected in traps placed on the eastern side of Teluk Datai (Traps X3 and X4). The coarser sediment fractions having sizes ≥ 250 μm were mainly collected in Traps X1 and X2 and these traps were located on the western region of the reef flat and reef slope of Teluk Datai respectively. Except for

Trap X2, larger quantities of sediment fractions > 1000 um were collected in traps during the wet season.

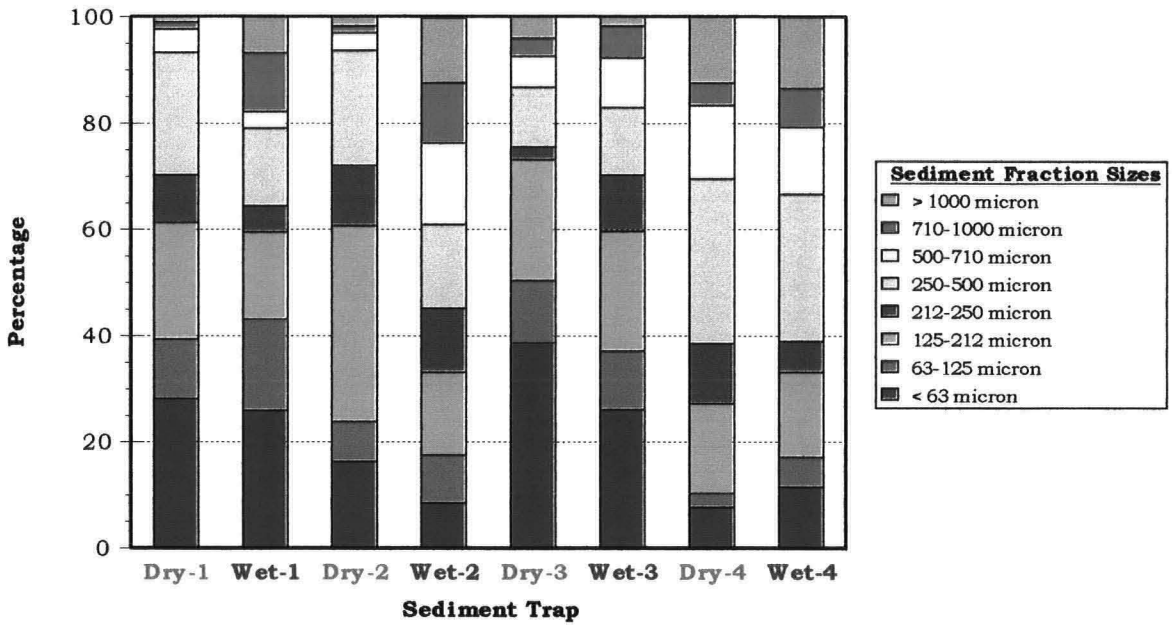

Figure 5.12: A comparison of Particle Size Fractions at Teluk Dedap, Pulau Langkawi during the Dry and Wet Seasons in 1999

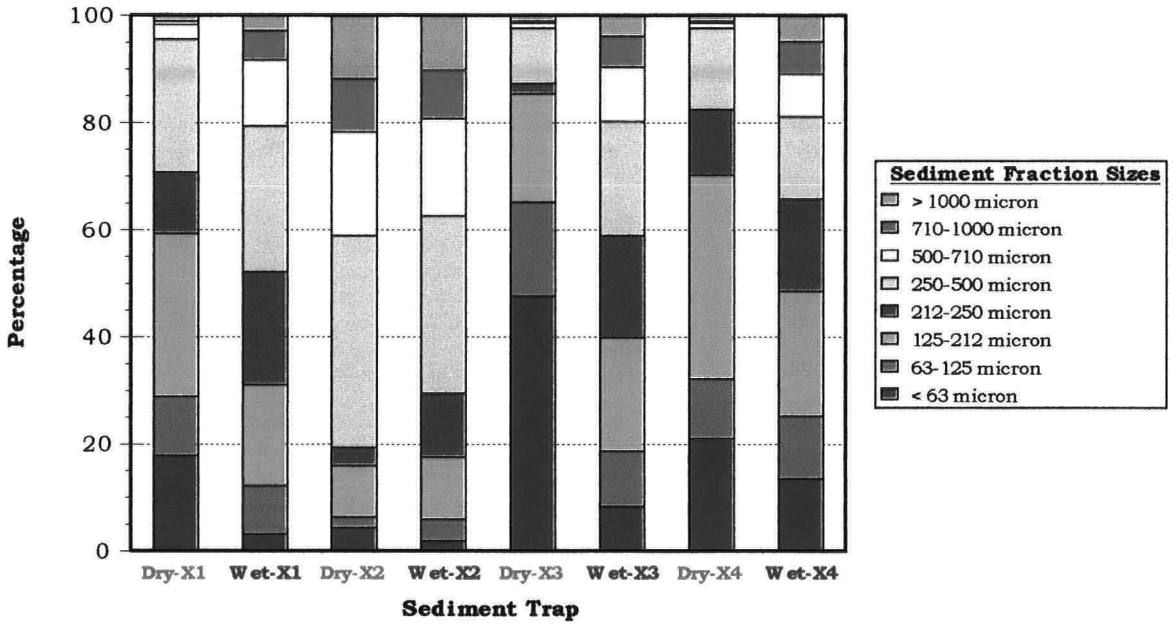

Figure 5.13: A comparison of Particle Size Fractions at Teluk Datai, Pulau Langkawi during the Dry and Wet Seasons in 1999

5.6 SEDIMENT FALLOUT RATES DURING THE DRY AND WET SEASONS

Table 5.4 compares the calculated sediment fallout rates in $g/m^2/day$ for Teluk Dedap and Teluk Datai reefs based on the sediment fallout collected during the dry and wet seasons in 1999. (Calculation of sediment fallout rates is provided in subsection 5.2.3.1).

In Teluk Dedap, the sediment fallout rate is almost similar on the reef flat during the dry season. The range calculated is 1,580.49 ± 419.22 $g/m^2/day$ to 1,674.62 ± 380.44 $g/m^2/day$. During the wet season, the range of fallout rate is much higher, 2,738.02 ± 75.91 $g/m^2/day$ to 2,830.14 ± 36.17 $g/m^2/day$. The variation of sediment fallout rates calculated from results obtained in these traps is not high. However, the variation of sediment fallout rates calculated for the reef slopes of Teluk Dedap is high both amongst the traps and also between the two seasons. The range fell within the 1,403.48 ± 125.60 $g/m^2/day$ to 4,754.12 ± 538.07 $g/m^2/day$ during the dry season, and 3,113.32 ± 176.73 $g/m^2/day$ to 6,550.77 ± 641.43 $g/m^2/day$ during the wet season.

In Teluk Datai, most of the sediment fallout rates calculated varied from season to season, from trap to trap and from location to location. The ranges calculated vary from the lowest of 1,532.99 ± 201.81 $g/m^2/day$ (Trap X3; reef flat east; dry season) to the highest of 12,446.45 ± 237.81 $g/m^2/day$ (Trap X2; reef slope west; wet season).

In general, based on seasons the sediment fallout rates were lower during the dry season and much higher during the wet season for both Teluk Dedap and Teluk Datai. It is observed too that in general (with the exception of Traps 1 and 2, dry season; Traps X3, and X4, wet season) sediment fallout rates were lower on the reef flats compared to the reef slopes in Teluk Dedap and Teluk Datai for both seasons.

Table 5.4: A comparison of calculated sediment fallout rates ($g/m^2/day$) for Teluk Dedap and Teluk Datai during the dry and wet seasons.

☐ Reef Flat

Teluk Dedap			Teluk Datai		
Trap	**Dry Season**	**Wet Season**	**Trap**	**Dry Season**	**Wet Season**
1	1,580.49 ± 419.22	2,738.02 ± 75.91	X1	4,003.39 ± 968.47	5,980.99 ± 211.71
2	1,403.48 ± 125.60	3,113.32 ± 176.73	X2	10,162.22 ± 397.65	12,446.45 ± 237.81
3	1,674.62 ± 380.44	2,830.14 ± 36.17	X3	1,532.99 ± 201.81	5,155.32 ± 214.61
4	4,754.12 ± 538.07	6,550.77 ± 641.43	X4	2,018.11 ± 254.50	3,536.39 ± 229.28

5.7 MICROSCOPIC ANALYSIS

Since the study area is located within a continental shelf, the sedimentation fallout occurring within this region would be considered shelf sedimentation where the major sediments are of biogenic type that occurs within the coral reef region. Biogenic sediments, both macroscopic and microscopic, are derived from the hard parts of organisms, such as shells and skeletons. The macroscopic biogenic sediments are clearly observed for sediment fractions collected from Teluk Dedap and Teluk Datai particularly the coarser sediment fractions having sizes ≥ 250 μm. Biogenic sediments collected from Teluk Dedap are shown in Figures 5.14(a)-(d) while for Teluk Datai these are shown in Figures 5.15(a)-(d). Smaller sediment fractions appear to consist mainly of feldspar and quartz, and also some remnants of microscopic biogenic sediments particularly of molluscs shells and crustaceans (Figures 5.14(e)-(g) and Figures 5.15(e)-(g)). Some fine remnants of coral debris, foraminifera, siliceous materials and calcareous shell remnants of polychaete housing were also observed in the sediment fractions collected in both Teluk Dedap and Teluk Datai. Some of these sediments were long eroded and broken off during its repeated transportation and deposition by wave actions within the area. This is proven by the rounded ends and edges of the broken pieces of shells in particular. Based on Figures 5.14 and 5.15, it is also clearly seen that the type of sediments collected in both reefs are similar, of which the coarser sediments are basically biogenic in nature and the finer sediment fractions were made up of mainly feldspar, siliceous and quartz materials.

Other forms of sediments observed are lithified sediments as schematically shown in Figure 5.16

Lithified sediments were found in most of the sediment fractions collected from Teluk Dedap and Teluk Datai. This form of sediment is easily observed in the larger sediment fractions such as those in the > 1000 μm sizes. An example of macroscopic lithified sediment is shown in Figure 5.17 which was taken from Trap 4 placed on the reef slope of Teluk Dedap during the dry season. The lithified sediments observed are probably of terrigenous origin (Thurman and Trujillo, 1999). The observed lithified sediments could have originated from weathered sedimentary rocks within the study area.

(a) Sediment fraction > 1000 μm, Trap 1(reef flat), Teluk Dedap (Dry season, 2-19 February 1999)

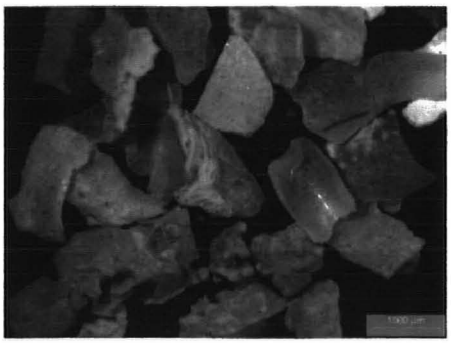

(b) Sediment fraction 710μm - 1000 μm, Trap 1 (reef flat), Teluk Dedap (Dry season, 2-19 February 1999)

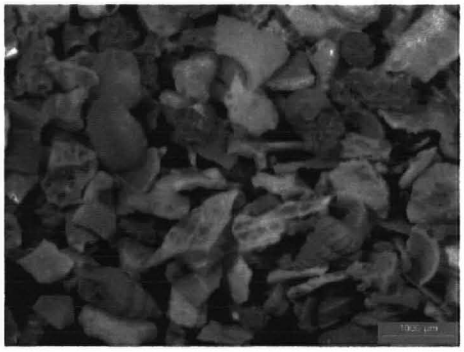

(c) Sediment fraction 500 μm - 710 μm, Trap 1 (reef flat), Teluk Dedap (Dry season, 2-19 February 1999)

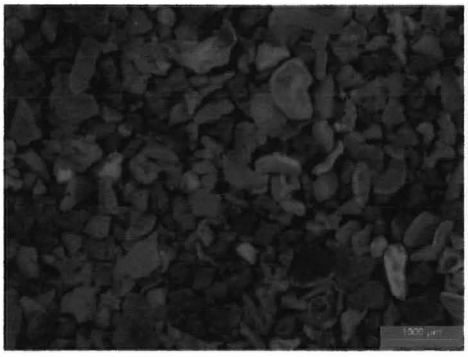

(d) Sediment fraction 250 μm - 500 μm, Trap 1 (reef flat), Teluk Dedap (Dry season, 2-19 February 1999)

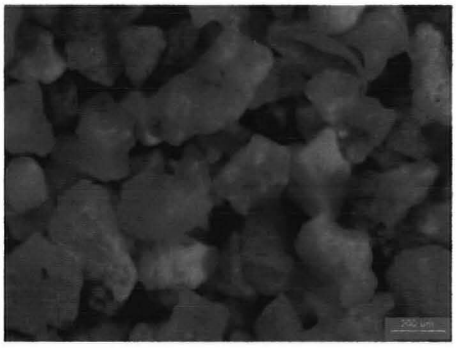

(e) Sediment fraction 212 μm - 250 μm, Trap 1 (reef flat), Teluk Dedap (Dry season, 2-19 February 1999)

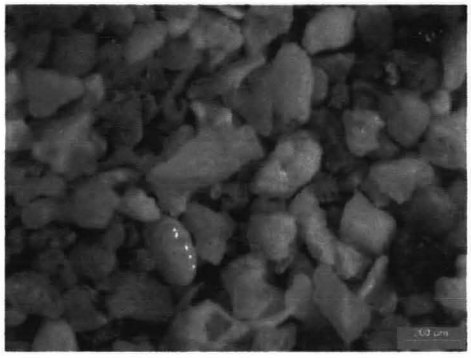

(f) Sediment fraction 125 μm - 212 μm, Trap 1 (reef flat), Teluk Dedap (Dry season, 2-19 February 1999)

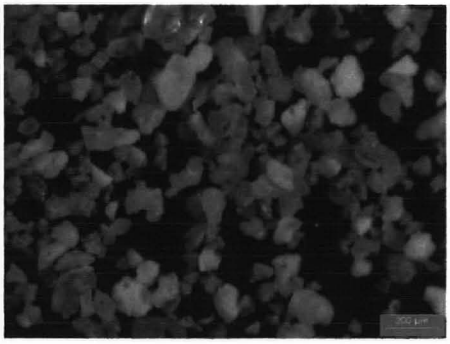

(g) Sediment fraction 63 μm – 125 μm, Trap 1 (reef flat), Teluk Dedap (Dry season, 2-19 February 1999)

Figure 5.14. Sediment particles observed under microscope for sediment fractions collected from Teluk Dedap (1999).

(a) Sediment fraction > 1000 μm, Trap 1 (reef flat), Teluk Datai (Dry season, 2-19 February 1999)

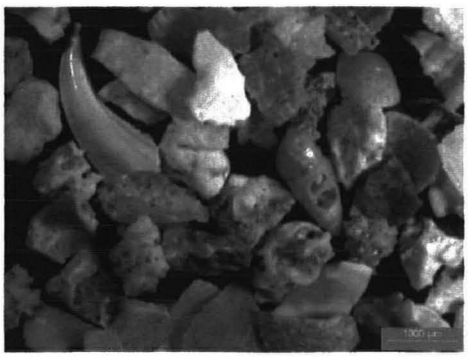

(b) Sediment fraction 710μm - 1000 μm, Trap 1 (reef flat), Teluk Datai (Dry season, 2-19 February 1999)

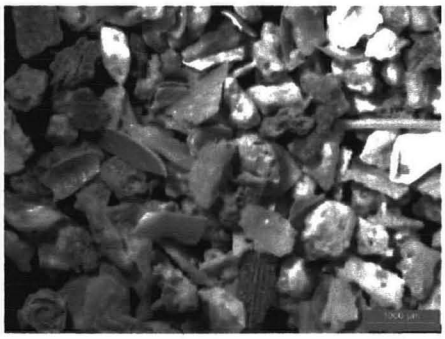

(c) Sediment fraction 500 μm - 710 μm, Trap 1 (reef flat), Teluk Datai (Dry season, 2-19 February 1999)

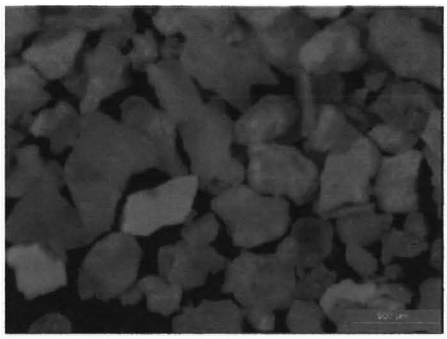

(d) Sediment fraction 250 μm - 500 μm, Trap 41 (reef slope), Teluk Datai (Dry season, 2-19 February 1999)

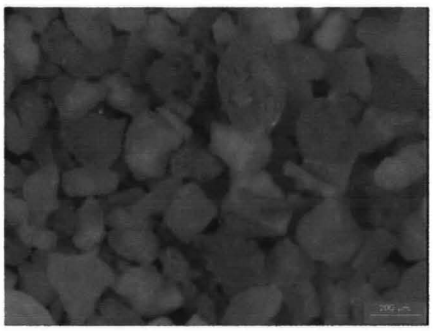

(e) Sediment fraction 212 μm - 250 μm, Trap 41 (reef slope), Teluk Datai (Dry season, 2-19 February 1999)

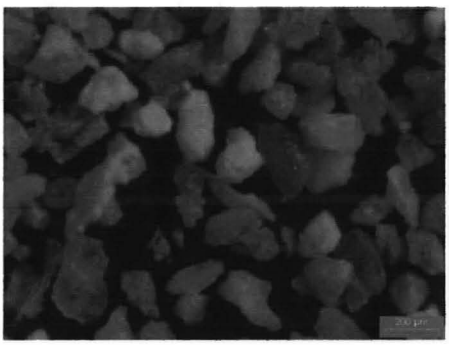

(f) Sediment fraction 125 μm - 212 μm, Trap 4 (reef slope), Teluk Datai (Dry season, 2-19 February 1999)

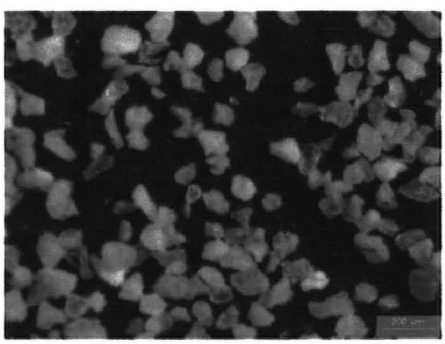

(g) Sediment fraction 63 μm – 125 μm, Trap 4 (reef slope), Teluk Datai (Dry season, 2-19 February 1999)

Figure 5.15 Sediments particles observed under microscope for sediment fractions collected from Teluk Datai (1999).

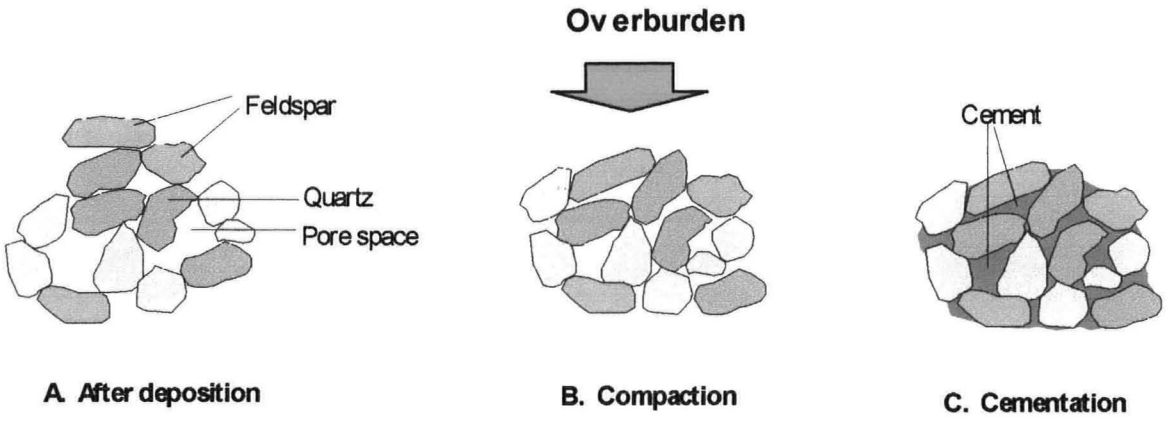

Figure 5.16: A schematic diagram on lithification of reef sediments: (a) deposition of loose grains, (b) weight of overburden compacts sediment particles into tighter arrangement, reducing pore space, (c) precipitation of cement in the pores to bind structure to form clastic texture. (Adapted from: Plummer *et al.*, 2003)

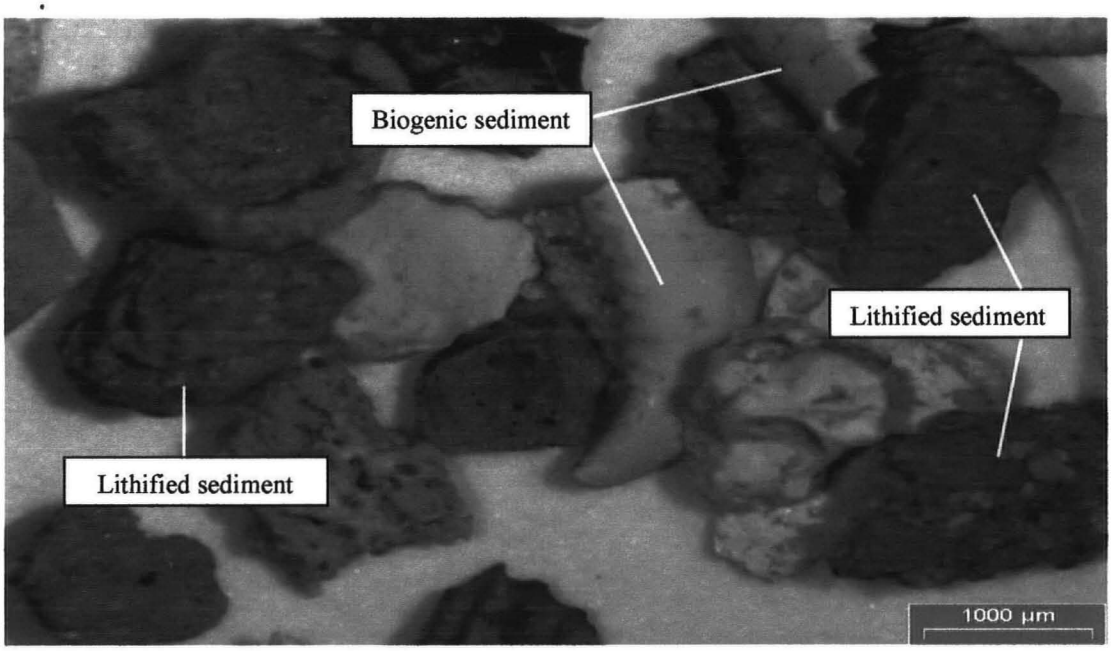

Figure 5.17: Lithified and biogenic sediments observed using microscope from sediment fraction size > 1000µm in Teluk Dedap during dry season (2-19 February 1999).

5.8 SUMMARY

By comparing the distribution of sediment fractions collected during the dry and wet seasons for Teluk Dedap and Teluk Datai, it was observed that in general the sediment segregation is rather poorly-sorted on the reef flats and reef slopes.

The patterns of sediment fallout in the study area (Teluk Dedap) and its control site (Teluk Datai) were dissimilar. On the Teluk Dedap reef, the finer sediment fractions of ≤ 212 μm were collected mainly on the reef flat; while on the Teluk Datai reef, the finer sediment fractions of ≤ 212 μm were collected on the eastern region of its reef. In Teluk Dedap the larger quantities of finer sediment fraction ≤212 μm on reef flat explains the reason why the coral debris/dead coral coverage is larger here as compared to its reef slope. On the east side of Teluk Datai where less live coral coverage was detected (Chapter 4, section 4.4) coincides with the larger quantity of finer sediment fractions collected here.

The pattern and degree of transportation and deposition differ between the two reefs at Teluk Dedap and Teluk Datai. This could be the result of different water circulation patterns, the different reef structures, the wave energy involved and other physical influences. The amount of sediment depositions collected during the dry and wet seasons in this study may arise either from (i) settlement of transported materials when the waves lose energy and can no longer transport its load, and (ii) accumulation of dead reefal organisms or their remnants where no transportation is involved at all. Based on the results obtained from the sediment fallout study, the environment of deposition of finer sediment particles with ≤ 212 μm sizes for Teluk Dedap reef was the reef flat while the reef slope was the environment of deposition of coarser sediment particles. In Teluk Datai, such distinction is not clearly divided between the reef flat and the reef slope. However, in Teluk Datai, the environment of deposition of finer sediment particles with ≤ 212 μm sizes is located within the eastern region of the reef itself, while the western region of the reef is the environment of deposition of coarser sediment particles.

The main component of the coarser sediment fractions collected were mainly of biogenic materials namely the shell or remnants of molluscs, crustaceans, coral debris, siliceous materials and lithified sediments. For the finer sediment fractions, the main composition appears to be of feldspar, siliceous and quartz materials.

Calculated sediment fallout rate in Teluk Dedap showed a lowest level of 1,403.48 ± 125.60 g/m^2/day during the dry season to the highest of 6,550.77 ± 641.43 g/m^2/day during the wet season. In the control site the range of sediment fallout rate varied from 1,532.99 ± 201.81 g/m^2 during the dry season to the highest of 12,446.45 ± 237.81 g/m^2/day during the wet season. Sediment fallout

rate is typically lower during the dry season compared to the wet season and on the reef flats compared to the reef slopes. Results indicated that if local sedimentation was the cause of live coral coverage deterioration, then Teluk Datai reef would have higher percentage of dead reef relative to its size compared to Teluk Dedap reef. However, this was not the case. Therefore, there was great possibility that higher percentage of dead coral coverage in Teluk Dedap was caused by sediment plumes transported eastwardly during ebbing tides from the riverine-estuarine area resulting in coral death over time.

Chapter 6

MODELLING OF SURFACE WATER TOTAL SUSPENDED PARTICULATES OF TANJUNG RHU

6.1 LITERATURE REVIEW

6.1.1 Remote Sensing

Since suspended particulates in surface waters can be a visible indicator of erosion and soil loss, remote sensing can provide the synoptic view of the landscape and the ocean necessary to locate and monitor areas with significant suspended particulate problems. To monitor or detect changes within the vast and dynamic coastal and marine system, conventional or the classical methods used for environmental monitoring is no longer efficient although it is needed. Within the equatorial region, quantitative measurements from satellite remote sensing through analysis with coincidence sea-truth data are rarely conducted due to difficulty in obtaining cloud-free scenes (Abdullah *et al.*, 2000). It is therefore necessary to combine conventional with new and developing remote sensing technologies to enable human monitor the rapid and dynamic changes of the environment due to both human-induced and natural phenomena.

This chapter describes the methodology used to develop an algorithm for the purpose of detecting and estimating Total Suspended Particulates (TSP) on Malaysian coastal surface waters applicable to remote sensing (satellite) data. The simple and direct methods commonly used (e.g. simple regression analysis or linear relationships between remote sensing digital data and *in-situ* data) to produce such algorithms will not be described here. This was because many of such equations were only applicable for one-time only or for a very short period of time since other possible variations of environmental factors were not considered during the simple linear equation formations. This chapter aimed for a simple algorithm which takes into consideration these environmental factors. A simple algorithm is preferred because it allows easy and direct applications of remote sensing data.

6.1.2 Light and Water-Sediment Interaction

The interaction of light with a water-sediment mixture is complex because both materials scatter and absorb radiation. The depth to which light will penetrate into the ocean, and hence, the depth at which production can occur, is dependent upon a number of factors; these include absorption of light by the water, the wavelength of light, transparency of the water, reflection from the surface of the water, latitude, and season of the year. A number of meteorological features influence light before it even impinges on the surface of the water. Factors such as clouds and dust act to interfere with light in such a way that lesser amounts survive the passage through the atmosphere to impinge

on the surface of the water. This reduces the available light initially, without reference to water conditions (Nybakken, 1982). The apparent upwelling radiance measured remotely is not only a function of water and sediment properties, but also is a function of initial solar input, atmospheric transmission of the radiation, the upwelling radiance at the water surface, and the specular reflection off the water surface due to both sunlight and skylight. These variables in turn are dependent on the illumination geometry, atmospheric conditions, and water surface parameters such as water surface roughness. If all of these variables can be accounted for, it may be possible to determine accurately the relationship between remotely sensed reflectance and sediment concentration (Holyer, 1978; Curran and Novo, 1988). After the light is reflected and refracted through the air-water boundary, it is absorbed and scattered by the water and sediment particles. The water-leaving radiance produced by the upwelling light stream is the property measured by remote sensing detectors and is a function in part of the sediment concentration (Holyer, 1978). The upwelling light stream from the water is primarily due to backscattering from particles. As the number of particles increases, the amount of scattering increases, and, hence, the effective backscattering increases proportionally, depending on the specific optical characteristics of the sediment particles. The increase in the magnitude of the upwelling light due to scattering as the sediment concentration increases is not linear, because light is also being absorbed. As scattering increases, the path length of the light also increases. An increase in path length results in a decrease in light intensity as the light passes through more water and more particles and radiation is absorbed. The increased absorption with increased path length counteracts the increased scattering in a non-linear manner, and the effect varies with wavelength. These two interacting effects combined with the increased scattering with increased particle number result in a non-linear increase in reflectance as sediment concentration increases (Kirk, 1986; 1989). The water itself and the dissolved materials in the water primarily affect the rate of absorption of light in water-sediment mixtures.

The rate of scattering and backscattering by suspended particles is a function of the mineralogical and textural characteristics of the particles. Theoretical studies stated that variations in sediment colour, type and size have significant effects on the observed range of reflectance values (Kirk, 1986; Curran and Novo, 1988; Novo *et al.*, 1989a; Bhargava and Mariam, 1990; 1991; Nanu and Robertson, 1990; Chen *et al.*, 1991; Sui *et al.*, 2001). Due to the low rate of absorption and the high rate of scattering by water, the most effective range of wavelengths for estimating the concentration of sediment in water from reflectance fall between 400 nm to 1000 nm. Hence, the sensitivity of reflectance sediment concentration falls within the range of visible and near-infrared spectrum (Chen *et al.*, 1991).

Incident radiation that is reflected results from scattering at or just below the water surface. Suspended sediments are a common scatterer in open waters, a number of researchers have

reported a strong positive correlation between suspended sediment concentration (SSC) and spectral radiance (Ritchie *et al.*, 1976; 1987; Novo *et al.*, 1989a, b; 1991; Bhargava and Mariam, 1990; 1991; Hinton 1991). This relationship has been used in conjunction with remotely-sensed spectral radiance to estimate SSC over large areas of oceans reservoirs, lakes, rivers, and coastal waters as an aid to the management of water quality, the monitoring of pollution, and the modelling of sediment (Curran and Novo, 1988; Ritchie and Cooper, 1988; Weeks and Simpson, 1991). There are, however, considerable problems associated with matching remotely-sensed spectral radiance and SSC in space and time (Curran, 1987; Curran *et al.*, 1987). These problems are exacerbated by the low and relatively small range of spectral radiance that is associated with relatively large range of SSC (Moore, 1977). Rarely does water reflect more than 10% of its incident radiation and even in nonturbid waters a 50 mg/L increase in SSC is unlikely to increase reflected radiation by more than 1% (Chen *et al.*, 1991). A 1% variability in reflected radiation is smaller than the variability associated with the sensor, incoming irradiance, water surface, or atmosphere. The atmosphere is usually the largest source of variability and even atmospheric correction models developed for oceanography are unable to correct, to within a 1% error, the radiation reflected from water (MacFarlane and Robinson, 1984; Kaufman, 1989; Duggin and Robinove, 1990).

6.1.3 Water Quality Mapping Using Remote Sensing Techniques

The methods of estimating TSP from reflectance or radiance measurements above the sea are based mainly on statistical analyses of remotely sensed and field data. According to Ritchie and Cooper (1988), Allee and Johnson (1999) and Gons (1999), algorithms produced in this direction so far have limited applicability and accuracy for retrieving the global sediment or chlorophyll concentrations in the water surface layer.

The studies of sedimentation on coastal areas especially of the coral reefs were never direct. Sedimentation impact on these areas will have to rely heavily on many different factors such as the physical factors since the coasts or the sea is a very dynamic system. Due to this factor and the complexity of the system, most research is limited to the study of water quality.

Most common water quality parameters studied include turbidity, TSP, salinity, chlorophyll-a and sea surface temperature (SST). Remotely-sensed data utilized involves the Coastal Zone Colour Scanner (CZCS), Landsat Multispectral Scanner (MSS), Landsat Thematic Mapper (TM), National Oceanographic and Atmospheric Administration – Advanced Very High Resolution Radiometer (NOAA-AVHRR), and airborne scanners. This section outlines studies carried out on water quality mapping and modelling using remotely-sensed data.

Khorram and Cheshire (1985) utilized Landsat Multispectral Scanner (MSS) digital data and surface measurements for the water quality of the Neuse River Estuary, North Carolina. The approach used was the acquisition of water quality samples simultaneously with Landsat satellite overpass. Water quality parameters involved in their study involved salinity, chlorophyll-a, turbidity, and suspended solids. Based on their studies, it was concluded that Landsat digital data can be successfully used to map some surface water quality parameters. It was observed that coefficients of determination (R^2) are high for salinity and turbidity, relatively high for chlorophyll-a, and medium for suspended solids. No quantitative assessment could be made of the surface water quality parameters by visual interpretation of aerial imagery. They have also stated that additional studies are needed at different flow conditions in order to develop generalized models. It was suggested that further studies using Landsat data for surface water quality mapping should investigate the use of up-to-date Landsat data, particularly for mapping chlorophyll-a and TSP.

Tassan and Sturm (1986) have developed theoretically an algorithm for the retrieval of sediment of turbid coastal waters from CZCS data and had the developed algorithm tested against experimental values. The theoretical approach consisted of numerical variable with low sensitivity to chlorophyll-like pigments, and to uncertainties in the procedure for the determination of the atmospheric correction applied to remotely measured radiances. The theoretically predicted sensitivity to the atmospheric correction method been confirmed by the experimental evidence, the possibility of using a simplified correction procedure, even in turbid waters where sediment and chlorophyll contents are uncorrelated. The experimental exercise by Tassan and Sturm (1986) led to the identification of two water types in the northern basin of the Adriatic Sea, characterized by a different correlation between sediment and chlorophyll, and corresponding to coastal zones with different hydrological conditions.

According to Schiebe *et al.* (1988), initial examination of Landsat TM data indicated that Bands 1-4 have potential for use in analysis of SSC and that Band 3 demonstrated the greatest promise. Studies by Ritchie and Schiebe (1986) and Schiebe et al. (1988) proved that simple linear and multiple regression techniques indicated that MSS 3 (700-800 nm) was the best single band for explaining variations in suspended sediment. Examination of these data set provided substantial evidence to support a theoretical-based exponential relationship between suspended sediments and reflectance (Schiebe *et al.*, 1988).

Studies by Ritchie *et al.* (1987) have shown that it is possible to use digital spectral data from the Landsat MSS to estimate the concentrations of suspended sediments in the surface water of lakes and where the concentration exceeds 50 mg/L. The equations for estimating the concentration of suspended sediments in surface water used MSS Band 2 or Band 3 data. According to this study,

since MSS Band 4 spectral data have been shown to be useful for locating water bodies in Landsat scenes, it should be possible to develop an effective system using Landsat digital data to locate water bodies with significant suspended sediment problems prior to the application of MSS band 2 or 3 spectral data from the estimation of SSC. Coefficients of determination (R^2) greater than 0.81 were calculated between MSS Band 2 (0.6-0.7 μm) or Band 3 (0.7-0.8 μm) and suspended sediments or total solids. Coefficients of determination for multiple regression using three or four MSS bands were greater than 0.90.

Ritchie and Cooper (1988) compared measured SSC with SSC estimated from Landsat MSS data for Moon Lake in Coahoma County, Mississippi. The study showed that good estimates of SSC between 50 and 250 mg/L (the critical concentration range for assessing conservation needs) can be made using simple linear regression equations based on Landsat MSS data. SSC greater than 250 mg/L were underestimated by most of the equations indicating a saturation of reflected solar radiation at higher SSC. Ritchie and Cooper (1988) suggested that further studies are needed to determine if equations developed for one water body can be used to estimate SSC in other water bodies in the same Landsat scene (Path and Row) or other water bodies in a Landsat scene from a different area (different Path and Row).

The use of remotely-sensed optical data to estimate the SSC of water is dependent upon the correlation between SSC and reflectance (Novo *et al.*, 1989). The strength of the relationship was hypothesized to vary with sediment type, as it is known that sediments, when dry, differ in their particle size distributions, colour and therefore reflectance properties. Novo *et al.* (1989) measured the reflectance of pure water with four concentrations of white clay and red silt in the laboratory using a spectroradiometer. The correlation between SSC and reflectance varied with wavelength and sediment type. For white clay the correlations were very high ($r \approx 0.98$) in visible and near-infrared wavelengths, but for the red silt it was lower ($r \approx 0.8$) in blue wavelengths increasing to much higher levels ($r \approx 0.98$) in blue/green and longer wavelengths. It was concluded that sediment type can affect the strength of the correlation between SSC and reflectance and that this will be most noticeable at shorter wavelengths.

Doerffer *et al.* (1989) analyzed Thematic Mapper data with respect to its capability for mapping the complex structure and dynamics of TSP distribution in the coastal area of the German Bight (North Sea). The results of this study have shown that near surface TSP concentrations may be detected with an accuracy of factor < 2 by using an algorithm derived from a radiative transfer model calculation. Due to high spatial resolution, TM allows the analysis of scales of TSP distribution in coastal areas, which is important for monitoring programs. It was stated in this study the data analyzed have confirmed the hypothesis that the distribution of TSP

was mainly controlled by the sea bottom topography. Topliss *et al.* (1990) uses a numerical two-flow reflectance equation (simulated remote sensing algorithms) to predict high concentration inorganic suspended sediment. The algorithms worked equally well with both the Landsat MSS data and with Nimbus-7 CZCS data. However, the comparative analysis between image groundtruthing and model predictions encountered three major limitations:

(1) uncertainty in the atmospheric conditions and hence correction routines,

(2) the influence of high absorbing dissolved material associated with river runoff, and,

(3) the exact spectral shape for broad wavebands.

A laboratory experiment relating spectral reflectance to TSP was carried out by Novo *et al.* (1991). The experimental method involved the determination of water reflectance as produced by the simulation of different TSP concentrations. The oxisoil used in the experiment showed a linear correlation between spectral reflectance and TSP concentrations. This correlation was statistically significant and constant from 450 to 900 nm, but the rate of change in the spectral reflectance with TSP concentration peaked in the red region of the spectrum.

According to studies carried out by Bhargava and Mariam (1991), laboratory based studies related to reflectance response of suspensions carrying five different soil types and particle sizes of varying concentrations indicate dependence of reflectance measurements on soil type characteristics, particle size and concentration. Reflectance for any soil type and size increases with SSC and turbidity but decreases with an increase in the modified secchi depth of the suspension. Reflectance also increases with decrease in particle sizes for any soil type. Models have been evolved for the prediction of SSC, turbidity, and modified secchi depths from measured reflectance values for a given soil type and size, and also with due involvement of particle size in the predictive models. The predicted and observed values of SSC, turbidity, and modified secchi depth, by the various evolved models showed good agreement. In their study, it was concluded that percentage reflectance increases with SSC as well as with turbidity for all particle sizes, all soil types, and at all wavelengths in the 500 to 1000 nm range.

Studies carried out by Dick and Miller (1991), Philpot (1991) and Chen *et al.*, (1991) showed that there are three regions of the spectrum at wavelengths around 450-550 nm, 675-750 nm, and 800-1000 nm show particularly large changes in derivative reflectance with SSC. These are therefore candidate spectral regions for the estimation of SSC with derivative spectroscopy.

Studies by Chen *et al.* (1992) using added Holderness yellow clay in a tank to give SSC range of 0-590 mg/L had shown that six of the reflectance demonstrated the main reflectance properties of

sediment-laden water. High reflectance was found to be in the visible wavelength region, strong positive relationship between SSC and spectral reflectance within the wavelengths of 450-1000 nm.

Harrington *et al.* (1992) used two methods to examine the relationship between selected water quality parameters and the satellite data. First, the simple linear regression techniques were used to analyze the relationship between the water quality parameters and exoatmospheric reflectance, primarily because this technique has been widely used in previous studies (Ritchie and Schiebe, 1986; Ritchie *et al.*, 1987; Lyon *et al.*, 1988). In addition, simple linear regression was also performed following a natural logarithm transform of both variables. In general, the Landsat MSS bands that cover the visible red (600-700 nm) and the near infrared (700-800 nm) wavelengths are considered more appropriate than other wavelength bands for predicting surface water quality characteristics (Harrington *et al.*, 1992). Of the three variables that were analyzed in their research, the optical measures (*i.e.*, nephelometric turbidity and Secchi disk depth) were associated with larger coefficients of determination and nephelometric turbidity was consistently the highest (Harrington *et al.*, 1992).

Nanu and Robertson (1993) made a theoretical simulation on the effect of suspended sediment depth distribution on coastal water spectral reflectance in the visible region, (0.4-0.7 μm). The Mie theory for light scattering has been used to estimate extinction, scattering and absorption coefficients for a system of suspended spherical particles characterized by Junge size-distribution and containing absorbing and non- components. Significant changes in the shape of the simulated spectral reflectance have been obtained when the suspended sediment distribution in the water column, extending from the surface to the light penetration depth, varies. The preliminary theoretical results presented in their study seem to sustain the possibility of retrieving sediment depth profile from remote sensed spectral data.

The Coastal Zone Colour Scanner (CZCS) operated from the satellite Nimbus 7 has provided oceanographers with new insights into the complicated structure and dynamics of ocean water masses and their biological and chemical properties in time and space (Chen *et al*, 1992). It has been recognized early also that the potential of remote sensing as a tool could be very much improved by a higher number of spectral channels with narrow bandwidths and enhanced radiometric resolution and sensitivity with the expected new generation of sensors called imaging spectrometers (Doerffer, 1979). In order to exploit this new quality of data for remote sensing of sea water constituents, it is necessary to develop also a new generation of data evaluation techniques based on inverse modelling. The application of this technique requires a detailed knowledge of the optical properties of substances suspended or dissolved in sea water, and of the radiative transfer processes (Doerffer, 1992).

6.1.4 Ocean Colour Remote Sensing

All kinds of suspended particulates or dissolved constituents, which absorb or scatter radiation in the visible part of the electromagnetic spectrum, cause changes in the radiation field backscattered by the ocean. Furthermore, processes like fluorescence and Raman scattering contribute to the upward directed radiance. Thus, the colour of the sea, i.e. the spectrum of radiance leaving the ocean, contains information about the constituents dissolved or suspended within the near surface layer of the ocean, a lake or a river. This radiance spectrum can be measured in a number of single spectral bands. By knowing the relationship between radiances and type and concentrations of a substance, it is now possible to map its horizontal distribution with a radiometer from an aircraft or from space. The availability of high radiometric resolution and the possibility to program the selection of spectral channels for data recording has enabled the mapping of various substances present in the sea with a much higher reliability and accuracy. This formed the basis of the methodology used and results obtained in this study.

Sunlight is the information carrier in all passive ocean colour remote sensing techniques including spectroscopy. Since water is only transparent for the visible part of the electromagnetic spectrum, studies are restricted to this small spectral window including the near infrared (NIR) used for atmospheric correction procedures. The following processes are involved in the signal transfer (Doerffer, 1992) (Figure 6.1).

1. Sunlight penetrates the atmosphere, whereby part of the light is selectively absorbed by atmospheric gases, such as ozone, oxygen and water vapour. Another part of the radiation is scattered at air molecules and aerosols. Both processes, absorption and scattering in the atmosphere, are wavelength dependent. They determine the transmission of light through the atmosphere and the light backscattered from the atmosphere into the sensor, the *path radiance*. In clouds, scattering of light is so strong, that we cannot receive unscattered radiance from the ocean: remote sensing of ocean colour from above clouds is not possible.

2. At the sea surface, part of the direct sunlight and the scattered light is specularly reflected according to the Fresnel Law. The specularly reflected diffuse sky light is present at all viewing angles and has to be taken into account in the data evaluation process. According to the Fresnel Law, it increases with increasing viewing angles and is modified by the sea surface roughness. Substances floating on the water surface, such as mineralic or natural oil films, floating plankton (blue-green algae), foam and white caps, may mask the water leaving radiance.

Figure 6.1. Schematic diagram showing the processes involved in passive remote sensing of water constituents. (Source: Doerffer, 1992)

3. Within the water column, sunlight is partly absorbed and partly scattered by water molecules and dissolved and suspended constituents. Light energy absorbed by phytoplankton and gelbstoff is also partly re-emitted at longer wavelengths in the form of fluorescence. Depending on the wavelength, only a few percent of the light entering the ocean is scattered back into the atmosphere and can be detected by a radiometer. Substances may be inhomogeneously distributed within the water column with maxima in depths, which are not contributing to the water leaving radiance. However, normally a homogeneous water column within the signal depth is assumed.

4. In shallow and clear water, the bottom of the sea may also contribute to the reflected sunlight and change the ocean colour (e.g. from a dark blue to lighter blue). In cases where TSP is present in the water column, the ocean colour (as seen from the satellite image) will appear in shades of yellow-white depending on the concentrations of TSP. For instance, if concentration of TSP is high (e.g. 350 mg/L), the ocean colour will appear almost white.

6.1.5 The Light Field and the Optical Properties of Water Constituents

The knowledge of the optical properties of all water constituents and of the optical processes which modify the ocean leaving radiance is the fundamental requirement for interpreting remotely sensed radiance spectra (Jerlov, 1976). The optical properties of pure water and its constituents are

described by their *inherent* optical coefficients, which are the absorption and the scattering coefficients a and b, and the derived beam attenuation coefficient c. These coefficients describe the loss in radiant intensity (or energy) per meter of a parallel beam of light travelling through the water. Absorption means the change into another form of energy, scattering the change of the direction of the travelling photons, attenuation means both effects c = a + b. Since the coefficients a and b are wavelength dependent, all processes of the transport of light through the water column and the atmosphere depend also on the wavelength.

The radiant intensity dI scattered into a given direction γ with respect to the incident light beam which irradiates the water volume dV with E is described by the volume scattering function $\beta(\gamma)$:

$$\beta(\gamma) = dI(\gamma) / EdV \qquad \textit{(eq. 1)}$$

The total scattering coefficient b describes the flux scattered from the incident beam into all directions of the sphere surrounding the unit volume of water:

$$b = 2\pi \int_0^{\pi} \beta(\gamma) \sin \gamma d\gamma \qquad \textit{(eq. 2)}$$

Other useful definitions are the single scattering albedo $\omega_0 = {}^{b}/_{c}$; because $c = a + b$, $\omega_0 = 1$ means a total scattering medium and $\omega_0 = 0$ is a total absorbing medium. The optical length or optical depth τ is the geometrical length r of a path multiplied with the total attenuation coefficient c: $\tau = rc$.

The transmittance, i.e. the fraction of energy after a pass of the length r is the $t = e^{-\tau}$. Thus, the energy of a light beam after passing r is $I_r = I_o t$.

The following definitions were used to describe the light field and the transport of light through the water and the atmosphere.

Spectral radiance $L(\lambda)$: the radiant flux per unit solid angle $d\omega$, per unit projected area of a surface dA and per wavelength interval $d\lambda$, the unit is $L[W\mathrm{m}^{-2}sr^{-1}\mu m^{-1}]$.

Spectral irradiance $E(\lambda)$: the radiant flux F from all directions on an element of a surface, divided by the area of that element, unit is $E[W\mathrm{m}^{-2}\mu m^{-1}]$.

The irradiance on a horizontal flat surface, vector irradiance, is an integral of the radiances from all directions (zenith, θ and azimuth, ϕ) of a hemisphere. The upwelling irradiance is called E_u, and the downwelling, E_d, are both defined by:

$$E_x = \int^{2\pi}_{o} \int^{\pi/2}_{o} L(\theta, \phi) \cos\theta \sin\theta \, d\theta \, d\phi \qquad \textit{(eq. 3)}$$

The scalar irradiance is the illumination of a point from all directions:

$$E_x = \int^{2\pi}_{o} \int^{\pi}_{o} L(\theta, \phi) \sin\theta \, d\theta \, d\phi \qquad \textit{(eq. 4)}$$

The illumination of a small sphere, the spherical irradiance E_s, is:

$$E_s = 1/4 * E_o \qquad \textit{(eq. 5)}$$

The irradiance reflectance R is:

$$R = E_u / E_d \qquad \textit{(eq. 6)}$$

In the case of a perfect diffuse reflecting surface:

$$E = \pi L \qquad \textit{(eq. 7)}$$

The attenuation coefficient of the downward flowing irradiance E_d is defined as:

$$k_d = d(\ln E_d) / dz \qquad \textit{(eq. 8)}$$

Since E depends on the radiance distribution, k is not an inherent but an apparent parameter, although it is used in many applications, such as in two-flow models, approximately as inherent.

The transmittance of the downwelling irradiance is: $E_z = E_{z=0} e^{-k_d z}$ *(eq. 9)*

According to Hørjeslev (1975), combining measurements of E_d, E_u and E_0 at two different depths z_1 and z_2 would provide the determination of absorption coefficient a of a homogenous water body between z_1 and z_2 by using:

$$a = d(E_d - E_u) / -E_o dz \qquad \textit{(eq. 10)}$$

6.1.5.1 Optical Properties of Pure Water

The characteristics of optical properties of pure water are absorption and scattering including polarization (which is normally not considered in remote sensing).

The scattering of pure water into the angle γ normalized to the total scattering (into the sphere 4π) can be described by the Rayleigh phase function $P_r(\gamma)$:

$$P_r(\gamma) = 3/4 (1 + \cos^2 \gamma) \qquad \textit{(eq. 11)}$$

A better approach for liquids is the fluctuation theory, which includes the depolarization factor δ with a value of 0.09 for sea water. The phase function is:

$$P_r(\gamma) = 3/2 (1 + (1- \delta)/(1 + \delta) * \cos^2 \gamma) [(1 + \delta)/(2 + \delta)] \qquad \textit{(eq. 12)}$$

As a consequence, the forward and backward scattering coefficients (b_f and b_b) are both $0.5b$. The scattering coefficient $b(\lambda)[m^{-1}]$ is wavelength dependent. It decreases with increasing wavelength for pure sea water by $\lambda^{-4.32}$ (Morel, 1974). The scattering coefficient for pure sea water at $\lambda_0 = 0.45\mu m$ ranges from $0.00349m^{-1}$ to $0.00454m^{-1}$. It can be calculated for other wavelengths with the following formula (for sea water):

$$b(\lambda) = b(\lambda_0)(\lambda/\lambda_0)^{-4.32} \qquad \textit{(eq. 13)}$$

The absorption of water cannot be measured directly but derived from measurement of the total beam attenuation coefficient c, where $a = c - b$. The absorption shows a strong increase with increasing wavelength. Both, scattering and absorption, cause the transparency of pure water and pure sea water has its maximum around $\lambda = 0.47\ \mu m$ (Figure 6.2) and that remote observations of water constituents are only possible within the wavelength range $\lambda \sim 0.4 - 0.7\ \mu m$.

Another consequence for imaging spectroscopy is that it is possible to look deeper into clear water at shorter rather than longer wavelengths. In the case of an inhomogeneous vertical distribution of a substance this may imply difficulties in data interpretation. Particularly the use of the phytoplankton chlorophyll fluorescence, with its maximum around $\lambda = 0.685\mu m$, is limited to the upper ~ 2m of the sea due to the absorption of pure water (Figure. 6.3).

The increasing absorption of pure water towards the red can be used to estimate the vertical distribution of chlorophyll within the penetration depth $z_{90} = 1/k$ of case I water (i.e. where only phytoplankton chlorophyll is present), by combining measurements at different wavelengths using the absorption effect in the blue/green and the fluorescence in the red.

6.1.5.2 Optical Properties of Suspended Matter

Suspended matter is defined as all particles which do not pass a filter with a pore size of $0.47\mu m$. For remote sensing purposes all suspended particles in the water without particular pigments are summarized as suspended matter. This means the pigment-containing phytoplankton is treated separately. Thus, suspended matter consists mainly of mineralic particles, such as grains of quartz, and particulate degradation products of organisms, such as broken shells of diatoms, zooplankton and allochthonic material transported by river and through the atmosphere into the sea (Doerffer, 1979). The absorption spectrum of this class of constituents is characterized by a smooth and flat decrease (Figure 6.4) with increasing wavelength without any prominent maxima (Doerffer, 1979; Prieur and Sathyendranath, 1981). A similar shape exhibits the scattering spectrum, which depends on the size distribution of the particles. For particles with a size radius in the order of the wavelength or larger, scattering is described by the Mie theory ((Tanaka and Nakajima, 1977).

Figure 6.2: Scattering (b), absorption (a) and diffuse attenuation (k) of pure water. (Source: Morel, 1974)

Figure 6.3: Penetration depth z_{90} of pure sea water (1), of water with a chlorophyll concentration of 1μg/L (2), and (3) of water with concentrations: suspended matter = 5mg/L, chlorophyll = 5μg/L and Gelbstoff absorption at $\lambda = 0.38\mu m$ of $1m^{-1}$. (Source: Morel, 1974)

Figure 6.4: Diffuse attenuation k of suspended matter (1mg/L), phytoplankton (1µg/L) and Gelbstoff ($a_{380}2m^{-1}$). (Source: Doerffer, 1979; Sathyendranath, 1986)

The lower limit of the size distribution with the transition to the Rayleigh scattering is about: $r_a/\lambda <$ 0.5, i.e. for visible light particles with a radius $r_a < 0.5\mu m$, which are defined as dissolved. The most dominant feature of the scattering function of suspended particles which make measurements very difficult is the strong forward scattering with a very steep increase at small angles. According to Zanewald and Roach (1974) and Pak *et al.*(1971), it is possible to calculate the scattering function by the Mie theory if the particle size distribution, the refractive index of the particles against water and the absorption coefficient are known.

The Mie theory assumes particles with a spherical form and a homogeneous refractive index which, in fact, is often not the case. However, deviations from these assumptions seem not to cause significant problems when using the calculated scattering functions in the evaluation process of remotely sensed radiance spectra with a radiative transfer model (Kronfeld, 1988). By using the Mie theory, the phase function (the normalized scattering function, i.e. the integral over all scattering directions is normalized to 4π) can be calculated, which can be assumed as constant for all wavelengths within the visible part of the spectrum. The relationship between scattering and absorption can be assumed as constant for this wavelength range. It is described by single scattering albedo $\omega_0 = {}^{b}/_{c}$ with a value of about 0.92 for suspended matter (Fischer, 1983). According to Doerffer (1992), for areas or cases where material with other optical properties is dominant, one has to modify these "normal" assumptions and use other size distributions, absorption coefficients and another single scattering albedo.

6.1.5.3 Optical Properties of Phytoplankton

Absorption and Scattering

Phytoplanktons have been treated separately although they are known to be part of marine suspended matter, because of their pigments, which selectively absorb radiance within the visible spectrum. The most dominant pigment is chlorophyll *a*, which is used by photo-organisms to absorb light energy for photosynthesis. In remote sensing, chlorophyll or chlorophyll *a* is used in most cases not in a strict sense but as a measure of the concentration of phytoplankton and its *in vivo* absorption including all pigments. Carotenoids and other accessory pigments, assist the chlorophyll in harvesting light energy of those wavelengths for which the chlorophyll has no or only weak absorption bands (Stauber and Jeffrey, 1988; Rowan, 1989). Besides the concentrations of these pigments, the important influence on the absorption characteristics of the chlorophyll is the structure of the chloroplasts. This structure causes variable specific absorption coefficient a^*, i.e. the absorption per unit pigment concentration (Hitchcock, 1982; Sathyendranath *et al.*, 1989). The concentrations of various pigments per cell and the pigment structure within the cell are variable and depend on:

- the species or group of species comprising the plankton population,
- the light conditions under which the plankton population grows (season, climate, turbulence within water column, etc.)
- the nutrient conditions.

The scattering properties (scattering function, total, forward and backward scattering coefficients) of phytoplankton are determined by a narrow size distribution compared to other suspended particles, particularly in the case of a monospecies bloom (Kronfeld, 1988). These properties have to be calculated with the Mie theory using the size distribution, the refractive index and the absorption coefficient (Doerffer, 1992). The absorption spectrum cannot be derived from pigment extraction but determined through the *in vivo* or *in situ* absorption, which can be performed by vector or scalar irradiance measurements *in situ* or in cuvette systems, or by correcting the absorption spectra of a pigment extract (Sathyendranath, 1986). Biogenic detritus (faecal pellets of zooplankton or fragments of zoo- and phytoplankton) may also contain pigments and their degradation products. These are present particularly in coastal zones near the estuaries and during the process of decaying phytoplankton blooms or heavy grazing of zooplankton (Doerffer, 1979).

The sunlight stimulated fluorescence is the most prominent optical property of phytoplankton with respect to selective passive remote sensing. These are shown in Figure 6.5. According to Gordon (1979) and Doerffer (1992), the sunlight energy, re-emitted by phytoplankton chlorophyll in the form of fluorescence, augments the water leaving radiance around $\lambda = 0.685 \mu m$, where it produces

a small peak. The height of the peak called Fluorescence Line Height (FLH) can be calculated by constructing a baseline from radiances at wavelengths before and after the fluorescence peak (Figure 6.6). According to studies carried out in GKSS (1986), FLH can be linearly correlated with the chlorophyll concentration and thus used to determine its concentration (Figure 6.7). However, the regression coefficients may vary depending on area and season as a function of the phytoplankton population and its physiological state which depends on the actual light conditions, the light history and the nutrient conditions (Günther *et al*, 1986; Gower, 1980; 1981; Doerffer and Fischer, 1987; Doerffer, 1988). The presence of suspended matter, however, may attenuate the fluorescence signal (Fischer and Kronfeld, 1986) or phaeopigment containing detritus may mislead to a high chlorophyll concentration (Doerffer, 1988; Kim *et al.*, 1985).

Figure 6.5: Upwelling radiance in 10 m depth, exhibiting clearly the fluorescence (phytoplankton and result of a two-flow model simulation for the same depth ar concentration as measured: 1 mg/L suspended matter, 7 µg/L chlorophyll-a and Gelbstoff absorption at $\lambda = 0.38\mu m$ of 0.2 m^{-1}. (Source: Doerffer, 1992).

Figure 6.6: Scheme for the calculation of the fluorescence line height FLH of chlorophyll-a. (Source: Doerffer, 1992).

Figure 6.7: Relation between FLH, as measured from an aircraft with a spectrophotometer from 600m and the chlorophyll concentration measured in 2 m depth along a 90km profile in the Fladengrund (North Sea) during FLEX'76. (Source: Doerffer, 1992)

6.1.5.4 Optical Properties of Gelbstoff

Approximately 70% of the dissolved carbon in the ocean is formed by a mixture of various molecules, which can only be described by a sum of parameters and not by a single structure formula (Spitzy and Ittekkot, 1986). This fraction which passes a filter with a pore size of $0.45 \mu m$, for dissolved species is called gelbstoff. In case of high concentrations, it causes a yellow discolouration of the water by its high absorption of blue light (Kalle, 1966). Gelbstoff is formed from excretion or degradation products of organisms under the activity of microbes. After microbial degradation and decomposition new complex molecules are composed by biochemical and chemical condensation. The polymers have molecular weights in order of 100 – 100000 (Gjessing, 1976). These colloids can partly be bonded to floc-like particles exceeding even the $0.45 \mu m$ definition size for particles. The large number of conjugated double bonds cause various overlapping spectral absorption bands with the result of an absorption spectrum, which is decreasing approximately logarithmically with increasing wavelength within the visible spectrum (Bricaud and Morel, 1987).

Generally, most gelbstoff are transported by rivers into the sea, but it has also been found in patches of high phytoplankton concentrations. Gelbstoff molecules are very stable and thus can be used as natural tracers (Diebel-Langohr *et al.,* 1986). In coastal zones where estuaries are transporting large quantities of gelbstoff into the sea, the absorption of gelbstoff can be used to trace the distribution of fresh water within the coastal area. However, the maximum absorption is in the same wavelength range ($\lambda = 0.40 – 0.47 \mu m$) as the absorption bands of chlorophyll. In studies by Doerffer (1992) for inverse modelling, at least 3 spectral bands are used in the blue green range in order to separate chlorophyll *a* and gelbstoff.

6.1.6 The Influence of the Atmosphere

The contribution of the atmosphere measured from a satellite over ocean water is more than 90% (Figure 6.8) and a correction of the measured signal, L_t, with respect to the transmission of the water leaving radiance, L_w, and the path radiance, L_{atm}, is necessary (Plass *et al.*, 1976). This is known as atmospheric correction. According to Gordon (1978), the basic idea for atmospheric correction is to measure the radiance in near infrared (NIR) channels where the absorption of water is so high that nearly no light is leaving the water. All radiances measured at wavelength $\sim > 0.7$ μm have to stem from radiance scattered at air molecules and aerosols, and from light specularly reflected at the water surface. The wavelength dependence of light scattered by air molecules is known from the Rayleigh law where the scattering coefficient decreases with increasing wavelength by $\lambda^{-4.08}$ (Penndorf, 1957). This is similar to the scattering of pure water. The wavelength dependence of scattering by aerosols is variable and depends on the size distribution of the aerosols (Ångström, 1930). Based on the studies by Plass and Kattawar (1972), van de Hulst (1980) and Antoine and Morel (1998), two different types of aerosols are present:

(i) maritime aerosol with a flat decrease in the attenuation coefficient

(ii) continental aerosol with a strong decrease with increasing wavelength.

Figure 6.8: Water-leaving radiance spectrum at the top of the atmosphere (1), contribution by aerosol (2) and Rayleigh scattering (3), and the total radiance (4) calculated for a sun zenith distance of 40°, a horizontal visibility of 20km and coastal water. (Source: Doerffer, 1992)

The slope of this decrease is described by the Ångström wavelength coefficient α:

$$\alpha = \frac{\ln \tau_a(\lambda_1) - \ln \tau_a(\lambda_2)}{\ln \lambda_2 - \ln \lambda_1} \qquad \textit{(eq. 14)}$$

where τ_a is the aerosol optical thickness at the two wavelength λ_1 and λ_2. This Ångström coefficient can be determined by using at least two channels in the NIR with a high radiometric resolution because of low light levels. It is used to calculate the aerosol path radiance for all required channels in the blue – red part of the spectrum by extrapolating the aerosol path radiance from one of the NIR channels (Gordon, 1978; Sturm, 1981; Doerffer *et al.*, 1989). The water leaving radiance at the sensor L^*_w can be retrieved by subtracting the aerosol path radiance L_a and the calculated Rayleigh path radiance L_r from then total radiance. The water leaving radiance L_w is calculated by:

$$L_w = L^*_w / t \qquad \textit{(eq. 15)}$$

with t being the diffuse transmittance of the atmosphere in the direction of the sensor, which is mainly determined by the diffuse transmittance through the "Rayleigh atmosphere", t_r, and the transmittance by absorption of atmospheric gases, t_{ag} (André and Morel, 1989).

The following sections explain the basis of the modelling methodology used in this study. The method used in search of Suspended Particulate Algorithm for Coastal Remote Sensing (abbr. SPACoRS) is the Simple Radiative Transfer Model (section 6.2). A modified version of the Simple Radiative Transfer Model is also discussed in section 6.3.

6.2 *SIMPLE RADIATIVE TRANSFER MODEL* (SIRTRAM)

The simple model produced by Doerffer (1992) used in this study describes the radiative transfer within the ocean-atmosphere system. It is based on algebraic expressions in order to keep it simple for inverse modelling of imaging spectrometer data. This requires the separation of solar radiation transport into different processes, such as the molecule and the aerosol scattering and the absorption by different gases. Within the atmosphere, only single scattering is treated. A two-flow model describes the radiative transfer within the water; for simulating the sunlight stimulated chlorophyll fluorescence, an approximation procedure has been added. Refraction and reflection at the air/sea interface with specular reflection of sunlight at a rough sea surface are included.

Since in real situations, the actual values of many parameters that could be included are not known, this kind of a model is sufficient to describe the core processes. Moreover, it has been proven as sufficiently accurate with respect to the many unknowns in real situations.

The following variables have been included in the model:

- sun and viewing zenith angle, azimuth angle between the vertical planes of viewing and sun direction,

- atmospheric pressure (for Rayleigh scattering and absorption of mixed gases), concentration of ozone and water vapour,
- aerosol extinction derived from horizontal visibility,
- windspeed for calculating the specular reflection of direct sunlight at a rough sea surface,
- concentrations of phytoplankton pigment, suspended matter and gelbstoff absorption.

The model is based on equations published in Joseph (1950), André & Morel (1989), Sturm (1980, 1981), and Iqbal (1983). The data tables used in the model calculation are based on values presented in Prieur & Sathyendranath (1981), Iqbal (1983), Doerffer (1979), Morel (1974), Jerlov (1976), and Fischer (1983). Data are given for the spectral range λ: 400 - 750nm with a resolution of 5nm.

The total radiance L_t (λ, θ_s, θ_v, ϕ) which a sensor is receiving at the top of the atmosphere can be divided into 4 components:

$$L_t = L_a + L_\tau + L_{s\tau} + L^*_\omega \qquad \textit{(eq. 16)}$$

with L_a and L_τ the aerosol and the Rayleigh path radiance, including that part specularly reflected at the surface ('sky light glitter"), where the total atmospheric path radiance $L_{atm} = L_a + L_\tau$, , and L^*_ω the water-leaving radiance after transmittance through the atmosphere, and $L_{s\tau}$ the specularly reflected sun light ("sun glitter").

These radiance components are depending on wavelength (λ), on the viewing zenith angle of the instrument (pixel to sensor) (θ_υ), the sun zenith angle (pixel to sun) (θ_s), and the azimuth angle (ϕ) between the vertical planes of pixel to sun and the pixel to sensor. For simplicity the dependence on (λ) and on the angles is omitted within most of the further equations.

6.2.1 Transmittance of Solar Radiation through the Atmosphere

The transmittance of the solar radiation down to the water surface and of the water leaving radiance up to the sensor can be approximately separated into 5 terms:

τ_τ optical thickness for Rayleigh scattering

τ_a optical thickness for aerosol scattering

τ_{oz} optical thickness for ozone absorption

τ_{mg} optical thickness for absorption of mixed gas

$\tau_{\omega\upsilon}$ optical thickness for water vapour absorption

where τ, the optical thickness, is the attenuation coefficient c multiplied by the vertical path through the atmosphere.

According to Leckner (1978), τ_τ can be calculated with λ in (μm) as shown in equation 17:

$$\tau_\tau = 0.008735\lambda^{-4.08}m_a \qquad \textit{(eq. 17)}$$

where m_a is the air mass factor at actual pressure P_a; it can be calculated by the pressure ratio (equation 18)

$$m_a = p_a/1013.25 \qquad \textit{(eq. 18)}$$

The attenuation by aerosols can be calculated according to *Ångström's turbidity formula* (Ångström, 1930) as shown in equation 19:

$$\tau_a = \beta\lambda^{-\alpha} \qquad \textit{(eq. 19)}$$

β is the Ångström turbidity coefficient, ranging from 0 for a clean atmosphere to 0.4 for a turbid atmosphere with a horizontal visibility < 5 km, α is the wavelength exponent with an average value of $\alpha = 1.3 \pm 0.5$, for a maritime atmosphere $\alpha = 1.0$ is a good value.

For horizontal visibilities *Vis* greater than 5 km, the turbidity coefficient can be calculated by equation 20 (McClatchey and Selby, 1972):

$$\beta = (0.55)^{\alpha}(3.912/Vis - 0.01162)[0.02472(Vis - 5) + 1.1.32] \qquad \textit{(eq. 20)}$$

The transmittance of either the solar radiation through the atmosphere for the calculation of the irradiance at the sea surface or the transmittance of the signal from the sea surface up to the sensor with respect to scattering is then:

$$T_{sx} = \exp\left[-(1 - \omega_{0\tau}b_{f\tau})\tau_\tau + (1 - \omega_{0a}b_{fa})\right] / \cos\theta_x \qquad \textit{(eq. 21)}$$

with x either the diffuse transmittance for solar radiation using the solar zenith angle or the diffuse transmittance for the signal using the viewing zenith angle.

Single scattering albedo for a maritime atmosphere can be set to $\omega_{0\tau}$ and $\omega_{0a} = 1$, and the forward scattering factor for Rayleigh scattering $b_{f\tau}$ to 0.5 and for aerosol scattering b_{fa} to 0.9.

The optical thickness of ozone is simply calculated by:

$$\tau_{oz} = a_{oz}\tau_{oz} \qquad \textit{(eq. 22)}$$

with a_{oz} the ozone absorption coefficient per cm NTP and τ_{oz} the amount of ozone in the atmosphere in cm NTP.

The transmittance through the ozone atmosphere is then:

$$T_{ozx} = \exp (-\tau_{oz}/\cos\theta_x) \qquad \textit{(eq. 23)}$$

with θ_x either the viewing or sun zenith angle for upward or downward transport, respectively.

The calculation of transmittance due to atmospheric gases other than ozone cannot be calculated by the simple Lambert-beer law because of the highly oscillatory function of wavelength. Leckner (1978) has developed algorithms for the transmittance due to the molecular absorption of mixed gases (CO_2, O_2, etc.) t_{mg} and of water vapour $t_{\omega\upsilon}$:

$$t_{mgx} = \exp [-1.41\tau_{mgx} / (1 + 118.93\tau_{mgx})^{0.45}] \qquad \textit{(eq. 24)}$$

and

$$t_{\omega\upsilon x} = \exp [-0.2385\tau_{\omega\upsilon x}/(1 + 20.07\tau_{\omega\upsilon x})^{0.45}] \qquad \textit{(eq. 25)}$$

with

$$\tau_{mgx} = c_{mg} m_a/\cos\theta_x \qquad \textit{(eq. 26)}$$

and

$$\tau = c_{\omega\upsilon}\ \mathrm{Conc}_{\omega\upsilon}/\cos\theta_x \qquad \textit{(eq. 27)}$$

where c_{mg} is the absorption coefficient for mixed gas for the vertical path through the standard atmosphere, m_a the pressure ratio from eq. 18, $c_{\omega\upsilon}$ the absorption coefficient per cm precipitated water-vapour, $\mathrm{Conc}_{\omega\upsilon}$ the content of water-vapour in the atmosphere in cm, and θ_x the viewing or sun zenith angle and x either the downward d or upward u direction.

By using the corresponding zenith angle for calculatingτ, the total gas absorption for the solar radiation t_{gd} is:

$$t_{gd} = t_{ozd}\, t_{mgd}\, t_{wvd} \qquad \textit{(eq. 28)}$$

and the gas absorption for the signal (radiation in direction to the sensor) t_{gu}

$$t_{gu} = t_{ozu}\, t_{mgu}\, t_{wvu} \qquad \textit{(eq. 29)}$$

The total transmittance through one way of the atmosphere with x the direction is then:

$$t_{totx} = t_{sx}\, t_{ozx}\, t_{mgx}\, t_{wvx} \qquad \textit{(eq. 30)}$$

and for both ways:

$$t_{two} = t_{totd}\, t_{totu} \qquad \textit{(eq. 31)}$$

6.2.2 The Path Radiance

The solar radiation (F_s, above atmosphere) scattered by the atmosphere into our sensor L_{atm}, the path radiance, is separated into two streams, the Rayleigh path radiance L_r and the aerosol path radiance L_a with

$$L_{atm} = L_r + L_a \qquad \textit{(eq. 32)}$$

For both parts the direct scattered lights as well as the scattered light which is specularly reflected at the sea/air interface have to be considered:

$$L_x = F_s \tau \omega_0 p_x / (4\pi \cos\theta_v) \qquad \textit{(eq. 33)}$$

With $x = a$ for aerosol and r for Rayleigh, the scattered part of the radiance p_x is

$$p_x(\theta_v, \theta_s) = P_x(\gamma^-) + [\rho(\theta_v) + \rho(\theta_s)]P_x(\gamma^+) \qquad \textit{(eq. 34)}$$

where ρ is the Fresnel reflectance, which is wavelength independent, and P_x is the scattering phase function, the – superscript indicates the scattered light, the + superscript that part, which is also specularly reflected at the air/sea interface.

The scattering angles in direction to the sensor and in direction to the sensor via the air-sea interface are:

$$\cos\gamma^{\pm} = \pm\cos\theta_v\cos\theta_s - \sin\theta_v\sin\theta_s\cos(\phi) \qquad \textit{(eq. 35)}$$

The Rayleigh phase function is:

$$P_r(\gamma^{\pm}) = \tfrac{3}{4}(1 + \cos^2\gamma^{\pm}) \qquad \textit{(eq. 36)}$$

The aerosol phase function depends on the particle size and chemical composition; it can be approximated by the two-term Henyey-Greenstein phase function:

$$P_a(\gamma^{\pm}) = \alpha f(\gamma^{\pm}, g_1) + (1 - \alpha) f(\gamma^{\pm}, g_2) \qquad \textit{(eq. 37)}$$

where

$$f(\gamma^{\pm}, g) = \frac{1 - g^2}{(1 + g^2 - 2g\cos\gamma^{\pm})^{3/2}} \qquad \textit{(eq. 38)}$$

with $\alpha = 0.985$, $g_1 = 0.8$, $g_2 = 0.5$ according to Sturm (1980) and Gower (1981).

For the calculation of the specular reflectance at the air-sea interface, $\rho(\theta_v)$ and $\rho(\theta_s)$, Snell's Law is used:

$$\sin i / \sin j = n \qquad \textit{(eq. 39)}$$

where i is the incident zenith angle θ_v or θ_s ; j is the zenith angle of the refracted beam underwater and n is the refractive index, of which for sea water is 4/3. The Fresnel Law for unpolarized light is then:

$$\rho(i) = \tfrac{1}{2}[\sin^2(i-j)/\sin^2(i+j) + \tan^2(i-j)/\tan^2(i+j)] \qquad \textit{(eq. 40)}$$

6.2.3 The Subsurface Albedo

The subsurface reflectance R is described by the two-flow equation (eq. 41) as described in Joseph (1950) and Doerffer (1979), for a homogeneous water column with a bottom depth, $z >> z_{90}$:

$$R = (k - a)/(k + a) \qquad \textit{(eq. 41)}$$

Since k, the diffuse attenuation coefficient, is an apparent parameter, this equation is only an approximation. However, it has been proven as useful and sufficiently accurate for many applications, because in most cases the actual radiance distribution below the water surface due to a partly clouded sky and waves is not known anyway.

The coefficient a and k can be split into the components for pure water a_w, k_w, and into the specific coefficients (per unit concentration) for chlorophyll a_c, k_c; for suspended matter a_s, k_s; and for gelbstoff a_g, k_g with C_x the corresponding concentrations:

$$a_{tot} = a_w + C_c a_c + C_s a_s + C_g a_g \qquad \textit{(eq. 42)}$$

and

$$k_{tot} = k_w + C_c k_c + C_s k_s + C_g k_g \qquad \textit{(eq. 43)}$$

The subsurface upwelling irradiance E_{us} with E_{ds}, the subsurface downwelling irradiance, is then simply:

$$E_{us} = E_{ds} R \qquad \textit{(eq. 44)}$$

For the calculation of the contribution by the sun light stimulated chlorophyll fluorescence to the upwelling irradiance, the following procedure is used as an approximation:

The total solar radiation within the wavelength range λ_1 - λ_2 absorbed by the phytoplankton pigment is:

$$E_{af} = \int_{\lambda 1}^{\lambda 2} E_{ds}\,(1 - R(\lambda))[\, C_c a_c(\lambda)/a_{tot}(\lambda)]\, d\lambda \qquad \textit{(eq. 45)}$$

with values of $\lambda_1 = 0.4\mu m$ and $\lambda_2 = 0.675\mu m$.

The emitted energy into the upper hemisphere E_{uf} is:

$$E_{uf} = 0.5 E_{af} F_{eff} \qquad \textit{(eq. 46)}$$

with F_{eff} as the fluorescence efficiency with a mean value of 0.003 (Günther *et al,* 1986).

Since the fluorescence energy is emitted over a broad band which can be described by a Gaussian shape with a standard deviation of $\sigma = 10.6\ nm$ equivalent to a half bandwidth of 25 nm (Gordon, 1979; Kronfeld, 1988), the fluorescence energy has to be distributed over a wavelength band for each wavelength λ_f around the wavelength of maximum fluorescence energy, set to $\lambda_o = 0.685 \mu m$.

The weights $g(\lambda_f)$ for the wavelength intervals $d\lambda$ are calculated by:

$$g(\lambda_f) = (1/\sqrt{2\pi\sigma^2})\exp(-(\lambda_f - \lambda_{of})^2/2\sigma^2) \qquad \textit{(eq. 47)}$$

The effect of differences produced by the mean penetration depth for the absorbed solar radiation and the mean depth from which the fluorescence energy arrives at the surface (due to different attenuations in the blue-green and in the red spectral range) was calculated by a factor for each emission wavelength using the following procedure:

(i) The mean excitation depth z_{ex} weighted by the absorption of phytoplankton pigments for the spectral range $\lambda_1 - \lambda_2$ is:

$$z_{ex} = \sum C_c a_c(\lambda_i) / \sum k_{tot}(\lambda_i) C_c a_c(\lambda_i) \qquad \textit{(eq. 48)}$$

(ii) This mean depth is used to calculate the emission depth for fluorescence at each of the wavelength around $0.685 \mu m$, and with both weights the subsurface upwelling spectrum of fluorescence radiation becomes:

$$F_u(\lambda) = (E_{uf} g(\lambda)) / (z_{ex} k_{tot}(\lambda)) \qquad \textit{(eq. 49)}$$

(iii) The total subsurface upwelling irradiance including fluorescence is then:

$$E_{ustot}(\lambda) = E_{us}(\lambda) + F_u(\lambda) \qquad \textit{(eq. 50)}$$

6.2.4 Transport Through the Air/Sea Interface

The transmittance T_d through the air/sea interface for calculating E_{ds}:

$$T_d = (1 - \rho) \cos \theta_s \qquad \textit{(eq. 51)}$$

with ρ being the specular reflection of sun and sky light averaged over all directions, which is set to 0.06, and θ_s is the sun zenith angle.

5. the specularly reflected sun radiance $L_{sr}(\lambda)$ has to be added.

Therefore, the calculation of all wavelengths:

$$E_{ds} = F_s t_{sd} t_{gd} T_d \qquad \textit{(eq. 59)}$$

$$E_{us} = E_{ds} R \qquad \textit{(eq. 60)}$$

By using equations 30, 31, and 34, the fluorescence value, F_u, is calculated and substituted into the following equation to obtain the water leaving radiance for all wavelengths at sensor:

$$L^*_w = (E_{us} + F_u) T_u t_{totu} / Q \qquad \textit{(eq. 61)}$$

The total radiance at the sensor is then calculated as:

$$L_t = L^*_w + L_{atm} + L_{sr} \qquad \textit{(eq. 62)}$$

6.3 *MODIFIED SIMPLE RADIATIVE TRANSFER MODEL* (M-SIRTRAM)

The work of Doerffer (1992), which utilized the Simple Radiative Transfer Model (SIRTRAM, a Two-Flow Model), was selected as the main reference in this modelling study. Modifications were made to its original SIRTRAM programme written in C Language, to suit the existing characteristic environment of Tanjung Rhu, Pulau Langkawi. These modifications were necessary as the SIRTRAM was originally designed for the temperate oceanic atmosphere as well as the water quality. These modifications were made by Doerffer for the purpose of this study. The programme has been re-named *Modified Simple Radiative Transfer Model*, which will now be referred to as *M-SIRTRAM.*

Two M-SIRTRAM programmes, Single Scattering M-SIRTRAM and Random Computation M-SIRTRAM, were used in this study for the development of the algorithm. This is shown in the form of a flowchart in Figure 6.9. Modifications were based on the TSP characteristics specific to the coastal waters within the study area. Modified elements for the specific characteristics in the programme include TSP backscattering, TSP absorbance, gelbstoff slope and gelbstoff values. These values need to be included because the nature of the study area consisting of its various natural habitats such as mangroves, riverine, estuarine, and coral reefs (described in Chapter 2) contributed specific characteristics to the water quality as seen in remote sensing. These values, which were included, contributed to the modifications necessary in the original SIRTRAM.

The initial phase of M-SIRTRAM was to determine these specific characteristics because:

i. the type of suspended particulates in the waters of Tanjung Rhu was not measured,

ii. the specific characteristics of the suspended particulates such as its absorbing or backscattering properties are therefore not known,

iii. the amount of gelbstoff was not measured, and

iv. the specific absorbing and backscattering properties of gelbstoff are also not known.

The second phase of the modelling process was to determine the satellite imagery band or band combinations that would contribute the most information in the development of the algorithm with the highest accuracy possible for the dynamic aquatic system of Tanjung Rhu.

There are two key issues that govern the expectations of the final output, *i.e.* the algorithm:

1. The expected algorithm should be *as simple as possible*.
2. The expected algorithm should be applicable to both wet and dry seasons of the tropics.

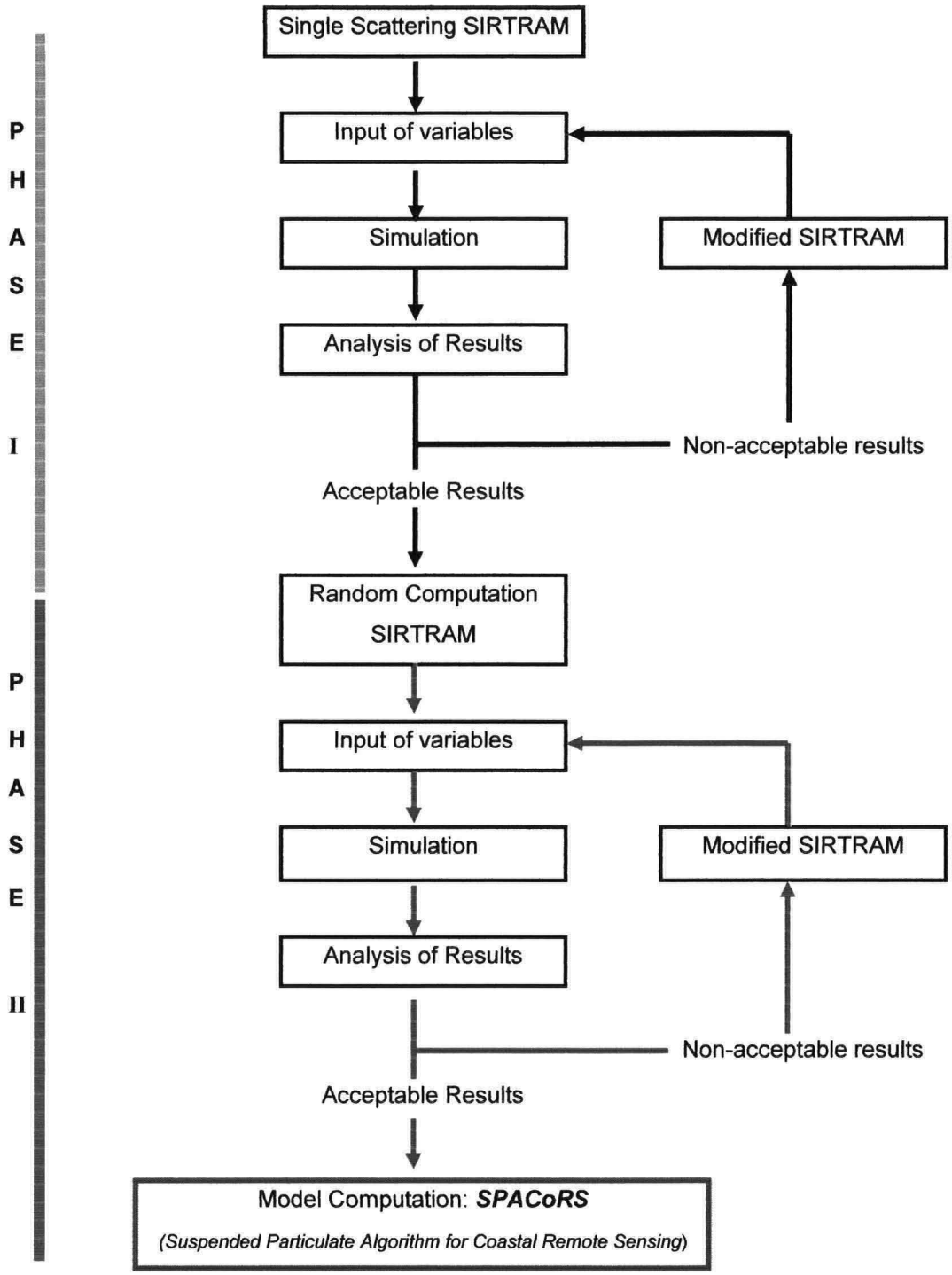

Figure 6.9: A Methodology Flowchart for the Development of SPACoRS.

6.3.1 Profiles of the Reflectances and Irradiances at Tanjung Rhu

The upwelling and downwelling irradiances in air measured at Tanjung Rhu at 1216hr on 16 January 1998 using Li-COR Spectroradiometer Model LI-1800 were used to determine the profiles of the irradiances and reflectances within the area (Figure 6.10a). The purpose of this measurement was to quantify the incoming radiation or irradiance incident upon the measurement site which was later used to prepare spectral reflectance curves for the measured site.

The calibrated downwelling irradiance ($W/m^2/\mu m$) measured against wavelength (300 – 1100 nm) is given in Figure 6.10b. The profile itself showed the typical peaks and valleys at specific wavelength region showing some main atmospheric absorption band region such as the O_3, O_2, and water vapour, and also its maximum irradiance or energy flux density. This measured profile was compared to a typical spectral distribution of solar radiation of a 'black body', extraterrestrial and direct beam/normal incidence at earth's surface plotted logarithmically together with the main atmospheric absorption bands (Figure 6.11).

The total solar output to space, assuming a temperature of 5,760K for the sun, is 3.84×10^{26} W, but only a tiny fraction of this is intercepted by the earth, because the energy received is inversely proportional to the square of the solar distance (150 million km) (Barry and Chorley, 1998). For solar radiation, 8% is ultraviolet and shorter wavelength emission, 39 % visible light (400 – 700 nm) and 53 % NIR (>700 nm). According to Stefan's Law, the total energy emitted by a black body is given by the area under each curve:

$$F = \sigma T^4 \qquad \textit{(eq. 63)}$$

where $\sigma = 5.67 \times 10^{-8}$ $W/m^2/K^4$; T = absolute temperature (K); and F = energy emitted (W/m^2). Since the mean temperature of earth's surface is 288 K (15°C), the energy emitted would be 370.08 W/m^2. This value is about 23% of a black body radiation curve of 6,000 K at the top of atmosphere (1.6 kW/m^2).

Figure 6.11 showed that in the case of a perfect situation, the direct beam (normal incidence) solar radiation at the earth's surface is 907 W/m^2. However, this is not the case in a real situation because solar radiation varies with latitude and season for the whole globe (Figure 6.12), the presence of interaction between atmospheric gases, aerosols and suspended particulates in air will then result in further absorption and scattering of the radiation.

The solar radiation is very intense and is mainly short-wave between 0.2 and 4.0 μm (200 – 4000 nm), with a maximum (per unit wavelength) at around 0.5 μm (500 nm) (Barry and Chorley, 1998).

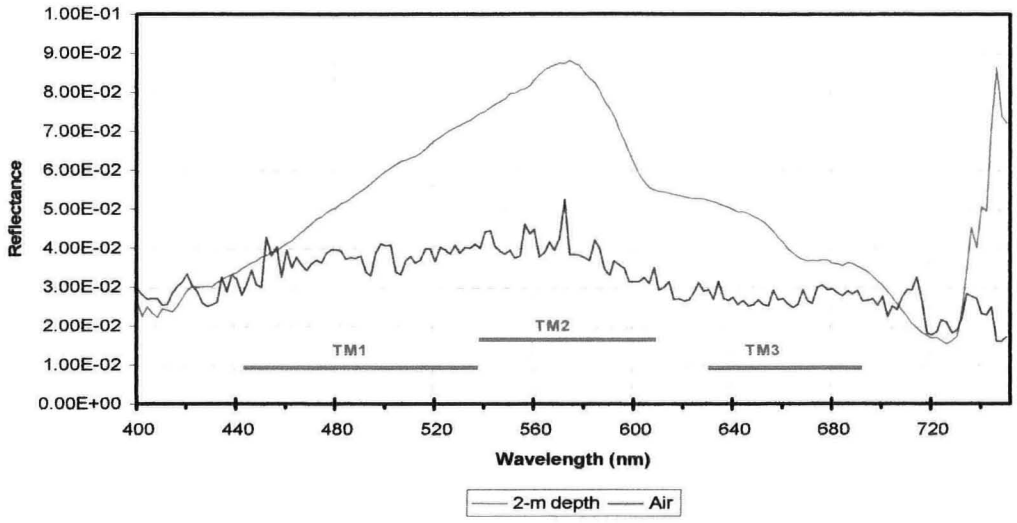

Figure 6.10a: Calculate reflectance (Ratios of Upwelling/Downwelling Irradiances) at Tanjung Rhu, 16 January 1998

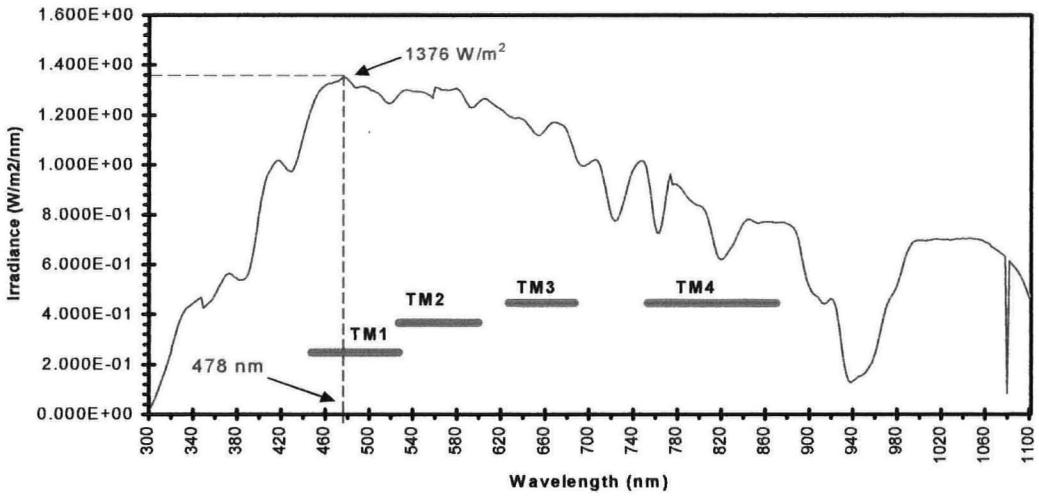

Figure 6.10b: Downwelling (calibrated) Irradiance in Air at Tanjung Rhu - 16 January 1998

Figure 6.11: Spectral distribution of solar and terrestrial radiation, plotted logarithmically, together with the main atmospheric absorption bands. (Source: Sellers, 1965).

From Figure 6.10b, the peak irradiance measured, 1,376 $W/m^2/\mu m$, was observed at 478nm. This value is a good indication of good atmospheric condition at the time of measurement because the maximum irradiance is similar to that projected in Figure 6.11. It is also an indicator of almost cloudless sky during measurement. About 18 % of the incoming energy is absorbed directly by ozone and water vapour. Ozone absorption is concentrated in three solar spectral bands (200-310 nm, 310-350 nm and 450-850 nm), while water vapour absorbs to a lesser degree in several bands between 900 – 2100 nm (Figure 6.11). These absorption characteristics were also observed in the irradiance curve of Tanjung Rhu shown in Figure 6.10a.

The relative roles of the atmosphere, clouds and the earth's surface in reflecting and absorbing solar radiation at different latitudes are illustrated in Figure 6.12. Of 100% radiation entering the top of atmosphere, about 20% is reflected back into space by clouds, 3% by air (plus dust and water vapour), and 8% by earth's surface. About 3% is absorbed by clouds, 18% by the air, and 48% by the earth (Sellers, 1965).

Figure 6.12: The average latitudinal disposition of solar radiation in Wm^{-2}. (Source: Sellers, 1965)

The upwelling irradiances had also been measured for several locations within Tanjung Rhu as shown in Figure 6.13. As expected the reflected values (50-200 $W/m^2/\mu m$) were much lower than those measured for downwelling because these irradiances would also have been absorbed by the earth surfaces. Only a fraction of 3-18% had been reflected during measurement.

Figure 6.13: Upwelling Irradiance (E_u) In Air at Tanjung Rhu, 18 January 1998

6.3.2 Determination of Satellite Band or Band Combinations for the Development of the Algorithm

To determine the satellite band or band combinations that could be used in the modelling process, a simulation of results was required for the range of TSP concentrations that characterize the water condition within the study area of Tanjung Rhu. Based on the results obtained in Chapter 3, a TSP concentration from 30 - 275 mg/L was preferred. The simulation of results requires the input of the TSP range into the SIRTRAM programme. This initial simulation process is important because there are 7 different bands in the Landsat Thematic Mapper data ranging from visible to NIR and Thermal IR of the electromagnetic spectrum, and not all the bands provide useful information in the development of the algorithm. This process narrows the number of bands that could possibly be used to detect TSP in surface waters. Since TSP is a visible pollution indicator, it would be more appropriate to limit the search of TM bands within the visible electromagnetic spectrum, *i.e.* TM1, TM2 and TM3.

Results computed in Figure 6.14 showed 3 distinguishable trends of XY scatter plots for radiance reflectance values of TM bands 1, 2 and 3 against concentrations of Suspended Particulates ranging between 30-275 mg/L. These results were based on fixed values of chlorophyll (1.0-2.0μg/L), z-depth (25 m), gelbstoff$_{abs440nm}$ (0.02-0.2).

Logarithmic trends drawn on these 3 TM bands produced the following equations and R^2 values:

TM1 : $y = 0.0005 ln x + 0.0081$ $R^2 = 0.7171$ *(eq. 64)*

TM2 : $y = 0.0006 ln x + 0.0073$ $R^2 = 0.9260$ *(eq. 65)*

TM3 : $y = 0.0016 ln x + 0.0013$ $R^2 = 0.9752$ *(eq. 66)*

where y = radiance, and x = [TSP] mg/L.

Based on these 3 different logarithmic trends, it was deduced that TM3 would project a better representation of TSP in water because the slope is greater indicating higher sensitivity to changes in [TSP] within the water column, and the computed R^2 was the highest (0.9752). The other possible band was TM2. It had the second highest slope factor and the R^2 was also high (0.9260). However, TM1 will not be considered here because TM1 generally contains most noise. Furthermore, the slope factor difference between TM1 and TM2 was very small and the trend scale was almost similar. There may also be a tendency to have too much overlapping information between TM2 and TM1.

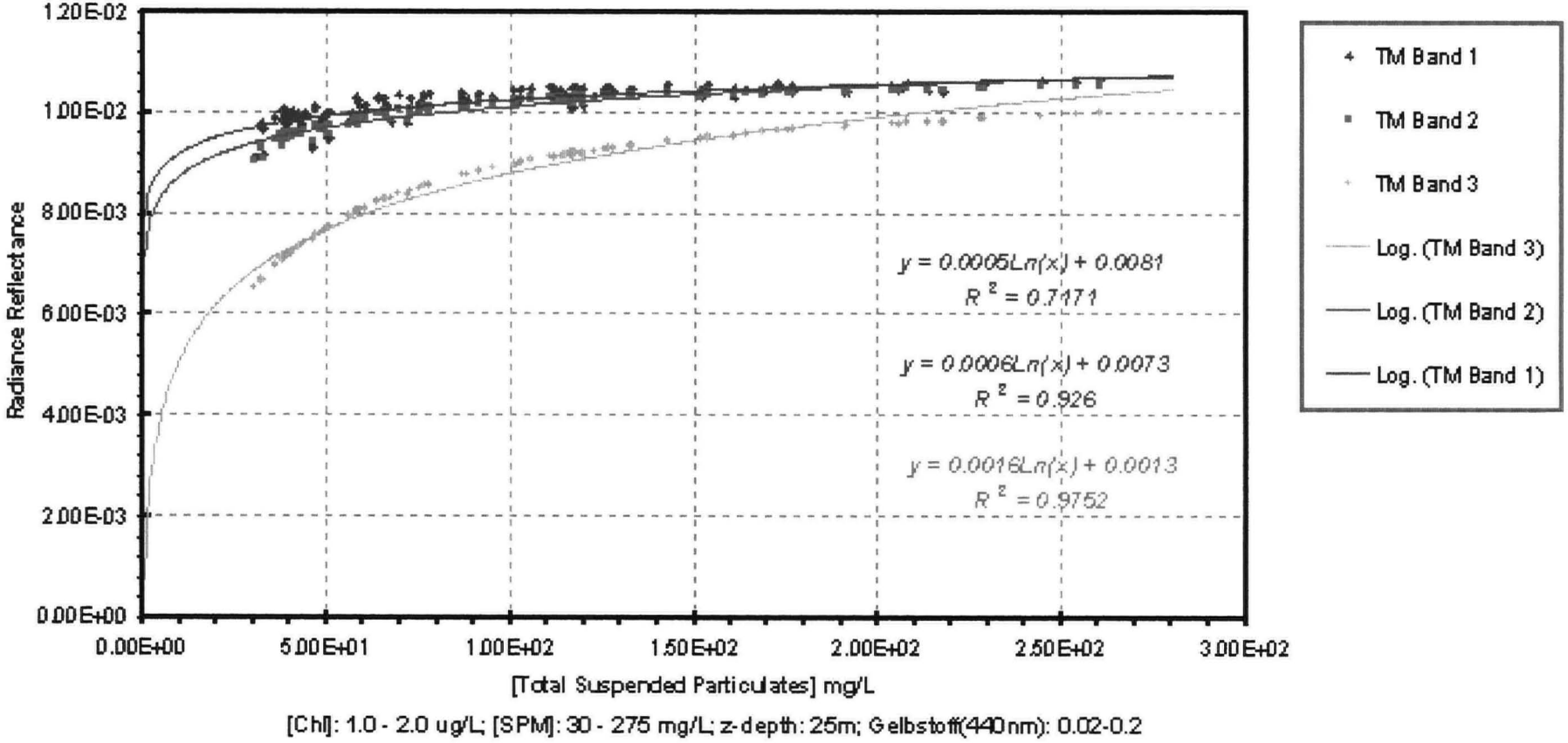

Figure 6.14: Reflectance values of TM Bands 1, 2, 3 for Total Suspended Particulates (30 – 275 mg/L)

Since TM3 and TM2 were the preferred bands here, the ratios of radiances between TM3/TM2 would produce a better and stable projection of the case. Computed ratios of TM3/TM2 against [TSP] were plotted (Figure 6.15). Similar logarithmic trend as projected in Figure 6.15 was also observed in this chart. The computed equation and R^2 were as follows:

TM3/TM2 : $y = 0.1112 ln x + 0.3543$ $R^2 = 0.9723$ *(eq. 67)*

where y = radiance, and x = [TSP] mg/L.

Computed log values of TM3/TM2 against log [TSP] were plotted in Figure 6.16 resulting in the following equations and R^2 values when the line is projected:

i. *linearly*: $y = 0.1324x - 0.3284$ $R^2 = 0.9604$ *(eq. 68)*

ii. *logarithmically*: $y = 0.2571 ln x - 0.2394$ $R^2 = 0.9797$ *(eq. 69)*

iii. *polynomially in the order of 2*:

$y = 0.1093x^2 + 0.5581x - 0.7352$ $R^2 = 0.9966$ *(eq. 70)*

where y = log(TM3/TM2), and x = log [TSP] mg/L

The results above showed that the band combinations of TM3 and TM2 provided the most sensitive band combination in the development of an algorithm for the retrieval of TSP in surface waters.

6.3.3 Computation of $R_{rs\text{-}Toa}$ Using Different Case Scenarios to Determine the Specific Characteristics of the Suspended Particulates and Gelbstoff.

To determine the specific characteristics of the suspended particulates and gelbstoff, computations of single scattering SIRTRAM need to be carried out based on different case scenarios. Based on the analysis of these computations, the most probable variables will be included or modified in the original SIRTRAM. This is a constant modification process.

There are 3 main steps in the determination of the specific characteristics of Suspended Particulates and the gelbstoff in the surface waters of Tanjung Rhu using the SIRTRAM. These steps are given in the flowchart (Figure 6.17). The first is to determine the general characteristics of gelbstoff, secondly to quantify the possible concentration range of gelbstoff, and thirdly to identify TSP backscattering and absorbing properties and the gelbslope.

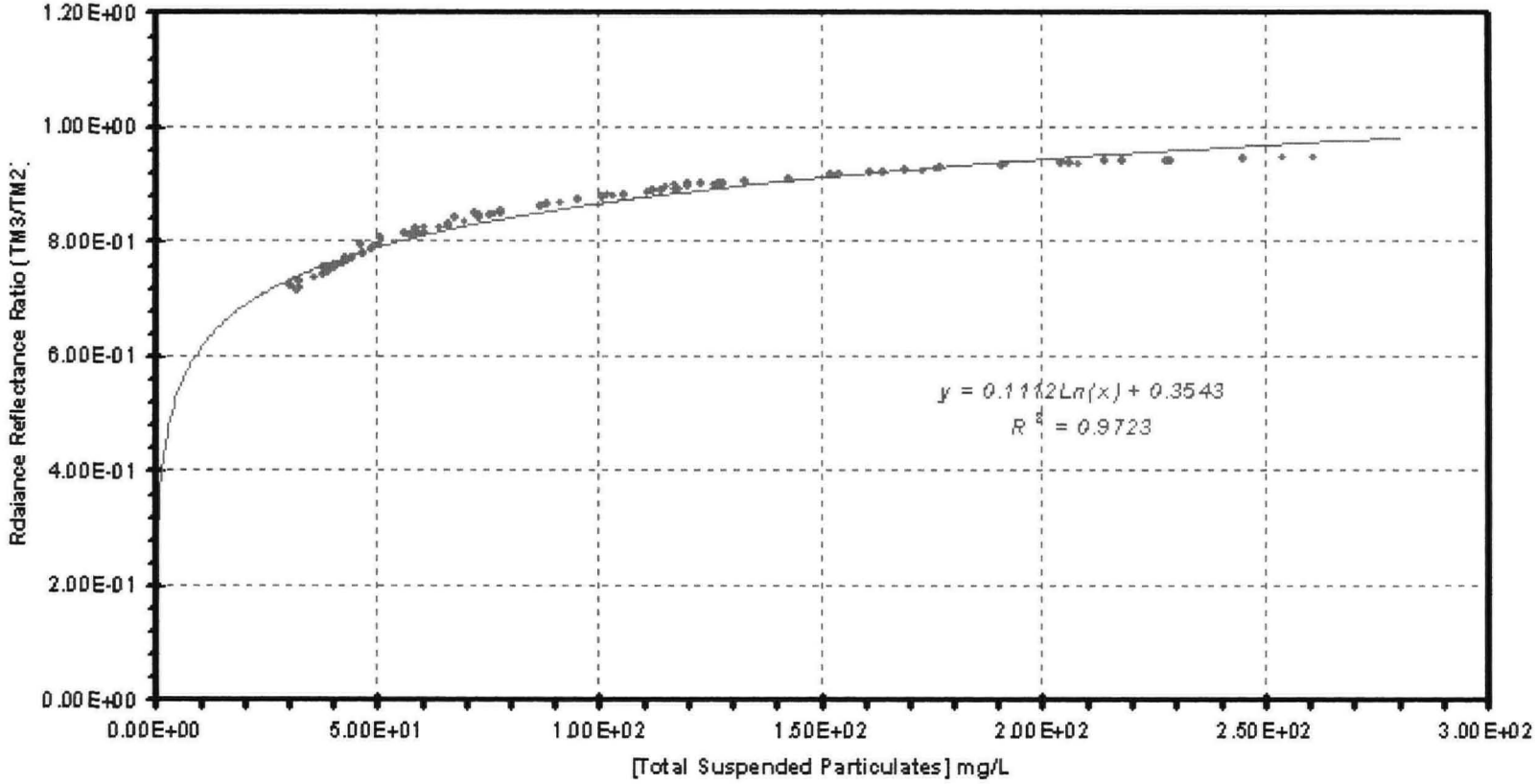

Figure 6.15: Radiance Reflectances of TM3/TM2 ratios for Total Suspended Particulates (30 – 275 mg/L)

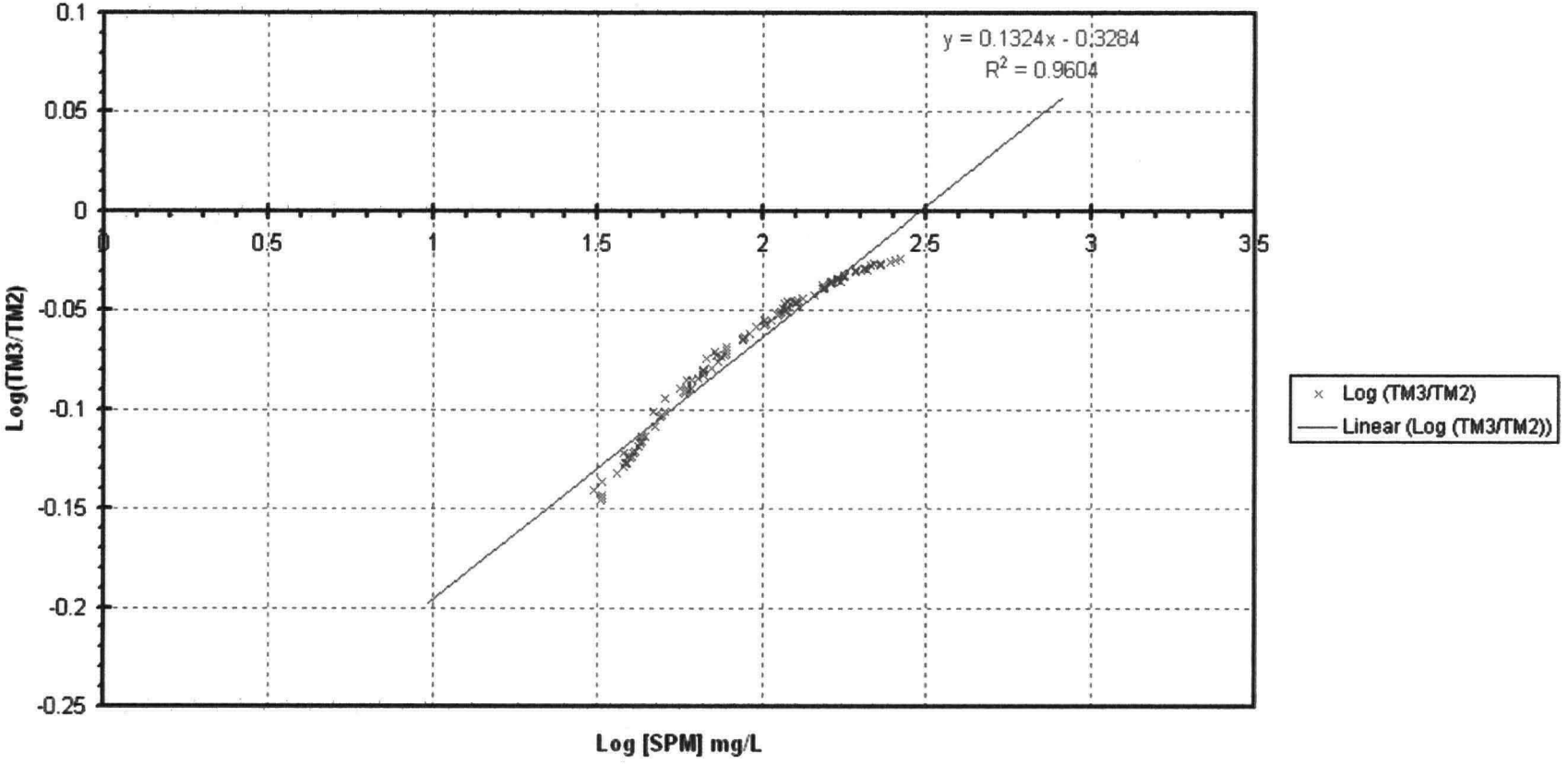

Figure 6.16: Log Radiance Reflectances Ratio of (TM3/TM2) vs. Log Total Suspended Particulates (30 – 275 mg/L)

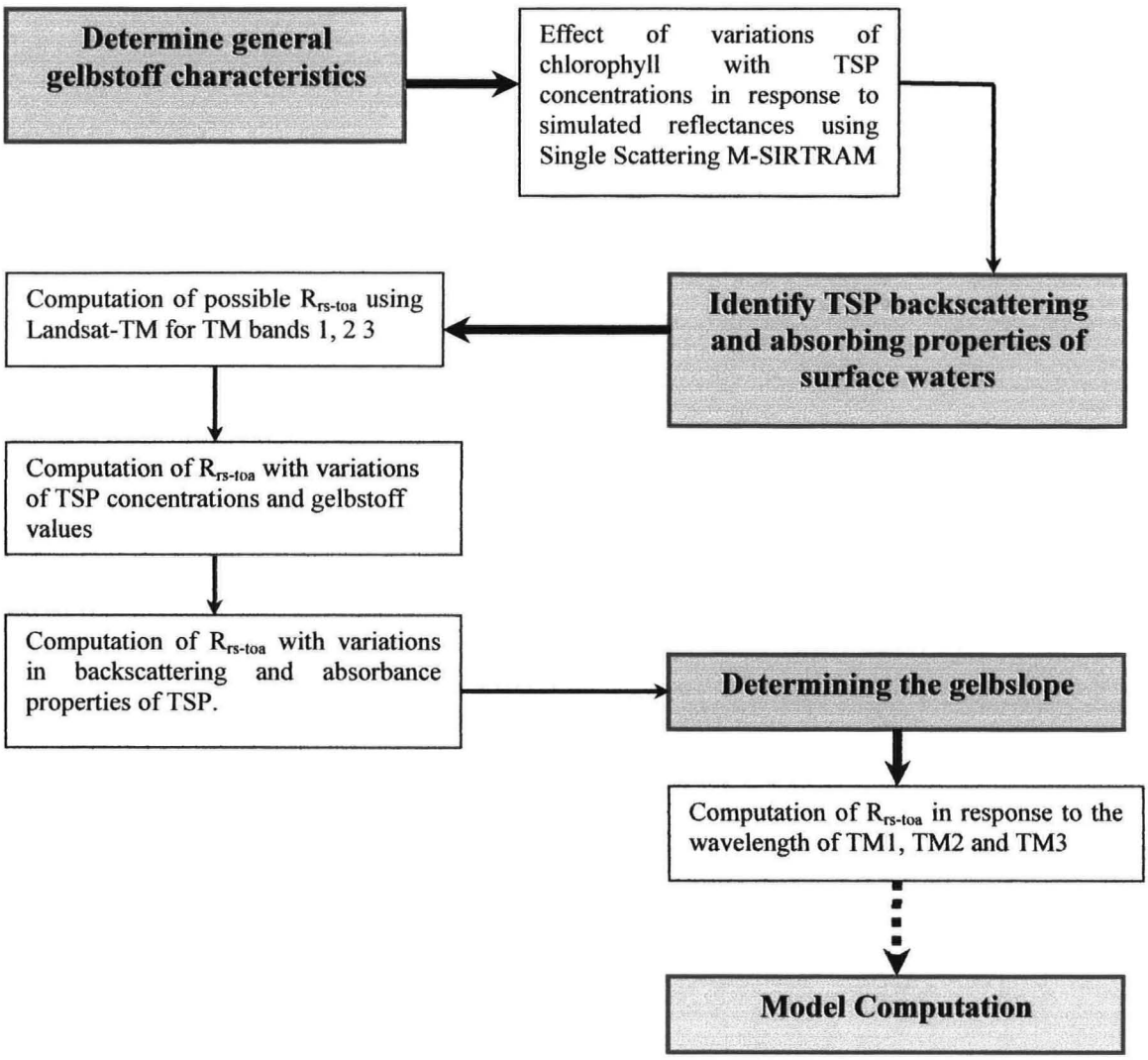

Figure 6.17. Flowchart for the determination of specific characteristics of gelbstoff and gelbslope.

6.3.3.1 Determination of General Characteristics of Gelbstoff

The presence of gelbstoff could have an effect on the reflectance values if the concentration is high. Since gelbstoff was not measured, it was necessary to determine this by varying the concentrations of chlorophyll with TSP concentrations and bottom depth using the Single Scattering SIRTRAM computation. Reflectance values computed were plotted against wavelength and the profile of the curves was compared to the reflectance curve obtained from the field on 16 January 1998 at 2m depth (Figure 6.10a).

Table 6.1 shows the range of information for Tanjung Rhu that was used in the modelling process.

Table 6.1: Physical information required in model computation using SIRTRAM

[TSP] mg/L	[Chlorophyll] μg/L	Bottom depth (m)
30 – 275	0 – 5	8m (min) 25m (max)

(a) Reflectance values computed for variations of chlorophyll concentrations ([Chl]) ranging from 2 – 15 μg/L for the 2 m depth at TSP of 1 mg/L, gelbstoff concentration of 0.2 and at bottom depth of 8 m and 25 m were plotted against wavelength (nm) as shown in Figures 6.18a and b respectively. The broad range of chlorophyll concentrations was chosen because the first aim here was to determine if variations of chlorophyll have any effect on the curve profiles. The concentration of 0.2 was used because this appears to be the normal measured value (Doerffer, 1992).

From Figures 6.18a and b, the curve profiles appeared to be similar to that obtained from *in situ* data measurement shown in Figure 6.10a. It also showed that regardless of the depth, the curve profile remained similar where there are 3 typical peaks. The most prominent of all is the peak at 565nm within the TM Band 2 range and the smaller or less prominent peaks are at 645 and 690nm which fall within the TM band 3 range. From these curve profiles, it showed that the higher the chlorophyll, the lower the reflectance values. However, there was a shift in the maximum reflectance between the two depths. Higher reflectance was computed for z_{bott} = 8m at λ = 450 – 580 nm. For the 25m depth, there appeared to be no change in the reflectance at λ = 565 nm. This was because at shallower depth and where water was clear, there was the bottom reflectance effect, hence the higher reflectance.

(b) Similar computations were carried then out as above but higher TSP was used (100 mg/L) resulting in the following curve profiles shown in Figures 6.19a and b. The curve profile had changed, although it still maintained the 3 typical peaks which no longer appeared to be very prominent, excepting the peak at 690nm. The curve slope at 400-550 nm range had weakened where the slope is approaching zero and this was similar to the weak gelbstoff characteristics mentioned earlier (Figure 6.10a). Similar reflectance values were computed for z_{bott} = 8 m and 25 m. This was an indication that:

(i) the z_{bott} has no effect on the reflectance curve profile when the [TSP] is higher and the gelbstoff is low within the 2-15 μg/L chlorophyll range,

(ii) in the real situation, gelbstoff concentration is probably much higher than the normal 0.2, and

(iii) there is good possibility that the reflectance curve profile is also strongly governed by the gelbstoff concentration.

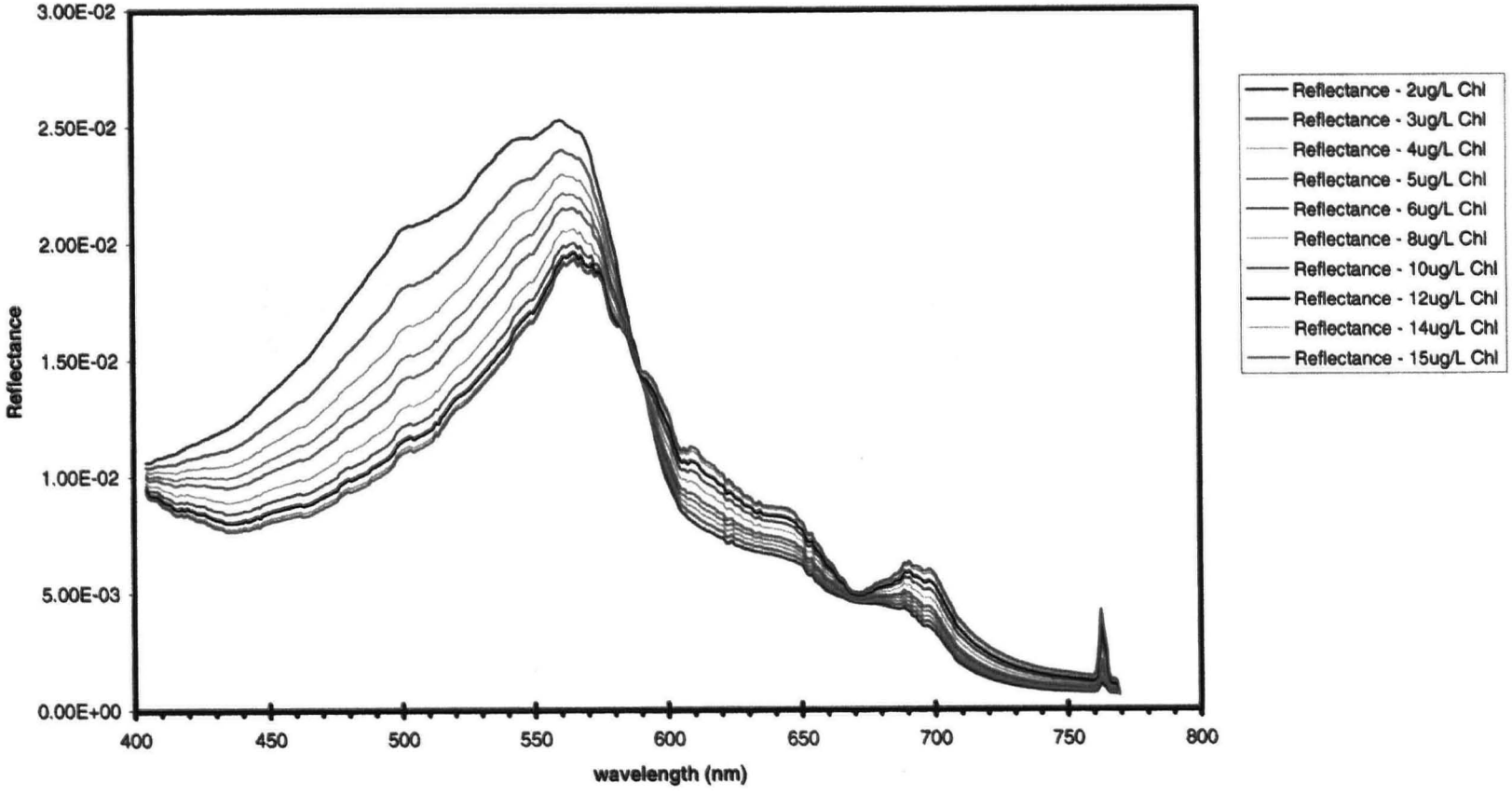

Figure 6.18a: Reflectance values for 2 m depth at TSP = 1 mg/L, Gelbs = 0.2 and z-depth = 8 m

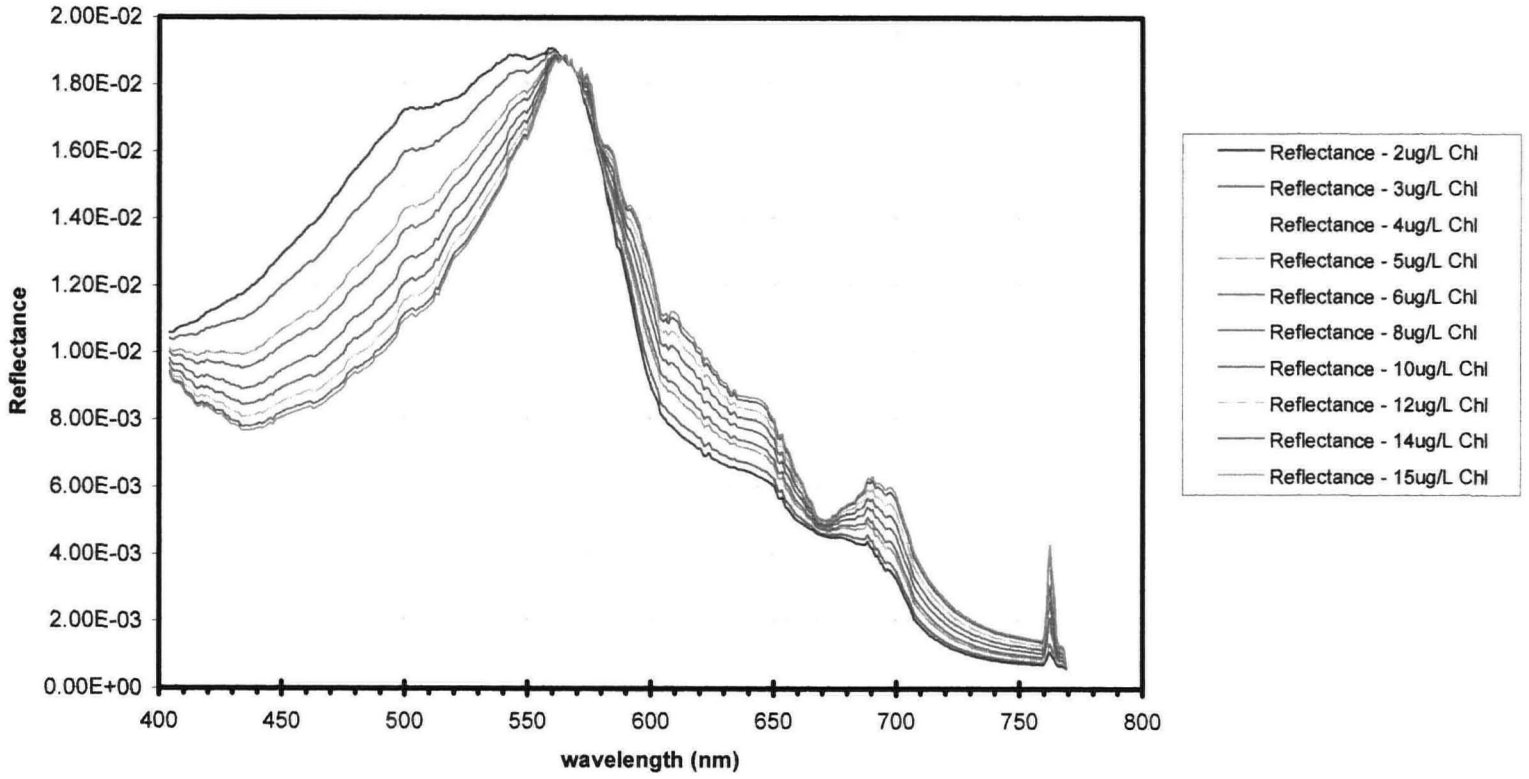

Figure 6.18b: Reflectance values for 2 m depth at TSP = 1 mg/L, Gelbs = 0.2 and z-depth = 25 m

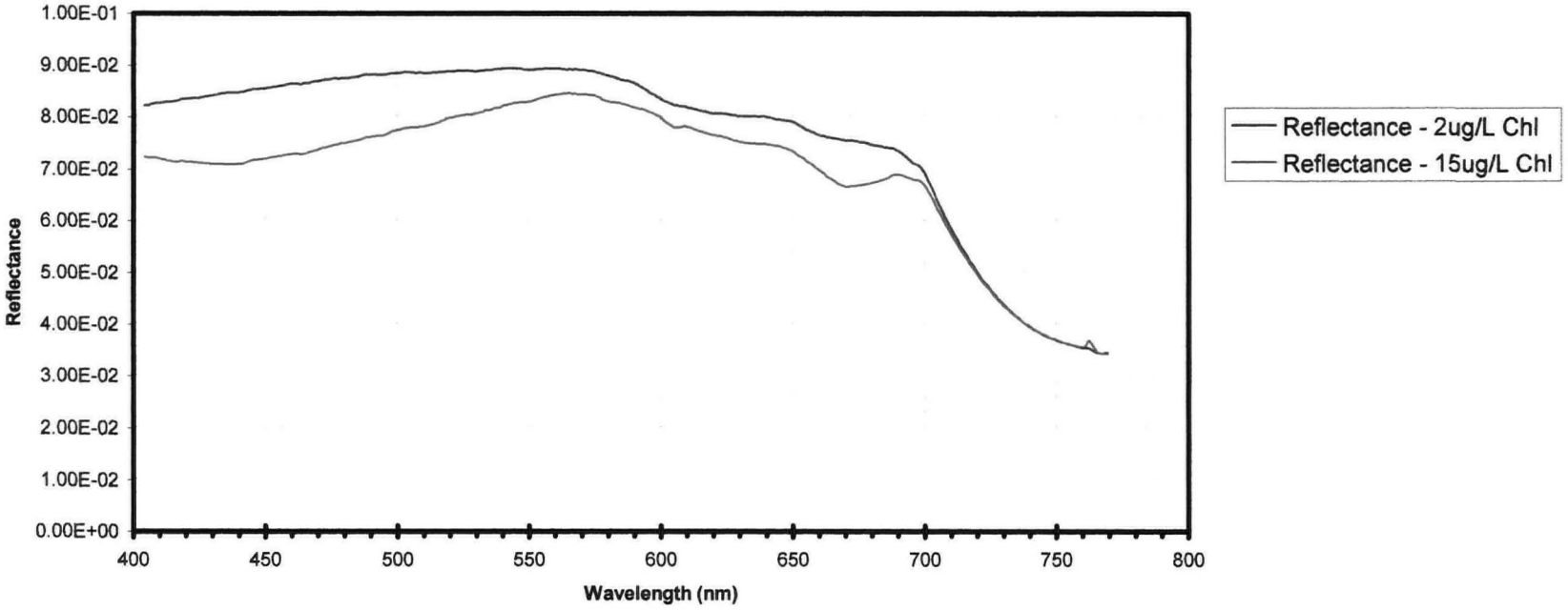

Figure 6.19a: Reflectance curve profiles for 2 m depth at TSP = 100 mg/L, Gelbs = 0.2 and z-depth = 8 m

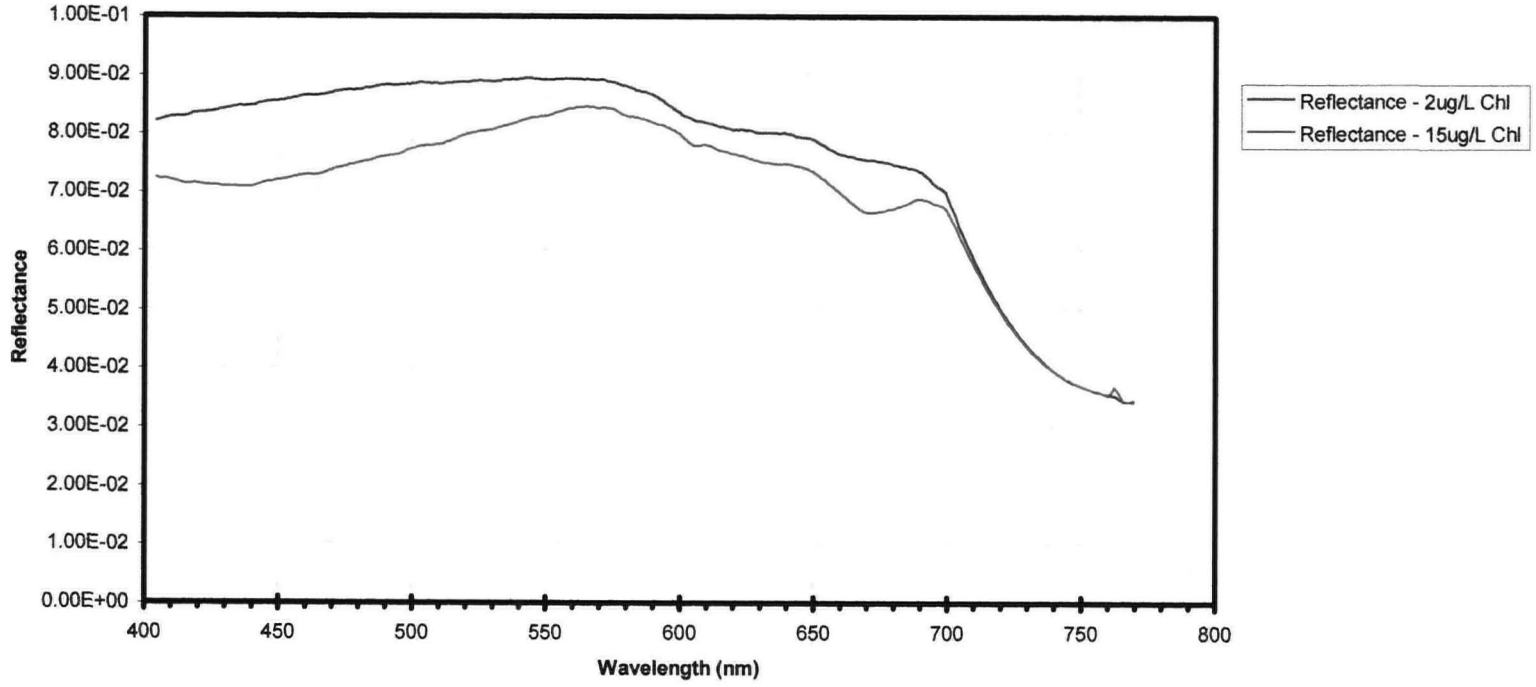

Figure 6.19b: Reflectance curve profiles for 2 m depth at TSP = 100 mg/L, Gelbs = 0.2 and z-depth = 25 m

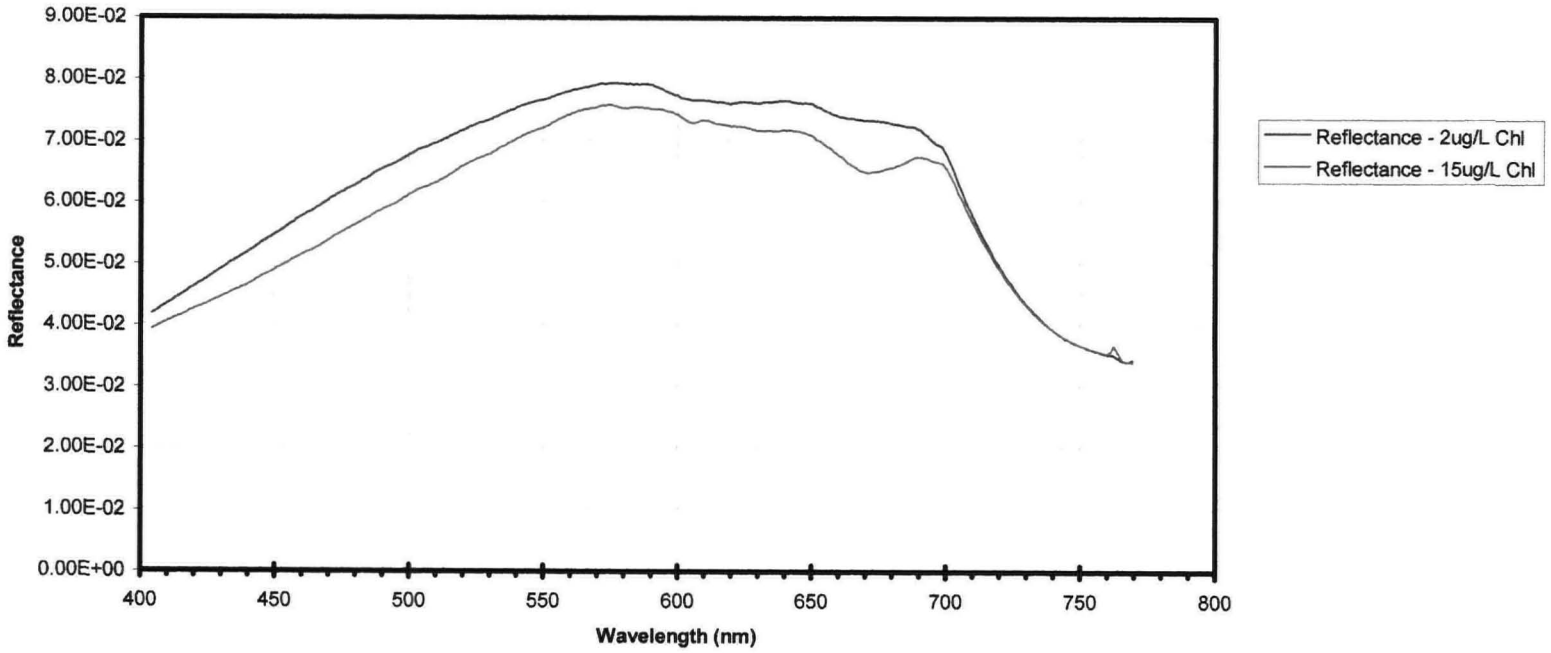

Figure 6.20a: Reflectance values for 2 m depth at TSP = 100 mg/L, Gelbs = 2.0 and z-depth = 8 m

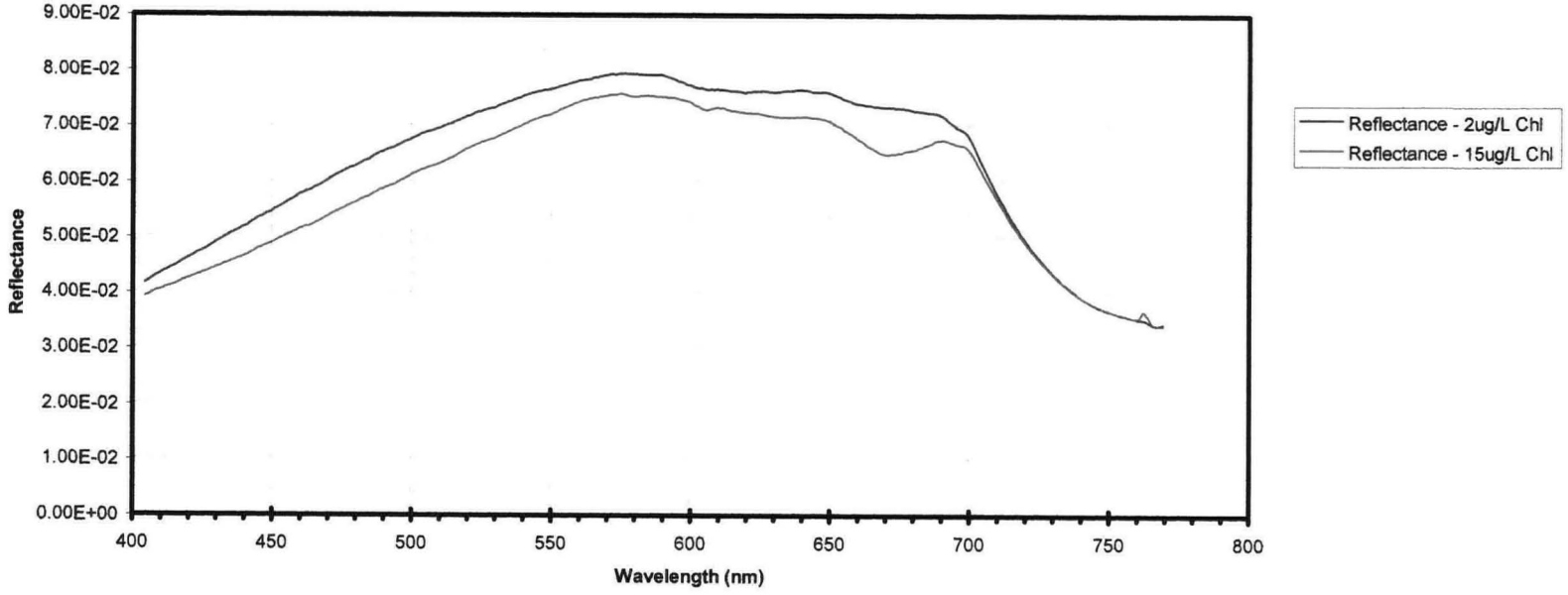

Figure 6.20b: Reflectance values for 2 m depth at TSP = 100 mg/L, Gelbs = 2.0 and z-depth = 25 m

(c) Reflectance curves were computed again using Single Scattering SIRTRAM with similar input variables except for a gelbstoff concentration of 2.0. The reflectance curve (Figures 6.20a and b) showed a changed profile where there appeared to be a shift to its curve slope at the $\lambda = 400 - 550$nm range. The curve slope had increased compared to the curve slopes shown in Figures 6.20a and b. There were still 3 distinguishable typical peaks in the reflectance curves. Results here had again indicated that:

(i) where [TSP] is high and gelbstoff is high, the z_{bott} has no influence on the reflectance curve,

(ii) in the real situation, gelbstoff concentrations in Tanjung Rhu surface waters were much higher than the normal level of 0.2 and also 2.0,

(iii) the reflectance curve is strongly influenced by the gelbstoff concentration.

(d) Reflectance curves were computed again using Single Scattering SIRTRAM with similar input variables but the gelbstoff concentration was increased to 8.0. A stronger curve slope at $\lambda = 400 - 550$ nm was observed as shown in Figures 6.21a and b. Again the z_{bott} has no effect on the reflectances where [TSP] and gelbstoff concentrations are high. This is because high [TSP] causes water turbidity, which will limit light penetration so that natural bottom reflection will be obstructed or non-existent. The 3 typical peaks were still distinguishable. These curves had provided an initial confirmation that in the real situation the gelbstoff concentration is much higher than 8.0. This had also allowed variation of [TSP] in relation to higher gelbstoff concentration in the next step, where a much more similar reflectance curve profile (as measured and shown in Figure 6.10a) would be expected.

(e) Based on reflectance curves projected with variations in [TSP], z_{bott}, and [Chl], it would be appropriate to observe the effect of higher [gelbstoff]:[TSP] on the reflectance curves. Reflectance values were computed again for [TSP] at 5 mg/L with gelbstoff at 0.4 and, z_{bott} at 25m. The reflectance computation for 8m depth was not done here because it was already deduced from earlier simulations that with high [TSP] and [gelbstoff], the z_{bott} plays an insignificant role. The [Chl] of 2 – 15 μg/L range was maintained for the purpose of comparison. Figure 6.22 showed reflectance curve profiles that were similar to those measured in Figure 6.10a. The peaks at 565 nm and 690nm were very distinctive while the peak at 645 nm was less prominent. The reflectance curve slopes of ≤ 5 μg/L [Chl] showed good approximation similar to the measured reflectance curve shown in Figure 6.10a.

(f) Computations of reflectance were then concentrated on obtaining the level of reflectance value measured as shown in Figure 6.10a. At 565 nm peak, reflectance was measured at 0.088 in

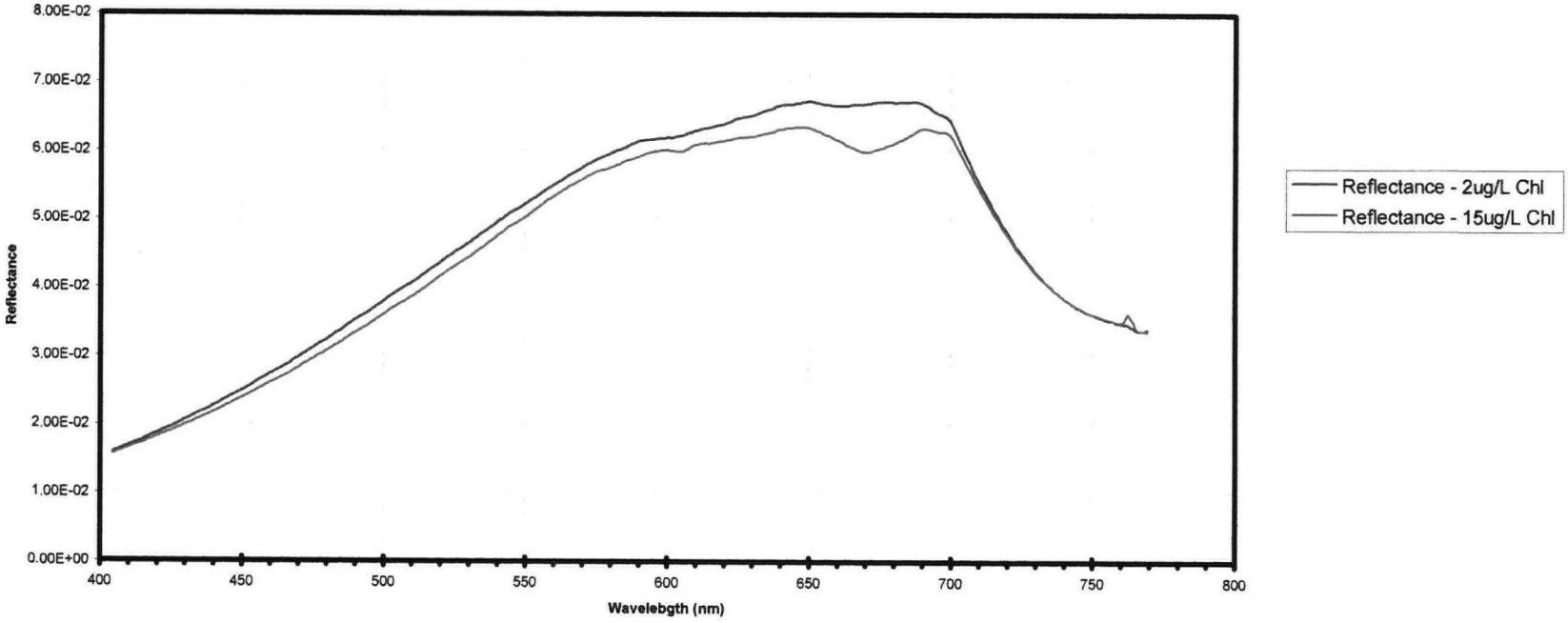

Figure 6.21a: Reflectance values for 2 m depth at TSP = 100 mg/L, Gelbs = 8.0 and z-depth = 8 m

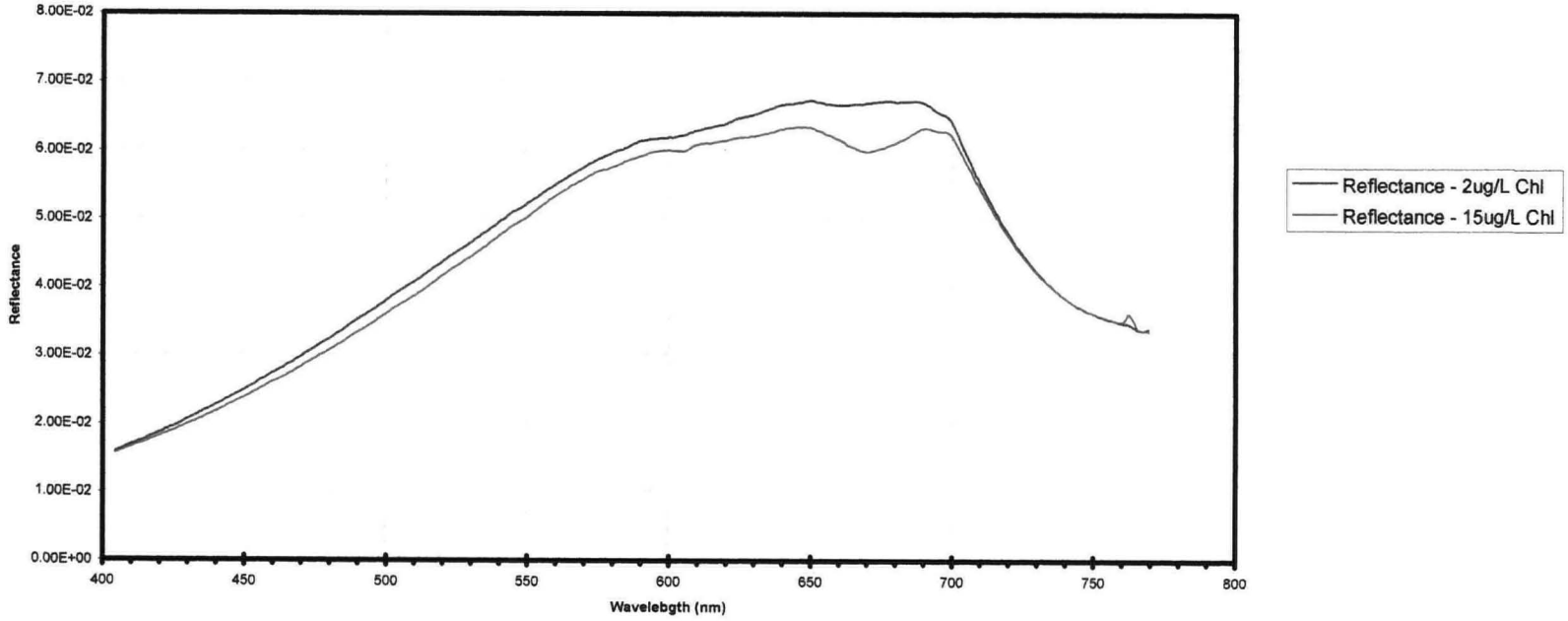

Figure 6.21b: Reflectance values for 2 m depth at TSP = 100 mg/L, Gelbs = 8.0 and z-depth = 25 m

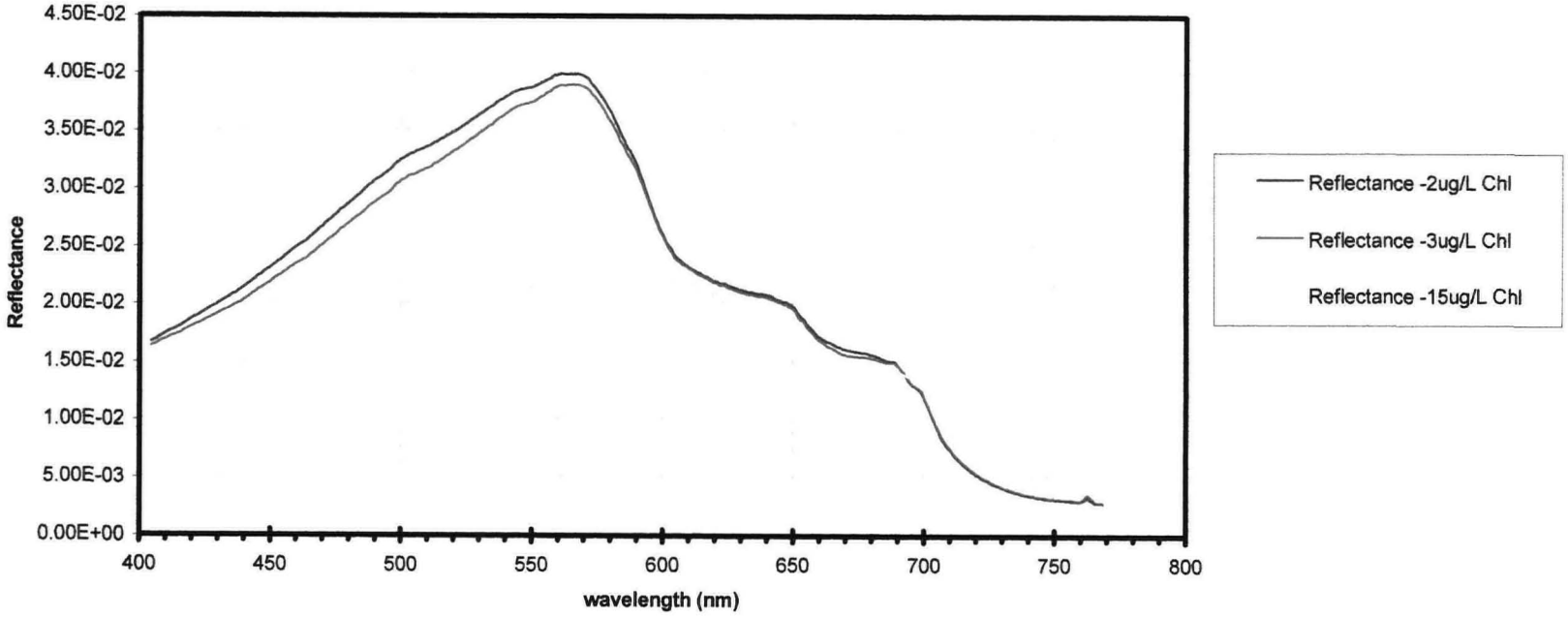

Figure 6.22: Reflectance values for 2 m depth at TSP = 5 mg/L, Gelbs = 0.4 and z-depth = 25 m

Figure 6.10a. It was necessary to observe if the reflectance values calculated at fixed [Chl] = 5 μg/L, z_{bott} = 25 m, and variations of [gelbstoff] with [TSP] range between 50 – 275 mg/L would produce a peak at 565 nm having the same or similar value of 0.088 reflectance. Values of the input variables were chosen as such because these were the measured values shown in Table 6.1.

Results from the computation showed that at gelbstoff = 2.0, maximum reflectance fell within the 0.08 – 0.90 range (Figure 6.23). Since measured reflectance shown in Figure 6.10a was recorded on 16 January 1998 having [TSP] between 160 – 200 mg/L at Station 5 (Sungai Ayer Hangat), it was necessary to observe whether the maximum reflectance simulated within the [TSP] range fell into the 0.088 – 0.090 reflectance. From Figure 6.24, the reflectance curve for 200mg/L TSP showed a maximum value of 0.086 and since this was near to the expected value of 0.088, it was considered acceptable.

From Figure 6.23 it was observed that it portrayed typical high [TSP] reflectance curves, where reflectance increased with [TSP], but the increments of reflectances were not linear. Based on the distances of these reflectance curves, it was observed that reflectance changes were no longer sensitive for [TSP] ≥ 150 mg/L. This set the limit to reflectance sensitivity to TSP = 150 mg/L.

6.3.3.2 Determination of TSP Backscattering and Absorbing Properties in Surface Waters of Tanjung Rhu

To determine the TSP backscattering and absorbing properties, the [gelbstoff] was set to zero in the Single Scattering M-SIRTRAM. This was because the [gelbstoff] was not measured and it would have been difficult to estimate the range of value through this method. Since the gelbslope would be determined later, therefore, it was no longer necessary to quantify the gelbstoff range.

So far, measurements and simulated results had been made for reflectances. However, in terms of remote sensing, the reflectance data recorded in the sensors were not simply reflectance as observed or measured on the ground but reflectances that had been altered by the atmospheric column such as through aerosol and Rayleigh scattering. Reflectance data measured at the satellite sensor would then be remote sensing reflectance at the top of atmosphere ($R_{rs\text{-}toa}$). It was then necessary to compute $R_{rs\text{-}toa}$ using the following equations:

$$R_{rs\text{-}toa} = L_{toa} / E_d \qquad \textit{(eq. 71)}$$

$$L_{toa} = L_{min} + DN*CF \qquad \textit{(eq. 72)}$$

where L_{toa} is radiance at the top of atmosphere or total radiance (L_{total}), L_{min} is the minimum radiance, DN is Digital Numbers, and CF is Conversion Factor.

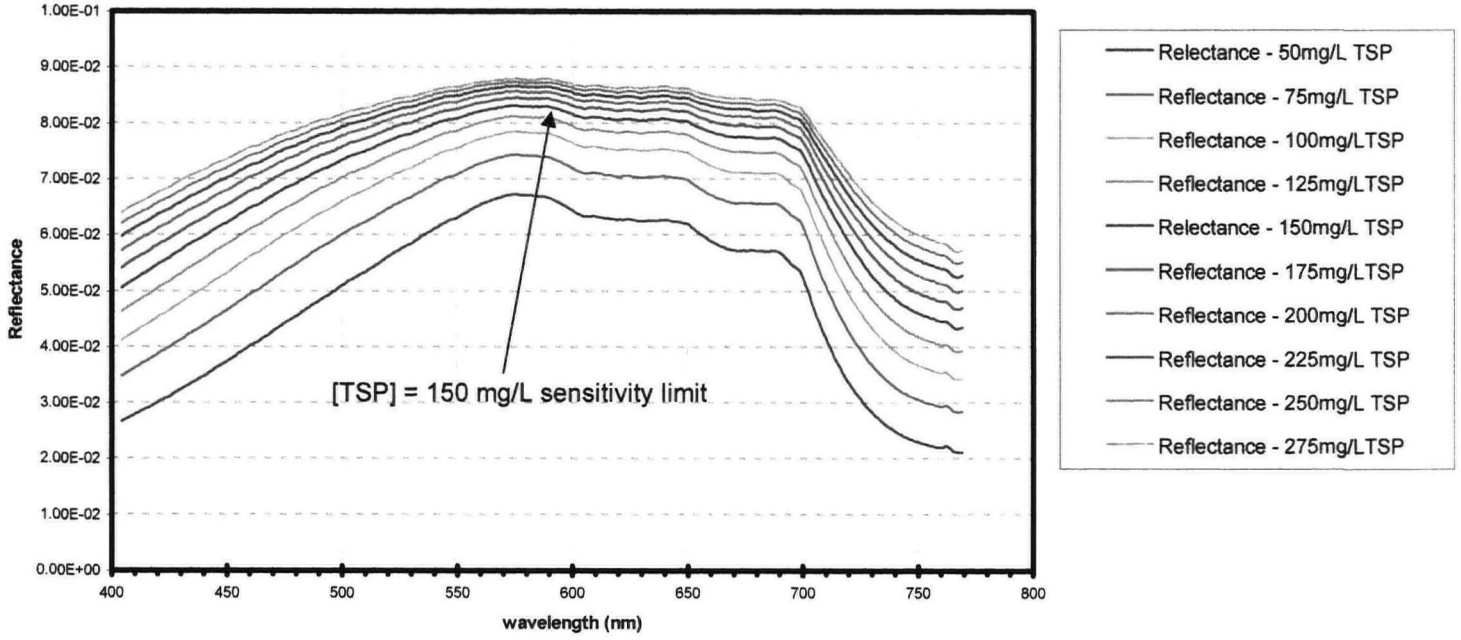

Figure 6.23: Reflectance values for 2 m depth at Chl = 5 µg/L, Gelbs = 2.0 and z-depth = 25 m.

L_{toa} and CF need to be calculated, DN are obtainable through Landsat TM images and L_{min} is the radiometric characteristics for Landsat TM data (Table 6.2). CF can be calculated by obtaining the maximum and minimum radiance difference and averaging the value with the DN range which is 0 – 255.

$$CF = (L_{max} - L_{min}) / 255 \qquad \textit{(eq. 73)}$$

CFs were required only for TM bands 1, 2, and 3. The middle wavelength λ_z for each TM band is used.

Results of the computation are given in Table 6.3

Before proceeding further, it was deemed necessary to extract information from Landsat TM uncorrected data of Tanjung Rhu to provide a clearer view of the surface water condition within Pulau Langkawi itself. This step would have made the final output, the algorithm, specific for the coastal waters of Pulau Langkawi. The northern waters of Pulau Langkawi (where Tanjung Rhu is located) are relatively clean as opposed to the southern waters where heavy maritime traffic and tourism had a noticeable effect on the water quality.

Table 6.2: Radiometric Characteristics of Thematic Mapper (Source: Doerffer *et al.*, 1989)

TM Channel	1	2	3	4	5	6	7
λ_z (nm)	485	570	660	840	1,675	11,000	2,250
L_{min}	-1.520	-2.840	-1.170	-1.510	-0.370	2.000	-0.150
L_{max}	158.420	308.170	234.630	224.320	32.420	15.600	17.000
diff S	0.800	0.500	0.500	0.500	1.000	0.500	2.400

Table 6.3: Conversion Factor (CF) for TM Bands 1, 2, and 3

TM Channel	1	2	3
λ_z (μm)	0.485	0.570	0.660
CF	0.6272	1.2196	0.9247
* E_s ($W/m^2/sr/\mu m$)	1861.72	1833.64	1580.64

* *Values taken from Doerffer (1992)*

To view these differences, a set of Landsat TM data dated 30 January 1992 of path/row ID of 128/56 was used. Ten locations were selected for both the north and south of Pulau Langkawi

where the DNs of TM1, TM2 and TM3 were extracted. Mean value of 3x3 pixel size had been used and these are shown in Table 6.4.

With the information calculated (Table 6.3) and provided in Table 6.2, total radiance (L_{total}), or radiance at the top of atmosphere (L_{toa}) was calculated for each of the mean DNs for clear and turbid waters of Pulau Langkawi where

$$L_{toa} = L_{min} + DN(CF) \qquad \textit{(eq. 74)}$$

The calculated values of L_{toa} are given in Table 6.5.

These values were then converted into remote sensing reflectance at top of atmosphere ($R_{rs\text{-}toa}$) using equation 75, as shown in Table 6.6:

$$R_{rs\text{-}toa} = L_{toa} / E_s \qquad \textit{(eq. 75)}$$

Table 6.4: Mean 3x3 DNs for clear and turbid waters of Pulau Langkawi

South Langkawi (Turbid water condition)					North Langkawi (Clear water condition)				
Position on image		Mean 3x3 DN			Position on image		Mean 3x3 DN		
x	y	TM1	TM2	TM3	x	y	TM1	TM2	TM3
1207	1184	94	40	39	583	838	78	30	33
1107	1205	101	45	47	638	830	75	28	29
1139	1322	96	41	41	692	824	77	30	32
994	1404	98	41	42	696	777	74	30	32
1297	1277	101	42	42	676	742	78	31	33
1322	1224	104	44	45	540	877	81	32	32
1262	1336	101	45	47	791	798	84	34	36
983	1401	99	41	42	679	743	74	29	32
976	1540	94	41	37	714	831	82	31	33
888	1505	92	39	40	536	882	80	32	31

Table 6.5: Radiances at top of atmosphere for clear and turbid waters of Pulau Langkawi

South Langkawi (Turbid water condition)					North Langkawi (Clear water condition)				
Position on image		L_{toa}			Position on image		L_{toa}		
x	y	TM1	TM2	TM3	x	y	TM1	TM2	TM3
1207	1184	57.44	45.94	34.89	583	838	47.40	33.75	29.35
1107	1205	61.83	52.04	42.29	638	830	45.52	31.31	25.65
1139	1322	58.69	47.16	36.74	692	824	46.77	33.75	28.42
994	1404	59.95	47.16	37.67	696	777	44.89	33.75	28.42
1297	1277	61.83	48.38	37.67	676	742	47.40	34.97	29.35
1322	1224	63.71	50.82	40.44	540	877	49.28	36.19	28.42
1262	1336	61.83	52.04	42.29	791	798	51.16	38.63	32.12
983	1401	60.57	47.16	37.67	679	743	44.89	32.53	28.42
976	1540	57.44	47.16	33.04	714	831	49.91	34.97	29.35
888	1505	56.18	44.72	35.82	536	882	48.66	36.19	27.50
	Mean	**59.95**	**48.26**	**37.85**		Mean	**47.59**	**34.60**	**28.70**

Table 6.6: Reflectance at top of atmosphere for clear and turbid waters of Pulau Langkawi.

South Langkawi (Turbid water condition)					***North Langkawi*** (Clear water condition)				
Position on image		$R_{rs\text{-}toa}$			Position on image		$R_{rs\text{-}toa}$		
x	y	TM1	TM2	TM3	x	y	TM1	TM2	TM3
1207	1184	0.030851	0.025056	0.022075	583	838	0.02546	0.01840	0.01857
1107	1205	0.033210	0.028382	0.026756	638	830	0.02445	0.01707	0.01623
1139	1322	0.031525	0.025721	0.023245	692	824	0.02512	0.01840	0.01798
994	1404	0.032199	0.025721	0.023830	696	777	0.02411	0.01840	0.01798
1297	1277	0.033210	0.026386	0.023830	676	742	0.02546	0.01907	0.01857
1322	1224	0.034220	0.027717	0.025585	540	877	0.02647	0.01974	0.01798
1262	1336	0.033210	0.028382	0.026756	791	798	0.02748	0.02107	0.02032
983	1401	0.032536	0.025721	0.023830	679	743	0.02411	0.01774	0.01798
976	1540	0.030851	0.025721	0.020905	714	831	0.02681	0.01907	0.01857
888	1505	0.030178	0.024391	0.022660	536	882	0.02613	0.01974	0.01740
	$R_{rs\text{-}toa}$	**3.0-3.4%**	**2.4-2.8 %**	**2.0-2.7%**		$R_{rs\text{-}toa}$	**2.4-2.7%**	**1.7-2.1%**	**1.6-2.0%**

Since Tanjung Rhu is located at the northeast of Pulau Langkawi, the range of $R_{rs\text{-}toa}$ that was considered in the computation of $R_{rs\text{-}toa}$ in the following procedure was concentrated within the 2.4 – 2.7% for TM1, 1.7 – 2.1% for TM2 and 1.6 – 2.0% for TM3.

With fixed values obtained from the previous procedures, the changes in the backscattering and absorbance properties of TSP are determined. These properties are the backscattering and absorbance factors and exponential values of TSP.

Presence of coral debris and its constant erosion of the debris due to the high physical activities within the existing natural environment of the adjacent coral reefs had resulted in high back-scattering effects from the surface waters. This fact was deduced from the computed results at the initial stage due to the shape of the curves obtained from SIRTRAM (Figure 6.24). The curves showed no absorbance characteristics from TSP presence within the water column of Tanjung Rhu. Calcium carbonate ($CaCO_3$), of which the coral skeletons were made, are white substances. This in itself provides the logical reason that none or very little absorbance was present and that high backscattering properties would be expected.

6.3.3.3 Determination of the Gelbslope

With the known backscattering and absorbing properties of TSP which are:

- Backscattering factor = 0.005
- Backscattering exponent = 0.01
- Absorbance factor = 0.0
- Absorbance exponent = 0.0

The final step was to determine the gelbslope. As mentioned earlier, since the [gelbstoff] was not measured, a trial and error process was necessary for this final step. Values of computed $R_{rs\text{-}toa}$ should have fallen within the range of 2.4-2.7% for TM1, 1.7-2.1% for TM2, and 1.6-2.0% for TM3. These values were for clear waters of Pulau Langkawi region, which is calculated and described in section 6.4.3.2 (Table 6.4 – Table 6.6). A range of gelbslope values were used to simulate $R_{rs\text{-}toa}$ to fall within the preferred range and the best level observed was at 0.005 (see Figure 6.25).

With this gelbslope, the next step was to generate $R_{rs\text{-}toa}$ for TM3 and TM2 for [TSP] ranging between 20 – 275 mg/L using Random Scattering M-SIRTRAM.

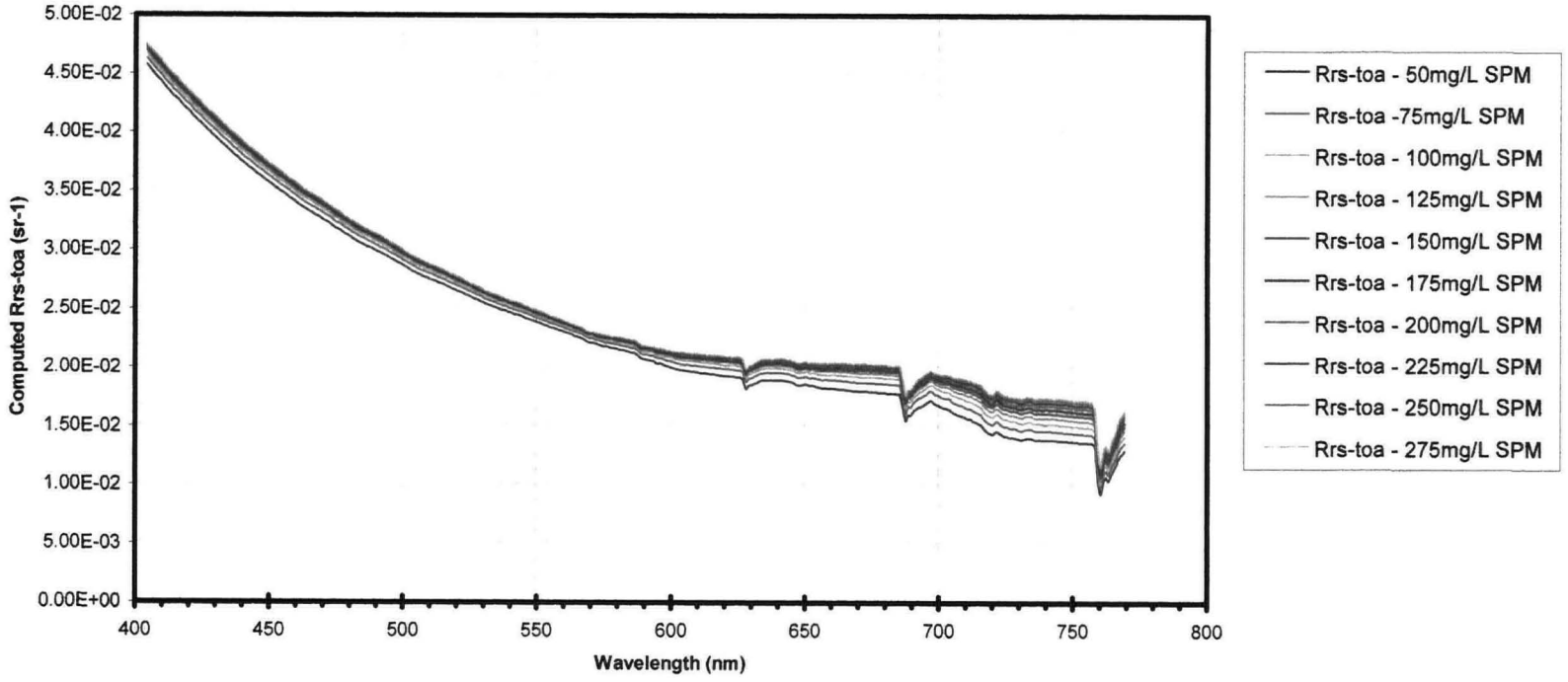

Figure 6.24: Computed Rrs-toa for Chl =5ug/L, Gelbs=0.4, subsurface sensor depth=0-m and z-bott=8-m. Horizontal vizibility = 10.0km Computations are for TM1, 2 and 3 only

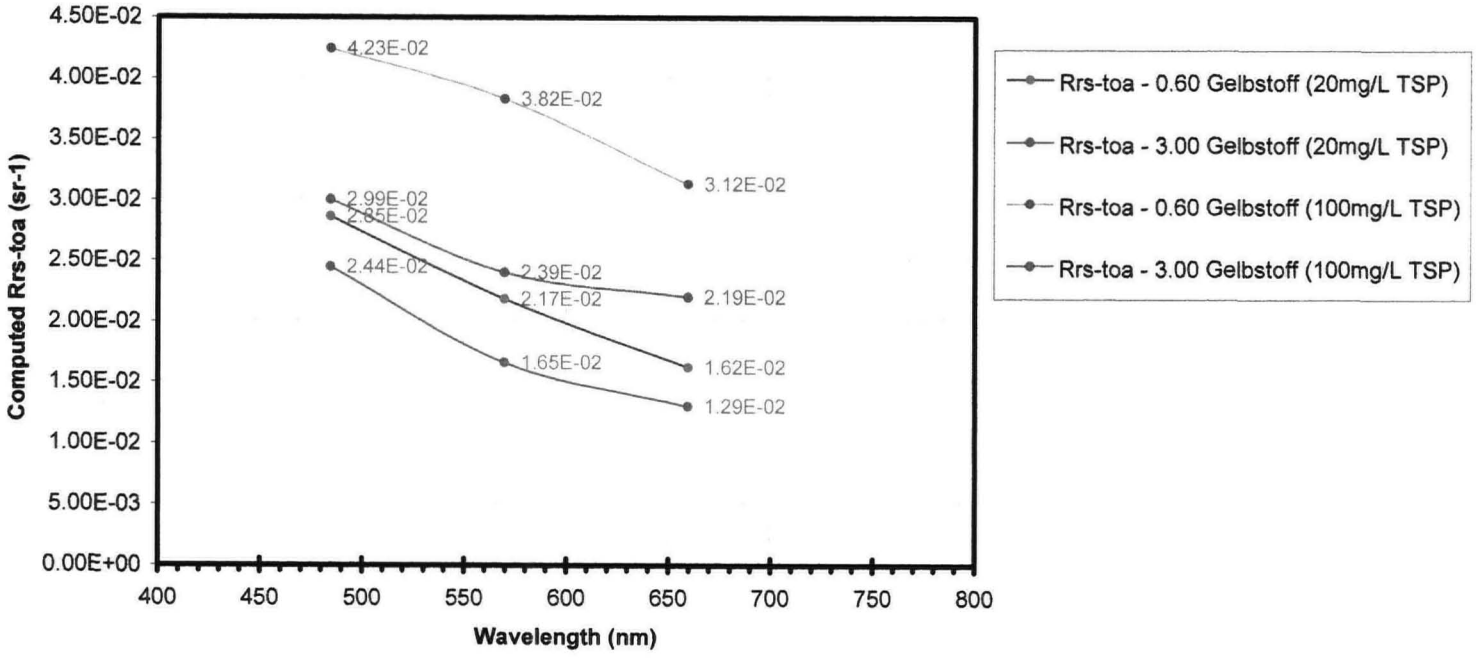

Figure 6.25: Computed $R_{rs\text{-}toa}$ for Chl – 5 µg/L, z-depth = 25 m, horizontal viz. = 20.0 km, SPM_bscat_exp = 0.01, SPM_bscat_fak = 0.005, SPM_abs_exp = 0.00, SPM_abs_fak = 0.00, Gelbslope = 0.005.

6.3.4 Formation of *Suspended Particulate Algorithm for Coastal Remote Sensing* (SPACoRS)

Based on the method described above, the information retrieved was pieced together and random scattering computation carried out. With reference to section 6.4.2, where the ratio of TM3/TM2 was found to produce high correlation, the ratio of simulated $R_{rs\text{-}toa}$ for TM3 and TM2 was calculated and plotted against [TSP] (mg/L) (Figure 6.26). A logarithmic equation was developed as follows:

$$y = 0.219\ ln(x) + 0.1299 \qquad \textit{(eq. 76)}$$

where $y = R_{rs\text{-}toaTM3}/R_{rs\text{-}toaTM2}$, and x = [TSP] mg/L.

This curve was then plotted in a reverse order because it was thought appropriate to have the [TSP] at the y-axis since the purpose of the modelling was to develop an algorithm to determine the concentrations of TSP.

The reverse plotting of the above logarithmic equation is shown in Figure 6.27 and the final output is a simple exponential algorithm, which is:

$$\mathbf{y = 0.6668e^{4.3892x}} \qquad R^2 = 0.9614 \qquad \textit{(eq. 77)}$$

where y = Total Suspended Particulates (mg/L)

and $x = R_{rs\text{-}toaTM3}/R_{rs\text{-}toaTM2}$

This algorithm is applicable to the Malaysian coastal waters having similar water quality characteristics during both dry and wet seasons such as Tanjung Rhu study area. As this algorithm is applicable to the coastal waters, it was termed *Suspended Particulate Algorithm for Coastal Remote Sensing* (abbr. SPACoRS).

From the exponential curve shown in Figure 6.27, [TSP] = 150 mg/L appears to be the sensitivity limit for TSP detection using remote sensing data. This was because at this point a small shift in the $R_{rs\text{-}toaTM3}/R_{rs\text{-}toaTM2}$ would result in a large change in the [TSP]. The exponential line beyond the 275 mg/L of TSP was a projected line. However, the importance of SPACoRS would be the applicability of it within waters having similar characteristics as that found in Tanjung Rhu and having [TSP] up to 275 mg/L.

The next phase following the formation of SPACoRS would be the application of the algorithm into Landsat TM imagery and the calculation of its accuracy level. These will be discussed in the following chapter.

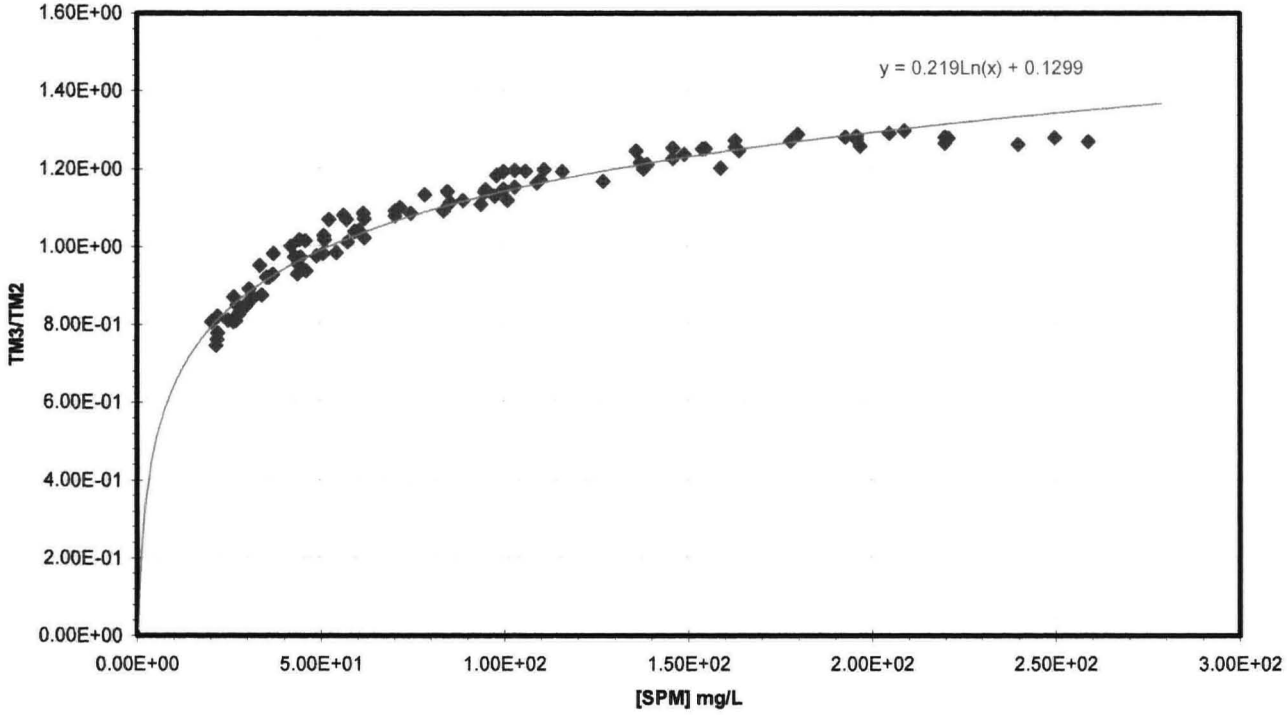

Chl=1-5ug/L; SPM=20-275mg/L; z-subsur=0-m; z-bott=8-m; horiz.viz=20-km. spm_bscat_exp=0.01; spm_ bscat_fak=0.005; spm_abs_exp=0.00; spm_abs_fak=0.00; gelb_slope=0.005; Gelbstoff range=2000-3000

Figure 6.26: Computed TM3/TM2 of $R_{rs\text{-}toa}$ at random.

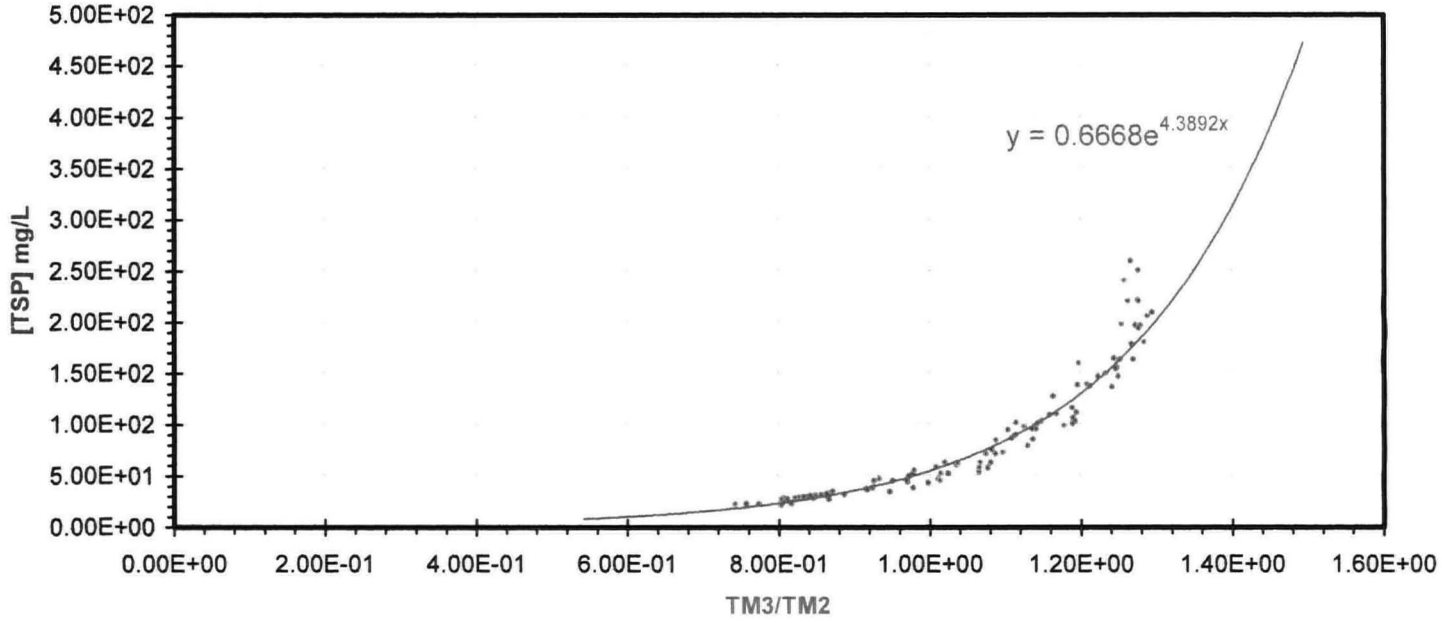

Computed TM3/TM2 of Rrs-toa for Chl=0-5ug/L; TSP=20-275mg/L; z-subsur=0-m; z-bott=25-m; horiz.viz=20-km. spm_bscat_exp=0.01; spm_ bscat_fak=0.005; spm_abs_exp=0.00; spm_abs_fak=0.00; gelb_slope=0.005.

Figure 6.27: Suspended Particulate Algorithm for Coastal Remote Sensing (SPACoRS) computed using Single Scattering and Random Scattering M-SIRTRAM for Tanjung Rhu surface waters.

6.4 SUMMARY

Based on the modified version of SIRTRAM which was originally written for temperate waters, the aim of producing an algorithm to be suitably applied to the tropical conditions was accomplished. Additional information that was not measured during the field data gathering phase was retrievable using SIRTRAM such as the backscattering and absorbance properties of TSP. It was observed that the TSP present within the water column of Tanjung Rhu appeared to have little or no absorbance, but had high backscattering properties. This was probably due to the presence of coral reef within the study area, where $CaCO_3$, which made up the coral skeletons, had contributed much to the TSP properties projected through M-SIRTRAM.

The Suspended Particulate Algorithm for Coastal Remote Sensing (SPACoRS) was found to be an exponential equation and not a linear equation. This was because in remote sensing, the grey values or the Digital Numbers (DN) that could be displayed from a satellite imagery were designed to range from 0 to 255 where DN=0 would mean full absorbance and no reflectance or backscattering, hence the black tone, while DN=255 would mean no absorbance but only reflectance or full backscattering, hence the white tone. This range of DN = 0 to 255 had limited the detection of TSP concentrations from satellite imagery. In this chapter, it was found that SPACoRS having the following equation:

$$\mathbf{y = 0.6668e^{4.3892x}}$$

where y = Total Suspended Particulates (mg/L), and $x = R_{rs\text{-}toaTM3}/R_{rs\text{-}toaTM2}$

has a sensitivity limit of [TSP] = 150 mg/L. It would mean that a slight change in the ratio of $R_{rs\text{-}toaTM3}/R_{rs\text{-}toaTM2}$ will result in a large shift in [TSP]. The R^2 of 0.9614 showed very good correlation. With this a high accuracy of predicted TSP was expected when SPACoRS was applied to Landsat TM data for the study area, which will be discussed in Chapter 7.

Chapter 7

THE APPLICATION OF *SPACoRS* TO LANDSAT THEMATIC MAPPER DATA AND ITS ACCURACY ASSESSMENT

7.1 INTRODUCTION

In recent years, many government agencies, environmental groups, hydrologists, and limnologists have expressed their concern about the problems of representative water quality. It has been of increasing concern as water bodies have shown a progressive increase in pollution. In order to investigate the impact anthropogenic activities on the water quality of rivers, lakes, and the coastal regions, it is essential to have an adequate data base which can be used to determine the temporal and spatial variability of water quality.

Many studies have shown that water quality variability is very complex and is influenced by hydrochemical, hydrobiological and hydrodynamical factors and processes (Tushinsky, 1991). The response of water bodies to these factors and processes can be assessed over three main temporal or spatial scales. Long-term temporal fluctuations of water quality are based on the seasonal variability of hydrological and other nature factors. The seasonal structure of spatial heterogeneity of water quality may also play a role in the whole water system. Short-scale temporal and spatial variations of water quality may be caused by physicochemical and biological factors and hydrodynamical processes such as current and mixing in rivers, estuaries, lakes and the coastal waters.

In this study, the developed algorithm, SPACoRS, was developed with a view to its utilization for both long-term and short-tem temporal and spatial variations since the aim of SPACoRS development was to produce a simple algorithm that could be applied both during the wet and dry seasons. SPACoRS was developed for the application using Landsat Thematic Mapper data. As there is availability of these data, it is therefore possible to analyze temporal variations using SPACoRS.

Accuracy Assessment

As resources become scarce, they become more valuable. Value is evidenced both by the increasing prices of resources and by problems in resource allocation and management. From forest harvesting and landuse conversion, to the fragmentation and loss of tropical habitats, acid deposition in continents and environmental degradation and pollution, the ecosystems of the world

have been significantly altered. Expanding population pressures continue to cause the price of resources to increase and to intensify conflicts over resources allocation and availability.

As resources become more available, the need for timely and accurate information about the type, quantity, quality and extent of resources increases. Allocating and managing the Earth's resources requires knowledge of their distribution across space. For example, to improve the habitat of endangered species such as corals, or fishes, we need to know what the species habitat requirements are, where that habitat exists, where the animals exist, and how changes to the habitat and surrounding environments will affect species distribution and population viability. To plan and conserve for the future requires decisions, and each decision (including the decision to do nothing) impacts (1) the status and location of resources and (2) the relative wealth of individuals and organizations that benefit from the resources. Knowing the location of resources and how they interact spatially is critical to their effective management.

Thus, effective decisions about resources require maps of known accuracy. If the accuracy of the map is known, the known expectations of accuracy can be incorporated into planning and contingency plans can be prepared for situations when the accuracy is low. This type of knowledge is critical for decisions such as endangered species preservation, resource allocation, emergency response, and management responses.

Remote sensing is the collection and interpretation of information about an object from a remote vantage point. Because there is high correlation between variation in remotely sensed data and variation across the earth's surface, remotely sensed data provides an excellent basis for making maps of landuse, landcover, and of pollution spread.

From the advent of the first aerial photographs to the launch of the latest satellite imaging system, the use of remotely sensed data has become an increasingly important and efficient way of collecting map information. Remotely sensed data are used to make maps because they:

1. are usually less expensive and faster than creating maps from information collected on the ground,
2. offer a perspective from above, allowing for a better understanding of spatial relationships, and
3. permit the capturing of types of data that humans cannot sense, such as the infrared portions of the electromagnetic spectrum.

The widespread acceptance and use of remotely sensed data has been and will continue to be dependent on the quality of the map information derived from it (Congalton and Green, 1999). However, map inaccuracies or error can occur at many steps throughout any remote sensing

project. Figure 7.1 shows the schematic diagram of the many possible sources of error. Accuracy assessment is conducted to understand the quality of map information by identifying and assessing map errors.

Accuracy assessments enabled the quality of the map information to be improved by identifying the sources of errors to be corrected. Analysts often need to compare various techniques, algorithms, analyses, or interpreters to test which is the best. Finally, if the information derived from the remotely sensed data is to be used in some decision-making process, then it is critical that some measure of its quality be known.

Figure 7.1. Sources of error in remotely sensed data. (Source: Lunetta *et al.*, 1981)

Accuracy assessment determines the quality of the information derived from remotely sensed data. Accuracy assessment can be qualitative or quantitative, expensive or inexpensive, quick or time-consuming, well-designed and efficient or haphazard. The purpose of *quantitative* accuracy assessment is the identification and measurement of map errors. Quantitative accuracy assessment involves the comparison of a site on a map against reference information for the same site. The reference data is assumed to be correct.

Usually funding limitations preclude the assessment of every spatial unit on the map. Because comparison of every spatial point is impractical, sample comparisons are used to estimate the accuracy of maps. Accuracy assessment requires:

i. the design of unbiased and consistent sampling procedures, and
ii. rigorous analysis of the sample data.

How a map is sampled for accuracy will partially be driven by how the information on the map is distributed across space by map category. This distribution will, in turn, be a function of how the categories of features of the earth being mapped are chosen – referred to as the *classification scheme*.

Map categories are specified by the project's classification scheme. Classification schemes are fundamental to any mapping project because they create order out of chaos and reduce the total number of objects (i.e. classes) that must be dealt with to some reasonably small number (Cowardin *et al.* 1979). The detail of the scheme is driven by (1) the anticipated uses of the map information, and (2) the features of the earth that can be discerned with the data (e.g., aerial photography, satellite imagery) being used to create the map. If a rigorous classification scheme is not developed before mapping begins, then any subsequent accuracy assessment of the map will be meaningless because it will be impossible to definitively state that an accuracy assessment sample area is of one class or another.

A classification scheme has two critical components: (1) a set of *labels* (clear water, turbid water, mangrove, etc.) and (2) a set of *rules* or definitions for assigning labels (Congalton and Green, 1999; Congalton, 1991). Without a clear set of rules, the assignment of labels to types can be arbitrary and lack consistency.

In addition to having labels and a set of rules, a classification scheme should be:
(1) *mutually exclusive,* and
(2) *totally exhaustive*.

Mutual exclusivity requires that each mapped area fall into one and only one category or class. A totally exhaustive classification scheme results in every area on the mapped landscape receiving a map label; no area can be left unlabeled (Congalton and Green, 1999; Congalton, 1991).

If possible, it is also advantageous to use a classification scheme that is *hierarchical.* In hierarchical systems, specific categories within the classification scheme can be collapsed to form more general categories.

There two basic analysis techniques in accuracy assessment and these are:
(1) Non-site Specific Assessments, and
(2) Site Specific Assessments.

In a non-site specific accuracy assessment, only total areas for each category mapped are computed without regard to the location of these areas. In other words, a comparison between the number of acres or hectares of each category on the map generated from remotely sensed data and the reference data is performed. In this way, the errors of omission and commission tend to compensate for each other and the totals compare favourably. However, nothing is known about any specific location on the map or how it agrees or disagrees with the reference data.

For site specific assessment, there was a need to know how the map generated from the remotely sensed data compared to the reference data on a locational basis.

The aims of this chapter are:

i. to successfully apply the developed Suspended Particulate Algorithm for Coastal Remote Sensing(SPACoRS) to Landsat Thematic Mapper data to produce a Total Suspended Particulate Distribution Map of Tanjung Rhu, Pulau Langkawi, and
ii. to assess the accuracy level of SPACoRS applied to Landsat Thematic Mapper data.

7.2 METHODOLOGY

To achieve the aims described in this chapter, the methodology adopted is described in the flowchart shown in Figure 7.2.

For Image Processing and Accuracy Assessment of SPACoRS, IDRISI for Windows Ver. 2.0 software was used.

An error matrix is computed to calculate the overall accuracy for the application of SPACoRS into Landsat Thematic Mapper imageries. The computation of error matrix is described in Chapter 4, section 4.2.1.5.

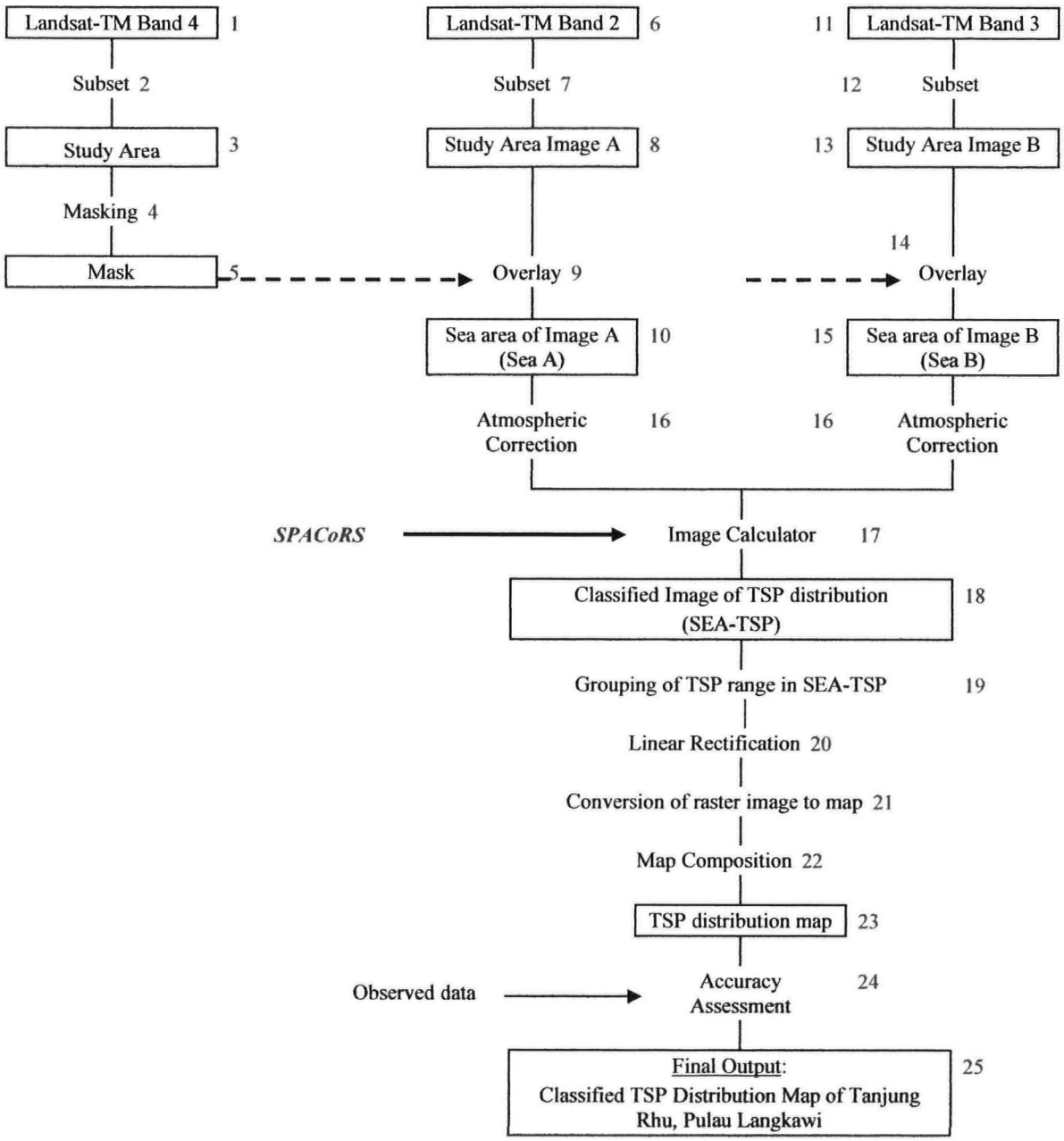

Note: Numbers in red denotes the procedures and each of these steps is described in the following sub-section (7.2.2).

Figure 7.2 A Methodology Flowchart on the Application of SPACoRS into Landsat Thematic Mapper.

7.2.1 Importing Data for use in IDRISI Version 2.0 for Windows.

The Landsat Thematic Mapper (Landsat TM) data dated 03 March 1998 with a path/row ID of 128/56 was used in the application of SPACoRS through IDRISI Version 2.0 for Windows. These data came in the form of a CD-ROM and needed to be imported or converted into the format readable in the IDRISI software. To accomplish this, the data file was imported using the ERDIDRIS command to convert the ".IMG" extension into the ".IMG" extension readable by IDRISI. This had to be done prior to the actual Image Processing phase.

Satellite data of 1997 or a more up-to-date satellite data especially of 1999 was not used for the application and accuracy assessment of SPACoRS because although available, they were very much clouded. These data would have been more appropriate to be used in assessing the applicability and the accuracy level of SPACoRS. If the images had appeared to be only hazy, atmospheric correction procedures would have been able to rid the problem. However, with thick cloud coverage in the 1997 and 1999 images, the application of atmospheric correction procedures without altering the original data is impossible. Should this be done, the results of accuracy assessment would have produced a substantial amount of errors.

7.2.2 Image Processing

The following steps described the method used in the image processing of Landsat TM data with the application of SPACoRS to produce the predicted Total Suspended Particulates of surface waters in Tanjung Rhu.

Step 1:

A full-scene of Landsat TM Band 4 was displayed through Launcher using IDRISI Version 2.0 for Windows.

Step 2:

To subset the study area, windowing using the Display in the Reformat module is used where the area of study can be resized.

The window is specified by row/column positions.

Upper left column: 990 Upper left row: 559

Lower right column: 1212 Lower right row: 815

Total size of the study area in the image is 223 columns x 257 rows

Step 3:

Saving the subset image which is the study area (Figure 7.3).

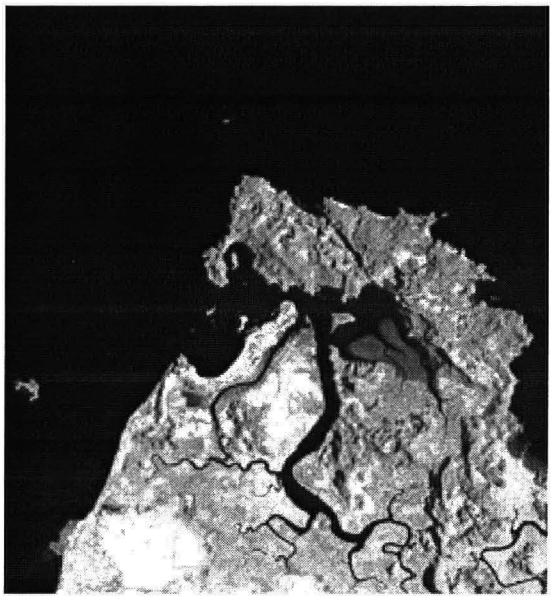

North

Image ID: 128/56 (Path/Row)
Image date: 03 March 1998
Displayed band : TM4
Image size: 257 rows x 223 columns

Figure 7.3. A subset image of the study area displayed in Landsat TM4.

Step 4:

To mask out the land features, Reclass of Database Query in the Analysis module is used. Prior to masking, the histogram of the study area is viewed to determine the range of DN values representing the land features that need to be masked out.

The normal DN threshold value of 30 is not used here for the masking because with this value, the two main rivers draining the study area will also be masked out as part of the land features. Therefore using the DN threshold value of 30 in this masking process would not produce a true picture of the study area, because both the rivers are relatively narrow and the reflectances of these rivers are low with the influences from the larger land features surrounding it.

Here, the threshold was set at DN = 44, where DN>44 will be masked out 'Class 0'. However, some shadows from the rugged limestone hills within the study area having DN < 44 will not be masked out. A further examination of the histogram showed that another 'Class 0' mask should be set at DN<25. In this case, only the land features will be masked out leaving the low DN values from the rivers undisturbed.

Step 5:

The generated mask is saved for use in steps 9 and 14.

Step 6:

A full-scene of Landsat TM Band 2 is displayed through Launcher using IDRISI. This band is used as the denominator in the band ratio of SPACoRS development.

Step 7:

Similar to Step 2, the study area is being subset through windowing using the Display in the Reformat module. Again, the window is specified by row/column positions.

Upper left column: 990 Upper left row: 559

Lower right column: 1212 Lower right row: 815

Total size of the study area in the image is 223 columns x 257 rows

Step 8:

Saving the subset image of Band 2 which is the study area, Image A (Figure 7.4)

Step 9:

An overlay of Image A and the Mask (from Step 5) is carried out to produce a Band 2 image of the study area with the masked out land and leaving only the sea area for further image processing in the application of SPACoRS.

In the Analysis module, the Overlay function in Database Query is used to perform this task. The selected overlay option is a multiplication between the two images.

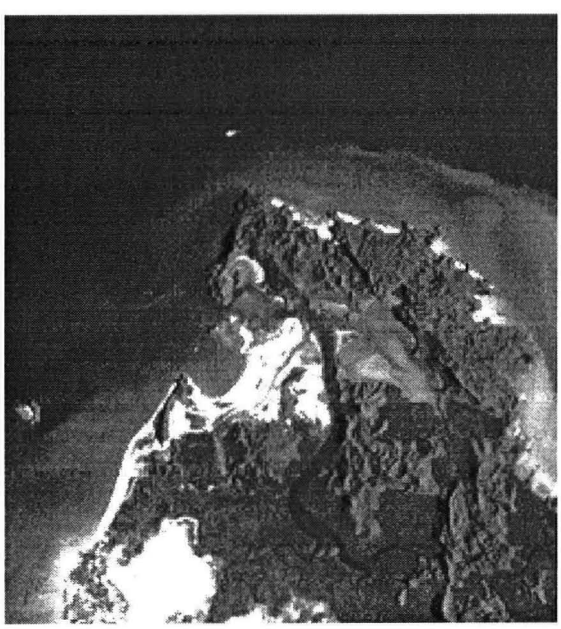

North

Image ID: 128/56 (Path/Row)
Image date: 03 March 1998
Displayed band : TM2
Image size: 257 rows x 223 columns

Figure 7.4. A subset image of the study area displayed in Landsat TM2.

Step 10:

The resultant image in the overlay function is a sea area of Image A which is now called Sea A.

Step 11:

This step is similar to steps 1 and 6 where a full-scene Landsat TM image is displayed through a Launcher. Here, TM Band 3 is displayed.

Step 12:

The study area is being subset using the same process as outlined in Steps 2 and 7. The same row/column positions are used to produce an image of an equal size.

Step 13:

The resultant image is called Image B (Figure 7.5)

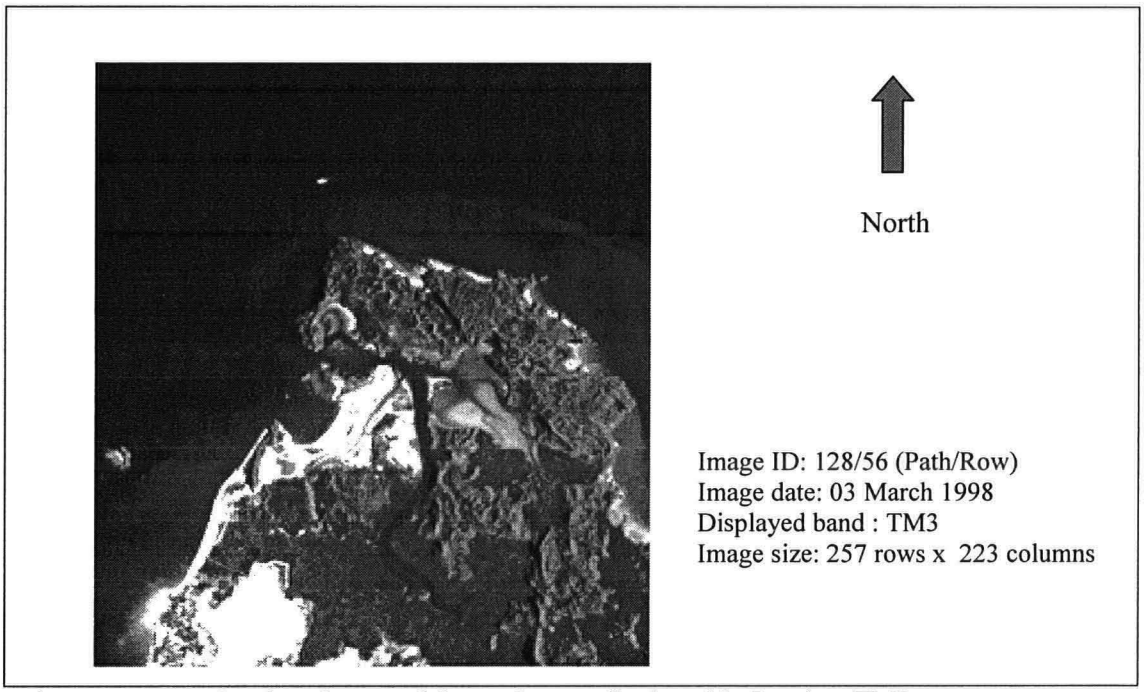

Figure 7.5. A subset image of the study area displayed in Landsat TM3

Step 14:

The same overlay process is applied to Image B as in Step 9.

Step 15:

The new sea area image (from Image B) is now called Sea B.

Step 16:

A simple Atmospheric Correction was applied to the cut images of Sea A and Sea B. Sea A which is a band 2 image was corrected by subtracting the DNs with 25 and the atmospherically corrected

image was called Sea A1; while for Sea B which is a band 3 image, the DNs were subtracted with 10 and the new atmospherically corrected image was renamed as SeaB1. These values (25 and 10) were the lowest DNs found in deeper clear waters within the image used in this study.

Step 17:

Both images of SeaA1 and SeaB1 were now ready to be applied with SPACoRS using Image Calculator in Database Query of the Analysis Module.

Since the input values required from the Landsat TM data were remote sensing reflectance at the top of atmosphere ($R_{rs\text{-}toa}$), the original DNs from the image would have to be converted into $R_{rs\text{-}toa}$ before the actual application of SPACoRS be carried out. These conversion values were incorporated into the SPACoRS as follows:

(i) To convert DNs into $R_{rs\text{-}toa}$ for the image

$$R_{rs\text{-}toaTM2} = \frac{(DN_2)CF_2 - L_{min2}}{E_{s2}}$$

$$R_{rs\text{-}toaTM3} = \frac{(DN_3)CF_3 - L_{min3}}{E_{s3}}$$

(ii) To convert DNs into $R_{rs\text{-}toa}$ for atmospheric correction

$$R_{rs\text{-}toaTM2d} = \frac{(25)CF_2 - L_{min2}}{E_{s2}}$$

$$R_{rs\text{-}toaTM3d} = \frac{(10)CF_3 - L_{min3}}{E_{s3}}$$

(iii) Merging of equations in (i) and (ii) for TM2 and TM3 for atmospheric correction:

$$R_{rs\text{-}toaTM2} = CF_2\,(DN_2 - 25)/E_{s2}$$

$$R_{rs\text{-}toaTM3} = CF_3\,(DN_3 - 10)/E_{s3}$$

(iv) The Ratio of TM3 and TM2:

$$R_{rs\text{-}toaTM3} / R_{rs\text{-}toaTM2} = [CF_3\,(DN_3 - 10) / CF_2\,(DN_2 - 25)] * (E_{s2}/E_{s3})$$

With E_{s2} and E_{s3} being constants, i.e.1833.64 $W/m^2/sr/\mu m$ and 1580.643 $W/m^2/sr/\mu m$ respectively, the ratio of E_{s2}/E_{s3} would be 1.16. The ratio of TM3 and TM2 would finally be:

$$R_{rs\text{-}toaTM3} / R_{rs\text{-}toaTM2} = 1.16* [CF_3\,(DN_3 - 10) / CF_2\,(DN_2 - 25)]$$

Using a Mathematical Expression as the Operation type, the SPACoRS was applied as follows:

$$\textit{SEA-TSP} = 0.6668 * \exp (4.3892* 1.16* [CF_3\,(\textit{SeaB} - 10) / CF_2\,(\textbf{SeaA} - 25)])$$

where *SEA-TSP* will be the output name for the generated map of TSP distribution and *SeaA* and *SeaB* are images of TM2 and TM3 respectively.

Step 18:

From Step 17, an image called *SEA-TSP* with Total Suspended Particulate distribution is produced.

In this image, the classes of TSP formed could be between 100-200 as each class represents only a single TSP value as a result of the mathematical expression applied.

Step 19 outlines the procedures used to further reduce these classes into groupings.

Step 19:

To group the TSP concentrations in SEA-TSP image, an Equal-Interval Reclass under the Reclass option of Database Query in the Analysis module is used. A number of 10 classes were selected based on the histogram of SEA-TSP. The range of TSP values mapped was 35.11 - 334.81mg/L. The lowest value was then set at 0 mg/L which represented the minimum, while the maximum for the Reclass option was 250 mg/L. The resultant image was then grouped with equal interval values of 50mg/L.

Step 20:

The classified TSP distribution image needed to be rectified as the original image had been slightly distorted during acquisition. No major georeferencing was required in this image because the distortion level was low. This is because the study area is located within the equatorial belt and there is less distortion of the acquired image as compared to a different geographic location e.g. 30° N or 30° S latitudes.

A Linear Rectification was required for the study area. The reference system used was UTM-5N in the Resample option in the Reformat module. A linear mapping function was selected with a nearest neighbour resampling method.

Step 21:

The rectified *SEA-TSP* image was then converted to map from its raster image. This is to enable the composition of map for the next step.

Step 22:

A full map composition was applied to produce a proper map of the classified and rectified *SEA-TSP map*.

Step 23:

This step produced the final output of the classified predicted TSP distribution map of Tanjung Rhu, Pulau Langkawi. This is shown in Figure 7.6. This map was then used for accuracy assessment described in section 7.5.

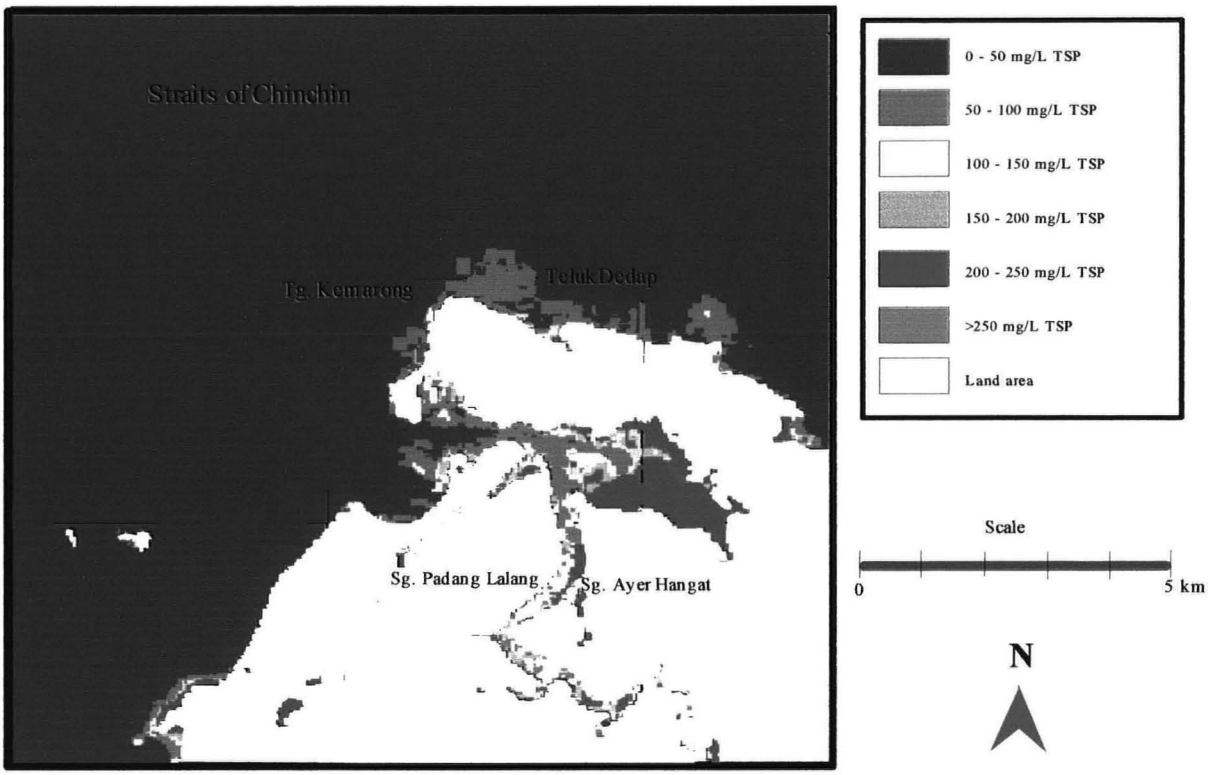

Figure 7.6: Distribution of Predicted Total Suspended Particulates in Surface Waters of Tanjung Rhu Based On the Application of SPACoRS in Landsat TM

7.3 THE DISTRIBUTION OF PREDICTED TOTAL SUSPENDED PARTICULATES ON THE TANJUNG RHU COASTAL WATERS

The range of [TSP] produced from the application of SPACoRS was between 30 mg/L to more than 300 mg/L. Six categories were chosen for this classified map where the interval was at 50 mg/L:

i. 0 – 50 mg/L
ii. 50 – 100 mg/L
iii. 100 – 150 mg/L
iv. 150 – 200 mg/L
v. 200 – 250 mg/L
vi. >250 mg/L

Although the result showed higher [TSP] *i.e.* ≥ 300 mg/L, categories of 250 – 300 mg/L TSP and ≥ 300 mg/L TSP were not selected because based on the monthly and mean annual measured [TSP] of Tanjung Rhu, the highest concentration was 243.00 mg/L (Station 7; April 1997). Taking into consideration the following factors:

(1) TSP measurements taken have included the varying environmental conditions of the study area, and
(2) the upper sensitivity limit of SPACoRS is assumed to be 150 mg/L TSP, which indicates the higher the [TSP] the higher the prediction inaccuracy,

therefore it is unnecessary to further separate the [TSP] into the 250 – 300 mg/L and ≥ 300 mg/L categories.

Most variations in the [TSP] were found to be within the riverine and estuarine areas of Tanjung Rhu where the [TSP] ranged from 50 mg/L to >250 mg/L. The high variation here was expected mainly because the rather enclosed riverine and estuarine systems would naturally have high physical interactions relative to its size as compared to the open sea. Physical activities such as erosion of river banks, anthropogenic inputs of possible pollutants, the stirring ups of bottom sediments etc. would not be fully flushed out of this enclosed system but rather contained within it. This had possibly resulted in the high concentrations detected within the inner estuary which is located on the eastern side. In conventional water quality sampling methods, these variations may not be clear if the area of study is too large or if the number of sampling points is inadequate to portray such visualization, or if the available resource for such sampling is limited. This is one of the major advantages of developing a remote sensing algorithm for application to a larger area where conventional methods may be too resource intensive and time consuming.

The inner estuary appeared to have high [TSP] concentrations from the classified map, where most areas showed >200 mg/L of TSP. This inner estuary is very shallow, so that during low water spring tidal conditions, the sand and mud flats are normally exposed. With the high physical activity occurring within this estuarine area, it was expected that the water column would contain high background concentrations of TSP. Another explanation may be the influx of water during a flooding tide which will naturally circulate around this region, creating an area of high physical activity resulting in high [TSP]. This possibility is supported by the green streaks of TSP having concentrations of 50 – 100 mg/L 'entering' the larger river (Sungai Ayer Hangat) and into the inner estuary. It is possible that the green streaks here (the second category of [TSP] classified in the map) may have represented an influx of the fresh water body that had just entered the riverine-estuarine system. Indeed, at the time of Landsat TM data acquisition by Landsat 5 satellite (03 March 1998 at 11:00 hr), the study area was experiencing flooding spring tidal conditions and no

distinctive turbidity or sediment plume was seen from the estuarine entrance in the classified map. This plume would have been seen and appeared in the classified map and imagery if it had been an ebb tidal condition.

From Figure 7.6, more turbid categories of water were classified in upstream sections of the rivers. The influx of marine water bodies from the sea into the estuary and then the rivers have resulted in higher TSP being flushed into the upper stream sections of the rivers. Although dilution may have occurred during the influxes, the clearer waters of 50 – 100 mg/L TSP category were not clearly mapped as found around the outer estuary. It can only be ascertained that influx had occurred.

Some sections of Sungai Padang Lalang, the smaller of the two main rivers draining Tanjung Rhu, were not classified or detected in the map. The widths of certain sections of the river were too narrow ($\leq$ 30 m) making them impossible to detect using the Landsat TM. During image processing classification i.e. with the application of SPACoRS, the low reflectance from these sections as a result of surrounding influences, were not classified as water bodies but as land. The reflectance value around these sections may either be <25 or >44 which had been masked out as land during the initial image processing procedure mentioned earlier.

Within the outer region of Tanjung Rhu, i.e. the seaward area, small turbidity plumes were detected in several locations having [TSP] mainly within the 50 – 100 mg/L category. A small area in Teluk Dedap showed higher variations of [TSP] ranging from 100 – 250 mg/L. The plume locations were found to be around Tanjung Kemarong, Teluk Dedap and Tanjung Gua Cherita facing northward of the study area. The small capes (Tanjung Kemarong and Tanjung Gua Cherita) formed interceptive points for the current flow. During a flood tide, the flow of the water is westward and the pattern of the plumes at Tanjung Kemarong and Tanjung Gua Cherita showed westward plume formation. The smaller plume size at Tanjung Gua Cherita may not clearly show the westward plume but the larger plume at Tanjung Kemarong allowed the swirl to be distinguished.

The open sea area of the Straits of Chinchin showed [TSP] that fell within the 0 –50 mg/L range depicting a clear water region.

7.4 AN ACCURACY ASSESSMENT OF THE PREDICTED TOTAL SUSPENDED PARTICULATES IN SURFACE WATERS OF TANJUNG RHU USING SPACoRS.

The Accuracy Assessment option in the Image Processing function of Analysis module in IDRISI for Windows Version 2.0 which produces the Error Matrix computation was not used to assess the accuracy of the map. The reasons were:

1. The coastal waters of the study area have a very dynamic nature which is typical of most coastal areas. Changes within this region occur on a constant basis. These changes depend on the tidal flow, the different seasons of the year, influences of the surrounding environment, and the time of the day, etc. The changes in the [TSP] probably occur on an hourly basis, although the magnitude of change may not be much during slower water movement in neap tides as opposed to during spring tidal conditions where more rigorous movement of water bodies may occur. However, the changes should fall within a certain measured range.

2. Neither Non-site specific or Site specific accuracy assessment could be applied here although the locations for accuracy assessment are fixed, because of the ever-changing dynamic system of Tanjung Rhu.

3. Due to the limited resources available, it was not possible to sample at measured point intervals within the study area to create a ground truth map that could be used for the accuracy assessment. Therefore, the methodology adopted here was simplified based on the Error Matrix procedure.

The methodology used for the accuracy assessment of the produced map was based mainly on the data collected on a monthly basis for 1997. This was made with the objective of producing SPACoRS that would be applicable for the study area during the dry and wet seasons. Therefore, regardless of the seasons or the tidal conditions, it hoped that the application of SPACoRS into Landsat TM data would be able to produce a map of relatively high accuracy and with validity at the time of map production for the purpose of reference.

In terms of accuracy assessment, it was not possible to use the exact Error Matrix method since, as mentioned earlier, the waters around Tanjung Rhu are a dynamic system. However, the Error Matrix procedure was used as the basis to assess the accuracy of the predicted [TSP] on surface waters of Tanjung Rhu.

Eight locations were used in the accuracy assessment process. These locations which have been described in Chapter 3 are shown in Figures 7.7. Table 7.1 shows the list of selected accuracy assessment points. Two of the sampling stations were not considered as accuracy assessment points because:

(i) these stations were located within the inner tributaries of Sungai Padang Lalang, and

(ii) the sizes of the tributaries were indistinguishable through Landsat TM data due to the 30m x 30m resolution of the imagery.

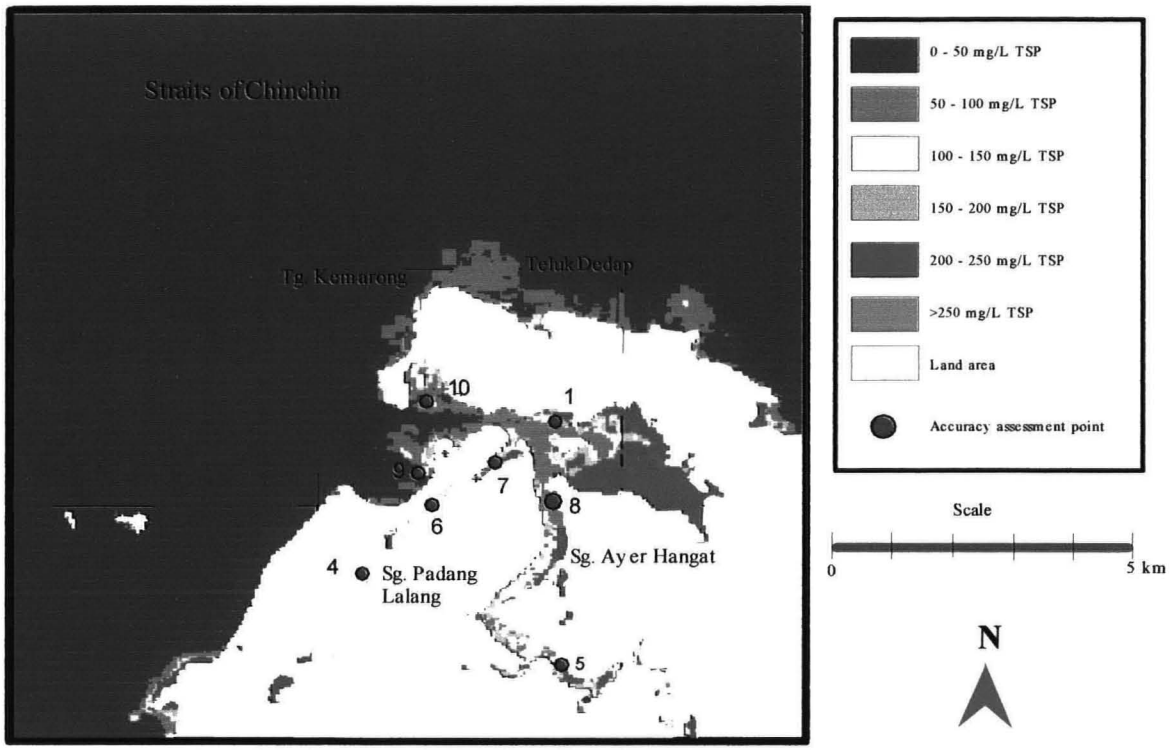

Figure 7.7: Location of Accuracy Assessment Points in the Predicted Total Suspended Particulate Map produced from the application of SPACoRS in Landsat TM

Table 7.1: Description of Accuracy Assessment Points for Tanjung Rhu

Accuracy Assessment Point	Location
1	Teluk Udang (Inner Estuary)
4	Sungai Padang Lalang (inner mid-stream)
5	Bakar Arang
6	Sungai Padang Lalang (outer midstream)
7	Sungai Padang Lalang river mouth
8	Sungai Ayer Hangat river mouth
9	Beach Front
10	Pulau Belibis (Outer Estuary)

Concentrations of TSP measured during 1997 (Table 7.2) were compared to the class of TSP mapped in Figure 7.6. If the range fell within the class, the particular category of TSP on the map was considered agreeable or accurate. For further examination of the predicted [TSP] distribution in the map, sections corresponding to the accuracy assessment points were enlarged according to the north and south regions. These regions were marked as shown in Figure 7.8 and Figure 7.9. The list of predicted [TSP] range was also tabulated in these figures.

Table 7.2: Measured Total Suspended Particulates (mg/L) in Surface Waters of Tanjung Rhu in 1997. (Source: Abdullah and Yasin, 2000)

	STATION									
MONTH	1	2	3	4	5	6	7	8	9	10
Jan	130.00	136.70	150.00	110.00	100.00	126.70	120.50	130.00	143.30	123.30
Feb	50.70	157.00	27.00	127.70	163.70	121.30	149.30	96.70	137.00	120.70
Mar	52.10	50.30	53.60	51.00	59.20	46.30	56.40	51.20	47.60	50.80
Apr	177.00	171.00	55.33	185.00	181.33	201.33	243.00	189.67	202.67	182.00
May	150.00	123.00	79.50	126.17	167.00	181.33	171.22	179.22	189.00	193.15
Jun	155.50	136.50	126.70	179.50	183.20	166.80	170.50	182.30	186.90	197.40
Jul	145.40	128.00	116.00	132.40	164.00	157.50	155.50	160.30	145.00	170.00
Aug	192.30	181.10	201.50	194.00	193.51	198.40	183.70	181.90	181.70	198.30
Sep	115.00	110.00	123.00	104.00	139.00	90.00	188.00	92.00	86.00	112.00
Oct	114.00	111.00	125.50	100.00	135.00	89.90	188.70	92.35	85.54	110.30
Nov	121.00	97.50	111.40	101.40	77.80	87.50	168.30	88.22	107.90	88.56
Dec	110.00	90.50	48.40	88.33	126.33	100.21	130.33	98.10	128.33	120.10
Mean	116.46	114.97	93.92	115.65	130.39	121.02	148.65	119.23	126.92	128.97
Std. Dev.	43.18	36.32	50.10	42.71	43.18	50.00	45.40	47.91	48.40	48.13

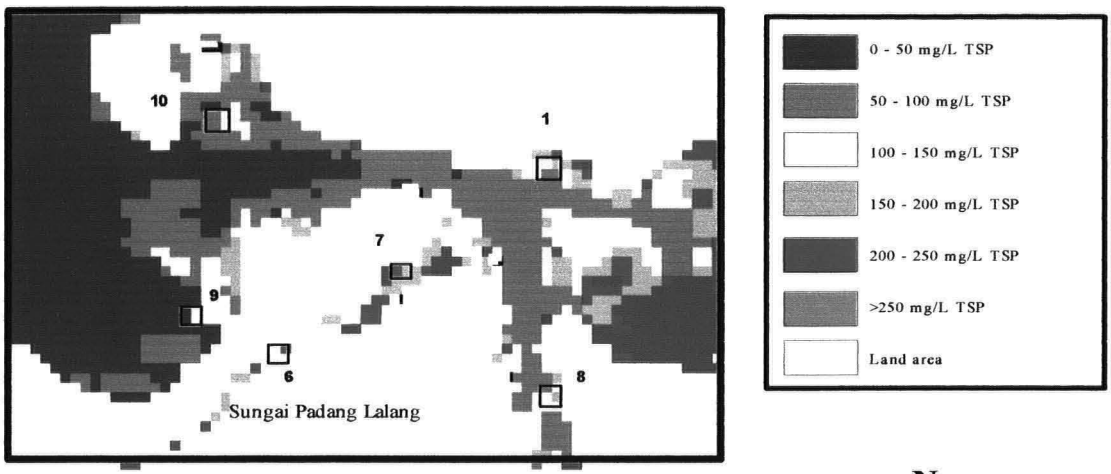

Range of predicted TSP (mg/L)	
Station 1	50 - 200
Station 6	100 - 150 & 200 - 250
Station 7	150 - 250
Station 8	50 - 200
Station 9	0 - 50 & 100 - 150
Station 10	50 - 150

Figure 7.8: Northern region of sampling points used for accuracy assessment.

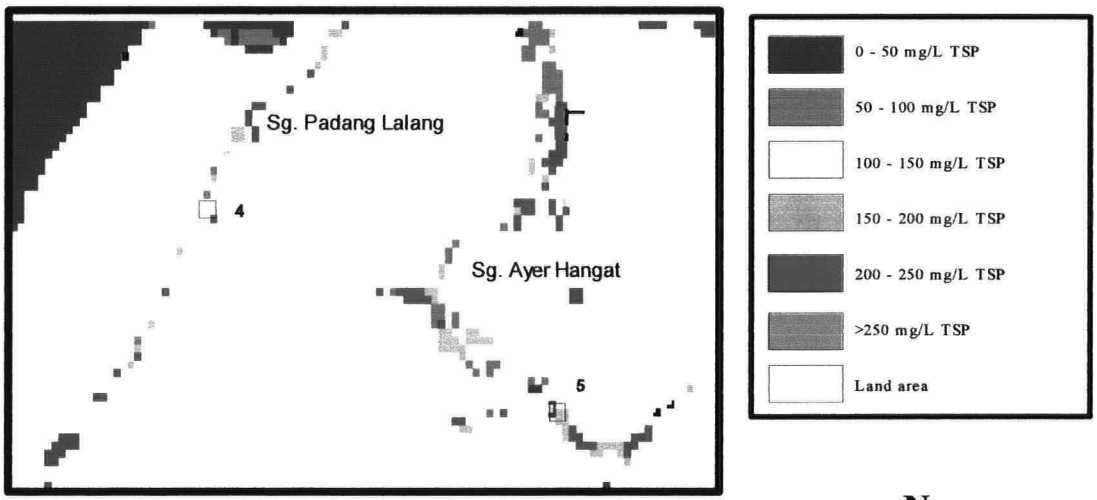

Range of predicted TSP (mg/L)	
Station 4	100 - 150 & 200 - 250
Station 5	100 - 200

Figure 7.9: Southern region of sampling points used for accuracy assessment.

The accuracy results determined through comparison between measured or observed data in Table 7.2, and predicted data in Figure 7.8 and Figure 7.9, are given in Table 7.3. The measured data for each month and for each station was noted as one occurrence. The number of occurrences or measurements for each station was 12 resulting in 96 occurrences for the 8 accuracy assessment points. This number was taken as an equivalent of the sum of diagonal as in the Error Matrix procedure. The number of correct occurrences, where the range of [TSP] measured and predicted coincided would be counted as correct. A summation of these correct occurrences was then used to calculate the percentage of overall accuracy.

As mentioned in Chapter 4 (subsection 4.2.1.5) on accuracy assessment using the Error Matrix procedure, errors of omission and commission, and producer's and user's accuracy are normally calculated. This is true for accuracy assessment of stable or static features, such as land use or land cover but not for the dynamic systems such as the Tanjung Rhu waters. Thus, the computation of those errors (of omission and commission) and levels of accuracies (by the producer and for the user) were not possible in these circumstances. This was omitted and only the overall accuracy was considered to have validity. Based on the calculations as shown in Table 7.3, the overall accuracy of SPACoRS applied to Landsat TM data is 66%. It is important however, to state the validity of the overall accuracy for such an assessment for the given time and space. In this study, it then had to be an overall accuracy for 1998 using SPACoRS, based on 1997 data. Because of this high accuracy is not expected and neither will the expectations be very low. An accuracy of at least 90% would have been expected if the measured data and the Landsat TM data used in the application of SPACoRS were of the same date and time.

The eight sampling stations used as accuracy assessment points can be grouped into 3 different categories which are:

(1) Riverine Stations

These are stations located within the rivers of Padang Lalang and Ayer Hangat namely stations 4, 5, and 6. These stations were located along the two main rivers.

(2) Estuarine Stations

These are stations located at the river mouth that are connected with the enclosed estuarine system and they are stations 1, 7, 8 and 10. Of these four, stations 7 and 8 were located at the river mouth of Sungai Padang Lalang and Sungai Ayer Hangat respectively. Station 1 represented the inner estuary while station 10 represented the outer estuary.

(3) Sea Stations

There is only one sea station in this group, i.e. station 9 located at the beach front facing northwest of the Straits of Chinchin.

Table 7.3: Accuracy Assessment of Predicted Total Suspended Particulates Produced from the Application of SPACoRS to Landsat TM Data

Range of [TSP] mg/L	Accuracy Assessment Point								Range of [TSP] mg/L
	1	**4**	**5**	**6**	**7**	**8**	**9**	**10**	
Measured: (#)									**Predicted**: (•)
0 – 50	0	0	0	1	0	0	1 •	0	0 – 50
50 – 100	2 •	3	3	3	1	6 •	2	2 •	50 – 100
100 – 150	7 •	6 •	3 •	3 •	3	1 •	5 •	5 •	100 – 150
150 – 200	3 •	3	5 •	4	7 •	5 •	3	5	150 – 200
200 – 250	0	0 •	0	1 •	1 •	0	1	0	200 – 250
> 250	0	0	0	0	0	0	0	0	> 250
No. correct occurrences	12/12	6/12	8/12	4/12	8/12	12/12	6/12	7/12	No. correct occurrences
Sum of occurrences = 8 x 12 = **96**						Sum of correct occurrences = **63**			
% correct occurrences	100.00	50.00	66.67	33.33	66.67	100.00	50.00	58.33	% correct occurrences
Overall Accuracy = (63/96) * 100 = ***66 %***									

Note: *Shaded area denotes correct occurrences of measured and predicted data used in the calculation of the overall accuracy.*

Based on the results obtained which were summarized in Table 7.3, there were 3 points that produced an accuracy level of ≤ 50%, namely the riverine stations 4 and 6, and the sea station 9. The reason for the low accuracy observed was probably the shallow depth. Riverine stations 4 and 6 had depths of 4 m and 3 m respectively during high water spring while station 9, a sea station had depths of about 4 m during the same tidal condition. Stations 4 and 9 had an accuracy level of 50% each, while station 6 had much less, i.e., 25 %. The low accuracy for station 6 was expected, because during low water spring, the river bottom was normally exposed for several hours and it also marked the shallowest portion of Sungai Padang Lalang since it actually divides the river with its sand/mud banks. The occurrence of this may well have been the effect of dredging to deepen the river at approximately 400m downstream where station 7 was located. The high fluctuation in the distribution of measured [TSP] at station 6 (0 – 250 mg/L) resulting in a low accuracy level, was expected. This was basically due to the pixel size (resolution) of Landsat TM data which was 30m x 30m. Although the distribution of [TSP] may vary within the width of station 6 (approximately 80m), the greater influences of reflectance within the pixel size would affect the final pixel value in the SPACoRS application process. The low accuracy levels for Station 4 and 9 may well be caused by constant mixing within the water column, again resulting in high fluctuations of [TSP].

Stations 1 and 10 gave a 100% accuracy level. Both were estuarine stations, with station 1 located at the inner estuary and station 10 in the outer estuary. The remaining stations showing an accuracy level of >50% were stations 5, 7, and 8. These were also estuarine stations except station 5. However, the higher accuracy may be attributed to the larger depth, the size or width of the sampling locations and the physical factors influencing the detection of [TSP] as seen through the application of SPACoRS into Landsat TM data.

It is normal procedure for the area coverage of each classified category in a map to be calculated. However, in this case, the dynamic nature of Tanjung Rhu system does not allow the validity of such a classified map (*i.e.* through an application with an algorithm). Such a classified map would only be valid for the purpose of temporal and spatial analysis in research, planning and management of a natural ecosystem or the conservation and preservation of natural resources.

7.5 FACTORS OR LIMITATIONS AFFECTING ACCURACY ASSESSMENT OF [TSP] DISTRIBUTION MAP PRODUCED BY SPACoRS.

There are several factors that need to be considered during accuracy assessment and these are:

1. Size of study area

The size of the study area is very important in relation to the resolution or pixel size of the satellite imagery in use. It would not be appropriate to have a study area the size of 1500m x 1500m (1.5km

x 1.5km) when one uses Landsat TM data for remote sensing studies. The small area of 1500m x 1500m area will contain only 50 x 50 pixels in a Landsat TM data because each pixel is 30m x 30m. A relatively large area would be more appropriate and cost effective for satellite imagery. Schematic examples for a small study area (A) and a large study area (B) using Landsat TM data are shown in Figure 7.10.

2. *Feature recognition*

The existing features recognizable in satellite imagery play a very important role as well. It would not be appropriate to map an area that contained features that are too small to be distinguished in the mapping process. Recognizable features on the satellite imagery provide further aid in speeding up the mapping process and reduce unnecessary error.

3. *Surrounding influences – neighbouring pixel effect*

If a general study area is large enough, but some features are too small, there tends to be a neighbouring pixel effect. An example is from this study itself which was mentioned in the earlier subsection (Section 7.4) where the width of certain sections of Sungai Padang Lalang was too narrow relative to the pixel size. The effect of the surrounding features (in this case the vegetation along the river banks) would have empowered the reflectance value detected and measured by the satellite concerned. This, in fact, is an error by itself but one that is unavoidable because of the way the sensor was designed.

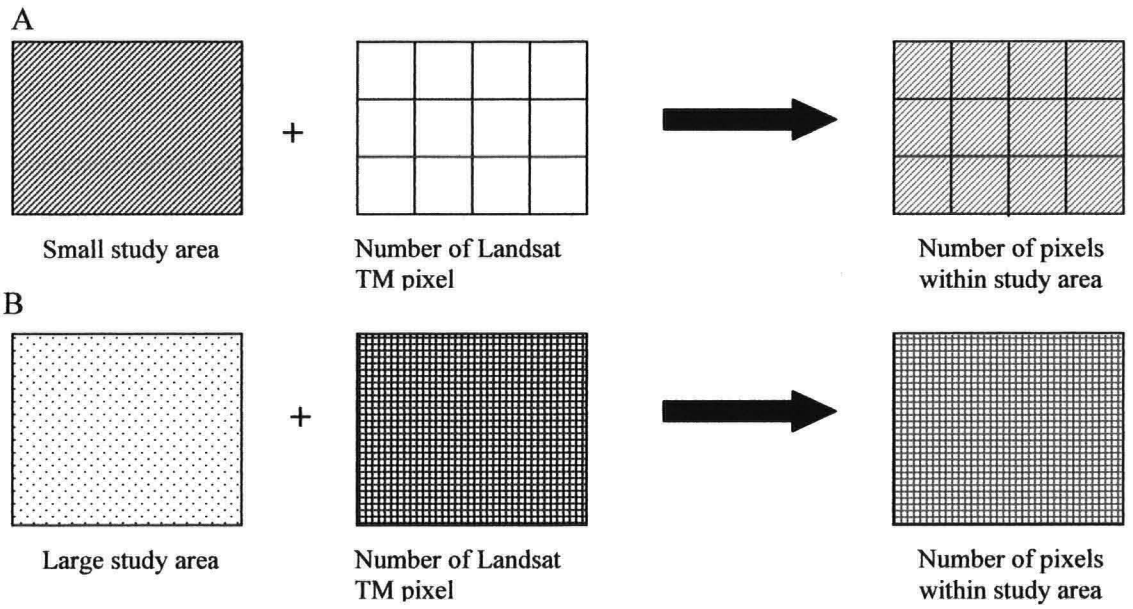

Figure 7.10. A schematic representation for a small study area (A) and a large study area (B) using Landsat TM data.

4. *Classification scheme.*

The formation of larger groups for the categories in the classification process can also contribute errors. This is particularly true for water quality classification with the application of an algorithm.

The dynamic nature of the coastal and marine system would have contributed the changes and errors for the map produced. An area classified as having 50.5 mg/L TSP may no longer fall within the 0 – 50 mg/L category but placed in the 50 – 100 mg/L category. Logically an additional 0.5 mg/L shall not be a concern but if accuracy assessment was to be done, this will already be considered a classification error. If the original value were rounded up to 50 mg/L and not 50.5 mg/L, then this area will be classified within the 0 – 50 mg/L category in the predicted map and the accuracy assessment would have been correct. Basically the classification scheme chosen in the image processing procedure will depend on the degree of detail required.

5. *Resource limitations for detailed sampling in the process of accuracy assessment.*

Another major factor affecting accuracy assessment is the availability of resources to compute more detailed and systematic ground truthing points. The higher the number of ground truthing or accuracy assessment points, the higher the probability of obtaining higher accuracy maps.

Figures 7.11(a)-(c) schematically explains the resource limitation factor here. Detailed and systematic ground truthing points will probably appear as shown in Figure 7.11(a). Figure 7.11(b) is the classified water quality map using an algorithm; while Figure 7.18c shows the actual number and locations of groundtruthing pints (due to lack of resources) used in the accuracy assessment of the map produced (Figure 7.11(b)). Naturally, the use of detailed groundtruthing points to assess the accuracy of the classified map will produce a higher accuracy than numbers of groundtruthing points. The possibility of obtaining the extreme ends of very good or very low accuracies in using the fewer groundtruthing points would probably be a 50% chance.

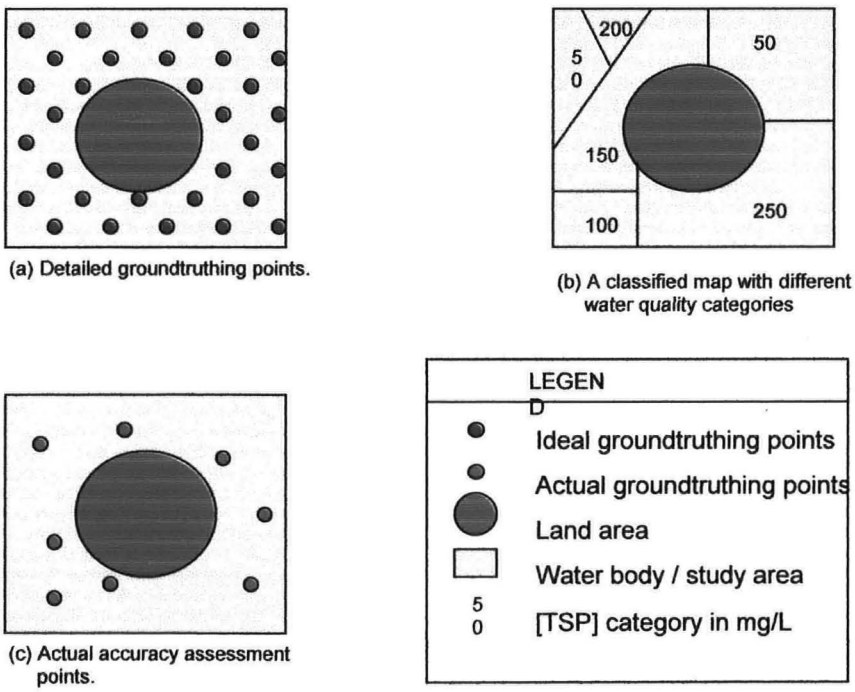

Figure 7.11. A schematic representation of resource limitation factor for detailed sampling in an accuracy assessment process.

6. Time and date of data acquisition

To achieve higher accuracy in a classification or mapping process, the time and date of both measured and satellite data should be identical or as similar as possible. However, this may not always be the case for coastal and marine systems because of limited access to the study area, which could be seasonal, or even the resources available. The time and date factor would be applicable to the terrestrial mapping purpose such as land use and land cover.

7.6 THE APPLICABILITY OF SPACoRS IN MALAYSIAN COASTAL WATERS

The development of SPACoRS appeared to be invaluable for Malaysian coastal waters. It enables the estimation of the extent of Total Suspended Particulates (TSP) on surface waters based on the availability of satellite data. The only limitation in using satellite data such as the Landsat TM is that when there is thick/heavy cloud coverage, the applicability and accuracy of results produced using SPACoRS will be limited. This is usually due to the fact that application of atmospheric correction procedures will alter the original data entirely and hence the accuracy level of TSP will also be altered greatly. However, SPACoRS is applicable not only to Landsat TM satellite data, but also other remote sensing data provided the wavelength bands cover similar range as in TM3 and TM2.

The higher the spatial and spectral resolutions of a particular satellite data will automatically enhance the accuracy of results produced using SPACoRS. Higher temporal resolutions will benefit the application of SPACoRS in that it will allow the monitoring of TSP pollution problem within the coastal waters.

As mentioned in Chapter 6, SPACoRS is very sensitive to [TSP] $\leq$ 150mg/L and less sensitive to [TSP] > 150mg/L. This showed that SPACoRS is also applicable within marine waters and not restricted only to coastal waters. Normally coastal waters are subjected to higher sedimentation problem and therefore usually higher [TSP]. The accuracy of surface waters with higher [TSP] (e.g. [TSP] = 300mg/L) will be lowered with SPACoRS. However, this does not mean that SPACoRS is inaccurate. It simply implies that SPACoRS will probably need finer tuning in its modeling process. To do so, very in-depth research methodology will probably be required.

In this study, the sensitivity level of SPACoRS is sufficiently good to be applied in Malaysian coastal waters where the coral reef ecosystem is of major concern. Waters within the coral reefs of Malaysia particularly within the west coast of Peninsular Malaysia normally have [TSP] < 150 mg/L while in the east coast Peninsular Malaysia (South China Seas) and East Malaysia (such as Sabah waters in the Sulu Seas), [TSP] is usually < 100mg/L (Yasin, *pers. comm.*).

The exact accuracy level of SPACoRS may be difficult to be determined because of the dynamic nature of the coastal and marine water ecosystem.

7.7 RECOMMENDATIONS

A further evaluation of the application of SPACoRS would be improved if temporal and spatial data analysis could be performed with the availability of more Landsat TM data of the same tidal condition. Ground truth data should also be available to assess SPACoRS's applicability.

SPACoRS could also be applied to Landsat TM data with haze problem within the atmospheric column. This may perhaps provide an insight into the applicability and effectiveness of SPACoRS in the mapping process of quantifying TSP in surface coastal waters within the tropical region.

The use of Landsat ETM data which contained the panchromatic band will also further improve the application of SPACoRS.

The applicability and accuracy of SPACoRS may be further tested if there is a possibility of utilizing MERIS products which are currently available within the European region. Since MERIS (Medium Resolution Imaging Spectrometer) has nine channels dedicated to retrieve water constituents (Schiller and Doerffer, 1999; Doerffer *et al.*, 1999; Gower *et al.*, 1999), it may prove valuable in its applicability to tropical coastal waters as well.

7.8 SUMMARY

The purpose of applying an algorithm (in this case SPACoRS) into imagery would certainly quantify the difference in tone of the displayed imageries as seen through visual observation. This saves both time and money. The knowledge that the application of SPACoRS into Landsat TM data is highly dependable on the time and date of the sources of data would certainly help to improve our ability to effectively use spatial data.

With the application of SPACoRS, the resultant Landsat TM image dated 03 March 1998 of Tanjung Rhu obtained a 66% of overall accuracy using 1997 data measured. The classification scheme used in the classification process was based on 50 mg/L TSP concentration intervals. A higher accuracy level will be expected if the time and date of measured TSP data used in the ground truthing coincided with clear satellite image i.e. cloudless image, captured during satellite data acquisition date. It is of no use if the time and date of measured TSP data coincided with heavily clouded satellite image because the cloud element in imagery cannot be technically removed in the image processing phase. In such case the image can be used in combination with a

radar image. However, the use of radar image in this study has to be ruled out since it is not available for the study region.

It may be possible to detect the different patterns and flow direction of turbidity plumes during the different tidal conditions i.e. flooding and ebbing tide during spring and neap tidal condition. This is because TSP is a natural tracer by itself which can be visually detected in the imagery. However, for research, planning and management purposes, TSP needs to be quantified and this is made possible with the development and application of SPACoRS.

SPACoRS was designed to estimate [TSP] during the dry and wet seasons of coastal tropical waters having similar dynamic nature as the study area. Similar to algorithms developed previously by environmental researchers, SPACoRS has its own limitation in terms of detection sensitivity. In this study, SPACoRS is sensitive to [TSP] of up to 150 mg/L. However, this sensitivity limit does not mean SPACoRS cannot detect or quantify [TSP] > 150 mg/L. SPACoRS can still detect higher [TSP] but perhaps less accurately. This is simply because SPACoRS was developed based on the range of [TSP] measured within Tanjung Rhu.

Chapter 8

SUMMARY

This study looked at the northern coast of Pulau Langkawi as a representative of the coastal environment of Malaysia where it covers the riverine-estuarine system.

The author particularly assessed the effect of sedimentation on the coastal habitats but the effect of sedimentation could not be separated out from all the other factors affecting these habitats without first ascertaining the possible linkage between sedimentation and the other factors. Therefore, the author had to consider and monitor the relevant physical, chemical and even the microbiological factors operating in these systems. The system was then monitored over a period of 3 ½ years of which in order to describe the existing environment and other interacting factors that affect the environment.

Given the nature of Tanjung Rhu (the study area), no heavy industries, low population pressure, a coastal environment which is tidal and now beginning to be exploited for development, several parameters were deemed important, particularly those relevant to organic pollution. Therefore, nitrates, phosphates, ammoniacal-nitrogen, etc. are in that group. The existing physical parameters such as salinity, dissolved oxygen, temperature, were also monitored since these changes with the tide and the season. One of the major factors that has affected coastal development in Malaysia is sedimentation and this of course was monitored in Tanjung Rhu.

The measured values of water quality parameters were compared with the Malaysian Department of Environment (DOE) Water Quality Standards, none of these parameters exceed the limits stipulated by standards except for the Total Suspended Particulates (TSP).

Increased TSP and settled solids in an area could affect the benthic habitats of which the coral reef areas are particularly sensitive. This is a significant component of the study area - because the corals are photosynthetic organisms which rely on the amount of light entering the water body for its well-being.

The distribution of Tanjung Rhu corals which had been affected by this sedimentation was mapped out. This was compared to a nearby control site (Teluk Datai) also in the north coast of Pulau Langkawi about 18 km to the west of Tanjung Rhu. Coastal development is almost absent in Teluk Datai and from literature review, the TSP concentrations of Teluk Datai waters is very low, i.e. below the Malaysian DOE standards of 50mg/L. The comparison also indicated that the diversity of the scleractinian/photosynthesizing corals are higher in Teluk Datai (76 species) compared to the study area of Tanjung Rhu (37 species).

Although as far as settled sediment is concerned, the amount of the settled sediment in Teluk Datai (the control site) was higher than the Teluk Dedap settled sediment. Observations on site indicated that for this type of reef and the amount of sedimentation involved, the reef organisms are able to withstand the input.

This type of point sampling provided a detailed temporal assessment of the effect of TSP in the coastal area. However, it does not provide a detailed spatial assessment as would remote sensing sampling. The latter, for several reasons discussed, did not provide as detailed a temporal assessment. This was because:

(1) the satellite overpass of Landsat Thematic Mapper data occurred in a 16-day cycle
(2) the cloud coverage is seasonable where on the months of January to possibly March would be cloud-free
(3) in developing countries, the purchasing of satellite imagery would be considered expensive.

The advantages of remote sensing sampling would be:

(1) it provides an instantaneous assessment over a wide area. Because of this it gives some sense of the dynamic of the TSP flow over a wide area.
(2) cost-effective
(3) provides detail because of its spatial resolution
(4) provides accessibility to areas difficult to sample as opposed to that accounted during point sampling.

Against this background, the most significant parameter affecting the coastal environment, i.e. the TSP, was modeled using remote sensing technique to determine its concentration and its distribution. The modeling chapter (Chapter 6) looked at:

(1) the computation of *Suspended Particulate Algorithm for Coastal Remote Sensing* (SPACoRS) which is a theoretical algorithm designed through the modification of Simple Radiative Transfer Program by the author and Doerffer for surface coastal water remote sensing of TSP, and
(2) assumptions made during the modeling process and these were high backscattering and low absorbance values of the water.

The developed SPACoRS defined as $y = 0.6668e^{4.3892x}$, where y is [TSP] in mg/L and x represents ($R_{rs\text{-}toaTM3}/R_{rs\text{-}toaTM2}$) ratio, quantified a concentration of TSP over a range of 0 – 275 mg/L at the study area. This range was divided into 6 classes which were 0-50 mg/L, 51-100 mg/L, 101-150 mg/L, 151-200 mg/L, 201-250 mg/L and >250 mg/L. SPACoRS also indicated habitats affected by the TSP and the ambient concentrations of TSP with respect to this particular habitat.

Following this, the application of the SPACoRS was made to the coastal areas of Tanjung Rhu. The accuracy of SPACoRS (66%) was determined based on the range of TSP concentrations measured by an error matrix. For a model developed for turbid waters, this was considered good if the accuracy was compared to existing literature. SPACoRS is robust since it can be applied over a temporal sequence. Previous linear models are very much less robust because these models can be applied only to the scene in question.

In Malaysia, the point sampling approach and the satellite remote sensing approach were used but the application of a model (in the satellite remote sensing approach) is newly introduced. Both approaches have their limitations. Some parameters cannot be revealed by modeling especially the chemical parameters. However, in this situation, this is not significant. Based on an earlier study by the author in 1997, the chemical levels did not exceed the permissible range provided by the Malaysian DOE. The study revealed the strengths and limitations of both approaches in the determination of a critical parameter such as TSP in the Malaysian coastal waters. SPACoRS also revealed the extent of TSP distribution, its source and its concentration. This was mapped out in Chapter 7 and its accuracy validated.

In conclusion, the physicochemical parameters measured at the study area were low. However, in view of the coastal development in that area, the concentrations of TSP are relatively high. The satellite model (SPACoRS) indicates a spread of TSP from the estuarine areas of Tanjung Rhu to the reef areas of Teluk Dedap, a considerable distance away. The satellite image also indicated associated areas of coastal development in the study area which may contribute to the TSP. In such instances the value of satellite remote sensing is further enhanced since point sampling could not reveal such association in detail.

The model produced here is robust enough to be used on a series of images in several locations. It can be used to assess this environment over a time series or it can be used at different locations. In addition, this study had also indicated the limitation of the model in revealing an environmental profile of the coastal habitat.

RECOMMENDATIONS

To further improve the accuracy of the model there should be an accuracy assessment of the assumptions made in the modeling process which were the backscattering and absorbance properties.

The Gelbstoff should also be measured to provide a more precise value to be fed in the Simple Radiative Transfer Model in fine-tuning the developed model, SPACoRS.

The accuracy of the model can be further improved by assessing images of other areas.

The drawback now to environmental profiling using remote sensing are also limitations associated with sensors mounted on space-borne platform. Such limitations are:

(1) the high levels of cloud cover which normally inhibit the study of coastal areas in Malaysia
(2) the frequency of image acquisition which for Landsat TM is 16 days and typically images taken from January to possibly March are useable.
(3) images are taken at approximately 11:00AM at the stipulated satellite overpass dates and at this time of the day, some areas are still covered by clouds/haze.

Recently Malaysia is considering the use of airborne sensors mounted on commercial flights which are not restricted to cloud cover or time of day. Data from these sensors could be fed to the model developed and this could provide a better environmental profile of the study area.

REFERENCES

Abdullah, A.L. and Z. Yasin (2000). Seasonal Distribution of Surface Water Total Suspended Solids and Associated Parameters of Tanjung Rhu, Pulau Langkawi, Malaysia. *Malayan Nature Journal 2000*, **54**(2): 109-125

Abdullah, A.L., Z. Yasin, W.R. Ruslan, B. Shutes and M. Fitzsimons (2002). The effect of early coastal development on the fringing coral reefs of Langkawi: a study in small scale changes. *Malaysian Journal of Remote Sensing & GIS,* **3**:1-10

Abdullah, A.L. and Z. Yasin (2003). The Fringing Reefs of Teluk Dedap, Tanjung Rhu: Its distribution and characteristics. Universiti Sains Malaysia short-term grant report 2003 (304/PHUMANITI/634031).

Abdullah, A.L., and Z. Yasin (2001). The Changes in the Fringing Reefs of North Langkawi. *Proceedings of the Asian Wetland Symposium 2001 – Bringing Partnerships into Good Wetland Practices* (in CD-ROM), Pulau Pinang, Malaysia, 27 – 30 August 2001

Abdullah, K., Z.B. Din, Y. Mahamod, R. Rainis, and M. Z. MatJafri (2000). Remote sensing of total suspended solids in Penang coastal waters, Malaysia. In: http://www.gisdevelopment.net/aars/acrs/2000/ps3/ps312pf.htm (Date: 29 March 2004).

Allee, R. J. and J.E. Johnson (1999). Use of satellite imagery to estimate surface chlorophyll-a and Secchi disc depth of Bull Shoals, Arkansas, USA. *International Journal of Remote Sensing*, **20**:1057-1072.

André, J.M. and A. Morel (1989). Simulated effects of barometric pressure and ozone content upon the estimate of marine phytoplankton from space. *Journal of Geophysicsical Research,* **94**(C1):1029-1037.

Ångström, A. (1930). On the atmospheric transmission of sun radiation. *Geografis. Annal.*, **2 and 3**:130-159.

Antoine, D., and A. Morel (1998). Relative importance of multiple scattering by air molecules and aerosols in forming the atmospheric path radiance in the visible and near infrared parts of the spectrum. *Applied Optics*, **37**: 2245-2259.

Antonius, A. (1981). Coral reef pathology – A review. *Proceedings, 4th International Coral Reef Symposium,* Manila, **2**:3-6.

APHA. (1985). *Water Quality and Treatment*, McGraw-Hill, Inc. 128pp.

Bak, R.P.M. (1978). Lethal and sublethal effects of dredging on coral reefs. *Mar. Poll. Bull.*, **2**: 14-16.

Barnes, J.D. (1973). Growth in colonial Scleractinians. *Bull. Mar. Sci.*, **23**:280-291.

Barry, R.G. and R.J. Chorley (1998). *Atmosphere, Weather and Climate. 7th Edition.* Routledge Publication. London. New York. 409 pp.

Benayahu, Y. and Y. Loya (1977). Space partitioning by stony corals, soft corals and benthic algae on the coral reefs of the northern Gulf of Eilat (Red Sea). *Helgolander wiss. Meeresunters*, **30**:362-382. In: English, S., C. Wilkinson and V. Baker (editors). *Survey Manual for Tropical Marine Resources*. Published by AIDAB on behalf of ASEAN-Australia Marine Science Project, Townsville, Australia.

Benayahu, Y. and Y. Loya (1981). Competition for space among coral-reef sessile organisms at Eilat, Red Sea. *Bulletin of Marine Science*, **31**:514-522.

Bhargava, D.S. and D.W. Mariam (1990). Spectral reflectance relationships to turbidity generated by different clay materials. *Photogrammetric Engineering and Remote Sensing*, **56**:225-229.

Bhargava, D.S. and D.W. Mariam (1991). Light penetration, depth, turbidity and reflectance related related relationships and models. *ISPRS. J. Phtogrammetric and Remote Sensing*, **46**:217-230.

Birkeland,C. (ed) (1997). *Life and Death of Coral Reefs* (New York: Chapman and Hall).

Bricaud, A. and A. Morel (1987).Atmospheric corrections and interpretation of marine radiances in CZCS imagery: Use of a reflectance model. *Oceanol. Acta,* 7:33-50.

Briggs, D. (1977). *Sources and Methods in Geography: Sediments*. Published by The Butterworths Group, London. 192 pp.

Brown, L.R. (1984). The global loss of top soil. *Journal of Soil and Water Conservation*, **39**:162-165.

Brown, L.R. and E.C. Wolf (1984). Soil Erosion: Quiet crisis in the world economu. Worldwatch Paper 60 (Washington D.C.: Worldwatch Institute).

Buchheim, J. (2002). Coral Reef Bleaching. Odyssey Expeditions.

Buddemeier, R.W. (1999). Is it time to give up? Plennary paper in Proceedings of the International Conference on Scientific Aspects of Coral Reef Assessment, Monitoring, and Restoration, 14-16 April 1999.

Cameron, W.M. and D.W. Pritchard, (1963). Estuaries In: *The Sea* (ed. M.N. Hill), Vol. 2, John Wiley & Sons, New York, pp. 306-324.

Chapman, D.W. (1962). Effects of logging upon fish resources of the West Coast. *J. Forest.* **60**:533-537.

Chen, Z., J.D. Hansom, and P.J. Curran (1991). The form of the relationship between suspended sediment concentration and spectral reflectance and its implications for the use of Daedalus 1268 data. *International Journal of Remote Sensing*, **12**:215-222.

Chen, Z., P.J. Curran, and J.D. Hansom (1992). Derivative Reflectance Spectroscopy to estimate suspended sediment concentration. *Remote Sensing of Environment*, **40**:67-77.

Chua. T.E., and J.K. Charles (eds.) (1980). *Coastal resources of east coast Peninsular Malaysia.* Publ. Universiti Sains Malaysia, Penang. 507pp.

Congalton, R. (1991). A review of assessing the accuracy of classifications of remotely sensed data. *Remote Sensing of Environment.* **37**: 35-46.

Congalton, R.G. and K. Green (1999). *Assessing the accuracy of remotely sensed data: Principles and Practices.* Lewis Publishers. Boca Raton London New York Washington D.C. pp.137.

Cooper, C.M. (1986). Benthos in the sediment-laden delta stream system. Fourth Federal Interagency Sedimentation Conference. pp 7-51.

Cordone, A.J. and D.W. Kelley (1961). The influences of inorganic sediments on the aquatic life of streams. *Calif. Fish and Game*, **47**:189-228.

Corfitzen, W.E. (1939). A study of the effect of silt on absorbing light which promotes the growth of algae and moss in canals. Bur. Reclam. U.S. Dept. Int. Washington, D.C. 14pp.

Cowardin, L.M., V. Carter, F. Golet, and E. LaRoe (1979). *A Classification of Wetlands and Deepwater Habitats of the United States.* Office of Biological services. U.S. Fish and Wildlife Service, U.S. department of Interior, Washington, D.C.

Cox, C. and W. Munk (1954). Measurement of the roughness of the sea surface from photographs of the sun`s glitter. *J. Opt. Soc. Am.*, **44**(11):838-850.

Cox, C. and W. Munk (1955). Some problems in optical oceanography. *Journal of Marine Reseearch*, 14:63-78.

Curran, P.J. (1987). Airborne multispectral scanner data for estimation of dye dispersion from sea outfalls. *Proc. Inst. Civil Eng., Part 2,* **83**:213-241.

Curran, P.J. and E.M.M. Novo (1988). The relationship between suspended sediment concentration and remotely-sensed spectral radiance: A review. *Journal of Coastal Research*, **4**:351-368.

Curran, P.J., J.D. Hansom, S.E. Plummer, and M.I. Pedley (1987). Multispectral remote sensing of nearshore suspended sediments: a pilot study. *International Journal of Remote Sensing*, **8**(1):103-112.

Dick, K., and J. Miller (1991). Derivative analysis applied to high resolution optical spectra of freshwater lakes. *Proceedings, 14th Canadian Symposium and Remote Sensing*, Canadian Remote Sensing Society, Ottawa, pp. 400-403.

Diebel-Langohr, D., T. Hengstermann, and R. Reuter (1986). Identification of hydrographic fronts by airborne lidar measurements of Gelbstoff distributions In: *Marine Interfaces Ecohydrodynamics*, J.C.J. Nihoul (ed). (Amsterdam: Elsevier Scientific Publishing Company), pp 569-590.

Dodge, R.E, and J.R. Vaisnys (1977). Coral populations and growth patterns: Responses to sedimentation and turbidity associated with dredging. *J. Mar. Res.* **35**: 715-730.

Doerffer, R, and J. Fischer (1987). Measurements and model simulations of sun-stimulated chlorophyll fluorescence within a daily cycle. *Advances in Space Research.* **7**:117-120.

Doerffer, R. (1988). Remote sensing of sunlight induced phytoplankton fluorescence. In: H.K. Lichtenthaler (ed) *Application of chlorophyll fluorescence*, pp:269-274. Kluwer Academic Publ., Amsterdam.

Doerffer, R. (1992). Application of a two-flow model for remote sensing of substances in water. *Boundary-Layer Meteorology*, **18**:221-232.

Doerffer, R.(1979). Untersuchungen über die Verteilung oberflächennaher Substanzen im Elbe-Aestuar mit Hilfe von Fernmesverfahren. *Arch. Hydrobiol./Suppl.* 43 2/3 119-224. In: Doerffer, R., Imaging Spectroscopy for Detection of Chlorophyll and Suspended Matter. A GKSS Forschungzentrum Geesthacht GmbH Report No. GKSS 92/E/54, 1992.

Doerffer, R., J. Fischer, M. Stossel, C. Brockman, and H. Grassl (1989). Analysis of Thematic Mapper data for studying the suspended matter distribution in the coastal area of the German Bight (North Sea). *Remote Sens. Environ.* **28**:61-73

Doerffer, R., K. Sørensen, and J. Aiken (1999). MERIS potential for coastal zone applications. *International Journal of Remote Sensing*, **20**(9):1809-1818.

DuBois, R. and E.L. Towle (1984). Coral and Sand Mining. CaseStudy No. 6. U.S. Agency of International Development and U.S. National Park Service, Washington, D.C.

Duggin, M.J. and C.J. Robinove (1990). Assumptions implicit in remote sensing data acquisition and analysis. *International Journal of Remote Sensing*, **11**:1669-1694.

Dunne, T. and L.B. Leopold (1978). *Water in Environmental Planning*. W.H. Freeman and Company, NY.

Dyer, K.(1973). Estuaries: A Physical Introduction. John Wiley & Sons, A Wiley-Interscience Publications. 1973. 140pp.

Ellis, M.M. (1936). Erosion silt as a factor in aquatic environments. *Ecology* **17**:29-42.

Ellis, M.M. (1937). Detection and measurement of stream pollution. U.S. Bureau of Fisheries Bull. **22**(48): 365-437.

English, S. and C. Wilkinson (editors) (1991). *Survey Manual for Tropical Marine Resources.* Published by AIDAB on behalf of ASEAN-Australia Marine Science Project, Townsville, Australia. 215pp.

Fischer, J. (1983). Fernerkundung von schwebstoffen im Ozean. *Hamburger geophysikalische Einzelschriften, herausg. Von den Geophysikalischen Instituten der Universität Hamburh, Reihe A, Heft 65.* In: Doerffer, R., Imaging Spectroscopy for Detection of Chlorophyll and Suspended Matter. A GKSS Forschungzentrum Geesthacht GmbH Report No. GKSS 92/E/54, 1992.

Fischer, J. and U. Kronfeld (1986). Sun-stimulated chlorophyll fluorescence.1: Influence of oceanic properties. *International Journal of Remote Sensing*, **11**(12):2125-2147.

Friedman, G.M. (1999).

Gardner, W.D. (1977). Sediment trap dynamics and calibraton: a laboratory evaluation. *Journal of Marine Research,* **38**: 17-39.

Gates, C.E. (1979). Line transect and related issues. In: Cormack, R.M., G.P. Patil and D.S. Robson (editors). *Sampling Biological Populations.* Inter. Co-op Publishing House, Fairland, Maryland.

Gjessing, E.T. (1976). *Physical and chemical characteristics of aquatic humus.* Ann Arbor Science, Ann Arbor, USA, 1976.

GKSS (ed) (1986). *The use of chlorophyll fluorescence measurements from space for separating constituents of sea water, ESA contract No. RFQ 3-5059/84/NL/MD.* GKSS Forschungzentrum, D-2054 Geesthacht, F.R.G.

Gons, H.J. (1999). Teledetection of chlorophyll-a in turbid inland waters. *Environmental Science Technology*, **33**:1127-1132.

Gordon, H.R. (1978). Removal of atmospheric effects from satellite imagery of the oceans. *Applied Optics,* 17:1631-1636. In: Doerffer, R., Imaging Spectroscopy for Detection of Chlorophyll and Suspended Matter. A GKSS Forschungzentrum Geesthacht GmbH Report No. GKSS 92/E/54, 1992

Gordon, H.R. (1979). Diffuse reflectance of the ocean: the theory of its augmentation by chlorophyll-a fluorescence at 685 nm. *Applied Optics,* 18(8). In: Doerffer, R., Imaging

Spectroscopy for Detection of Chlorophyll and Suspended Matter. A GKSS Forschungzentrum Geesthacht GmbH Report No. GKSS 92/E/54, 1992.

Gower, A.M. (1980). *Water Quality in Catchment Ecosystems*. John Wiley & Sons: NY, New York.

Gower, J.F.R., R. Doerffer, and G.A. Borstad (1999). Interpretation of the 685nm peak in water-leaving radiance spectra in terms of fluorescence, absorption and scattering, and its observation by MERIS. *International Journal of Remote Sensing*, **20**(9):1771-1786.

Gower, J.R. (ed.) (1981). *Oceanography from space.* Plenum Press, New York.

Gross, M.G. (1972). *Ocenaography: a view of the earth.* Publ. Prentice-Hall, Inc. Englewood Cliffs, New Jersey. 581 pp.

Günther, K.P., D. Ernst, and H. Maske (1986). Biophysical processes of chlorophyll-a fluorescence. In: GKSS (ed), *The use of chlorophyll fluorescence measurements from space for separating constituents of sea water, ESA contract No. RFQ 3-5059/84/NL/MD.* GKSS Forschungzentrum, D-2054 Geesthacht, F.R.G., pages appendix 1: 1-32.

Harrington, J.A., Jr., F.R. Schiebe, and J.F. Nix (1992). Remote sensing of Lake Chicot, Arkansas: Monitoring suspended sediment, turbidity, and Secchi depth with Landsat MSS data. *Remote Sensing of Environment*, **39**:15-27.

Hinton, J.C. (1991). Application of eigenvector analysis to remote sensing of coastal water quality. *International Journal of Remote Sensing*, **12**:1441-1460.

Hitchcock, G.L. (1982). A comparative study of the size-dependent organic composition of the marine diatoms and dinoflagellates. *Journal of Plankton Research*, **4**(2).

Hoegh-Guldberg, O. (2000). Climate Change, Coral Bleaching and the Future of the World's Coral Reefs. A Greenpeace International Report. The Coral reef Research Institute, Univ. of Sydney, 28 pp.

Højerslev, N.K. (1975). A spectral light absorption meter for measurements in the sea. *Limnol. Oceanogr.*, **20**(6):1024-1034.

Holdgate, M.W. (1979). A Perspective of Environmental Pollution. Cambridge University Press. Cambridge.

Holyer, R.J. (1978). Towards universal suspended sediment algorithms. *Remote Sensing of Environment*, 7:323-338.

International Maritime Organization (IMO) Regional Program for the Preventation and Management of Marine Pollution in the East Asian Seas (MPP-EAS) (1999). *Total Economic Valuation: Coastal and Marine Resources in the Straits of Malacca.* MPP-EAS Technical

Report 24 (Quezon City, Philippines: Global Environment Facility, UNDP, and IMO, 1999). pp.14

Iqbal, M. (1983). *An introduction to solar radiation.* Academic Press, Toronto, New York, London.

Jameson, S. and D. Smith (1997). Coral Reef Management on the New Red Sea Riviera. *Proceedings of Coastal Zone 1997* **2** (1997): 784-86

Jameson, S.C., J.W. McManus, and M.D. Spalding (1995). *State of the Reefs: Regional and Global Perspectives* (Washington, D.C. ICRI., U.S. Department of State), ICRI report, 24pp.

Jerlov, N.G. (1976). *Marine Optics.* Elsevier Scientific Publishing Company, Amsterdam, Oxford, New York, 2nd Edition.

Jones, J.R.E. (1964). *Fish and River Pollution.* Butterworth, London. 220 pp.

Jones, O.A.and R. Endean (1981). Coral reefs: the coming crisis. *Proceedings of the Fourth International Coral Reef Symposium*, pp:33-36.

Joseph, J. (1950). Untersuchungen über Ober- und Unetrlichtmessungen im Meere und über ihren Zusammenhang mit Durchsichtigkeitsmessungen. *Dt. Hydrogr. Z. 3:324-335.* In: Doerffer, R., Imaging Spectroscopy for Detection of Chlorophyll and Suspended Matter. A GKSS Forschungzentrum Geesthacht GmbH Report No. GKSS 92/E/54, 1992.

Kalle, K.(1966). The problem of the Gelbstoff in the sea. *Oceanogr. Mar. Biol. Anu. Rev.*, **4**:91-104.

Kaufman, Y.J. (1989). The atmospheric effect on remote sensing and its correction. In: *Theory and Applications of Optical Remote Sensing* (G. Asrar, Ed.), Wiley, New York, pp. 336-428.

Khorram, S. and H.M. Cheshire (1985). Remote sensing of water quality in the Neuse River estuary, North Carolina. *Photogrammetric Engineering and Remote Sensing*, **51**(3):329-341.

Kim, H.H., H. van der Piepen, V. Amann, and R. Doerffer (1985). An evaluation of 685nm fluorescence imagery of coastal waters. *ESA Journal*, **9**:17-27.

Kinsey, D.W. (1988). Coral Reef System Response to some Natural and Anthropogenic Stress. *Galaxea*, **7**:113-128.

Kirk, J.T.O. (1986). *Light and Photosynthesis in Aquatic Ecosystems*, Cambridge University Press, Cambridge, 401pp.

Kirk, J.T.O. (1989). The upwelling light stream in natural waters. *Limnology and Oceanography*, **34**:1410-1425.

Kronfeld, U. (1988). Die optischen Eigenschaften der ozeanischen Schwebstoffe und ihre Bedeutung für die Fernerkundung von Phytoplankton. In: GKSS Forschunzentrum, D-2054 Geesthacht, F.R. Germany, Report GKSS 88/E/40, pp 153.

Langlois, T.H. (1941). Two processes operating for the reduction in abundance or elimination of species from certain types of water areas. *Trans., North American Wildlife Conf.* **6**:189-201.

Leckner, B. (1978). The spectral distribution of solar radiation at the earth's surface - elements of a model. *Sol. Energy,* 20 (2):143-150. In: Doerffer, R., Imaging Spectroscopy for Detection of Chlorophyll and Suspended Matter. A GKSS Forschungzentrum Geesthacht GmbH Report No. GKSS 92/E/54, 1992.

Lee, J.W.L. (1994). *Impact Of Coastal Development On The Natural Coastal Ecosystems Of Northwest Langkawi (1985 - 1994).* Unpublished MSc. Thesis NR-94-5, Asian Institute Of Technology, Bangkok, Thailand. 132pp.

Leletkin, V.A. (1981). Analysis of the influence of substrate variables on coral reef fish communities. Mar. Biol., **49**:317-323.

Liew, H.C. and R. Hoare (1979). The effects of sediment accumulation and water turbidity upon the distribution of scleractinian corals at Cape Rachado, Malacca Straits. *Proc. Conf. Trends in Appl. Biol. In S.E. Asia VII.* Universiti Sains Malaysia, Penang. pp.14

Lillesand, T.M., and R.W. Kiefer (1987). *Remote Sensing and Image Interpretation.* Second Edition. John Wiley and Sons Publ. New York.-Chichester-Brisbane-Toronto-Singapore. 721 pp.

Lorenzen, C.J., F.R. Schuman and J.T. Bennett (1981). In-situ calibration of a sediment trap. *Limnology and Oceanography,* **26**: 580-585.

Loya, Y. (1978). Plotless and transect methods. pp. 197-217. In: Stoddart, D.R. and R.F. Johannes (editors). *Coral Reefs: Research Methods.* UNESCO, Paris.

Lunetta, R., R. Congalton, L. Fenstermaker, J. Jensen, K. McGwire and L. Tinney (1981). Remote sensing and geographic information system data integration: error sources and research issues. *Photogrammetric Engineering and Remote Sensing.* **57**(6):677-687.

Lyon, J.C., K.W. Bedford, J.C. Yen, D.H. Lee and D.J. Mark (1988). Detremination of suspended sediments from multiple day Landsat and AVHRR data. *Remote Sensing of Environment,* **25**: 107-115.

MacFarlane, N. and Robinson, I.S. (1984). Atmospheric correction of Landsat multispectral scanner data for a multidate suspended sediment algorithm. *International Journal of Remote Sensing,* **5**:561-576.

Mansueti, R.J. (1961). Effects of civilization on striped bass and estuarine biota inChesapeake Bay and tributaries. *Proc. Gulf Caribbean Fisheries Inst.* pp: 110-136.

Mapstone, B,D., J.H. Choat, R.L. Cumming and W.G. Oxley (1989). The fringing reefs of Magnetic Island: benthic biota and sedimentation. A baseline study. A report to the Great Barrier Reef Marine Park Authority. March 1989. 88pp.

Marsh, L.M., R.H. Bradbury and R.E. Reichelt (1984). Determination of the physical parameters of coral distributions using line transect data. *Coral Reefs*, **2**: 175-180.

Maurer, D. and K.S. Price (1969). Shellfish: From here and extinction. *Delaware Cons.* **13**:3-10.

Maurer, D., L. Waling and R. Keck (1971). A Delaware oyster industry: A reality? *Am. Fish. Soc. Trans.* **100**:100-111.

McCabe, J.M., and C.L. Sandretto. (1985). *Some Aquatic Impacts of Sediment, Nutrients, and Pesticides in Agricultural Runoff.* Publication No. 201. Limnological Research Laboratory, Dept. of Fisheries and Wildlife, Michigan State University.

McClatchey, R.A., and J.E. Selby (1972). Atmospheric transmittance from 0.25 to 38.5 μm: computer code LOWTRAN-2. *Air Force Cambridge Research Laboratories, AFCRL-72-0745, Environ. Res. Paper 427.* In: Doerffer, R., Imaging Spectroscopy for Detection of Chlorophyll and Suspended Matter. A GKSS Forschungzentrum Geesthacht GmbH Report No. GKSS 92/E/54, 1992.

Milliman, J.D. and R.H. Meade (1983). World-wide delivery of river sediment to the ocean. *Journal of Geology*, **91:** 1-21.

Moore, G.K. (1977). Satellite surveillance of physical water quality characteristics. *Proceedings of 12th International Symposium on Remote Sensing of Environment*, University of Michigan, Ann Arbor, MI, pp.445-461.

Morel, A. (1974). Optical Properties of pure water and pure sea water. In: Jerlov, N.G., and E. Steemann Nielsen (eds.) *Optical aspects of oceanography.* Academic press, London and New York. p. 1-24.

Morel, A.(1980). In-water and remote measurements of ocean colour. *Boundary-Layer Meteorology*, **18**:177-201.

Nanu, L. and C. Robertson (1993). The effect of suspended sediment depth distributionb on coastal water spectral reflectance: theoretical simulation. *International Journal of Remote Sensing*, **14**(2):225-239.

Newman, H.E. (1984). *Effects of sediment fallout and turbidity on hermatypic corals.* Unpublished MSc. thesis. School of Biological Sciences, Universiti Sains Malaysia, Penang Malaysia. 186 pp.

Novo, E.M.M., C.A. Steffan, and C. Z.F. Braga (1991). Results of laboratory experiment relating spectral reflectance to total suspended solids. *Remote Sensing of Environment*, **36**:67-72.

Novo, E.M.M., J.D. Hansom, and P.J. Curran (1989a). The effect of sediment type on the relationship between reflectance and suspended sediment concentration. *International Journal of Remote Sensing*, **10**(7): 1283-1289

Novo, E.M.M., J.D. Hansom, and P.J. Curran (1989b). The effect of viewing geometry and wavelength on the relationship between reflectance and suspended sediment concentration. *International Journal of Remote Sensing*, **10**(8): 1357-1372

Nybakken, J.W. (1982). *Marine Biology: An Ecological Approach.* Harper and Row Publications. New York.

Odum, H.T. (1955). Trophic structure and productivity of a windward coral reef community on Eniwetok Atoll. *Ecol. Monogr.*, **25**:291-320.

Pastorok, R.A., and G.R. Bilyard (1985). Effects of sewage pollution on coral-reef communities. *Mar. Ecol. Prog. Ser.*, **21**: 175-189

Pearson, R.G. (1981). Recovery and recolonization of coral reefs. Mar. Ecol. Prog. Ser.. **4**:105-122.

Penndorf, R. (1957). Tables of the refractive index for standard air and the Rayleigh scattering coefficient for the spectral region between 0.2 and 20.0 μm and their application to atmospheric optics. *J. Opt. Soc. Am.*, **47**(2):176-182.

Phelps, E.B. (1944). *Stream sanitation.* John Wiley and Sons. New York, N.Y., 276pp.

Philippines Ministry of Natural Resources (1979). Forum on Philippine Corals: issues on Conservation and Management. 9th Natural Resources Management Forum. *Jour. Of NaturalRresources Management Forum,* 50pp.

Philpot, W.D. (1991). The derivative ratio algorithm: avoiding atmospheric effects in remote sensing. *IEEE Trans. Geosci. Remote Sens.* **29**:250-357.

Pimentel, D., J. Allen, A. Beers, L. Guenand, R. Linder, P. McLauughlin, B. Meers, D. Musonda, D. Purdue, S. Poesson, S. Seebert, K. Stoner, R. Salazar, and A. Hawkins (1987). World Agriculture and Soil Erosion. *Bioscience,* **37**:277-283

Plass, G.N., and G.W. Kattawar (1972). Effects of aerosol variation on radiance in the earth's atmosphere-ocean system. *Applied Optics*, **11**:1598-1604.

Plass, G.N., G.W. Kattawar, and J.A. Guinn, Jr. (1976). Radiance distribution over a ruffled sea: contribution from glitter, sky and ocean. *Applied Optics* **15**:3161-3165.

Plummer, C.C., D. McGeary, and D.H. Carlson (2003). *Physical Geology*. Ninth Edition (International Edition). Published by McGraw-Hill. 574pp.

Prieur, L. and S. Sathyendranath (1981). An optical classification of coastal and oceanic waters based on the specific spoectral absorption curves of phytoplankton pigments, dissolved organic matter, and other particulate materials. *Limnology Oceanography* **26**:671-689.

Pritchard, D.W. (1952b). Estuarine hydrography. *Advan. Geophy.*, **1**:243-280.

Randall, R.H. and C. Birkeland (1978). Sedimentation studies at Fouha Bay and Ylig Bay. In: Guams reefs and beaches II. University Guam Tech. Report **47**: 77-77.

Ray, G.C. and G.F. Grassle (1991). Marine Biological Diversity. *Bioscience*, **41**:453-457.

Ritchie, J.C. (1972). Sediment, fish and fish habitat. *Journal of Soil and Water Conservation,* **27**:124-125.

Ritchie, J.C. F.R. Schiebe, and J. McKhenry (1976). Remote sensing of suspended sediments in surface waters. *Photogrammetric Engineering and Remote Sensing* **42**(11): 1539-1545.

Ritchie, J.C., and C.M. Cooper (1988). Comparison of measured suspended sediment concentrations with suspended sediment concentrations estimated from Landsat MSS data. *International Journal of Remote Sensing*, **9**(3): 379-387

Ritchie, J.C., and F.R. Schiebe (1986). Monitoring suspended sediments with remote sensing techniques. *Hydrologic Applications of Space Technology*, (Proceedings of Cocoa Beach Workshop, Florida, August 1985). IAHS Publ. No. 160, pp233-242.

Ritchie, J.C., C.M. Cooper and I. Yongong (1987). Using landsat Multispectral Scanner data to estimate suspended sediments in Moon Lake, Mississippi. *Remote Sensing of Environment*, **23**(1):65-81.

Robinson, A.R. (1971). Sediment. *Journal of Soil and Water Conservation,* **26**:61-61.

Rowan, K.S. (1989). *Photosynthetic pigments of algae*. Cambridge Univ. Press, Cambridge.

Sathyendranath, S. (1986). Remote sensing of phytoplankton: A review with special reference to picoplankton. In: T. Platt and W.K.W. Li (eds), *Photosynthetic Picoplankton*, Vol. 214 of Canadian Bulletin of Fisheries and Aquatic Science, pp. 561-583.

Sathyendranath, S. L. Prieur and A. Morel (1989). A three-component model of ocean colour and its application to remote sensing of phytoplankton pigments in coastal waters. *International Journal of Remote Sensing*, **10**(8):1373-1394.

Schiebe, F.R., J.A. Harrington Jr., and J.C. Ritchie (1988). Remote sensing of suspended sediments of Lake Chicot, Arkansas. *Proceedings of the 6th U.S. Army Corps. Of Engineering Remote Sensing Symposium*, Galveston, TX, pp.77-85.

Schiller, H. and R. Doerffer (1999). Neural network for emulation of an inverse model – operational derivation of Case II water properties from MERIS data. *International Journal of Remote Sensing*, **20**(9):1735-1746.

Sellers, W.D. (1965). *Physical Climatology*. University of Chicago Press, Chicago. Ill. 272 pp.

Sheppard, C. R. C. (1980). Coral cover, zonation and diversity on reef slopes of Chagos atolls, and population structures of the major species. *Mar. Ecol. Progr. Ser.*, **2**:193-205.

Spitzy, A. and V. Ittekkot (1986). Gelbstoff: an uncharacterized fraction of dissolved organic carbon. In: GKSS (ed) *The influence of yellow substances on remote sensingof seawater constituents from space, ESA contract No. RFQ 3-5060/84/NL/MD.* GKSS Forschungzentrum, D-2054 Geesthacht, F.R.G., pages appendix 1:1-31.

Stauber, J.L. and S.W. Jeffrey (1988). Photosynthetic pigments in fifty-one species of marine diatoms. *J. Phycol.*, **24**:158-172.

Stoddart, D.R. (1968). Catastrophic human interference with coral atoll ecosystems. *Geography* **53**:25-40.

Stoddart, D.R. (1981). Coral Reefs: The Coming Crisis. *Proceedings of the Fourth International Coral Reef Symposium*, Manila, The Philippines. Vol. 1.

Sturm, B. (1980). The atmospheric corrections of remotely sensed data and the qualitative determination of suspended matter in marine water surface layers. In: A.P. Cracknell (ed.) *Remote Sensing in Meteorology, Oceanography and Hydrology,* Ellis Horwood Ltd., Chichester. p. 163-197.

Sturm, B. (1981). Ocean colour remote sensing and quantitative retrieval of surface chlorophyll in coastal waters using Nimbus CZCS data. In: Gower, J.R. (ed.) (1981). *Oceanography from space.* Plenum Press, New York. p. 267-279.

Sui, X., D.L. Muirhead, W.A. Jackson, and C. Zhang (2001). The Colour of Total Suspended Solids: Potential Use in Remote Sensing and Water Quality Monitoring. Proceedings of the 7th Annual Student Conference, University of Houston-Clear Lake, Houston, TX, April 18-19, 2001.

Summerfield, M.A. (1998). *Global Geomorphology.* Wiley, New York, pp. 73-111.

Tanaka, M., and T. Nakajima (1977). Effects of oceanic turbidity and index of refraction of hydrosols on the flux of solar radiatrion in the atmosphere-ocean system. *J. Quant. Spectrosc. Radiant. Transfer*, **12**:93-111.

Tarzwell, C.M. and A.P. Gauffin (1953). Some important biological effects of pollution often disregarded in stream surveys. *Purdue Univ. Eng. Bull. Proc., 8th Ind. Waste Conf.*, Lafayette, Ind. 38 pp.

Tassan, S., and B. Sturm (1986). An algorithm for the retrieval of sediment content in turbid coastal waters from CZCS data. *International Journal of Remote Sensing*, **7**:643-655

Thevathassapillai, R. (1990). *Kesan sedimentasi terhadap terumbu karang di Pulau Kendi.* Unpublished BSc. thesis. Universiti Sains Malaysia. 115pp.

Thurman, H. and A. Trujillo (1999). *Essentials of Oceanography.* Sixth Edition. Published by Prentice-Hall, Inc., New Jersey. 527 pp.

Tide Tables Malaysia Volume 1. (1999). Published by Hydrographic Branch, Royal Malaysian Navy. 165 pp.

Topliss, B.J., C.L. Almos and P.R. Hill (1990). Algorithms for remote sensing of high concentration, inorganic suspended sediment. *International Journal of Remote Sensing*, **11**(6):947-966.

Tushinsky, S. (1991). Spatial and temporal variability of water quality and optimization of pollution monitoring networks in the Upper Volga River Basin. In: Water Pollution: Modelling, Measuring and Prediction. (Eds. Wrobel. L.C. and C.A. Brebbia), First International Conference on Water Pollution: Measuring and Prediction 91. Computational Mechanics Publications & Elsevier Applied Science, Southampton, London New York. p:211-221.

UKM (1995). *Preliminary Environmental Impact Assessment of the Proposed Tanjung Rhu Integrated Resort Development, Langkawi: A Final Report.* 180pp.

United Nations Environment Programme (UNEP) (1990). GESAMP: The State of the Marine Environment. UNEP Regional Seas reports and Studies, **115**:i-vii, 1-111.

United Nations Environment Programme (UNEP) and World Conservation Union (IUCN) (1988). *Coral Reefs of the World. Volume 1: Atlantic and Eastern Pacific* (Gland, Switzerland: IUCN, 1988), xvi.

United Nations Education, Scientific and Cultural Organization (UNESCO) (1985). Considerations on analytical and sampling methods and information on intercalibration exercises *(18 p. in various pagings), illus.; IOC/WC/GIPME.I/17;*

van der Hulst, H.C. (1980). *Multiple light scattering, tables, formulas and applications. Vols. 1 and 2.* Academic Press, New York.

Weeks, A. and H. Simpson (1991). The measurement of suspended particulate concentrations from remotely-sensed data. *International Journal of Remote Sensing*, **12**:725-737

White, A.T. and A. Cruz-Trinidad (1998). *The values of Philippines Coastal Resources: Why Protection and Management are Critical.* Cebu City, Philippines: Coastal Resource Management Project. 1998.

Wilber, C.G. (1983). *Turbidity in the Aquatic Environment: An Environmental Factor in Fresh and Oceanic Waters*. Charles C. Thomas Publishers, Springfield IL.

Wood, E.M. (1984). *Reef Corals of the World: Biology and Field Guide*.256 pp.

World Resources Institute (2000*).* *Coral Reefs: A World Resources Report.* WRI Publication. 132pp.

World Resources Institute (2002). *Reefs at Risk in South East Asia.* WRI Publication. 164 pp.

Yasin, Z. (1993). Sedimentation on the coral reefs of Malaysia: Interpretation of sedimentation data for coastal zone management. Paper presented at the "International Seminar on Remote Sensing for Coastal Zone and Coral Reef Applications" at Asian Institute of Technology, Bangkok, Thailand, 25 October – 1 November 1993.

Yasin, Z. (*pers. comm.)*. Centre for Marine and Coastal Studies, Universiti Sains Malaysia, Penang, Malaysia.

Zaneveld, J.R.V. and D.M. Roach (1974). The determination of index of refraction of distribution of oceanic particulates. *Journal of Geophysical Research*, **79**:4091-4095.

APPENDIX 1

A flowchart showing the effect of rainfall erosion from a forested area and its typical sediment pathway into an existing coastal ecosystem.

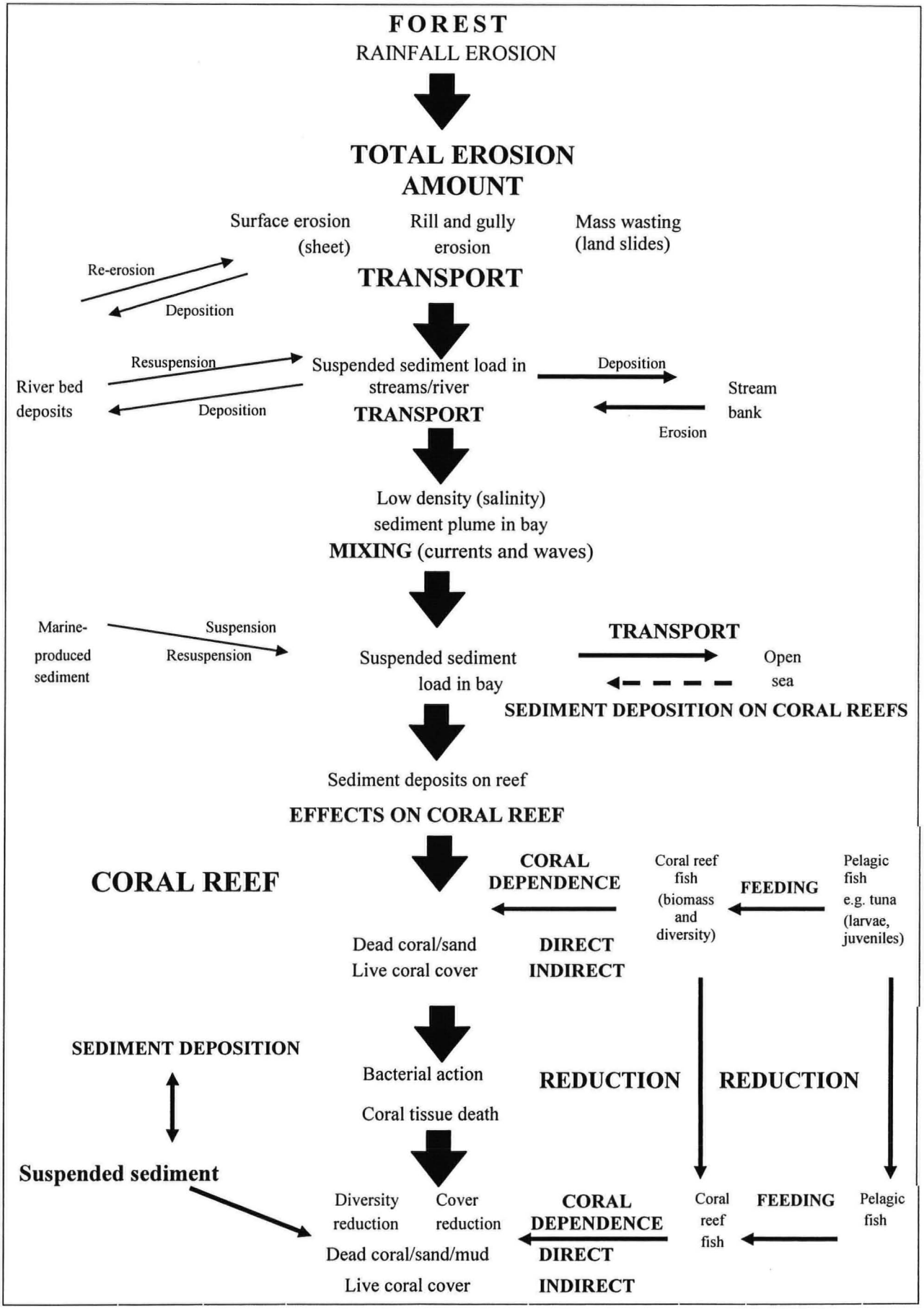

A typical rainfall erosion and sediment pathway from a forested area to an existing coastal ecosystem.

APPENDIX 2

Flowcharts showing typical examples of the degree of impact of deforestation on the terrestrial, freshwater stream and the marine environments of Malaysian coasts.

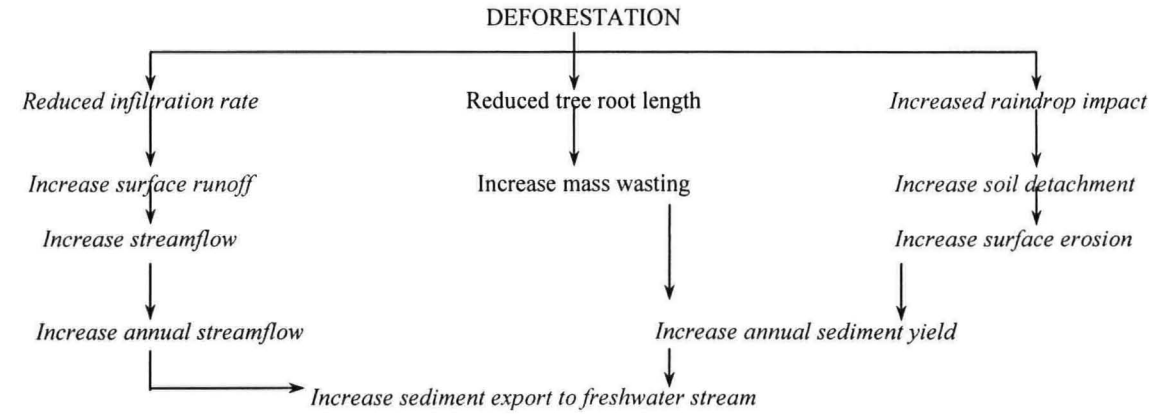

Impact of deforestation on the terrestrial environment. (Source: Lee,1994)

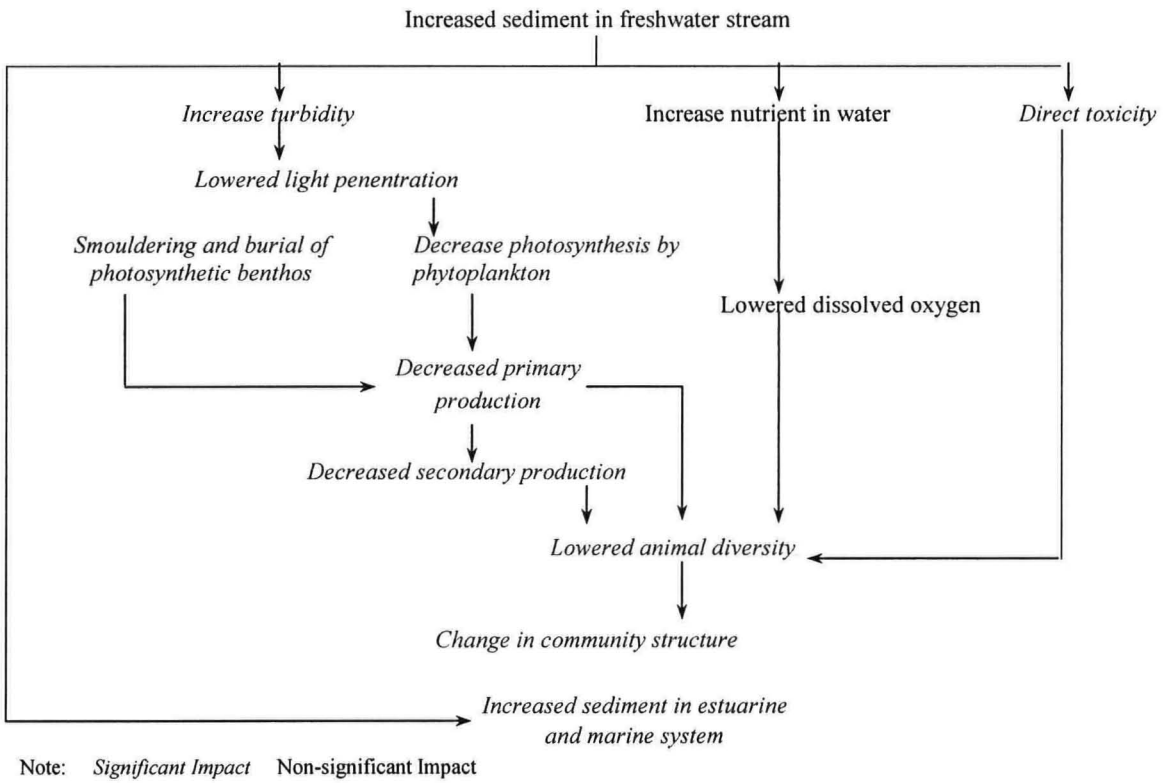

The impact of deforestation on the freshwater stream environment. (Source: Lee, 1994)

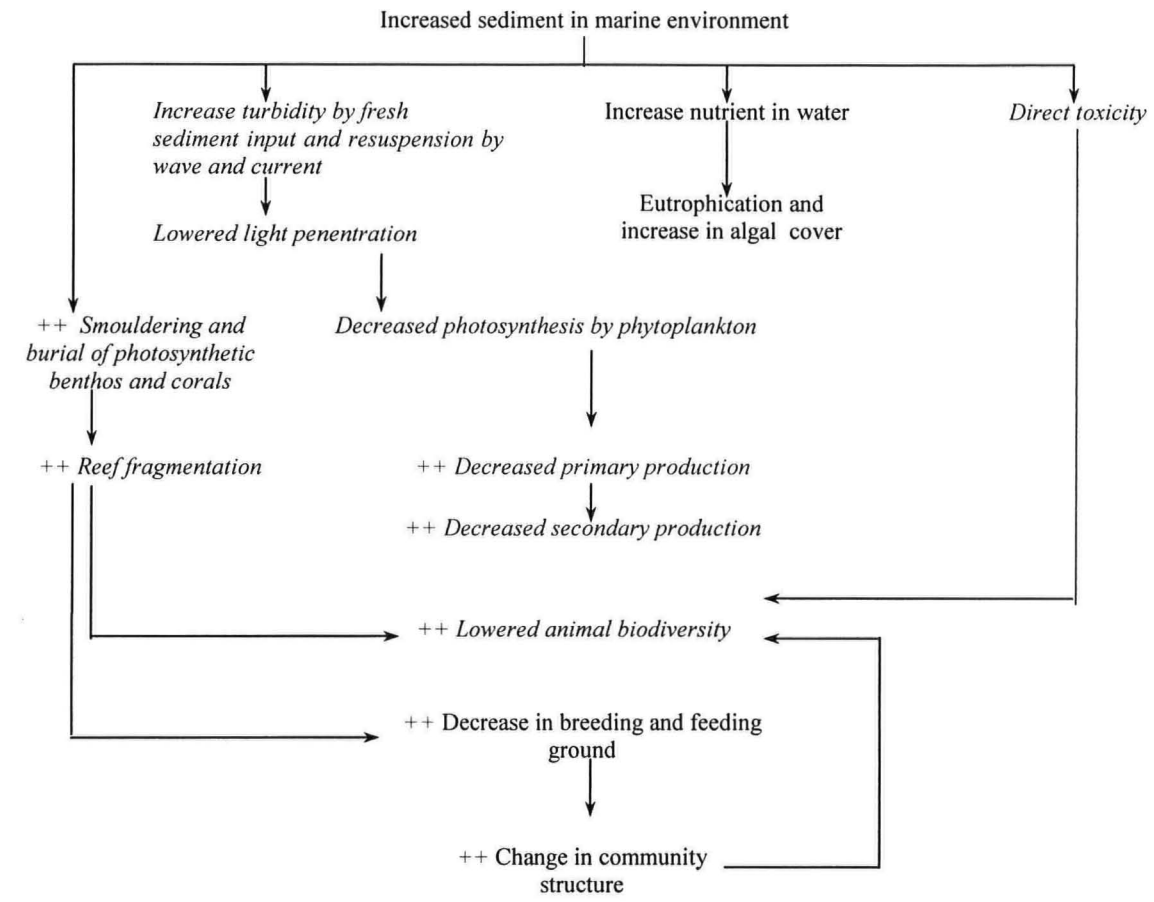

Note: *Significant Impact* Non-significant Impact '++' Long-term impact

The impact of deforestation on the marine environment (Source: Lee, 1994)

APPENDIX 4

Summary of the marine water quality of Teluk Datai, Pulau Langkawi for 1985, 1989 and 1994.

Summary of the marine water quality of Teluk Datai, Pulau Langkawi (1985, 1989 and 1994). (Source: Lee, 1994)

	1985	1989	1994
Physical parameters			
Seasurface temperature (C)	29.2	29.0	29.4
Dissolved Oxygen (mg/L)	7.44	6.35	6.0
Total Suspended Particulates (mg/L)	10.0	20.0	40.0
Salinity (ppt)	29.0	29.0	30.5
pH	8.1	8.0	8.1
Chemical parameters			
Phosphate (mg/L)	0.04	0.03	0.10
Ammoniacal nitrogen (mg/L)	0.11	1.30	0.10
Nitrate nitrogen (mg/L)	0.10	1.20	0.08
Oil and Grease	ND*	ND*	ND*
Microbiological parameters			
Total coliforms (MPN/100ml)	0	0-100	0
Faecal coliforms (MPN/100ml)	0	0-100	0

*ND: *Not detectable*

APPENDIX 6

List of coral species found within the study area (Teluk Dedap fringing reefs) and the control site (Teluk Datai fringing reefs).

Coral species of the study area (Teluk Dedap fringing reefs) and the control site (Teluk Datai fringing reefs). (Note: √ indicates presence of species)

Class: **ANTHOZOA**

Sub-class: **ZOANTHARIA**

Order: **SCLERACTINA**

		TELUK DEDAP	TELUK DATAI	Commonly shared species
Sub-order	**ASTROCOENIIA**			
Family	**Thamnasteriidae**			
	Psammocora contigua		√	
	Psammocora digitata		√	
Family	**Pocilloporiidae**			
	Madracis kirbyi	√		
	Pocillopora damicornis		√	
	Pocillopora eydouxi		√	
	Pocillopora verrucosa	√	√	√
Family	**Acroporiidae**			
	Acropora tubicinaria	√		
	Acropora abratanoides		√	
	Acropora formosa		√	
	Acropora hyacinthus		√	
	Acropora variabilis		√	
	Acropora sp. 1		√	
	Acropora sp. 2		√	
	Acropora sp. 3		√	
	Asteropda myriopthalma		√	
	Montipora digitata	√	√	√
	Montipora fruticosa		√	
	Montipora levis		√	
	Montipora solanderi		√	
	Montipora tuberculosa		√	
	Montipora sp. 1		√	
Sub-order	**FUNGIINA**			
Family	**Agariciidae**			
	Pachyseris crinata	√	√	√
	Pachyseris speciosa		√	
	Psammocora contigua	√		
	Pavona cactus	√		
	Pavona crassa	√	√	√
	Pavona decussata		√	
	Pavona frondifera		√	

(continue)

Coral species of the study area (Teluk Dedap fringing reefs) and the control site (Teluk Datai fringing reefs). (Note: √ indicates presence of species)

Class: **ANTHOZOA**

Sub-class: **ZOANTHARIA**

Order: **SCLERACTINA**

		TELUK DEDAP	TELUK DATAI	Commonly shared species
Sub-order	**FUNGIINA**			
Family	**Fungiidae**			
	Fungia echinata	√	√	√
	Fungia fungites	√	√	√
	Fungia rependa	√	√	√
	Herpolitha limax		√	
	Palahalomitra robusta		√	
	Podabacia crustacea	√	√	√
Family	**Poritidae**			
	Goniopora norfolkensis	√		
	Porites lobata	√		
	Goniopora lobata	√	√	√
	Goniopora sp.		√	
	Porites convexa	√	√	√
	Porites lutea	√	√	√
	Porites nigrescens	√	√	√
	Porites sp. 1 (branching)		√	
	Porites sp. 2 (encrusting)		√	
	Porites sp. 3		√	
Sub-order	**FAVIINA**			
Family	**Faviidae**			
	Cyphaestrea chalcidium		√	
	Cyphaestrea micropthalma		√	
	Diploastrea heliopora		√	
	Echinopora lamellosa		√	
	Echinopora horrida		√	
	Favia favus	√	√	√
	Favia speciosa	√	√	√
	Favia amicorum	√	√	√
	Favia sp. 1		√	

(continue)

Coral species of the study area (Teluk Dedap fringing reefs) and the control site (Teluk Datai fringing reefs). (Note: √ indicates presence of species)

Class: **ANTHOZOA**

Sub-class: **ZOANTHARIA**

Order: **SCLERACTINA**

		TELUK DEDAP	TELUK DATAI	Commonly shared species
Family	**Faviidae**			
	Favites abdita	√	√	√
	Favites sp. 1		√	
	Favites complanata	√		
	Oulastrea crispata	√		
	Goniastrea aspera	√	√	√
	Goniasteria pectinata	√	√	√
	Goniastrea rectiformis	√	√	√
	Hydnopora excesa		√	
	Hydnopora rigida		√	
	Platygyra daedala	√	√	√
	Platygyra lamellina		√	
	Platygyra sinensis	√	√	√
Family	**Meralinidae**			
	Merulina ampliata		√	
Family	**Oculinidae**			
	Galaxea clavus	√	√	√
	Galaxea fascicularis	√	√	√
Family	**Mussidae**			
	Symphyllia recta	√		
	Scomylia vitiensis	√		
	Lobophyllia hemprichii		√	
	Symphyllia nobilis		√	
Family	**Caryophyllidae**			
	Plerogyra sinuosa		√	
	Euphyllia ancora	√		
	Euphyllia fimbriata		√	
	Euphyllia glabrescens		√	
	Paracyathus stokesi		√	
Family	**Pectiniidae**			
	Pectinia lactuca		√	
	Echinophyllia aspera		√	
	Turbinaria frondens	√		

(continue)
Coral species of the study area (Teluk Dedap fringing reefs) and the control site (Teluk Datai fringing reefs). (Note: √ indicates presence of species)

		TELUK DEDAP	TELUK DATAI	Commonly shared species
	Class: **ANTHOZOA**			
	Sub-class: **ZOANTHARIA**			
	Order: **SCLERACTINA**			
Sub-order	**DENDROPHYLLINAE**			
Family	**Dendrophyllidae**			
	Dendrophyllia micranthus		√	
	Dendrophyllia diaphana		√	
	Tubastrea aurea	√	√	√
	Turbinaria reniformis	√		
	Balanophyllia sp.		√	
	Turbinaria crater		√	
	Turbinaria mollis		√	
	Class: **HYDROZOA**			
	Order: **MILLEPORINA**			
Family	**Milleporidae**			
	Millepora platyphyllia		√	
	Millepora tenera		√	